ESCOLA DE DOUTORAMENTO
INTERNACIONAL DA USC

Amelia
MacKay Anderson

Tese de doutoramento

THE MOLECULAR MAGIC OF CYCLODEXTRINS DECODING COMPLEX INTERACTIONS WITH COMPUTATIONAL MODELING

Santiago de Compostela, 2024

Programa de Doutoramento en Ciencia de Materiais

ESCOLA DE DOUTORAMENTO
INTERNACIONAL DA USC

DOCTORAL THESIS

THE MOLECULAR MAGIC OF CYCLODEXTRINS

DECODING COMPLEX INTERACTIONS WITH COMPUTATIONAL MODELING

Amelia MacKay Anderson

Supervisor/s: Ángel Piñeiro & Rebeca Garcia Fandiño

Tutor: Ángel Piñeiro

PHD PROGRAMME IN MATERIALS SCIENCE

SANTIAGO DE COMPOSTELA

Table of Contents

ACKNOWLEDGEMENTS.....8

ABSTRACT.....10

Resumo en galego.....10

CHAPTER 1. INTRODUCTION.....18

1.1. Cyclodextrins: Versatile Molecules with Exceptional Applications.....19

1.1.1. Applications of Cyclodextrins.....20

1.1.2. Selective Sequestration of Toxic Oxidized Cholesterols for Atherosclerosis Treatment.....22

1.1.3. Cyclodextrin Summary.....23

1.2. Computational Modeling of Molecules and Molecular Interactions.....23

1.2.1. Docking Calculations.....24

1.2.2. Molecular Dynamics Simulations.....25

1.2.3. Metadynamics and Potential of Mean Force Calculations.....27

1.3. Computational Studies on CDs: Unraveling Complex Host-Guest Interactions.....29

1.4. The Importance of Validation and Corroborating Assays.....31

CHAPTER 2. HYPOTHESIS AND OBJECTIVES.....33

CHAPTER 3. GENERAL METHODOLOGICAL FRAMEWORK.....35

3.1. Computational simulations.....36

3.1.1. Initial Molecule Parameterization and Building of the Complexes.....36

3.1.2. Molecular Docking.....36

3.1.3. Molecular Dynamics.....36

3.1.4. Metadynamics.....37

3.1.5. Potential of Mean Force.....38

3.2. Wet lab experiments.....40

3.2.2 Isothermal Titration Calorimetry.....40

3.2.3 Electronic Spectroscopy.....41

CHAPTER 4. UNRAVELING THE MOLECULAR DYNAMICS OF SUGAMMADEX-ROCURONIUM COMPLEXATION: A BLUEPRINT FOR CYCLODEXTRIN DRUG DESIGN.....42

4.1. Preface.....42

4.2. Introduction.....43

4.3. Specific Methods.....45

4.3.1. Parameterization and Geometry Optimization.....45

4.4. Results.....45

4.4.1. Docking.....45

4.4.2. Molecular Dynamics.....46

4.4.3. Metadynamics and PMF.....49

4.5. Discussion.....50

4.6. Conclusion.....52

CHAPTER 5. CYCLODEXTRINS: ESTABLISHING BUILDING BLOCKS FOR AI-DRIVEN DRUG DESIGN.....53

5.1. Preface.....53

5.1. Introduction.....55

USC UNIVERSIDADE DE SANTIAGO DE COMPOSTELA

5.2. Specific Methods....57
5.2.1. Description of the Systems....57
5.2.2. Simulation Parameters....58
5.2.3. Metadynamics Simulations....58
5.2.4. Potential of Mean Force....59
5.2.5. Statistical analysis....59
5.3. Results....60
5.3.1. General description of the PMF profiles....60
5.3.2. Statistical Results....64
5.4. Discussion....68
5.6. Conclusion....69

CHAPTER 6. ADDRESSING THE COMPLEXITIES IN MEASURING CYCLODEXTRIN-STEROL BINDING CONSTANTS: A MULTIDIMENSIONAL STUDY....70

6.1. Preface....70
6.1. Introduction....72
6.2. Materials....74
6.3. Specific Methods....75
6.3.1 Computational methods....75
6.3.1.1. Description of the structures employed for the computational simulations....75
6.3.1.2. Simulation Parameters....76
6.4. Results....77
6.4.1. Metadynamics Simulations....77
6.4.2 Competitive Isothermal Titration Calorimetry....79
6.4.3 Circular Dichroism....82
6.5. Discussion....84
6.6. Conclusion....86

CHAPTER 7. GENERAL CONCLUSIONS....87

Final Thoughts....89

REFERENCES....91

SUPPLEMENTAL INFORMATION....105

ANNEX 1: PUBLICATIONS INCLUDED IN THE THESIS AND AUTHORIZATIONS FOR THE PUBLISHED CONTENT....134

USC
UNIVERSIDADE DE SANTIAGO DE COMPOSTELA

Acknowledgements

As this chapter of my formal education draws to a close, I feel overwhelmed with gratitude for the many people who have supported me, trained me, and given me so many incredible opportunities along the way. I feel so lucky to be on this path, and I would like to extend my deepest thanks to everyone who has been a part of this extraordinary adventure.

To my family, who have cheered me on and kept me on track since the start, I love you, and I could not have done it without you. Thank you for inspiring my scientific career, pushing me to overcome the challenges, and being there for me every step of the way. As for the ongoing debate of chemistry vs. physics...I say, why argue? Physical chemistry is where it's at!

To Gert Kiss - my partner in every sense, my steady flame, and a catalyst in my scientific journey - I don't need to know how this chemistry works, I love stirring up trouble with you. You always ask the hardest questions, and then help me find the answers (when in doubt, 42 usually works). Now, before I put my foot where my mouth is, thank you for your tenacity, humor, and wisdom, and for tolerating lots and lots of pet hair. I love you.

To my dear friends: Mihir Athavale, Andrew Yang, Kavya Raman, Guneet Kaur, Rinky, Yogi, and Rudy Sahu, Milorad Andjelkovic, Colton Green, Diana Carr, Evan Atwater, (Alex) Zuvich, and especially my beloved frenemy Nick Church for actually reading and editing this thesis...thank you for keeping me sane (most of the time) and for putting up with my nerdy antics. I truly cherish every single one of the Redwolves, Gauchos, Underdogs, and otherwise certified weirdos who have stood by my side for the many laughs, tears, and late nights we've shared. Life without you all would simply be boring.

I am also immensely grateful for the dedication and mentorship of my professors, Ángel Piñeiro and Rebeca Garcia-Fandiño. It has been an absolute pleasure to be your student, and it is a privilege to be guided by you. Your innovative, passionate minds have shaped my approach to research and greatly influenced my view of the world. I am beyond excited to see what the next chapter holds - I hope it involves many more visits to Santiago de Compostela.

Finally, I am deeply indebted to Oki O'Connor and Mike Kope, for their unwavering support and steadfast belief in me. Oki and Mike propelled me from undergraduate intern to company cofounder, and helped me navigate my ongoing education along the way. They connected me with the best resources for what I wanted to do, and sent me on a path - this path - that I could have only dreamed of. I am forever grateful. Thank you, Mike and Oki, for not just believing in the underdog, but for helping me become a leader of the pack.

After all these heartfelt thanks, let's dive in – before my dogs start thinking this thesis is about them!

USC
UNIVERSIDADE DE SANTIAGO DE COMPOSTELA

This work was supported by Cyclarity Therapeutics, the European Union's Horizon Europe research and innovation programme (Marie Sklodowska-Curie grant agreement Bicyclos N° 101130235), the Spanish Agencia Estatal de Investigación (AEI) and the ERDF (PID2019-111327GB-I00 and PDC2022-133402-I00), by Xunta de Galicia and the ERDF (ED431B 2022/36 and Centro Singular de Investigación de Galicia, 2019-2022, Grant ED431G2019/03). All calculations were carried out at CESGA Supercomputing Center.

Declaration of Generative AI and AI-assisted technologies in the writing process: During the preparation of this work the author(s) used OpenAI's ChatGPT in order to improve the readability and flow of the writing. After using this tool/service, the author(s) reviewed and edited the content as needed and take full responsibility for the content of the publication.

USC
UNIVERSIDADE DE SANTIAGO DE COMPOSTELA

Abstract

Cyclodextrins (CDs) are cyclic oligosaccharides recognized for their ability to form inclusion complexes with diverse guest molecules. Through advanced computational techniques, enhanced by custom protocols designed for CDs' unique attributes, these complex interactions can be modeled *in silico*. Computational methods can help us understand the mechanisms of these widely used encapsulators, including prominent drugs like Bridion™ and Trappsol®. Building on such knowledge of CDs in drug design, CDs are being investigated for atherosclerosis therapy by targeting the toxic oxidized cholesterol, 7-ketocholesterol (7KC).

Removal of 7KC, however, necessitates selective encapsulation of 7KC over essential cholesterol - a tall order, given that the two differ by a mere atom. Initial simulations of CD monomers with 7KC and cholesterol revealed little to no specificity and low affinity. However, upon expanding the method and exploring 1:2 stoichiometries by covalently linking two CD monomers into a dimer, greatly enhanced affinity and marked specificity towards 7KC emerged. The CD dimer, designed for 7KC encapsulation, showed promising results at the qualitative level. However, understanding the differences in encapsulation between 7KC and cholesterol at a quantitative level is fraught with challenges due to the heterogeneity of modified CDs, multiple stoichiometries of CD dimer inclusion complexes, and the inherent solubility issues of sterols. These multifaceted interactions demanded a more sophisticated analytical approach than computational studies alone. By merging the strengths of *in silico* and *in vitro* methods, the intricacies of these interactions were unraveled. Both unbiased molecular dynamics (MD) and metadynamics simulations offered quantitative and qualitative insights into binding constants and mechanisms of particular systems and stoichiometries, while competitive isothermal titration calorimetric (ITC) and circular dichroism (CiDi) measurements provided evidence for the actual distribution of CDs synthesized and tested on the bench.

These findings underscore that covalently linked CD dimers, with certain modifications, exhibit enhanced affinity for 7KC over cholesterol. This extraordinary discernment between molecules as similar as cholesterol and 7KC accentuates CDs' adaptability and potential in tailored applications across disciplines, and particularly places CD dimers as an exciting new therapeutic avenue for combating atherosclerosis. The research presented in this doctoral thesis was conducted within the scope of a project financed by Cyclarity Therapeutics, which aimed to fulfill the company's objectives and contribute to the broader scientific community. The findings disclosed in this dissertation represent the portions of the research that are suitable for public dissemination. The work, supported by Cyclarity Therapeutics, underscores the vast potential of CDs and especially CD dimers to specifically encapsulate a range of molecular targets, marking significant strides in the field of targeted therapy.

Resumo en galego

As ciclodextrinas (CDs), unha ampla familia de moléculas oligosacáridas con forma de anel, destacan pola súa capacidade para encapsular distintas substancias grazas á súa estrutura composta por seis (αCD), sete (βCD) ou oito (γCD) unidades de glicosa. A súa superficie hidrofílica e a cavidade interior hidrofóbica convértenas en formadoras excepcionais de complexos de inclusión solubles na auga con moléculas hóspede de variados tamaños. Poden ser quimicamente modificadas mediante a substitución dos seus hidroxilos por outros grupos funcionais, como metilo, hidroxipropilo (HP) ou sulfobutilo (SB). Estas modificacións resultan en distribucións de estruturas con diferentes números e localizacións das substitucións, o que pode mellorar a solubilidade da CD e alterar as súas propiedades de diversas maneiras.

USC DE SANTIAGO DE COMPOSTELA

O número medio de grupos funcionais presentes na distribución das CDs quimicamente modificadas denomínase grao de substitución/saturación (DS). Estas modificacións tamén poden modular a selectividade para a encapsulación de certas moléculas, así como a súa taxa de liberación, abrindo así unha oportunidade para desenvolver utilidades específicas.

Presentes na nosa vida cotiá moito máis do que poida parecer, as CDs teñen unha ampla gama de aplicacións en varios ámbitos científicos e industriais. Na industria alimentaria, na creación de fragrancias e no desenvolvemento de cosméticos, as CDs contribúen a eliminar sabores e cheiros desagradables, mellorando a bioaccesibilidade e protección dos compoñentes. Son igualmente valiosas na remediación ambiental, onde eliminan eficazmente os contaminantes hidrofóbicos, e na ciencia dos materiais e química analítica, destacando pola súa capacidade de selección quiral e na innovación de novos materiais. No ámbito farmacéutico, as CDs, grazas á súa versatilidade, potencian a solubilidade e estabilidade dos fármacos hidrofóbicos. Ademais, mostran un prometedor potencial como axentes terapéuticos autónomos. Esta tese doutoral, inserida no contexto investigador impulsado por Cyclarity Therapeutics, centra o seu foco no aproveitamento das CDs no tratamento de patoloxías como a aterosclerose, particularmente a través da captura selectiva de metabolitos tóxicos do colesterol (CHOL), destacando o 7-ketocholesterol (7KC). Deste xeito, as CDs reafírmanse non só como elementos cotiáns senón tamén como axentes de progreso terapéutico, revelando así a súa omnipresencia e o seu amplo potencial no desenvolvemento de estratexias de terapia dirixida.

Na investigación das CDs, os estudos computacionais emerxen como unha ferramenta imprescindible para desentrañar as complexas interaccións entre as CDs e as súas moléculas hóspede, proporcionando detalles que resultan difíciles de conseguir mediante experimentación tradicional en laboratorio. A diferenza do que acontece no ámbito do descubrimento de fármacos relacionados con proteínas (onde estas técnicas computacionais aplícanse de maneira rutineira), a investigación centrada nas CDs aínda se apoia considerablemente en métodos de proba e erro. A pesar de que se desenvolveron múltiples estudos computacionais sobre as CDs, este campo aínda non alcanzou o mesmo grao de madurez que a investigación en sistemas proteicos. Dentro das metodoloxías máis utilizadas, o docking molecular destaca pola súa capacidade para ofrecer unha imaxe detallada da afinidade potencial e os patróns de interacción entre as CDs e as moléculas hóspedes. No entanto, o docking presenta certas limitacións, como a súa incapacidade para considerar axeitadamente a flexibilidade das moléculas e o impacto do disolvente no proceso de interacción, o que pode levar a unha representación incompleta ou inexacta do comportamento molecular. Fronte a estas limitacións do docking, a dinámica molecular (MD) proporciona unha visión máis profunda da natureza dinámica dos complexos de inclusión. A través da MD, é posible non só observar o proceso de encapsulación da molécula hóspede, senón tamén avaliar a estabilidade do complexos CD-hóspede e explorar o comportamento das CDs en diferentes contextos disolventes, tendo en conta a súa flexibilidade e as interaccións co medio.

Existe unha necesidade crecente de desenvolver ferramentas computacionais avanzadas e fiables específicas para o estudo das CDs nos procesos de traballo automatizados, particularmente nas plataformas de descubrimento de fármacos. Esta integración é fundamental para mellorar a eficiencia e a precisión na identificación e desenvolvemento de novos compostos terapéuticos, semellante ao que xa se está facendo no estudo das proteínas. A implementación destas tecnoloxías avanzadas nos fluxos de traballo automatizados facilitará a exploración e optimización no deseño e desenvolvemento de novas terapias baseadas en CDs, aproveitando ao máximo as oportunidades nesta área de investigación. No entanto, para

USC
UNIVERSIDADE
DE SANTIAGO
DE COMPOSTELA

lograr este avance, enfróntanse varios desafíos. Primeiramente, é esencial representar con precisión a flexibilidade das CDs, o que implica unha coidadosa selección dos campos de forzas para captar as complexas interaccións moleculares. Ademais, a validación experimental cobra unha importancia crucial para asegurar a fiabilidade dos modelos computacionais. Establecer unha forte correlación entre os resultados teóricos e os experimentais é chave para garantir que as simulacións computacionais reflictan fielmente a realidade molecular. Este paso é vital para fortalecer a validez e a aplicabilidade práctica das investigacións sobre as CDs, especialmente cando se pretende a súa integración en sistemas automatizados de descubrimento de fármacos.

Esta tese doutoral, fundamentada en métodos computacionais avanzados e ensaios de laboratorio, ten como obxetivo desentrañar o modo en que as CDs forman complexos de inclusión cos seus hóspedes e analizar as repercusións destas interaccións no desenvolvemento e na descuberta de fármacos. Os estudos desenvolvidos aquí exploran tres facetas distintas das interaccións das CDs con moléculas hóspede de especial interese, achegando de maneira conxunta á comprensión do amplo panorama do recoñecemento molecular e a encapsulación. Estas investigacións son a pedra angular dunha plataforma computacional exhaustiva que, en última instancia, permitirá a predición automática de pares CD-hóspede ideais, xerando novos candidatos para o emprego das CDs en diversos ámbitos, incluíndo o desenvolvemento farmacéutico. A hipótese central destes traballos sostén que un coñecemento profundo sobre a natureza complexa das interaccións das CDs con variadas moléculas hóspedes permitirá a creación de sistemas moleculares a medida para diversas aplicacións. Esta hipótese xeral establece varios obxectivos específicos, cada un deles abordado individualmente en tres estudos diferenciados:

1. Sugammadex e a Reversión do Bloqueo Neuromuscular utilizados en anestesia:

O primeiro estudo céntrase no sugammadex, un medicamento baseado en CDs e comercializado como Bridion™, aprobado para a reversión do bloqueo neuromuscular en adultos sometidos a ciruxía. O sugammadex forma un complexo de inclusión co axente bloqueador neuromuscular (NMBA) rocuronium, permitindo unha rápida reversión da parálise muscular. Neste caso, o complexo sugammadex-rocuronium é tomado como un modelo ideal para validar varios métodos computacionais propostos para caracterizar a interacción entre CDs e moléculas hóspede. Este sistema foi escollido debido ao interese clínico de Bridion™ e á subseguinte dispoñibilidade de información experimental precisa sobre a interacción de ambas as moléculas. Ademais, é de destacar a singularidade deste sistema no que respecta ao patrón de substitución (DS) do sugammadex, xa que non está suxeito á variabilidade presente noutras CDs modificadas, onde se atopan distintos isómeros con diferentes grupos modificados. No caso do sugammadex, todos os grupos hidroxilo na posición O6 están substituídos polo grupo carboxil tioéter. O obxetivo do primeiro estudio é proporcionar información detallada sobre este sistema e empregalo como un modelo para validación.

A aproximación computacional multifacética aplicada abarca docking, dinámica molecular non dirixida e simulacións de metadinámica, cada método ofrecendo visións únicas sobre a estrutura, mecanismo de interacción, dinámica, cinética e tamén sobre os perfís enerxéticos correspondentes á formación do complexo de inclusión. Os estudos de docking ofreceron resultados altamente consistentes, mostrando o rocuronium principalmente no interior da cavidade da CD, o que subliña a forza da súa interacción co sugammadex. De maneira notable, as simulacións revelaron que o rocuronium mostra unha preferencia marcada pola orientación que coincide coa evidencia empírica proporcionada por estudos cristalográficos,

USC UNIVERSIDADE DE SANTIAGO DE COMPOSTELA

onde a carga positiva do rocuronium está orientada cara as sustitucións negativas do sugammadex na formación do complexo. É interesante sinalar que tamén se identificou unha preferencia menos pronunciada pola orientación contraria á que se podería supor con base en interaccións electrostáticas, o que suxire que ambas as orientacións poden existir en solución. As simulacións de MD non dirixida reforzaron as conclusións obtidas nos estudos de docking, proporcionando información máis detallada. A interacción duradeira entre o sugammadex e o rocuronium ao longo das traxectorias sinala unha interacción estable e específica. A maioría das simulacións e os valores enerxéticos obtidos para a interacción entre a CD e o hóspede corroboraron a orientación predominante onde a carga positiva do rocuronium interacciona coas sustitucións aniónicas do sugammadex. A consistencia entre os resultados computacionais e a estrutura cristalina real é un indicador da fiabilidade do protocolo computacional empregado.

É importante ter en conta que os valores de enerxía de enlace derivados do docking ou da MD non dirixida non son directamente comparables cos obtidos por métodos experimentais. A metadinámica, unha ferramenta poderosa para explorar o panorama de enerxía libre, foi aplicada para proporcionar un perfil completo do PMF (potencial de forza media) da interacción sugammadex-rocuronium, que pode ser directamente comparado cos experimentos. Este método rigoroso proporciona información mecanística e estrutural vinculando a cinética da interacción coas barreiras enerxéticas ao longo das rutas consideradas, tal como ven definido polas variables colectivas (CV). Os cálculos de metadinámica/PMF xeraron resultados en liña cos valores obtidos experimentalmente, reforzando a confianza nos métodos desenvolvidos. Ademais da precisa predición da constante de asociación das simulacións de metadinámica, comparable á experimental, a estrutura excelente obtida das simulacións de metadinámica tamén coincide moi ben coa obtida a partir da estrutura cristalina de raios X.

A visión conxunta obtida deste primeiro estudo computacional proporcionou unha comprensión completa da interacción sugammadex-rocuronium. Máis aló das ideas específicas sobre este complexo particular, o potencial dos métodos explorados para prever o comportamento de complexos de CDs foi validada neste estudo. É importante resaltar que, desde unha perspectiva computacional, as simulacións de MD e docking molecular demostráronse como métodos eficientes e atinxíbeis en canto a custo computacional para o estudo destes sistemas, especialmente en comparación coa complexidade doutras biomoléculas como as proteínas. Este estudo mostra que é posible elucidar rapidamente as características dos complexos de inclusión de CDs utilizando estas técnicas. Ademais, este estudo validou os resultados obtidos mediante comparación directa con propiedades experimentais, asegurando así a súa relevancia e precisión. Por outra banda, a metadinámica, aínda que computacionalmente máis custosa, destaca como unha ferramenta poderosa para prever constantes de afinidade realistas de CDs coñecidas e novas antes da súa síntese co obxectivo de descubrimento de fármacos e deseño molecular. Esta capacidade pode acelerar significativamente o proceso de identificación e desenvolvemento de novos candidatos terapéuticos, reducindo tanto o tempo como os custos asociados á síntese e proba experimental.

2. β-CDs e Complexos de Inclusión con Esteroides:

Neste segundo estudo, adaptamos e probamos diversos enfoques baseados en simulacións de metadinámica para simular e avaliar complexos de inclusión baseados en CDs. O obxectivo é aprofundar na enerxía de unión, na dinámica estrutural e nas preferencias de interacción, establecendo as bases para o desenvolvemento de sistemas moleculares personalizados. Para probar estes métodos, empregáronse sistemas βCD-esteroides 1:1. O colesterol (CHOL) e a súa forma oxidada 7-ketocholesterol (7KC) foron

USC UNIVERSIDADE DE SANTIAGO DE COMPOSTELA

usados como ligandos para estruturas de βCD con diferentes tipos, número e localización de substitucións. A diferenza entre o 7KC nativo CHOL é pequena: só un átomo adicional no 7KC, un átomo de oxíxeno formando un grupo cetona na posición 7. Esta diferenza, por pequena que sexa, é aparentemente clave para o desenvolvemento de moitas enfermidades como a aterosclerose e o Alzheimer. Por iso, ao contrario do colesterol, que é esencial para varios roles fisiolóxicos, incluíndo a composición da membrana celular e as funcións precursoras de hormonas, o 7KC ten efectos desastrosos en organismos vivos. Esta é a principal razón para buscar métodos para extraer selectivamente o 7KC das células sen afectar significativamente a concentración de CHOL. A encapsulación do esteroide oxidado por CDs foi proposta para este fin. Nesta estratexia, a especificidade para a encapsulación do 7KC sobre o CHOL é crucial.

Así, neste estudo, empregamos cálculos PMF obtidos de simulacións de metadinámica para caracterizar os complexos de inclusión 1:1 entre catro βCDs modificadas diferentes, con diferentes tipos, número e localización de substitucións, e dúas moléculas esteroides (CHOL e 7KC). Os métodos desenvolvidos, validados para a reproducibilidade a través de catro simulacións independentes repetidas por sistema e diferentes técnicas de procesamento posterior, ofrecen información nova sobre a formación e estabilidade dos complexos de inclusión CD-esteroides. Os resultados mostran unha preferencia sistemática por unha orientación na que a cauda do esteroide proxéctase desde a cara máis grande da CD, así como impactos significativos das substitucións do CD na formación dos complexos. De maneira notable, o mostraxe só da cara ampla do CD durante as simulacións produciu enerxías de unión comparables ás da mostraxe completa, pero en menos tempo e con menor incerteza estadística, o que suxire un enfoque máis eficiente.

O exame detallado dos sistemas βCD-esteroides 1:1 con CHOL e 7KC serve como un modelo preliminar para un obxectivo máis amplo, que é desenvolver métodos computacionais precisos e eficientes que poidan ser implementados nun fluxo de traballo automatizado para producir constantes de afinidade para miles de complexos de inclusión. Ademais dos novos detalles que as simulacións desenvolvidas proporcionan sobre as interaccións específicas entre diferentes CDs e as dúas moléculas esteroides estudadas, este estudio propón un protocolo que podería empregarse en cálculos masivos de PMF de sistemas CD-ligando. Este protocolo baséase en simulacións de metadinámica que só requiren o mostraxe nunha dimensión (o desprazamento do ligando ao longo do eixo de simetría do CD) na dirección da cara ampla da cavidade da CD cunhas restricións (a orientación relativa do ligando respecto do CD e a distancia do ligando ao eixo de simetría do CD). Os valores de ΔG^0 e constante de asociación obtidos destes cálculos foron altamente reproducibles e permitíron aforrar recursos computacionais significativos en comparación con outros métodos. Estes resultados abren as portas ao futuro adestramento de algoritmos de aprendizaxe automática para deseñar CDs modificadas excelentes para fins específicos.

3. Dímeros de CDs e Tratamento da Aterosclerose:

O terceiro estudo abre un novo camiño ao investigar o potencial dos dímeros de CDs como tratamento innovador para a aterosclerose. Este estudo fai parte dun proxecto máis amplo destinado a deseñar CDs modificados capaces de encapsular biomoléculas tóxicas con alta afinidade e especificidade. Recentemente, Cyclarity Therapeutics deseñou dímeros de CD como APIs (Active Pharmaceutical Ingredients) innovadoras para o tratamento da aterosclerose, unha das principais causas das enfermidades cardiovasculares. Os tratamentos actuais para a aterosclerose céntrase principalmente en xestionar os factores de risco e aliviar os síntomas, pero proponse que os dímeros de CD poden reverter eficazmente a formación de placas arteriais encapsulando de forma específica os oxisterois ateroscleróticos e citotóxicos.

USC UNIVERSIDADE DE SANTIAGO DE COMPOSTELA

Neste caso, o reto radica en encapsular selectivamente o citotóxico 7KC sobre o CHOL. Esta investigación centra a atención nos dímeros de CD, xa que presentan varias vantaxes sobre os monómeros, incluíndo a súa maior afinidade para encapsular moléculas de esterol e unha maior densidade de grupos funcionais que poden ser substituídos dentro dunha única molécula, facilitando a potencialidade da especificidade da estrutura modificada. Ademais, o ligador químico que conecta os dous monómeros de CD pode ser adaptado para optimizar o recoñecemento e encapsulación de ligandos particulares.

A caracterización das interaccións entre os dímeros de CD e os oxisterois presenta desafíos formidables debido á baixa solubilidade dos esteróis, á síntese de CDs modificadas que resultan nunha mestura de numerosas especies con diferentes números e ubicacións de grupos modificados, e á diversidade dos mecanismos de interacción. Para abordar estes desafíos e iluminar os matices das interaccións CD-esterol, utilizamos varios enfoques ortogonais para unha caracterización exhaustiva. Neste estudo presentamos resultados obtidos de tres técnicas independentes: simulacións de metadinámica, calorimetría isotérmica de titulación competitiva e dicroísmo circular, para cuantificar a interacción CD-esterol. Cada un destes métodos requireu unha optimización significativa para estes tipos de sistemas anfitrión-hóspede. Os resultados obtidos ofrecen ideas cooperativas sobre a interacción entre o dímero de CD e as moléculas de esterol, incluíndo perfís de enerxía, estruturas optimizadas para os complexos supramoleculares e estimacións independentes cuantitativas das afinidades de enlace correspondentes. O obxectivo deste estudo é obter as constantes de afinidade así como información estructural e dinámica do sistema, tendo en conta as vantaxes e limitacións de cada método.

Os resultados suxeriron que a complexidade dos complexos de inclusión dímero de CD-esterol require a integración de múltiples métodos no canto de confiar nunha única aproximación. Factores como a flexibilidade, variacións na solubilidade, diversas substitucións e múltiples estequiometrías contribúen a esta complexidade, e a aproximación multimétodo empregada ilumina o comportamento do dímero de CD-esterol de maneira máis exhaustiva que unha aproximación individual. Estas técnicas ortogonais estiman de forma independente os valores de K_A e ΔG^0, mostrando a encapsulación selectiva de 7KC polo dímero de CD. Esta aproximación destaca como unha análise multidimensional que profunda na comprensión da formación do complexo de inclusión CD-esterol, tanto cualitativa como cuantitativamente. Os resultados combinados destes experimentos demostraron que o dímero de CD ten unha afinidade aproximadamente 1000 veces maior por 7KC que por CHOL. As constantes de afinidade obtidas dos métodos *in vitro* encaixan ben cos obtidos das simulacións de metadinámica, e son comparables ou mesmo superiores a outros valores reportados na bibliografía para sistemas similares de complexos de esteroides con dímeros de CD. Aínda que algunhas propiedades do complexo de inclusión seguen sendo difíciles de caracterizar, os métodos combinados demostran a capacidade dos dímeros de CD para diferenciar cuantitativamente entre moléculas hóspede moi similares.

Este último estudo subliña os desafíos para obter constantes de afinidade realistas para sistemas complexos, así como as vantaxes e desvantaxes de tres métodos diferentes. Aquí, desenvolvéronse protocolos específicos para optimizar a caracterización destes sistemas, realizando un estudo ortogonal baseado en tres métodos diferentes para obter información complementaria. En particular, o poder de iterar entre múltiples simulacións de isómeros individuais e datos empíricos *in vitro* de mesturas non isoméricas de moléculas anfitrións non debe subestimarse. Aínda que os datos computacionais sempre necesitan ser validados con datos experimentais, as simulacións permiten predicións, enriquecen a interpretación de experimentos empíricos e respostan as preguntas que non se poden facer en experimentos reais. A combinación das

USC UNIVERSIDADE DE SANTIAGO DE COMPOSTELA

técnicas experimentais e as computacionais axuda a explicar a verdadeira natureza do complexo mellor que calquera por si sóa. Este estudo espera servir como un referente na caracterización doutros sistemas igualmente complexos. Por outra banda, a notable capacidade destes dímeros de CD para discriminar entre moléculas tan similares como CHOL e 7KC, tanto cualitativa como cuantitativamente, destaca o potencial para aproveitar os CDs na encapsulación específica de pequenas moléculas particulares para diversas aplicacións.

O traballo exposto nestes tres estudos independentes, publicados cada un nas súas respectivas revistas, aspira a converterse nun referente na caracterización de sistemas complexos de inclusión con CDs. Empregáronse diversas ferramentas computacionais, integradas nun fluído fluxo de traballo, para avaliar un amplo espectro de complexos de inclusión de CD, tanto en forma de monómeros como de dímeros. Resalta a importancia de combinar técnicas computacionais e experimentais de laboratorio para desvelar as complexidades das interaccións moleculares. Este estudo demostra a capacidade dos métodos desenvolvidos para replicar con éxito características de sistemas xa coñecidos, como o sugammadex-rocuronio. Ademais, procurouse validar o método do PMF en varios sistemas de monómeros de CD, incluíndo complexos entre monómeros de βCD e esteroides. O último estudo centrouse na cuantificación computacional da especificidade da unión de do 7KC fronte ao CHOL polos novos dímeros de CD desenvolvidos por Cyclarity Therapeutics, conducindo á síntese de novos dímeros de CD para o tratamento da aterosclerose. Estes dímeros demostran un gran potencial como ferramentas polivalentes para a encapsulación selectiva de biomoléculas específicas, destacando a súa capacidade de diferenciar entre moléculas estruturalmente semellantes, como o colesterol e 7KC, o que ten implicacións significativas no tratamento de enfermidades e na comprensión dos mecanismos das enfermidades complexas relacionadas con 7KC. En Cyclarity Therapeutics, o obxectivo principal destes estudos foi desenvolver, avaliar e validar unha tecnoloxía de plataforma para a análise *in silico* de complexos de inclusión de CD. As simulacións e análises desenvolvidas nesta tese doutoral están agora eficazmente automatizadas e almacenadas nunha base de datos privada, que contén miles de simulacións de CDs. O propósito desta base de datos é empregar algoritmos de intelixencia artificial (IA) e aprendizaxe automática (ML) para profundar na comprensión do complexo de inclusión de CD e as súas múltiples facetas, así como para propor novas estruturas de CD para usos específicos.

A investigación presentada nesta tese de doutoramento foi realizada no marco dun proxecto financiado por Cyclarity Therapeutics, que tiña como obxectivo cumprir cos obxectivos da empresa e contribuír á comunidade científica máis ampla. Os achados revelados nesta disertación representan as partes da investigación que son axeitadas para a súa difusión pública. O traballo, apoiado por Cyclarity Therapeutics, subliña o enorme potencial dos dímeros de CD para encapsular especificamente unha gama de obxectivos moleculares, marcando avances significativos no campo da terapia dirixida..A través desta tese doutoral, demostrouse non só a eficacia dos métodos computacionais no estudo das CDs, senón tamén a súa relevancia práctica para o deseño e desenvolvemento de novas aplicacións. As posibilidades que se abren grazas á unión destas dúas áreas son amplas e prometedoras, abrindo camiños para futuras investigacións que poderían revolucionar o campo da bioloxía molecular e a farmacoloxía. A capacidade de simular e prever interaccións moleculares complexas con precisión *in silico* pode acelerar significativamente o proceso de investigación e desenvolvemento, reducindo os custos e o tempo necesario para alcanzar resultados prometedores. Ademais, esta aproximación ofrece unha ferramenta valiosa para a comprensión profunda de mecanismos biolóxicos e patolóxicos, o que pode traducirse en avances terapéuticos significativos.

USC
UNIVERSIDADE DE SANTIAGO DE COMPOSTELA

Abbreviations

2-hydroxypropyl (HP)
7-ketocholesterol (7KC)
Active pharmaceutical ingredient (API)
Artificial intelligence (AI)
Automated topology builder (ATB)
Center of mass (COM)
Cholesterol (CHOL)
Circular dichroism (CiDi)
Collective variable (CV)
Configuration interaction (CI)
Coupled cluster theory (CC)
Cyclodextrin (CD)
Degree of substitution/saturation (DS)
Density functional theory (DFT)
Dimethyl sulfoxide (DMSO)
Double inclusion complex (DIC)
Ethanol (EtOH)
Glucopyranoside unit (GPU)
Hartree-Fock (HF)
Hydroxyl (OH)
Hydroxypropyl (HP)
Hydroxypropyl-β-cyclodextrin (HPβCD)
Isothermal titration calorimetry (ITC)
Machine learning (ML)
Molecular dynamics (MD)
Molecular mechanics (MM)
Neuromuscular block (NMB)
Neuromuscular blocking agent (NMBA)
Nuclear magnetic resonance (NMR)
Per- and poly-fluoroalkyl substances (PFAS)
Potential of mean force (PMF)
Quantum mechanics (QM)
Randomly methylated βCD (RAMEB)
Simple point charge (SPC)
Singular value decomposition (SVD)
Steered molecular dynamics (SMD)
Sulfobutyl (SB, SBE)
Quantitative structure activity relationship (QSAR)
Weighted histogram analysis method (WHAM)

USC
UNIVERSIDADE DE SANTIAGO DE COMPOSTELA

Chapter 1. Introduction

USC
UNIVERSIDADE
DE SANTIAGO
DE COMPOSTELA

1.1. Cyclodextrins: Versatile Molecules with Exceptional Applications

Cyclodextrins (CDs) are a family of versatile molecules that have numerous applications across various scientific and industrial domains. These unique, ring-shaped oligosaccharides are generally composed of six (αCD), seven (βCD), or eight (γCD) glucose units bound together in a cyclic structure by α-(1,4)-glycosidic linkages (Garrido et al., 2020; Kurkov & Loftsson, 2013; Szejtli, 1998) (Fig. 1). Their shape allows them to encapsulate and sequester a wide variety of guest molecules, making them extremely useful. CDs have a hydrophilic exterior and a hydrophobic interior cavity, and the size of the CD determines the size of the guest molecules that can be encapsulated in a water-soluble inclusion complex (Fig. 1C, 2). The characteristics of the inclusion complex can be further modified by adding chemical groups (e. g., hydroxypropyl (HP) groups) to the hydroxyl (OH) units of the CDs - up to 3 per glucose unit (Kurkov & Loftsson, 2013; Szejtli, 1998). This distinctive, modifiable structure has led to a plethora of seemingly unrelated uses for CDs, spanning from pharmaceuticals to food science and beyond (Crini et al., 2018; É. Fenyvesi et al., 2016; Loftsson & Duchene, 2007).

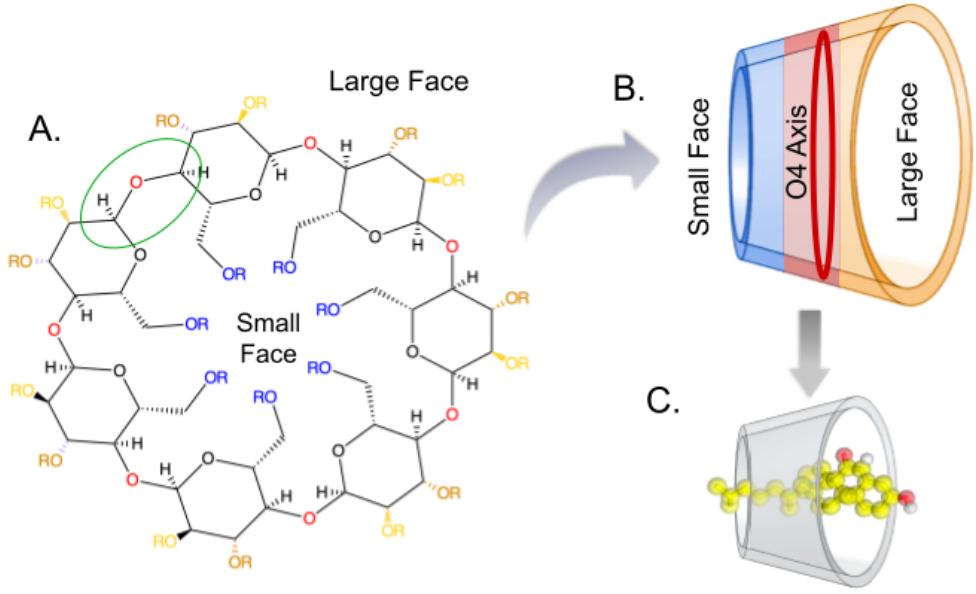


Figure 1. Anatomy of a CD. βCD is used as an example. (A) Chemical structure of βCD where R groups denote locations where a chemical modification group can be added. O4 atoms shown in red, O6 (small face) in blue, O2 in light orange, O3 in dark orange (large face). One α-(1,4)-glycosidic linkage is circled in green. (B) Rotated, simplified cone representation. Again, the small face is blue, the large face is orange, and the O4 axis is red. (C) Example of a 1:1 inclusion complex where a guest molecule (yellow) is encapsulated in the CD (gray).

CDs are primarily derived from the enzymatic degradation of starch by cyclodextrin glycosyltransferases (CGTases). It was French scientist Villiers in 1891 who observed the crystallization of a peculiar substance when a certain bacteria, *Bacillus amylobacter*, interacted with starch (Villiers, 1891). In the early 20th century, Schardinger identified these compounds more comprehensively and described α, β, and γ CDs, differing in the number of glucose units, and gave them a name: "Schardinger dextrins" (French, 1957), which was later changed to cyclodextrins for improved clarity. Following these foundational studies, the mid-20th century saw a rise in the interest surrounding CDs and in particular understanding their inclusion

USC UNIVERSIDADE DE SANTIAGO DE COMPOSTELA

complexation behavior, and by the 1980s, CDs were an integral part of several industries. Today, CDs are particularly useful in pharmaceutical formulation, where they are used as excipients for therapeutic agents (Kurkov & Loftsson, 2013; Loftsson & Duchene, 2007; Szejtli, 1998). Interest has also been sparked in using CDs as therapeutic agents themselves (Anderson et al., 2021; *Safety and Efficacy of Intravenous Trappsol Cyclo (HPBCD) in Niemann-Pick Type C Patients from ClinicalTrials.Gov*, 2019).

When a guest molecule fits snugly into the CD's central cavity, it results in the formation of a stable, water soluble, non-covalent inclusion complex (Fig. 1C, 2). Encapsulating compounds within CDs can improve their solubility, stability, and bioavailability, while also offering controlled release, taste masking, and environmental remediation capabilities. It is important to consider that CD inclusion complexes do not always adapt a 1:1 stoichiometry of CD to a guest molecule, which adds a layer of complexity to their study. The stoichiometry of CD complexes usually depends on the size and compatibility of the guest molecule with the CD cavity; while CDs commonly form 1:1 complexes with guest molecules, other stoichiometries such as 2:1 or 1:2 have been reported depending on the size and characteristics of the guest molecules (Loftsson et al., 2019; Messner et al., 2010; Piñeiro et al., 2021). Notably, the βCD-cholesterol complex has been shown to be a 1:2 ($cholesterol_1$:CD_2) complex in both crystal structure (Christoforides et al., 2018) and NMR (Kučáková & Dolenský, 2020) studies. Apart from forming inclusion complexes, CDs can also self-aggregate or induce the aggregation of guest molecules, leading to the formation of binary, ternary, or even more extensive molecular assemblies in solution. Aggregation can be influenced by several factors, such as the concentration of CDs, temperature, pH, and the presence of other substances; CD-induced aggregation of guest molecules can result in the formation of nanoparticles, micelles, or other supramolecular structures (Fig. 2) (Jansook et al., 2010; Loftsson & Duchene, 2007; Messner et al., 2010; Piñeiro et al., 2007; Szejtli, 1998; Yang et al., 2017).

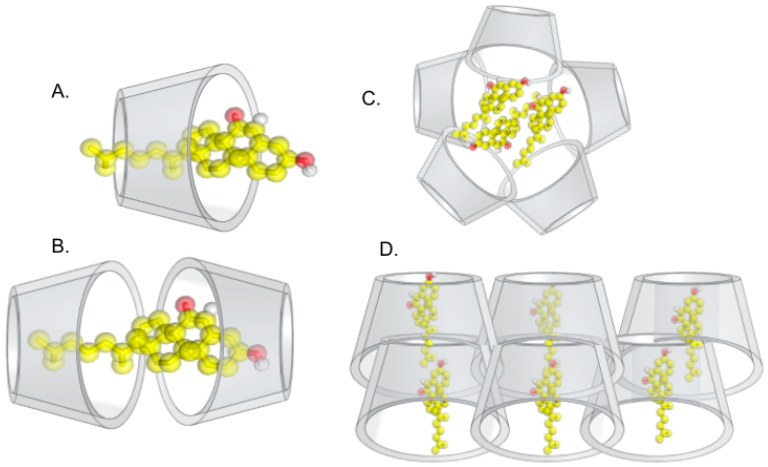


Figure 2. Description of several different CD-target interaction mechanisms. (A) 1:1 inclusion complex. (B) 1:2 inclusion complex. (C) Aggregation. (D) Self - Assembly of many 1:1 inclusion complexes.

1.1.1. Applications of Cyclodextrins

CDs, with their unique molecular structure and ability to form inclusion complexes, have found a multitude of applications across various fields. The diverse uses of CDs are seemingly endless, underscoring the importance of CDs in modern scientific and industrial applications. The following section aims to highlight

USC
DE SANTIAGO
DE COMPOSTELA

how their distinct properties enable them to function in different contexts – from enhancing molecular stability to innovative environmental solutions and advanced material design.

Drug Delivery: CDs have gained prominence in drug delivery by encapsulating hydrophobic drugs, which augments their solubility, stability, and bioavailability. This encapsulation facilitates a controlled drug release, accentuating therapeutic efficacy and attenuating side effects (Arima et al., 2017; Garrido et al., 2020; Irie & Uekama, 1997; Loftsson & Duchene, 2007). HPβCD is one particularly safe CD derivative, and it is used to improve the water solubility of many compounds, including poorly soluble drugs. The inclusion complex with HPβCD allows for intravenous administration of drugs which would be challenging or impossible otherwise (Pahuja et al., 2014). For example, paclitaxel is a chemotherapy drug with poor solubility - formulations using HPβCD can make it easier to administer in clinical settings and may even help with drug resistance issues (Shen et al., 2020). CD-based formulations were also employed to improve the solubility of Remdesivir, an antiviral for the treatment of COVID-19 (Almeida et al., 2023). In fact, the commercial formulation of Remdesivir is actually ~96% CD (solid, by weight) (Ramsey et al., 2022).

Food, Fragrance, and Cosmetics: The utility of CDs in food, fragrance, and cosmetics industries includes important functions like removing unpalatable tastes or smells, improving bioavailability of compounds, and stabilization. CDs can encapsulate volatile molecules, which are generally strong in taste and smell, optimizing the release of flavors, fragrances, or active ingredients. The inclusion of these molecules within the CD cavity can also offer protection against degradation due to light, oxygen, or other external factors, which improves quality and appeal of these products (Archambault et al., 2004; Astray et al., 2020; Buschmann & Schollmeyer, 2002; É. Fenyvesi et al., 2016; Hedges et al., 1995; Holland et al., 2000). Moreover, many essential nutrients and flavors are not water-soluble, making them difficult to incorporate into many products; CDs can enhance the solubility of these compounds, making them more bioavailable (Szente & Szejtli, 2004). CDs can also encapsulate and neutralize undesirable flavors or odors, which is especially beneficial in products like fish oil capsules, where CDs can mask the strong fishy taste (E. Fenyvesi & Szente, 2016; Marques, 2010; Szente et al., 2021). One of the most known applications of CDs in consumer products is in Procter & Gamble's Febreze® - this mechanism of encapsulating bad odors is different from many other deodorizers which may simply mask or overlay unwanted smells with a more pleasant scent (Williams et al., 2016). In cosmetics, hydrophobic compounds are often employed for their beneficial effects on skin or hair, and can be solubilized using CDs, enhancing their delivery and efficacy (Buschmann & Schollmeyer, 2002).

Environmental Remediation: CDs offer innovative solutions to some of the longstanding challenges in pollution control. CDs can encapsulate hydrophobic contaminants, making them particularly suited for the removal of pollutants from both water and soil (É. Fenyvesi, 2011). Their inclusion complex formation aids in the immobilization and subsequent removal of various environmental toxins, including heavy metals and organic pollutants (Barbosa et al., 2019; É. Fenyvesi, 2011; *Final Progress Reports*, 2018; Landy et al., 2012; Yadav et al., 2022). The environmentally friendly nature of CDs, coupled with their effective pollutant-capture capability, has driven researchers and environmentalists to explore them further for large-scale applications. CDs are increasingly being incorporated in filtration systems, ground-water treatment, and soil-washing processes, underscoring their potential in contributing to a cleaner and more sustainable environment (Landy et al., 2012). As an example, CDs demonstrate high selectivity and efficiency in capturing and immobilizing emerging environmental contaminants such as per- and polyfluoroalkyl substances (PFAS) because the CD cavity is well-suited for trapping and sequestering PFAS in water

USC UNIVERSIDADE DE SANTIAGO DE COMPOSTELA

(Halford, 2019; W. Wang et al., 2021). Moreover, in conjunction with other adsorbent materials or techniques, CDs can form hybrid systems, enhancing the overall filter efficiency. CDs have been studied for the removal of various contaminants, such as pesticides, pharmaceuticals, and endocrine disruptors, with promising outcomes (Crini et al., 2018).

Analytical Chemistry and Materials Science: In chromatography and capillary electrophoresis, CDs have been utilized as chiral selectors to distinguish between enantiomers, thereby facilitating the separation and analysis of complex mixtures. Their ability to selectively interact with specific analytes has significantly improved detection and quantification in these analytical methods (S. Li & Purdy, 2002; Szente & Szemán, 2013). In materials science, CD-based materials including nanoparticles, nanofibers, and hydrogels, have been synthesized for a myriad of applications. CDs can be grafted onto polymers to create materials with enhanced solubilization properties (Badruddoza et al., 2013; Prabaharan & Mano, 2006) or form nanoparticles that can be used in disease therapy (Guo et al., 2019). and CD membranes can be used for controlled release of active agents or for selective filtration processes (Topuz et al., 2021). CDs have even found applications in organic electronics, where they can improve the solubility and processability of organic semiconductors (Crini et al., 2018; Feng et al., 2005; Hata et al., 2020; Prochowicz et al., 2017). They can also be incorporated into sensor systems, enhancing their specificity and sensitivity towards certain analytes (de Jong et al., 2000; Ogoshi & Harada, 2008).

Active Pharmaceutical Ingredient: Recent strides have spotlighted CDs as potential pharmaceutical agents themselves, not just formulation superheroes. Sugammadex, marketed as Bridion™, is a CD derivative used to reverse neuromuscular blocks post-surgery. This allows patients to come out of anesthesia more easily by directly binding and sequestering the neuromuscular blocking agent, rocuronium, and has been hailed by anesthesiologists since its approval in 2015 (Ezri et al., 2016). Today, clinical explorations are underway to employ CDs, specifically HPβCD, in treating Niemann Pick Type C, a debilitating disease of cholesterol metabolism (*Safety and Efficacy of Intravenous Trappsol Cyclo (HPBCD) in Niemann-Pick Type C Patients from ClinicalTrials.Gov*, 2019), and prospective trials for atherosclerosis are on the horizon (Anderson et al., 2021).

1.1.2. Selective Sequestration of Toxic Oxidized Cholesterols for Atherosclerosis Treatment

CDs have shown promise in selectively encapsulating cholesterol and its oxidized derivatives, particularly 7-ketocholesterol (7KC), a toxic compound implicated in various health issues (Fig. 3). 7KC is an oxidized form of cholesterol formed during oxidative stress and aging processes; it is considered a pro-inflammatory and cytotoxic compound, and is implicated in many diseases including atherosclerosis and neurodegenerative disorders (Anderson et al., 2020). Because some derivatives of CDs have been shown to have specificity for 7KC over cholesterol (Kritharides et al., 1996), interest has been growing around using CDs to selectively encapsulate 7KC over cholesterol (Anderson et al., 2021, 2024). Ensuring this selectivity for 7KC over cholesterol is crucial to ensure important biological processes involving cholesterol are not perturbed, but the structures of these two molecules differ by only a single atom (Fig. 3). Computational study of this system offers invaluable insights into the interactions at play in the CD/cholesterol inclusion complex vs. the CD/7KC complex, so that the interaction can be optimized to favor 7KC over cholesterol. If this CD dimer is to be a successful drug, a validated and in-depth understanding of its interaction mechanisms with both 7KC and cholesterol will be necessary. Computational methods are, in many ways, ideal for studying such an intricate system. The next sections will focus on unraveling and addressing these

USC UNIVERSIDADE DE SANTIAGO DE COMPOSTELA

intricacies. Rigorous validation and stepwise advancements were necessary to tailor the computational and *in vitro* methods for CD dimer-sterol inclusion complexes, but the results of these efforts will contribute to the first yet atherosclerosis drug specifically addressing oxidized cholesterol accumulation.

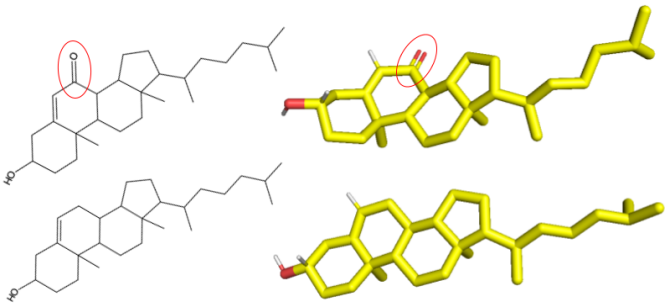


Figure 3. 2D (left) and 3D (right) structures of 7KC (top) and cholesterol (bottom). The 7-keto group in 7KC is circled in red.

1.1.3. Cyclodextrin Summary

From revolutionizing drug delivery systems and stabilizing pharmaceuticals to enhancing food products and contributing to environmental remediation, it is clear that CDs are remarkably versatile and have a far-reaching impact. Their ability to form inclusion complexes is a key feature that has been effectively utilized across different sectors. This overview not only highlights the current uses of CDs, but also suggests their potential for continued innovation and application in new areas. As we look to the future, the diverse applications of CDs are likely to expand and evolve, maintaining their relevance in both scientific research and practical applications.

1.2. Computational Modeling of Molecules and Molecular Interactions

Computational modeling of molecules is a large and ever-growing area of research that encompasses a range of techniques and methods to understand, predict, and simulate molecular and atomic level phenomena. These techniques range from foundational quantum mechanics (QM) methods to long-range molecular mechanics (MM) simulations that can capture protein-ligand interactions.

The Schrödinger equation serves as the cornerstone of QM, governing the time evolution of the wave function concerning the system's Hamiltonian operator, which represents its total energy. QM methods are able to capture electron interactions and provide a detailed, fundamental understanding of molecular behavior. These methods include Hartree-Fock (HF) (Hartree, 1928; Slater, 1951; Szabo & Ostlund, 1996) and density functional theory (DFT) (Kohn et al., 1996) and are widely used in quantum chemistry, but they are often far too computationally expensive to use for larger molecules. HF approximates electron-electron interactions by averaging the effect of all electrons on any given one, employing a self-consistent field approach and iteratively fine-tuning the wave function to minimize energy (Hartree, 1928). DFT on the other hand, focuses on electron density rather than wave functions, and postulates that the ground state energy is a functional of this density, simplifying calculations (Kohn et al., 1996).

The accuracy of QM methods is closely tied to the choice of computational level and basis set, with higher accuracy often necessitating increased computational resources. Other post-Hartree-Fock methods can

USC UNIVERSIDADE DE SANTIAGO DE COMPOSTELA

provide precise results, but still require substantial computational investments. These methods include coupled cluster theory (CC) (Bartlett & Musiał, 2007; Shavitt & Bartlett, 2009; Szabo & Ostlund, 1996) and configuration interaction (CI) (Bartlett & Purvis, 1978; Szabo & Ostlund, 1996), where the accuracy is improved by considering electron correlation and excitation to higher energy orbitals. A plethora of software packages, including Gaussian (Frisch et al., 2016), NWChem (Aprà et al., 2020), and Quantum Espresso (Giannozzi et al., 2009) facilitate QM calculations, and these simulations often demand high-performance computing resources.

In contrast, MM methods provide a classical description of molecular systems and are often used for larger molecules like proteins. Instead of solving the Schrödinger equation for electron distributions, MM uses classical physics to describe molecular motions and interactions; it does not explicitly consider the electronic structure of atoms. The main assumption is that molecules behave like interconnected balls (atoms) and springs (bonds), following Newtonian laws; the energy of a system is calculated as a sum of different potential energy functions. These potential energy functions are based on empirical parameters derived from experimental data or high-level QM calculations, and are assembled into "force fields" that can be applied to simulations. These parameters include values for bond stretching, angle bending, torsional rotations, and non-bonded interactions like van der Waals forces and electrostatic interactions (Arsiccio et al., 2021; Jorgensen & Tirado-Rives, 1988; Mackerell Jr., 2004; Ott & Meyer, 1996; Vanommeslaeghe et al., 2010; J. Wang et al., 2004). The accuracy of these MM simulations, therefore, depends heavily on the applicability of the chosen force field to the system in question, and extrapolating beyond the range of the training data can lead to misleading results. Additionally, MM methods cannot observe quantum phenomena such as bond breaking/forming (Frenkel et al., 1997; Hann et al., 2001; Poltev, 2015; Vanommeslaeghe et al., 2010). The key advantage of MM is its computational efficiency, making it suitable for simulating a myriad of systems and phenomena over relatively long time scales, such as protein folding, ligand binding, membrane dynamics, polymer morphology, and, in this case, molecular encapsulation (Poltev, 2015).

Hybrid QM/MM methods also exist, in which a part of the molecule (e.g., the active site of an enzyme) is modeled by QM, while the rest is modeled using MM. This partitioning enables the detailed study of chemical reactions in large systems, such as enzymatic reactions, by capturing the electronic changes in the reaction center while also considering the environmental effects from the surrounding matrix. One of the critical challenges in QM/MM simulations is the treatment of the QM-MM boundary, ensuring smooth energy and force translations across the interface, and different QM/MM schemes manage the interactions at this boundary differently. The choice of which QM method to use can also impact results. QM/MM is a powerful tool, especially in the study of enzyme mechanisms, where it has provided insights into the role of enzyme environments in catalysis (Gao & Truhlar, 2002; Senn & Thiel, 2009). This combined approach can provide a balance between accuracy and computational efficiency.

In this work, we will focus on three different MM-based methods: docking calculations, unbiased molecular dynamics (MD) simulations, and guided metadynamics simulations paired with potential of mean force (PMF) calculations.

1.2.1. Docking Calculations

USC
UNIVERSIDADE DE SANTIAGO DE COMPOSTELA

In general, docking involves predicting the optimal orientation of one molecule (often a small ligand) when bound to another molecule (often a larger protein or macromolecule). The goal is to predict the binding

affinity and the preferred orientation of the ligand (pose). Early endeavors in the 1980s, such as the DOCK program by Kuntz et al., introduced algorithms to navigate the orientation and position of ligands in protein binding sites (Kuntz et al., 1982). These pioneering efforts focused mainly on geometric matching, fitting the ligand into a protein based on shape alone. As the field advanced, the 1990s witnessed the integration of more detailed scoring functions to evaluate binding affinities, adding depth to the purely geometric considerations (Meng et al., 1992). By the turn of the century, algorithms became more sophisticated, incorporating flexibility for both the ligand and receptor, recognizing the dynamic nature of biomolecular interactions (Morris et al., 1998). Programs like AutoDock, and later AutoDock Vina, used in this work, became popular for their effective scoring functions and enhanced accuracy (Trott & Olson, 2009). Recently, researchers have been exploring using docking augmented by machine learning techniques and high-throughput virtual screenings, setting the stage for the next era of drug discovery and molecular understanding (Lyu et al., 2019; Z. Xu et al., 2021).

In modern docking calculations, the binding energy between the ligand and the protein is typically evaluated using MM force fields, which provide empirical potential energy functions based on the positions of atoms and their interactions including bond stretching, bond angles, torsion angles, van der Waals interactions, and electrostatic interactions. There are also scoring functions specifically developed for docking that are used to rank and evaluate the binding affinities of the ligand poses (Sousa et al., 2006; Trott & Olson, 2009). These scoring functions can be based on force field terms, empirical data, knowledge-based potentials, or a combination thereof. While MM-based docking is computationally more efficient and is the standard, it's worth noting that there are QM and QM/MM docking approaches (Cho et al., 2005; M. Xu & Lill, 2013). However, they are less common, primarily due to the significantly higher computational cost associated with QM methods.

The rigidity of the system is of crucial importance to docking calculations. Traditional docking methods typically treat the protein as a rigid entity, which can limit the accuracy of the predicted interactions. Flexible docking allows both the ligand and the target protein to adjust their conformations during the docking process (Bursulaya et al., 2003; Morris et al., 2009). By acknowledging some of the dynamic nature of biomolecular systems and permitting conformational changes, flexible docking aims for a more realistic representation of how molecules interact in a biological setting. This adaptability often leads to improved accuracy in predicting ligand binding poses and affinities, but it also comes with increased computational demands compared to rigid docking approaches.

Docking provides a fast but relatively crude method to determine how two molecules might interact. Limited flexibility can be introduced to the system, and there is no time component so the molecules cannot respond to each other in solution. In fact, there is not even a solution present because docking calculations do not consider solvent. However, the speed of these calculations makes them useful for studying certain systems, and high-throughput studies using docking are now relatively common.

1.2.2. Molecular Dynamics (MD) Simulations

In contrast to docking calculations, which provide a snapshot of a favorable conformations between two molecules frozen in time, molecular dynamics (MD) allows a molecular system to evolve over time, showing the dynamic behavior of the molecular interactions. At its core, MD operates on Newtonian physics, where forces on atoms are calculated based on their interactions with surrounding atoms; these

USC
UNIVERSIDADE DE SANTIAGO DE COMPOSTELA

forces are used to compute the accelerations, velocities, and ultimately the new positions of the atoms over discrete time steps (Frenkel et al., 1997).

In recent decades, the field of molecular simulation has seen dramatic advances, both in terms of technology and methodology. The first MD simulation of a protein at atomic level was conducted by J. Andrew McCammon at Harvard in 1977 (McCammon et al., 1977); this was followed by the introduction of water models in the 1980s, pioneered by Berendsen et al.'s Simple Point Charge (SPC) (Berendsen et al., 1981), which revolutionized our understanding of protein dynamics. This also coincides with the first simulations reaching nanosecond timescales, allowing for processes like protein folding and ligand binding to be observed. By the turn of the century, simulations expanded massively in complexity and could handle nearly 10,000 atoms over extended durations - up to a millisecond. Today's advanced technology can simulate systems containing billions of atoms with reasonable performance (Jung et al., 2021), and many researchers have their eyes set on achieving simulations on the timescale of seconds (Wolf et al., 2020). The technique has enabled insights into dynamic processes like ligand-receptor interactions, enzyme catalysis, and phase transitions in materials (Hansson et al., 2002; Karplus & Petsko, 1990). However, MD simulations, like their experimental counterparts, are not without limitations. They demand a keen understanding of the system's experimental aspects and a deep knowledge of appropriate methods. Blindly applying techniques, especially those honed for specific molecules or systems, to other situations can have profound effects. Therefore, the validation of force fields and simulation parameters, ensuring their suitability for the chosen system, is paramount.

The accuracy of simulations often hinges on the chosen force field, and errors in its selection or formulation can lead to misleading results. Additionally, the timescales achievable in MD—typically nanoseconds to microseconds—might not always be sufficient for certain phenomena. A force field is a set of mathematical equations and associated parameters used to approximate the quantum mechanical forces between atoms. These equations define how energy varies with atomic positions, typically breaking down the energy into bonded (e.g., bond stretching, bond angle bending, and torsion angles) and non-bonded interactions (e.g., van der Waals and electrostatic interactions). The parameters are constant, and include values like bond lengths, bond angles, and atomic charges, which are often derived from experimental data or quantum mechanical calculations (Cornell et al., 1995; Mackerell Jr., 2004).

Numerous force fields have been developed, each with specific design philosophies, and intended for particular applications. For instance, while the AMBER (J. Wang et al., 2004) and CHARMM (Vanommeslaeghe et al., 2010) force fields are popular for simulating proteins and nucleic acids, the OPLS (Jorgensen & Tirado-Rives, 1988) and GROMOS (Ott & Meyer, 1996) force fields have been applied to a wider range of molecular systems. Importantly, no force field is universally perfect, and challenges arise from the inherent approximations made in their formulation, leading to potential discrepancies between simulation results and experimental observations. Continuous refinement and validation against experimental and quantum mechanical data are essential to enhance their accuracy and reliability (Ponder & Case, 2003). However, unbiased MD simulations, despite their ability to calculate even improbable events, have limitations, such as difficulty in overcoming high energy barriers and adequately exploring rare transition states. In this context, metadynamics offers significant advantages (Barducci et al., 2011; Bussi & Laio, 2020). These types of simulations are usually referred to as metadynamics simulations; as the name suggests, they offer a deeper insight beyond typical MD as the molecules are guided to fully explore their energy landscape.

USC
UNIVERSIDADE
DE SANTIAGO
DE COMPOSTELA

1.2.3. Metadynamics and Potential of Mean Force (PMF) Calculations

In order to calculate the probability of an unfavorable event, the event must first be captured by a simulation. While typical unbiased MD simulations will not usually capture these kinds of events effectively, they can be guided using different methods to move along a defined pathway (Fig. 4). Steered Molecular Dynamics (SMD) is one of these methods, allowing for improved sampling of rarely-visited conformations and therefore the calculation of the energy profile, which can be used to deduce many important qualitative and quantitative properties of the system, such as molecular recognition or conformational changes. SMD was introduced in the 1990s as a technique to induce transitions by applying an external force to certain atoms, guiding the system from one state to another (Park & Schulten, 2004). SMD can rapidly induce specific molecular transitions, which is beneficial for observing particular reactions or conformations, but it is important to consider that applying an external force can introduce artifacts or non-physical behaviors in the simulation. Metadynamics, suggested in 2002 by Laio and Parrinello (Laio & Parrinello, 2002), is an improvement to this, in which the bias is defined by a chosen collective variable (CV) or set of CVs, which can be fully sampled throughout the simulation. A CV in molecular simulations is a parameter or set of parameters that encapsulates vital transitions or conformational changes between two states of a system. A simple example of a CV would be the distance between two atoms, or two centers of mass (COM) of two molecules (Fig. 5) that are expected to interact. Serving as a dimensionality reduction tool, CVs are used to bias MD simulations to explore specific trajectories or hurdles on an energy landscape that may not be sampled by a freely evolving simulation, without necessitating an external force.

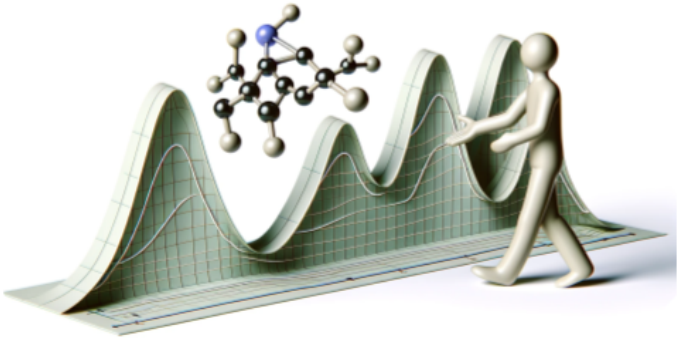


Figure 4. DALL·E 3 rendering of guided MD such as SMD or metadynamics.

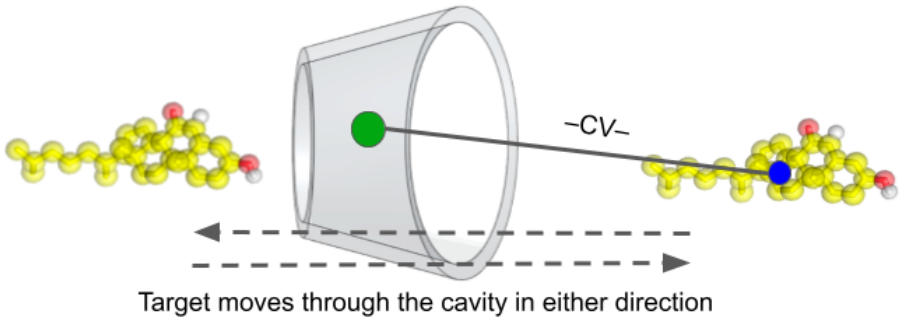


Figure 5. Description of CV. CD is represented as the rotated, simplified cone representation and the target is shown in yellow. The approximate COM of the CD is shown as a green dot while the approximate COM of the target is shown as a blue dot. The CV is the distance between the green dot and the blue dot as the target moves through the cavity.

The concept of Potential of Mean Force (PMF) has its roots in statistical mechanics, where it represents the free energy as a function of the CV(s). Thus, a free energy profile that is well sampled by MD can be used to calculate the PMF of a certain pathway, such as the recognition and interaction of two molecules, as

USC UNIVERSIDADE DE SANTIAGO DE COMPOSTELA

defined by the CV. This yields quantitative binding information that can be used to dissect the thermodynamics and kinetics of molecular processes, deepening our understanding of myriad biological and chemical phenomena.

Initial PMF methods relied on direct integration of forces, which was computationally expensive and limited to simple systems. In the late 1970s, umbrella sampling was introduced. This technique divides the entire range of the CV into overlapping "windows", where each window has a biasing potential applied to focus the simulation around a specific value of CV (Fig. 6) (Torrie & Valleau, 1977). After performing simulations for each window, the data is combined using methods like the Weighted Histogram Analysis Method (WHAM) to yield an unbiased PMF profile, revealing energy barriers and stable states (Ferrenberg & Swendsen, 1989; Kumar et al., 1992). This method is particularly valuable because it enables detailed exploration of rarely accessed regions in the reaction coordinate, although it can be computationally intensive (Torrie & Valleau, 1977).



Figure 6. DALL·E 3 rendering of umbrella sampling.

In this work, metadynamics has been used to calculate PMF profiles. Metadynamics works by appending a history-dependent potential to specific CVs, which is iteratively constructed as the sum of Gaussian functions over the trajectory. The goal of this is to prevent the system from revisiting previous conformations. Metadynamics can also employ repulsive potentials, or walls, to a system, which serve to confine the simulation to specific areas or to prevent the system from venturing into regions that are either physically meaningless or not of interest.(Barducci et al., 2011; Bussi & Laio, 2020; Laio & Parrinello, 2002) By applying a wall, the sampling of the simulation can be focused on specific regions of the free energy landscape, which can be particularly useful when studying transition pathways or when the simulation might otherwise drift into unfavorable states. This also allows a particular CV space to be fully explored, and ensures that the simulation proceeds in a manner relevant to that CV and does not waste computational time.

Metadynamics continuously modifies the system's Hamiltonian by adding biasing potentials, and the accumulated bias directly yields the free energy landscape (or PMF) associated with the chosen CVs (Bussi & Laio, 2020; Laio & Parrinello, 2002). However, as the biasing potential continuously grows, overfilling of the energy wells can occur. This means that at extended timescales, the Gaussian additions might become too excessive, leading to a loss of resolution in the free energy surface (Laio & Parrinello, 2002). Well-tempered metadynamics is an improvement over traditional metadynamics; instead of adding a constant height Gaussian, the height of the Gaussian decreases as the simulation progresses. This is achieved by introducing a bias factor, which modulates the height of the added Gaussians. As a result, well-tempered metadynamics provides a better estimation of the free energy surface with reduced computational cost (Barducci et al., 2008).

The PMF can be deduced from the history-dependent biasing potentials that are added during the simulation; the PMF as a function of the CV can be computed as the negative of the accumulated bias. As

USC UNIVERSIDADE DE SANTIAGO DE COMPOSTELA

the simulation progresses and converges, this derived PMF approaches the true PMF of the system. To obtain a smoother PMF, post-processing and averaging over multiple metadynamics runs might be necessary, and tools like PLUMED offer utilities (ie, sum_hills) to assist in processing and obtaining the PMF from metadynamics simulations (Bonomi et al., 2009, 2019; Tribello et al., 2014).

It is crucial to note that, no matter what sampling method is used, calculating PMF requires careful selection of the CV(s). An improper choice can lead to misrepresentative or incomplete energy landscapes, which can have large effects on the resulting PMF. Also, the chosen sampling method and the accuracy of the underlying molecular mechanics force fields can significantly influence the PMF results (Bonomi & Parrinello, 2010).

1.3. Computational Studies on CDs: Unraveling Complex Host-Guest Interactions

Computational studies are useful in elucidating many characteristics of CD-guest interactions that are difficult to measure in typical wet laboratory experiments. There are many different types of computational models and experiments, but in drug discovery most of these simulations are focused on protein-receptor interactions. Compared to CDs, proteins are immense. The relatively small size of CDs makes them ideal for modeling the complex phenomena of molecular encapsulation, which is critical for the design of novel drug delivery systems. Computational modeling of CDs can also serve as a scaffold for studying drug molecule stability and predicting the release kinetics, to screen and refine drug interactions with CDs, to enhance the affinity for target molecules, and/or to fine-tune the resulting complex's properties. This can lead to the creation of more effective and targeted drug delivery systems with potentially fewer side effects. As a result, the field of computational chemistry continues to push the boundaries of CD research and provide valuable insights that drive innovation in pharmaceutical design and development.

Various computational studies of CDs have been conducted, but the field is still in a relatively nascent state in comparison to studies on protein systems. CDs can be studied using a variety of computational techniques including Quantitative Structure Activity Relationship (QSAR) modeling, MD, and docking. QSAR can be powerful for predicting binding constants between CDs and guest molecules, but depends on the availability of large amounts of accurate data. Therefore, for CDs, the method faces challenges as it continues to evolve. In the future, effective and precise QSAR modeling may be the standard for CD inclusion complexes (Ding et al., 2022). On the other end of the spectrum, docking calculations with CD inclusion complexes are becoming more and more common. Flexible systems are expected to behave more realistically than rigid ones, but require more computational resources, and docking scoring systems are typically developed with protein systems in mind, not CDs (Ding et al., 2022; T. Li et al., 2022). Thus, docking represents an easy and fast method for cheap results, but there is a real need for a more refined CD docking function. Finally, MD is particularly useful for studying CD inclusion complexes because the dynamic nature of the inclusion complex can be observed, and the flexibility of CDs has been shown to be particularly important (Bonnet et al., 2002; Cézard et al., 2011; Christoforides et al., 2018; Hayashino et al., 2018; Kerdpol et al., 2019; Mazurek et al., 2021; Mixcoha et al., 2014; Piñeiro et al., 2007). Some QM studies have also been conducted with promising results, but they remain a niche endeavor (Mazurek & Szeleszczuk, 2022).

Biased MD simulations are useful for studying CD inclusion complexes and particularly guest encapsulation. By guiding the target towards and eventually out of the CD cavity, the entire energy landscape can be connected to a simple CV. For CD inclusion complexes, this CV is usually taken as the distance between the COM of the guest and the COM of the CD. These metadynamics simulations can be

USC
UNIVERSIDADE DE SANTIAGO DE COMPOSTELA

coupled with PMF calculations to determine binding constants, and have been successfully used as 'models' for studying ligand-receptor dynamics (the CD cavity can be treated similarly to a protein binding site) (You et al., 2019). Computational studies on CDs have made substantial contributions to our understanding of host-guest interactions and have helped pave the way for numerous applications. However, these studies are not without their challenges, which encompass various aspects of CD behavior and their interactions with guest molecules. CDs, although relatively small compared to proteins, exhibit considerable conformational flexibility, allowing them to adapt to the shape and size of guest molecules, which makes them excellent host molecules. However, capturing this conformational flexibility accurately in simulations can be computationally demanding. Achieving meaningful results often requires long simulation times, extensive sampling, and customized analysis to account for the various conformations that CDs can adopt during host-guest interactions (Dodziuk, 2002; F. Garrido et al., 2020).

Addressing Stoichiometry and Aggregation: MD studies on CD systems are becoming more and more common, but careful setup and a deep understanding of the system is necessary for good MD results with CDs. A recurring theme across many MD studies on CDs is the commonly held assumption of solely considering 1:1 CD complexes. Many underscore the inadequacy of this simplification, advocating for a broader exploration of stoichiometries and aggregation (Bonnet et al., 2001; Choi et al., 2000; Hayashino et al., 2018; Mixcoha et al., 2014; Piñeiro et al., 2007), but it is also clear that exploring all of the possible CD inclusion complex interactions for a given system can be exceptionally challenging. Those studies that do examine more complex binding modes and interactions of CDs, usually with cholesterol, often reveal higher affinity in 2:1 complexes (Christoforides et al., 2018; Hayashino et al., 2018; López et al., 2011), which also corresponds to the crystal structure of this interaction. Many different types of CD interactions may be taking place at once, so it is important to choose a particular complex and investigate it in a stepwise manner, incrementally accounting for more stoichiometries and degrees of complexity.

Addressing Solvent Effects: The role of water and the choice of method/force field are also central to computational studies. Early studies sometimes did not even consider solvent (Choi et al., 2000), as it was too computationally demanding, but it has become apparent that water profoundly impacts the CD inclusion complex. Multiple studies have shown that water can exhibit unexpected behavior around CD molecules (F. Garrido et al., 2020; Makieła et al., 2018; Sandilya et al., 2020), and some studies even suggest that the AMBER forcefield does not properly reproduce some of the structural and dynamic properties for CD systems due to how it characterizes water (F. Garrido et al., 2020).

Addressing Flexibility: CDs, contrary to how they are often represented, are highly flexible rings that behave differently depending on how they interact with each other, the solvent, or the guest molecule(s). CDs can exhibit significant differences in both aggregation and flexibility based on their size or substitution type and pattern (Makieła et al., 2018; Mixcoha et al., 2014; Schönbeck et al., 2014), and thus the setup of the MD simulation should be considered based on what is known and what is being tested. Similarly, the more substitutions on the CD, the more flexibility it will have. The impact of the substitution groups is significant, and can have large effects on guest encapsulation (Kerdpol et al., 2019). Flexible CDs can adapt their shape to better accommodate various guest molecules with more or less specificity, which is vital for applications like drug delivery. Computational studies that accurately model this flexibility can predict how changes in CD structure influence their binding properties, but many still represent the CD as a simple truncated cone with little flexibility.

USC
UNIVERSIDADE DE SANTIAGO DE COMPOSTELA

Choosing a Force Field: The choice of force fields also significantly influences the accuracy of predictions. Force fields comprise the underlying laws that the simulation will follow, and different force fields may yield different results for CD-guest systems. Combine this with the fact that most force fields are designed with proteins in mind, enormous molecules compared to CDs, and it becomes clear why researchers often grapple with the challenge of selecting an appropriate force field for their specific study (Gebhardt et al., 2018). In previous work, we have tested various force fields for use with CDs, and we have found that the GROMOS G54a7 forcefield (Oostenbrink et al., 2004) effectively captures the aforementioned flexibility as well as critical hydrophobic interactions in our CD systems.

Addressing the Structural Distribution of CDs: Computational studies must also be validated against experimental data to ensure their reliability and relevance. However, experimental determination of binding constants and complex structures for CD-guest systems can be especially challenging. Discrepancies between computational predictions and experimental results can pose difficulties in validating simulation outcomes, emphasizing the need for robust experimental validation. In addition to these challenges, modified CDs are mostly synthesized as a distribution of isomers (with a notable exception being sugammadex), which would be impossible to simulate in entirety for every CD. A representative structure, ideally a series of representative structures, must be selected to simulate; if the simulations are not representative, they could give misleading results. Additionally, validation with a native or single-isomer CD such as sugammadex can help with this problem.

Finally, challenges arise from the diversity of guest molecules that can form inclusion complexes with CDs. CDs can interact with a wide range of guest molecules, from small drugs to large biomolecules. Modeling this diversity in computational studies is complex, and the simulation protocol often must be adapted for different guest molecules to ensure accurate predictions. The structural and chemical diversity of guest molecules adds complexity to computational investigations. Computational studies on CDs have significantly advanced our understanding of host-guest interactions and their diverse applications. Despite facing challenges related to size, flexibility, guest diversity, and experimental validation, computational approaches continue to provide valuable insights into the behavior of CDs in complex environments. As computational techniques evolve and computational resources become more accessible, researchers are poised to overcome these challenges and continue unraveling the secrets of CD host-guest systems, driving innovation in fields such as drug delivery, materials science, and environmental remediation.

1.4. The Importance of Validation and Corroborating Assays

A thesis reporting on the computational methods used to assess a system would be incomplete without a discussion on validating experiments. Each computational method presents its own benefits as well as challenges and limitations, and is intended to provide an independent perspective on the interactions at play in a particular inclusion complex. Because of this, it is difficult to use computational studies alone to make conclusive remarks about a system, unless that system has been properly validated against bench experiments. Complementing the computational simulations in this work are *in vitro* experiments performed using isothermal titration calorimetry (ITC) and circular dichroism (CiDi, so as not to be confused with CD for cyclodextrin) techniques. These experiments aim to measure the binding constants, thermodynamic parameters, and complex stoichiometry of CD dimer-sterol complexes.

ITC is a precise laboratory technique that directly measures the heat (energy) changes associated with a binding process (Bouchemal & Mazzaferro, 2012; Connors, 1987; Piñeiro et al., 2019). In the case of this

USC
DE SANTIAGO
DE COMPOSTELA

research, ITC is used to explore the interaction between CD dimers and sterols, and is a very useful tool for validating binding constants (Peluso et al., 2023; Piñeiro et al., 2022). Circular dichroism (CiDi) spectroscopy is another laboratory technique employed in the study which allows for the examination of spectral changes that occur when CD dimers interact with sterols (Allenmark, 2003; Harata & Uedaira, 1975; Kiss et al., 2019). ITC and CiDi are also useful for exploring the stoichiometries of inclusion complexes, offering additional insights into how to computationally capture the nature of the complex most effectively.

A crucial aspect of this research is the comparison between computational and wet laboratory methods. Both approaches offer unique advantages and challenges. Computational simulations provide predictive insights into molecular interactions, enabling researchers to understand the fundamental mechanisms governing binding. However, they are limited to studying specific isomeric structures. In contrast, laboratory experiments like ITC and CiDi provide empirical data that consider the entire distribution of molecular structures present in a non-isomeric mixture of CDs and, except in certain cases, represent a distribution of structures. These methods capture complex stoichiometry and thermodynamic parameters, providing valuable insights into real-world interactions.

USC
UNIVERSIDADE DE SANTIAGO DE COMPOSTELA

Chapter 2. Hypothesis and Objectives

USC
UNIVERSIDADE DE SANTIAGO DE COMPOSTELA

This thesis, guided by advanced computational methods as well as wet laboratory assays, aims to reveal how CDs form inclusion complexes with their guests and the implications that this interaction may have for drug development and discovery. The following studies delve into three distinct facets of CD interactions, collectively contributing pieces to the broader puzzle of molecular recognition and encapsulation. These studies form the basis of a comprehensive computational platform which will ultimately be able to automatically predict ideal CD-guest pairs, producing new candidates for CD applications in various fields, including drug development.

The central hypothesis of the works presented here is that an advanced understanding of the intricate nature of CD interactions with various guest molecules will empower us to design tailored molecular systems for diverse applications. This overarching hypothesis guides specific objectives, each addressed within the context of individual publications:

1. **Sugammadex and Neuromuscular Blockade Reversal**: The first study focuses on sugammadex, a well characterized CD-based drug marketed as Bridion™, celebrated for its rapid reversal of rocuronium-induced neuromuscular blockade. Using this system, we endeavor to establish and validate advanced computational methods for studying and quantifying CD inclusion complexes.

2. **β-CDs and Sterol Inclusion Complexes**: In the next study, we employ our computational techniques to investigate β-CDs and their 1:1 inclusion complexes with sterol molecules, with a primary focus on cholesterol and 7KC. The objective is to unravel the binding energetics, structural dynamics, and interaction preferences, thus laying the groundwork for the development of customized molecular systems.

3. **CD Dimers and Atherosclerosis Treatment**: The third study charts an unexplored path, investigating the potential of CD dimers as a novel treatment for atherosclerosis by forming specific inclusion complexes with 7KC. Ridding the body of 7KC (but, importantly, not cholesterol) could potentially aid in the reduction and healing of arterial plaques. Characterizing these interactions presents formidable challenges, including low sterol solubility and intricate interaction mechanisms. To overcome these hurdles, we employ a multifaceted approach, integrating metadynamics simulations, competitive isothermal titration calorimetry, and circular dichroism.

USC
UNIVERSIDADE DE SANTIAGO DE COMPOSTELA

Chapter 3. General Methodological Framework

USC
UNIVERSIDADE
DE SANTIAGO
DE COMPOSTELA

3.1. Computational simulations

Simulations were conducted using compatible parameters and a standardized methodology across various systems. This approach is the result of extensive testing and validation steps, leading to an automated process that ensures compatibility and consistency in our simulations, thereby enhancing the reliability and comparability of our results.

3.1.1. Initial Molecule Parameterization and Building of the Complexes

Both the initial coordinates for the CD and the corresponding topologies were built using our own tools (Anderson et al., 2021, 2024), based on the GROMOS 54A7 forcefield (Oostenbrink et al., 2004). Initial coordinates and the topology file for the targets (rocuronium, cholesterol and 7KC) and the linker (in the case of CD dimers) were obtained from the ATB server (Malde et al., 2011). To ensure consistency with the force field, manual adjustments were made to the parameters, preventing unreasonable interaction constants for bonds and angles. Furthermore, the common atomic groups were assigned identical interaction parameters, while differences in interaction parameters were limited to the parts of the molecules that are not equivalent.

After the CD and target were built and parameterized, the target was introduced into the CD cavity, with both molecules sharing the same center of mass, at approximately 0 or 180 degrees ("up" and "down" orientations, respectively) with the angle defined between the main axis of the target and that perpendicular to the plane that best fit the O4 atoms (those joining the glucopyranoside groups) of the CD (Fig. 1). These atoms were taken as a reference because they were observed to correspond to the most stable internal coordinates of the CD molecule in previous works (Mixcoha, 2014; Piñeiro, 2007; Garrido, 2020). These structures are placed in a dodecahedron simulation box (7x7x7 nm^3) and solvated with explicit SPC water molecules, removing those overlapping the solute molecules and neutralizing negative charges with Na^+ ions. The solvated structures are then minimized to remove any high-energy conformations. Simulations with the “up” and “down” relative orientations of the target within the CD are conducted separately.

3.1.2. Molecular Docking

In the docking calculations, the target was first removed from the CD cavity. For the CD monomers and the ligand, flexibility was introduced using MGLTools. This approach introduced torsional flexibility around the O2, O3, and O6 atoms of the CD. The ligand search grid was defined as a 30 Å cube positioned about the center of mass of the CD monomer or CD dimer. Autodock Vina (Trott & Olson, 2009) was used to conduct the docking calculations. Snapshots of the optimal poses were generated using PyMOL.

3.1.3. Molecular Dynamics

All MD simulations were performed using the NPT ensemble (Andersen, 1980) at 298 K and 1 bar. The temperature and pressure were controlled using the v-rescale thermostat (Hünenberger, 2005) and the Parrinello-Rahman barostat (Parrinello & Rahman, 1981) with coupling times of 0.1 and 0.5 ps, respectively. The long-range interactions were determined using the Particle Mesh Ewald algorithm (Darden et al., 1993) with a grid spacing of 0.15 nm and a direct-space cut-off of 1.2 nm. The same cut-off was employed for the short-range interactions. A timestep of 2 fs was employed in all cases using the leap-frog integrator algorithm (Van Gunsteren & Berendsen, 1988). All bonds were constrained (where applicable) using the SETTLE algorithm (Miyamoto & Kollman, 1992) for water and the LINCS algorithm

USC DE SANTIAGO DE COMPOSTELA

(Hess et al., 1997) for the solute molecules. These simulations were executed using the GROMACS 2021.4 (Abraham et al., 2015; Berendsen et al., 1995) engine and the GROMOS54a7 forcefield (Oostenbrink et al., 2004).

Analysis: A number of quantitative parameters as a function of time were determined along the trajectories. These parameters were designed to easily understand at a glance how the host and the guest molecules behave during the simulations. The angle between both molecules (the CD and the target), determined using the principal axis of the targets (rocuronium, cholesterol or 7KC) and the axis perpendicular to the best plane containing the O4 atoms (Fig. 1), was determined to illustrate variations in the relative orientation of both molecules and is expected to be sensitive to the disassembly of the complex as well as to potential flipping of the target inside the cavity. The distance between the COM of both molecules was also determined, which is a clear direct sensor of the separation of the molecules. The number of hydrogen bonds and the number of contacts (using a cutoff of 6 Å) between the two molecules are also expected to provide complementary insight in how the molecules behave, since it is possible that both the angle and the distance are compatible with significantly different values of these features. Another important parameter for CD systems is the number of water molecules inside the CD cavity, since the encapsulation of the target is expected to displace a significant number of solvent molecules from this region. For this calculation, a sphere centered in the COM of the O4 atoms with a radius of 6 Å was considered. Finally, the Coulomb and Lennard-Jones energy contributions between the two molecules were determined as a function of time. For all these properties, both the average values along the trajectories and the corresponding standard deviations were determined. The standard deviation was taken as a measurement of the fluctuation in the corresponding property. Snapshots of representative structures were generated using PyMOL.

3.1.4. Metadynamics

In order to derive the free energy profile leading to the formation of the complexes, as well as the optimal structure of the inclusion complex, well-tempered metadynamics simulations were performed. Coupled metadynamics simulations of twelve slightly different complexes built for each system and relative orientation of the ligand in the CD cavity were executed in parallel. Simulations with the up and down relative orientations of the ligand were conducted separately. All simulations were conducted for a minimum of 300 ns per walker.

For CD monomers, the projection of the COM of the target on the symmetry axis of the CD, defined by the O4 atoms, was set as the CV (Fig. 1, 5). Many tests were conducted to determine the ideal parameters for the PLUMED metadynamics simulations, and the best were determined to be a Gaussian Height = 0.1 kJ/mol, σ = 0.1 nm, biasfactor = 15 at 298 K, and a grid spacing of 0.02 nm between -3.4 and 3.4 nm. The following restraints were devised to focus the investigation on inclusion complex structures: permitting the ligand movement solely along the axis perpendicular to the plane of the O4 atoms of the CD and constraining the relative orientation of the ligand. The O4 atoms of the CD were selected as reference points for distance measurements and defining reference planes and axes in the restraints, due to their relatively static nature compared to the other atoms in the CD. All restraints in these simulations were implemented using harmonic potentials with a constant force of 1000 $kJ \cdot mol^{-1} \cdot nm^{-2}$.

For CD dimers, the method was similar except that two CVs and additional restraints were employed. CD dimers possess numerous degrees of freedom, resulting in significant flexibility, which complicates the identification of a small set of generalized coordinates able to represent their dynamic behavior in a proper

USC DE SANTIAGO DE COMPOSTELA

way. The movement of CD dimers was constrained to focus on the characterization of double inclusion complexes (DIC, where "double" refers to both of the CD rings in the complex encapsulating the guest, as opposed to a "single inclusion complex" in which the stoichiometry is the same, but only one of the two CD rings encapsulates the guest), thus reducing the number of degrees of freedom and facilitating sampling. To maintain this DIC complex, the CD was restrained to maintain both CD monomers in parallel to each other without angular or lateral shifts between their symmetry axes. For the CVs, we decided to use the distance between the COM of the ligand and the COM of the O4 atoms (those joining the glucopyranoside rings in the CD molecules) of *each monomer* as CVs. The metadynamics calculations were carried with PLUMED 2.8 (Bonomi et al., 2009, 2019; Tribello et al., 2014).

3.1.5. Potential of Mean Force (PMF)

The PMF profiles were determined from the sum of the gaussian functions generated by the 12 coupled walkers corresponding to each relative orientation of the target molecule with each CD during the metadynamics trajectories, using the sum_hills tool of PLUMED.

For dimers, the 2D PMF profiles (resulting from two CVs) must be converted into 1D PMFs. The 1D projections of the profiles along each CV were obtained by performing the numerical integration of the probability distribution associated with the 2D PMF with respect to the complementary CV, using the s*um_hills* tool of PLUMED. Subsequently, the resulting integrated values were transformed back into a PMF by taking the logarithm of these values, and then multiplying by the negative Boltzmann factor. The convergence of each simulation was also considered by plotting the evolution of the 1D PMF profiles in time periods of 1 ns. The dispersion of these curves over the last 20 ns can be considered as a fingerprint of the convergence.

The resulting 1D PMF profiles, for both monomers and dimers, were post-processed to determine the corresponding standard binding constant, which for a bimolecular interaction (A+B ↔ AB) can be determined from the partition function of each chemical species (Z_i):

$$K_A = N_A \frac{Z_{AB}/V}{Z_A/V \; Z_B/V} \quad [1]$$

where N_A is the Avogadro's number, Z_i is the partition function of the compound *i* and *V* is the volume of the system. Neglecting the internal degrees of freedom of A and B, the corresponding Hamiltonian is:

$$H_i = \sum_{j=1}^{3} \frac{p_j^2}{2m_i} \quad [2]$$

where p_j is the *j* component of the linear momentum and m_i is the mass of the molecule *i*. The partition function corresponding to that Hamiltonian is:

$$Z_i = V\left(\frac{2\pi m_i K_B T}{h^2}\right)^{3/2} \quad [3]$$

with K_B representing the Boltzmann constant and *h* the Plank constant. The Hamiltonian corresponding to the complex would be:

$$H_{AB} = \sum_{j=1}^{3} \frac{(p_j^{com})^2}{2(m_A+m_B)} + \sum_{j=1}^{3} \frac{(p_j^R)^2}{2\mu} + E(r) \quad [4]$$

USC UNIVERSIDADE DE SANTIAGO DE COMPOSTELA

p_j^{com} being the *j* component of the linear momentum of the COM of the complex, p_j^R the j component of the linear momentum of the relative movement between A and B in the complex, $\mu = \frac{m_A \cdot m_B}{(m_A + m_B)}$, and $E(r)$ is the potential energy of interaction between A and B as a function of the relative coordinates between both molecules. The corresponding partition function is:

$$Z_{AB}=\mathrm{V}\left(\frac{2\pi(m_A+m_B)K_BT}{h^2}\right)^{3/2}\left(\frac{2\pi\mu K_BT}{h^2}\right)^{3/2}\int e^{-E(r)/RT}\,dv \qquad [5]$$

where R and T are the gas constant and the temperature, respectively, and *dv* is the volume elment expressed int erms of the r coordinates. Replacing equations 2-5 in equation 1, we obtain (Piñeiro et al., 2022):

$$\mathrm{K_A} = \mathrm{N_A}\int e^{-E(r)/RT}\,dv \qquad [6]$$

Given the symmetry of the CD monomer and the restraints applied to the relative movement of the ligand with respect to the macromolecule, the interaction energy $E(r)$ and the volume element *dv* are naturally expressed in cylindrical coordinates (φ, ρ, z). Since the rotations around the CD symmetry axis are not restrained, and the interaction energy is assumed to be independent on the corresponding angle, the volume element can be directly integrated over φ (from 0 to 2 π). The distance from the ligand to the axis perpendicular to the O4 atoms that passes throughout their COM is restrained with a harmonic potential, so it is not exactly constant, but the PMF is assumed to be independent of this parameter. Thus, the volume element is also integrated over ρ from 0 to the maximum radius of the cylinder where the ligand can move (ρ_{max}). Importantly, the simulations were not performed in the standard state, so a correction should be performed for this aim. This correction is performed by dividing the volume of each molecule in the simulation box by the volume available for one molecule at 1M concentration (1660 $\mathrm{Å}^3$). After simplifying this implies an additional factor of the Avogadro's number ($\mathrm{N_A}$) in the expression for $\mathrm{K_A}$. Taking account all these approaches and considerations, the final expression for the association constant would be:

$$\mathrm{K_A} = \pi\,\mathrm{N_A}\,\rho_{max}^2\int e^{-E(\xi)/RT}\,d\xi \qquad [7]$$

where the cylindrical coordinate *z* was replaced by the collective variable ξ employed in our simulations and $E(\xi)$ can be replaced by the PMF. Using this equation, the binding constant for each system was computed by numerical integration of the PMF along the CV. For our calculations a constant value of 0.4 nm was taken for ρ_{max}.

For dimers, the binding constant for each system was computed by numerical integration of the *two* possible projections of the PMF along each CV.

In order to estimate the uncertainty of the $\mathrm{K_A}$ values, multiple integrations were considered for each 1D-PMF, with different integration limits in the unbound region. Then, the ΔG^0 values obtained in this way for each PMF profile were clusterized with the k-means algorithm with the optimal number of clusters determined using the Silhouette (Rousseeuw, 1987) method. The final ΔG^0 values, together with the corresponding standard errors, were taken as the average and standard deviation of the ΔG^0 values of the most populated cluster. Then, the corresponding association constant was obtained as $\mathrm{K_A} = \exp(-\Delta G^0/RT)$ and its uncertainty determined by standard error transmission. This procedure allows the automatic detection and elimination of outliers without any human bias. For the calculation of average values we

USC UNIVERSIDADE DE SANTIAGO DE COMPOSTELA

decided to work in the ΔG^0 space due to the exponential nature of the association constants, whose direct averaging can be heavily skewed by values that differ significantly in magnitude. However, energies are additive, a property that makes it well suited to operations such as summation and averaging. By converting K_A to ΔG^0 values, one can obtain a more representative average, which can then be transformed back into the K_A space for interpretation. This method ensures that the derived average value is not disproportionately influenced by constants that are significantly larger or smaller than the others, providing a more accurate and meaningful representation of the dataset. This approach resulted in a fully automated 1D and 2D PMF method, providing a reasonable quantitative approach for obtaining binding constants for the formation of CD monomer or dimer inclusion complexes using a reasonable amount of computational resources. The final values of K_A and the corresponding ΔG^0 were obtained using a Python script that uses the pandas (McKinney, 2010; team, 2023), numPy (Harris et al., 2020), matplotlib (Hunter, 2007), and kmeans1d (Grønlund et al., 2018; Wu, 1991) libraries.

The process is identical for monomers and dimers except that there is only one CV/dimension for monomers, and thus the conversion from 2D to 1D PMF is not necessary.

3.2. Wet lab experiments

3.2.2 Isothermal Titration Calorimetry

ITC experiments are widely recognized as the gold standard for characterizing the thermodynamics of molecular interactions. This is because they rely on a direct measurement of the interaction energy as a function of time (heat power), which, when integrated, yields the enthalpy as a function of the concentration ratio of the involved compounds. The analysis of the corresponding isotherms offers insights on the interaction mechanism (stoichiometry), as well as the corresponding binding constants for the applied model. Additionally, no chemical labeling is required to perform the experiments, but they do require that the compounds are well-dissolved at concentrations that yield significant signals. The low solubility of the studied solute, in this case sterol molecules, is a common limitation in such studies, since their solubility is lower than that required to get a clear signal in the calorimeter. Thus, we designed an alternative strategy to characterize interactions with CD dimers, using randomly methylated βCD monomers (RAMEB) as a competitor to encapsulate sterol molecules. This is similar to the "release protocol" found effective for analysis of CD monomers, in which a saturated solution of Target 1 encapsulated CD is titrated with a second target solution capable of displacing the Target 1 from the CD (Bertaut & Landy, 2014; Bouchemal & Mazzaferro, 2012). For our assay, 40 small (12 μL) aliquots of approximately 10-20 mM RAMEB and around 1 mM sterol solutions were injected into the sample cell of a VPT-ITC from Microcal containing either pure water (for dilution experiments) or CD dimer aqueous solutions at about 0.04-0.08 mM (for competitive experiments). The employed RAMEB to sterol concentration ratio (10-20:1) was required to fully solubilize the sterol molecule. The sample cell and the syringe were carefully cleaned with DMSO and water between experiments.

The ITC raw data were processed (baseline correction + integration of the power profile) using the AFFINImeter software (Piñeiro et al., 2019), since it allows a flexible definition of several coupled equilibrium processes to be simultaneously considered as a global interaction model. The results were then fitted with a competitive model where the sterol (S) can be encapsulated either in the monomer (M) or in the dimer (D) with different stoichiometries represented by the following equilibria:

USC
UNIVERSIDADE DE SANTIAGO DE COMPOSTELA

$$M + S \leftrightarrow M_1S_1 \Rightarrow K = \frac{[M_1S_1]}{[M][S]} \quad [8]$$

$$2M + S \leftrightarrow M_2S_1 \Rightarrow K = \frac{[M_2S_1]}{[M]^2[S]} \quad [9]$$

$$D + S \leftrightarrow D_1S_1 \Rightarrow K = \frac{[D_1S_1]}{[D][S]} \quad [10]$$

$$D + 2S \leftrightarrow D_1S_2 \Rightarrow K = \frac{[D_1S_2]}{[D][S]^2} \quad [11]$$

$$2D + S \leftrightarrow D_2S_1 \Rightarrow K = \frac{[D_2S_1]}{[D]^2[S]} \quad [12]$$

3.2.3 Electronic Spectroscopy

UV-Vis Absorption spectra have been registered on a Perkin Elmer 950 spectrophotometer. The intrinsic absorption of the triazole linker in the dimer was used with a molar absorption coefficient of 4000 $M^{-1}cm^{-1}$ at 215 nm to estimate the CD concentration. CiDi spectra have been registered on a Jasco J-715 spectropolarimeter. The CiDi experiments were performed in diluted aqueous solution of the sterol with a minimal amount of EtOH (1% V/V) in order to avoid aggregation phenomena or precipitation, and to circumvent the use of the intrinsic aqueous solubility value of the sterol during the estimation of the binding constants. The 7KC or CHOL concentration in the aqueous solution has been set to 20 μM, close to its solubility limit in water (6 μM) allowing the recording of reliable CiDi spectra, with the CD concentration varying in the 20-200 μM range. The CiDi spectra of the sterol/CD mixtures were corrected for the CiDi signal of the quartz cuvette with solvent. The best complexation model, binding constants, and single spectra of the complexes were determined by means of a multivariate global analysis of multiwavelength data using a set of spectra corresponding to different sterol/CD mixtures. The analysis was performed with the commercial software ReactLab™ Equilibria from JPlus Consulting developed by Matlab, considering the equilibrium processes in Eq. 10 - 12. The ReactLab™ Equilibria procedure is based on singular value decomposition (SVD) and nonlinear regression modeling by the Levenberg-Marquardt method. A matrix is created with all complete absorption or CiDi spectra, and each spectrum is assigned to a specific CD concentration of the titration. The analysis proceeds optimizing the single binding constants as well as the spectra of the single species. It eventually affords, upon convergence, the final binding constants of the chosen model together with the individual spectra of the complexes. The software allows comparison of experimental data and calculated values at single wavelengths to evaluate goodness of fit. Further statistical outputs include standard deviations for each fitted parameter as well as sum-of-squares and standard deviation for the residuals.

USC
UNIVERSIDADE DE SANTIAGO DE COMPOSTELA

Chapter 4. Unraveling the Molecular Dynamics of Sugammadex-Rocuronium Complexation: A Blueprint for Cyclodextrin Drug Design[1]

4.1. Preface to Contextualizing the Research: Insights into Authorship, Contributions, and Publication Specifics

As detailed in the introduction and methods, *in silico* methods for studying CD inclusion complexes can be developed for accurately predicting their structural, energetic, dynamic, and kinetic properties, as well as binding constants. Here, a computational study aimed at characterizing the sugammadex-rocuronium system from the perspective of docking calculations, unbiased MD simulations, and biased metadynamics simulations with PMF calculations is presented. The aim is to provide detailed information about this system, as well as to use it as a model system for validation of the methods. These methods predict results in line with experimental evidence for both the optimal structure and the quantitative value for the binding constant. Interestingly, there is a less profound preference for the orientation than might be assumed based on electrostatic interactions, suggesting that both orientations may exist in solution. These results show that this technology can efficiently analyze CD inclusion complexes and could be used to facilitate the development and optimization of novel applications for CDs.

Title: Unraveling the Molecular Dynamics of Sugammadex-Rocuronium Complexation: A Blueprint for Cyclodextrin Drug Design

Authors: Amelia Anderson, Rebeca García-Fandiño, Ángel Piñeiro, Matthew S. O'Connor

Year: 2024

Publisher: Elsevier Ltd.

ISSN/ISBN: 01448617

DOI: https://doi.org/10.1016/j.carbpol.2024.122018

Quality indexes: Carbohydrate Polymers is a journal covering the technologies/fields/categories related to Materials Chemistry (Q1); Organic Chemistry (Q1); Polymers and Plastics (Q1). It is published by Elsevier Ltd.. The overall impact score is 11.93.

Contributions: As the leading and corresponding author of this work, my involvement was multifaceted and critical to the project's success. My key contributions were: designing and conceptualizing the research study; developing and implementing the computational methodologies employed; analyzing and interpreting the resulting data; writing and preparing the manuscript for publication.

[1] This article/chapter was published in Carbohydrate Polymers, Available Online March 4, 2024, Reference Number CARP 122018, PII S0144-8617(24)00244-3
Copyright Elsevier 2024

4.2. Introduction

Within the realm of pharmaceuticals, CDs generally serve as excipients, enhancing the solubility and stability of poorly soluble drugs while increasing their bioavailability and controlled release profiles (Arima et al., 2017; Brewster & Loftsson, 2007; European Medicines Agency, 2017). Notably, however, sugammadex (Welliver, 2008), marketed as Bridion™ (Merck and Co, Inc., 2015) (Fig. 7), has achieved blockbuster status in neuromuscular blockade (NMB) reversal - this CD-based drug is able to form rapid and efficient inclusion complexes with steroidal neuromuscular blocking agents (NMBAs), allowing patients to come out of surgery safely and comfortably (Keating, 2016; Nag et al., 2013).

NMBAs are essential medications for relaxing the muscles during a surgical procedure. Sugammadex works by directly and rapidly encapsulating the NMB-inducing drug rocuronium (Fig. 7), shielding it from receptors and escorting it out of the body via the kidneys (Isik et al., 2016). This effectively reverses NMB at all levels, without impacting nicotinic or muscarinic receptors and preventing cholinergic side effects like respiratory muscle weakness, excessive salivation, or arrhythmias (Haerter & Eikermann, 2016). Sugammadex is a γCD with each glucopyranose unit substituted at the O6 position (the so-called 'small' or 'primary' face of the CD, as opposed to the 'large' or 'secondary' face of the CD, where the O2 and O3 atoms reside) by a negatively charged carboxyl thioether group (Bom et al., 2002; Keating, 2016; Kovac, 2009; Merck and Co, Inc., 2015; Nag et al., 2013; PubChem, n.d.; Welliver, 2008). The position of these substitutions elongates the cavity and allows rocuronium to fit more snugly, while the negative charges enhance both the electrostatic binding of positively charged rocuronium and the structure of the inclusion complex by forcing the cavity open due to the substitutions repelling each other (Haerter & Eikermann, 2016; Nag et al., 2013).

The negative charges on sugammadex are physically close to the positive charge on rocuronium in the X-ray crystal structure (Bom et al., 2002), while the uncharged side of rocuronium protrudes slightly from the uncharged large face of the CD. This favorable interaction results in a tight inclusion complex in which rocuronium is fully encapsulated and solubilized, allowing the reversal of neuromuscular blockade. The published K_A for this inclusion complex is 1.05e7 M^{-1}, measured by Isothermal Titration Calorimetry (ITC) (Bom et al., 2002). CDs can exhibit a wide range of affinities for various CD/guest combinations (Tahıl et al., 2023) but a typical use case in drug formulation would have a K_A of approximately 1e3 to 1e4 M-1 (Angelova et al., 1999; Z. Wang et al., 2020). Considering this, it is clear that the strong affinity of sugammadex for rocuronium is what makes it such an effective drug. Kinetic assessments reveal that a 90% recovery from NMB is achieved in less than 3 minutes following specific intravenous doses of Bridion™ (0.5 mmol·kg-1) (Balaka et al., 2011). The efficiency of Bridion™ in encapsulating and neutralizing rocuronium highlights the significance of understanding these interactions, laying the foundation for developing targeted treatments that effectively address specific medical requirements. Atomic-resolution computational simulations represent a multifaceted approach to understanding the behavior of molecules, offering cost-effective and time-efficient predictions prior to lab experiments. In particular, unbiased and biased molecular dynamics (MD) simulations account for all possible degrees of freedom, allowing the observation of spontaneous interactions in a virtually recreated environment, including the explicit presence of the solvent or any possible co-solute, ionic strength, temperature, and even local pressure fluctuations (Blanco-González et al., 2023; Bonnet et al., 2002; Piñeiro et al., 2007). Simulations not only have the capability to replicate or predict quantitative parameters that can be found from experiments, but also provide more detailed information that is not accessible by any experimental method.

USC
UNIVERSIDADE DE SANTIAGO DE COMPOSTELA

Past computational and experimental studies revealed that, despite their conventional depiction as rigid truncated cone structures, CDs exhibit significant flexibility and noncovalent interactions in both solid and solution states, a dynamic trait that holds significant relevance for capturing precise interactions in computational studies (Anderson et al., 2024; Choi et al., 2000; F. Garrido et al., 2020; Hernandez-Pascacio et al., 2016; Irani et al., 2023; L. Li et al., 2018; Piñeiro et al., 2007, 2021, 2022). Accurate simulations of CD systems require careful parameterization of the involved molecules, i.e. the use of a reliable forcefield and of the involved parameters (bond lengths, angles, force constants, partial charges, Lennard-Jones constants and any other interaction or geometrical parameter) as well as of the algorithms involved in the control of temperature, pressure and sampling. The analysis of this data is also crucial, given the substantial amount of information they provide. Unlike protein systems, there is a lack of publicly available computational tools and algorithms specifically designed for analyzing CD systems. While traditional analyses performed for protein systems, such as calculating the RMSD of fluctuations and radius of gyration, may yield some useful insights for CD systems, other standard analyses like determining secondary structures, as defined for proteins, are not applicable to CDs. However, specific analyses are pivotal for CD systems, such as the calculation of the number of water molecules within the CD cavity, the establishment of reference axes to define orientations or displacements, and the accurate determination of affinity constants for the target encapsulation process. It's noteworthy that, unlike proteins, CDs are well-suited for atomic resolution computational simulations due to their relatively small size, enabling the generation of significantly longer trajectories compared to larger molecular entities.

Another issue that should be seriously considered for CD-systems is the location and distribution of chemical substitutions along the glucopyranoside rings and their impact in the experimental observables, as well as in the practical applications. Most applications of CDs are based on chemically modified structures, which are typically synthesized as a heterogeneous distribution of many different entities where the new chemical groups replace the hydroxyls of the CD at positions O2, O3, or O6 of the glucopyranoside rings (with different probabilities). Thus, the validation of new computational methods to obtain accurate information of CD-systems is much easier for a molecule where this problem is not present, such as that of rocuronium and sugammadex. This system is distinct in that, unlike other CDs which may have a variety of substitutions leading to different regioisomers and numbers of modifications, sugammadex, by design, possesses only one specific regioisomer.

In this chapter, our goal is to offer a comprehensive and precise account of the formation of the rocuronium and sugammadex complex. Computational simulations are expected to not only replicate the quantitative parameters observed in experiments, but also uncover detailed information that traditional experimental methods cannot access. This approach will fill knowledge gaps about the sugammadex-rocuronium complex, and validate the simulation methodologies for broader applicability to other CD-based complexes. The availability of these methods is of key importance for the development of CD-based applications because they are quick and cheap compared to wet-lab approaches, and can be massively employed for hundreds or even thousands of systems with a reasonable effort. By leveraging the lessons learned from the rocuronium-sugammadex interaction, we can potentially create a blueprint for future endeavors in molecular engineering, expanding our toolkit for addressing an array of challenges, from toxin neutralization to targeted drug delivery and beyond.

USC
UNIVERSIDADE DE SANTIAGO DE COMPOSTELA

4.3. Specific Methods

4.3.1. Parameterization and Geometry Optimization

Initial coordinates and the topology file for rocuronium were obtained from the ATB server (Malde et al., 2011). The up orientation corresponds to the complex where the *N*-allyl-pyrrolidinium group of rocuronium is oriented towards the eight carboxyl thioether groups of the CD; in the down orientation, this group faces the unsubstituted side of the CD, where the secondary OH groups are located. These structures are placed in a 7x7x7 nm^3 dodecahedron simulation box and solvated with approximately 7800 explicit SPC water molecules, removing those overlapping the solute molecules and neutralizing negative charges with Na^+ ions. All the methods used in this chapter are described in **Chapter 3. Methodological Framework**.

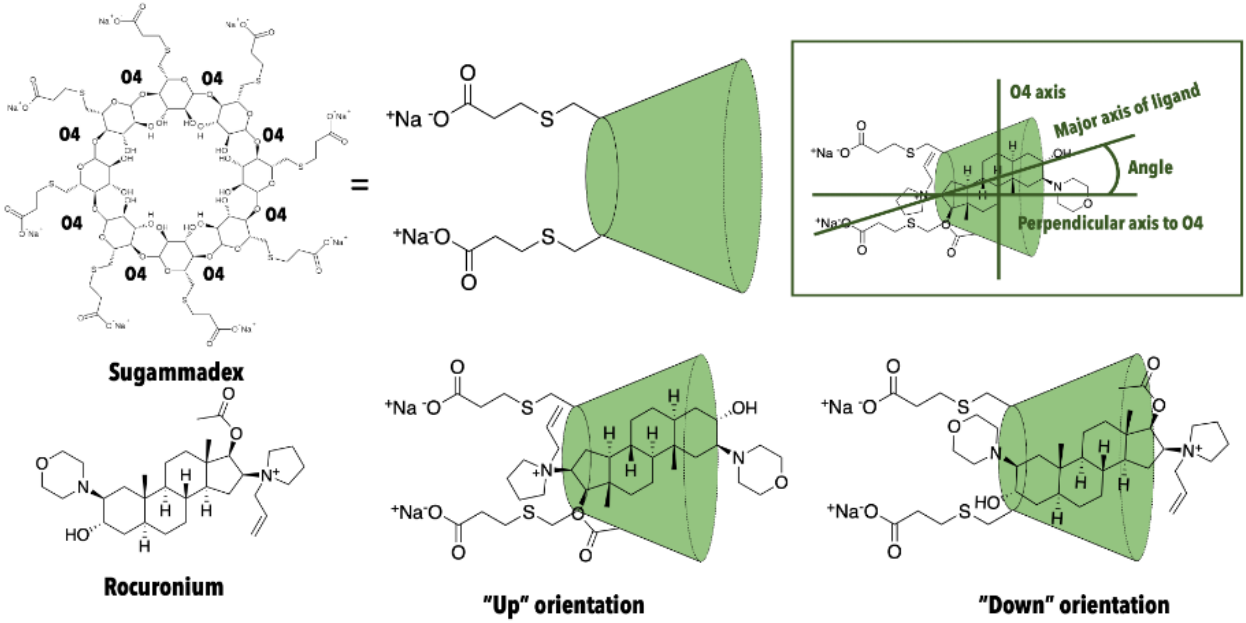


Figure 7. 2D chemical structure of sugammadex, marketed as Bridion™, highlighting the O4 oxygens, alongside the structure of rocuronium. The complex is presented in both 'up' and 'down' orientations. In the 'up' orientation, the *N*-allyl-pyrrolidinium group of rocuronium is oriented towards the eight carboxyl thioether groups of the CD. In the 'down' orientation, this group faces the CD's unsubstituted side, where the secondary OH groups reside. The principal axes of both the target and the CD are also depicted, including the angle between them.

4.4. Results

4.4.1. Docking

The docking results for the sugammadex - rocuronium complex were highly conserved, with all of the top outputs having the rocuronium deeply embedded in the CD cavity (Fig. 8). The binding energy calculated by Vina ranged from -5.38 to -5.76 kJ/mol. The orientation of rocuronium was also highly conserved in the up orientation for the top 8 outputs. Importantly, the input orientation of rocuronium for docking is agnostic, as the two molecules are combined with no starting conformation. However, the structure of the CD may be slightly different if the geometry is optimized for one target orientation or another, so half of the input structures were optimized in up, and the other half in down. Thus, the orientation of the complex is

USC UNIVERSIDADE DE SANTIAGO DE COMPOSTELA

normalized, and a strong preference for the up orientation is detected by docking calculations and in agreement with the crystal structure (Bom et al., 2002).

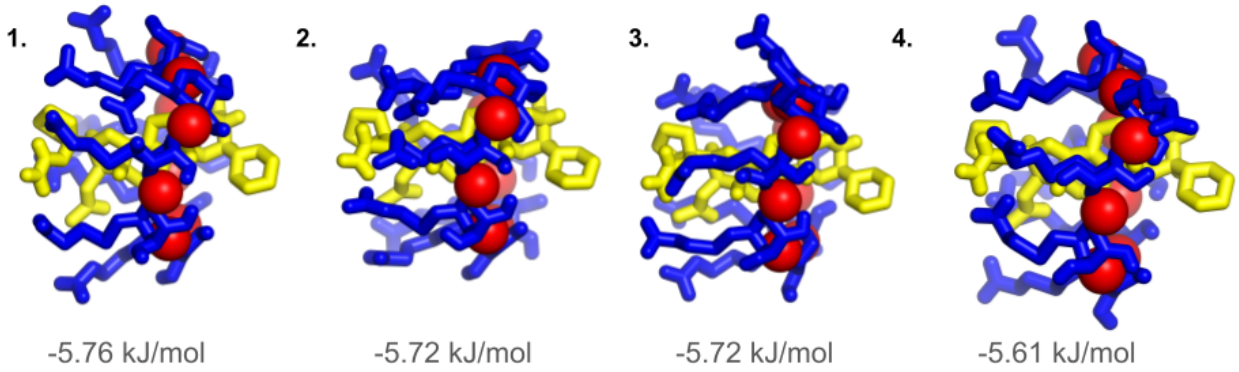


Figure 8. Four most favorable docking poses obtained from the protocol analyzing the interaction between sugammadex and rocuronium, derived from 10 unique initial conformations, ordered by their docking binding energy.

Additionally, there is good alignment between the top docking output and the minimum suggested by the more rigorous PMF calculations in the up orientation (RMSD = 1.875 Å for the entire complex [Fig. S1]), but the complex is quite flexible, especially regarding the CD substitutions.

4.4.2. Unbiased Molecular Dynamics

The MD simulations also showed strong, consistent interaction between rocuronium and sugammadex, where none of the complexes disassociates within the first 500 ns of unbiased MD (even without restraints). However, some of the simulations (ie #3 and #4 in Fig. 9) do show the rocuronium less deeply embedded in the CD cavity, probably showing the sampling of a local minimum where rocuronium directly interacts with the substituted groups without threading the CD cavity (see PMF results). The total MD interaction energy for the strongest and most ideal inclusion complex had a total MD energy of -269 kJ/mol, with -94 kJ/mol coming from Coulombic contributions and the remaining -175 kJ/mol from Lennard-Jones contributions. The weakest interaction was found to be -158 kJ/mol, with -34 kJ/mol coming from Coulomb and -124 kJ/mol coming from Lennard Jones, and the the *N*-allyl-pyrrolidinium moiety of rocuronium was situated towards the large face, protruding from the unsubstituted side of the cavity (SI, #8). Notably, when rocuronium was less deeply embedded in the cavity in more energetically favorable simulations (#3 and #4), it tended to be on the opposite (small, substituted) face of the CD.

It is important to note that the input structures of the simulations are not equivalent to each other - they correspond to the centroids of structural clusters and were designed to represent a variety of realistic structures as different starting points. Consequently, some initial structures are expected to be less stable than others.

Fig. 9 shows the top four outputs, ranked by total MD energy, as well as input conformations and the evolution of the analyzed quantitative properties along the trajectories (see methods section). Generally, a flat, consistent pattern for all the computed features was observed, indicating high stability of the structures. The ‘angle’ analysis (top row) shows the orientation of rocuronium; in Fig. 9, output #1, #3, and #4 are in the up orientation (angle ≅ 180°) while output #2 is in the down orientation (angle ≅ 0°). The number of

USC
UNIVERSIDADE DE SANTIAGO DE COMPOSTELA

water molecules in the CD cavity is a clear indicator of the conformation of the inclusion complex; this descriptor is also sensitive to the relative orientation of the ligand. Fig. 9 shows this property in the bottom row of the plot for each trajectory. Trajectories #1 and #2 both show rocuronium well inside the CD cavity throughout the duration of the MD simulations, but with opposite orientation with respect to the CD main axis. The number of water molecules inside the CD cavity is significantly higher and more variable in #1 than in #2, showing that the down orientation is more restrictive than the up orientation for the approaching of solvent molecules to the core of the CD. The evolution of water molecules in Fig. 9, #3 and #4 is even more informative - at a glance, it is clear that the ligand moves in and out of the cavity throughout the trajectories, reaching a relatively stable interaction with the CD that is compatible with up to 10 water molecules inside the cavity. The energies extracted from these simulations using GROMACS tools are described in Table 1.

Table 1. Summary of the top four MD systems energies, extracted using GROMACS tools.

Ranking	Orientation	Total Energy (kJ/mol)	Coulomb (kJ/mol)	L-J (kJ/mol)
1	Up	-269 ±37	-94 ±24	-175 ±13
2	Down	-244 ±44	-75 ±31	-169 ± 13
3	Up	-238 ±53	-72 ±30	-166 ±23
4	Up	-236 ±49	-68 ±28	-168 ±21

These values account only for the direct interaction between the target and the CD molecule, so they are not thermodynamic binding energies, but they provide useful information to understand how the two molecules behave. It is notable that in all cases the L-J energy contribution is much higher than the Coulomb contribution, and also that the fluctuation of the LJ energy along the trajectories is significantly lower both in relative and in absolute terms. Thus, even if the rocuronium and the chemical modifications of the CD have charges of different sign, the combination of L-J contributions are strong enough to stabilize the structure. Interestingly, the L-J and Coulombic contributions of the optimal down orientation (trajectory #2) are comparable to the values corresponding to the trajectories #3 and #4, where the ligand oscillates between the global and a local minima. Both energy contributions corresponding to the optimal structure in the up orientation (trajectory #1) provide the most negative values amongst all the simulations (see Table 1).

USC
UNIVERSIDADE DE SANTIAGO DE COMPOSTELA

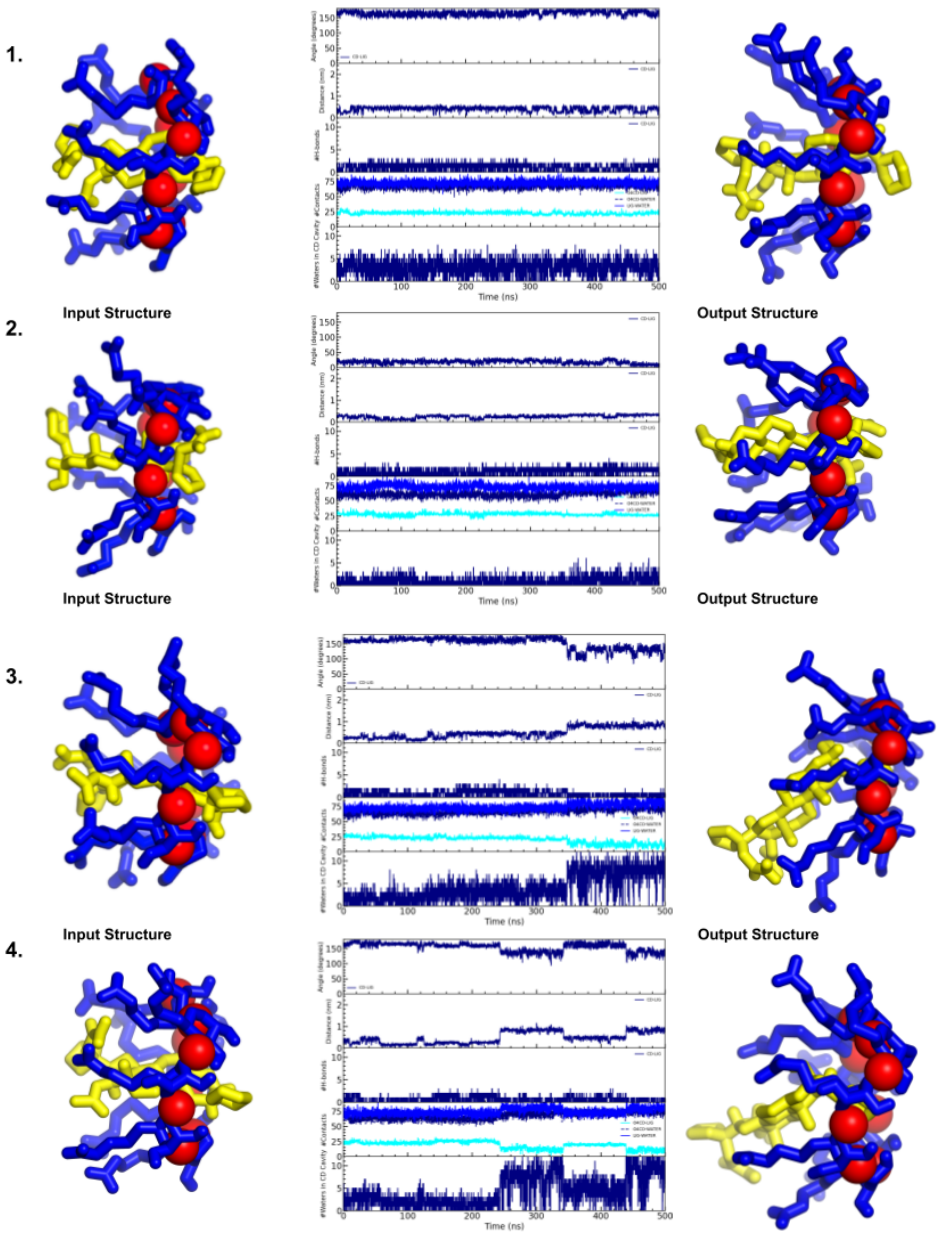


Figure 9. Four most favorable MD results from the protocol running sugammadex (blue) + rocuronium (yellow), ranked based on the final MD energy. Note that the 'angle' analysis shows the orientation of rocuronium - 1 and 3 are in the up orientation (angle ≅ 180°) while 2 is in the down orientation (angle ≅ 0°). Each simulation has five associated analyses (middle plots). From top to bottom, each plot shows, over 500 ns: the angle between the CD and rocuronium (degrees), the distance between the COM of the two molecules (nm), the number of H-bonds between the CD and rocuronium, the number of contacts between the CD and rocuronium (solid red), the CD and water (dotted red), and the rocuronium and water (blue), and finally the number of waters in the CD cavity.

Although docking calculations consistently indicate an up orientation of the complex aligning with crystal structures, MD simulations reveal that the down orientation is nearly as favorable, if we consider just the potential energy of interaction between both molecules. This is supported by the substantial Lennard-Jones energy contributions, indicating that electrostatic interactions are not the primary driving force, contrary to

USC
DE SANTIAGO
DE COMPOSTELA

what might be assumed. This somewhat surprising result has also recently been found by Irani et al (Irani et al., 2023) in a separate computational study using unbiased MD simulations. Furthermore, the total energy of interaction in the down orientation, while lower than the best up orientation structures, is still significant and practically equivalent, considering the uncertainty range. These results are consistent with docking and experimental X-ray structures, suggesting that the up orientation is more probable, but the down orientation could be notably present in the normal distribution of dynamic binding states. This will be better quantified by the thermodynamic binding energy (see metadynamics results in the following section).

4.4.3. Metadynamics and PMF

As explained in the methods section, twelve walkers were used, each contributing simultaneously to the metadynamics simulation. PMF profiles were obtained from the combined analysis of the twelve, 300 ns trajectories with the described parameters and restraints. These curves are rich in information and provide useful insight on how the molecules can be encapsulated (the binding pathway), but it is important to ensure that the calculation is of good quality before making conclusions. This can be determined by the overlapping of the different curves obtained for periods of 1 ns (see methods section) and by the value of the ΔG^0 in the unbound region for both sides of the CD because the energy interaction at long distances is expected to be minimal, and the thermodynamic ΔG^0 between the bound and unbound states should be independent of the path used to transition between these states. As observed in Fig. 10, this holds true to a very good approximation for both PMF profiles, and the convergence is very good since the PMF profiles are stable over the last 20 ns of the trajectory (Fig. 10).

Reproduction of experimental results also lends credibility to computational methods. In our case, the numerical values of the association constants calculated from the PMF profiles (see Methods), as well as the structures at the energetic minimums, are exceptionally well aligned with reported values (1.07e07 L/mol for PMF vs 1.05e07 L/mol reported by ITC (Bom et al., 2002). Note that the estimated uncertainties for both the computational and the experimental values are comparable (12% and 15% for the up and down orientations from PMFs and 15% for the value obtained from ITC). Note also that the K_A values obtained from the up and down simulations can be combined in a single K_A just by adding both values. This is very easy to demonstrate from the definition of the association constants, and thus the overall association constant obtained from the metadynamics simulations is:

$$K_A = \frac{[up] + [down]}{[CD] \cdot [ROC]}$$

where [up] and [down] represent the concentration in the solution of up and down species while [CD] and [ROC] represent the concentration of free (out of the complexes) sugammadex and rocuronium molecules. Thus, the metadynamics simulations predict that the up orientation dominates the solution, as supported by the X-ray structure, the docking studies and the unbiased MD simulations, but the presence of complexes with the down orientation is still possible and not negligible at all - our simulations suggest that it could comprise nearly 10% of the complexes if they exist in proportion to their calculated affinity constants. This quantitative result is important to understand the behavior of this system and it should be considered when designing other CDs for other purposes based on similar mechanisms.

USC
UNIVERSIDADE DE SANTIAGO DE COMPOSTELA

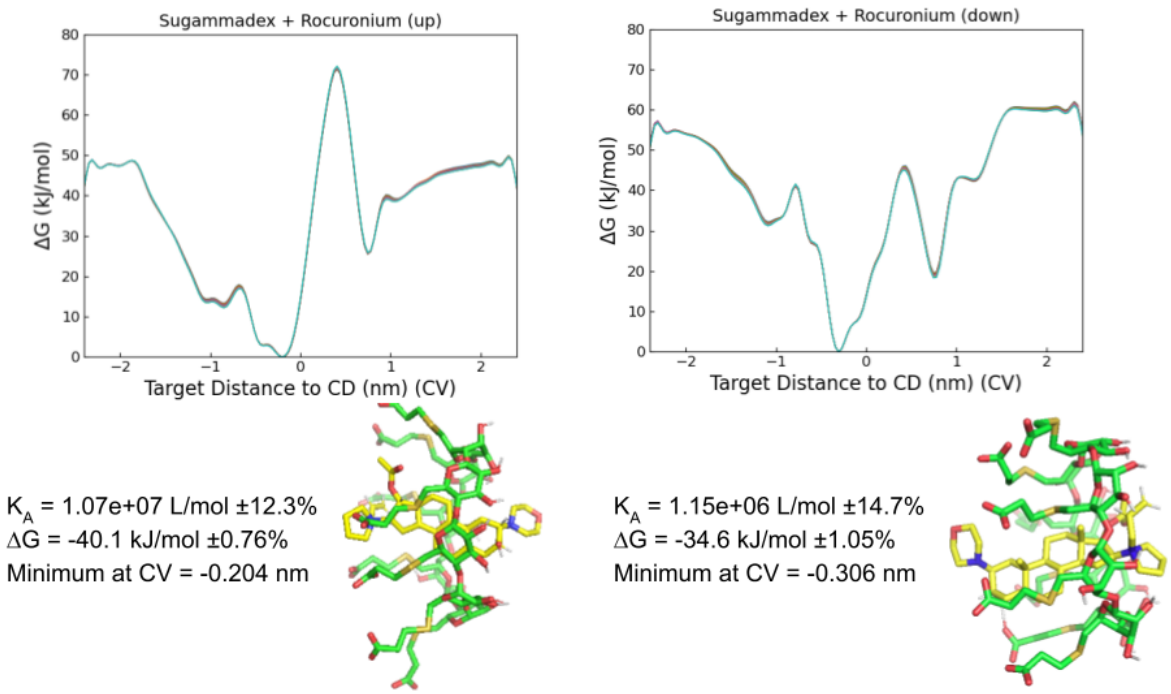


Figure 10. PMF profiles obtained from metadynamics simulations together with the minimum energy structure. The sugammadex is shown with green carbons while rocuronium has yellow carbons.

As stated above, the thermodynamic calculations clearly indicate that the up orientation is significantly more probable than the down, but the PMF profiles are non-symmetric in the bound region. Both PMFs exhibit an energy barrier at CV ~ 0.5 nm, but that of the up orientation is much higher than for the down counterpart, suggesting that the down orientation could associate equally well from both sides of the cavity, while the up orientation strongly prefers association via the small face. The energy barriers are connected to the kinetics of the process, so the encapsulation through the negative values of the CV (the substituted, narrow face) is much faster than that by the positive (unsubstituted, wide) side, especially in the up orientation. This demonstrates that the substitutions indeed contribute to the encapsulation of the target, mainly in the up orientation While the up orientation is still preferred, the stability of the down orientation highlights the importance of cooperative, nonspecific forces between the molecules and the solvent. It is noteworthy that, in the minimums suggested by PMF, the presence of a hydrogen bond between the OH of rocuronium and an oxygen in one of the carboxyl thioether groups may also contribute to the surprising favorability of the down orientation (Fig. S4-2), but the main contribution is still driven by the solvent effects.

4.5. Discussion

The ability to precisely characterize inclusion complexes in CD-target systems solely through computational methods, without the need for synthesizing new molecules in the lab, paves the way for conducting extensive simulations to develop or optimize many different CD-based applications. It is crucial, therefore, to demonstrate the reliability of these results and to fully leverage the insights offered by the methods used. In this case, the sugammadex-rocuronium complex is taken as an ideal and challenging model to validate several computational methods proposed to characterize the interaction between CDs and targets. This system was chosen because of the clinical interest of Bridion™ and the subsequent availability

USC UNIVERSIDADE DE SANTIAGO DE COMPOSTELA

of accurate experimental information on the interaction of both molecules. This system is also ideal for the fact that the substitution pattern cannot be contaminated by different species of the CD - all hydroxyl groups at position O6 are substituted by the carboxyl thioether group. A typical modified CD is only available as a distribution of many different isomers with different number and location of modified groups, making validation more challenging.

Our results demonstrate that computational methods can be effectively employed to quantify CD-target interactions. The applied multi-faceted computational approach encompasses docking, unbiased molecular dynamics, and metadynamics simulations, each method offering unique insights into the structure, interaction mechanism, dynamics, and kinetics, as well as on the energy profiles corresponding to the formation of the inclusion complex. We put special emphasis on preventing any human bias in our results, and all the employed methods have been fully automated to remove any potential irregularities or human errors. In principle, the methods presented here could be applicable to other macrocyclic molecules able to encapsulate ligands in their cavity, but this method has been specifically developed for inclusion complexes. Other types of complexes would probably require different CVs and approaches to determine association constants.

The docking studies yielded highly conserved results with rocuronium predominantly being situated deeply within the CD cavity, highlighting the strength of the interaction. Notably, the orientation of rocuronium showed a marked preference for the up conformation, in agreement with empirical evidence from crystallographic studies (Bom et al., 2002). However, the binding energy values provided by docking are based on scoring algorithms and cannot be directly compared to those obtained by other methods. Unbiased MD simulations reinforced the findings from the docking studies, providing much more detailed information. The enduring interaction between sugammadex and rocuronium across the trajectories is indicative of a stable and specific interaction, and the majority of the simulations as well as the energy values obtained for the interaction between the CD and the target further corroborated the predominant up orientation of the rocuronium molecule, accentuating its favored position in the complex formation. This consistency between our computational outputs and the actual crystal structure serves as a testament to the reliability of our computational protocol.

Metadynamics, a powerful tool in exploring the free energy landscape, was applied to provide a comprehensive PMF profile of the sugammadex-rocuronium interaction. This rigorous method provides mechanistic and structural information by linking the kinetics of the interaction to the energy barriers along the considered pathways, as defined by the CV. Metadynamics/PMF calculations generated results in line with reported values, fortifying our confidence in the methods (1.07e07 L/mol for PMF vs 1.05e07 L/mol reported by ITC (Bom et al., 2002). This suggests a robust and dependable computational methodology. Notably, two of the three MD simulations in the up orientation (Fig. 9, #3 and #4) sampled two stable positions, one in which the rocuronium was less deeply seated in the CD cavity, with #4 actually oscillating between the two positions. This was recapitulated by the presence of a peripheral energy well in the PMF profile of the up orientation (Fig. 10), at approximately CV = -1, suggesting that there are two favorable positions of the complex in this orientation. The other, less favorable energy wells in the PMF profiles were not observed by MD. The PMF profiles also suggest that the rocuronium is most likely to associate from the substituted (small) side of the CD in the up orientation, probably facilitated by electrostatic interactions as the negatively charged substitutions ‘grab’ the positively charged rocuronium and pull it into the cavity.

USC
UNIVERSIDADE DE SANTIAGO DE COMPOSTELA

In addition to the accurate prediction of the association constant from the metadynamics simulations, the optimal structure obtained from the metadynamics simulations also agrees very well to that obtained from the X-ray crystal structure. We have made significant effort to prevent any human bias in all the calculations, so all of our results are rigorously obtained. This provides additional confidence in results that are obtained from our simulations that are not accessible from physical experiments.

While each computational approach offers a different perspective on the interaction, a recurring theme is the consistent preference for the up orientation of rocuronium within the sugammadex complex. This preference, echoed across the methods, not only aligns with experimental evidence but also suggests the possibility of the lesser-observed down orientation existing in solution. While this down conformation is apparently less energetically favorable by an order of magnitude, its presence cannot be completely ruled out, suggesting a dynamic interaction in solution. The up orientation makes more structural sense, considering the charge interactions between the molecules, but the MD simulations suggest that the L-J interaction is quite strong - strong enough to still allow for a stable interaction even when the charges are not so close to each other. This is recapitulated by the PMF calculations, showing only an order of magnitude of preference for the up over the down orientation, which is not as strong of a preference as might be assumed. Interestingly, the PMF profiles also suggest that the substitutions at position O6 are key to facilitating the formation of the complex, primarily in the up orientation. This seems to be caused by the lack of energy barriers that the target encounters when traveling through the cavity of this gamma CD, which is the widest of the three predominant CDs.

The collective insights gained from this multi-pronged computational study provide a comprehensive understanding of the sugammadex-rocuronium interaction. Beyond the specific insights into this particular complex, the potential of our methods in predicting the behavior of CD complexes is validated as far as is possible in this study. MD and docking simulations are computationally efficient and inexpensive for these types of systems, compared to those for other biomolecules such as proteins, and this study shows that we can recapitulate known characteristics of CD inclusion complexes quickly using these methods. PMF, while more computationally expensive, stands out as a powerful tool in predicting realistic affinity constants of known and novel CDs prior to synthesis for the purpose of drug discovery and molecular design. This capability can greatly accelerate the process of identifying and developing novel therapeutic candidates, reducing both time and costs associated with experimental synthesis and testing.

4.6. Conclusion

The goal of this study was to use a series of computational methods to investigate the sugammadex-rocuronium inclusion complex. It was hypothesized that, using this series of in silico methods, a reasonable estimation of the affinity constant and structure of the inclusion complex could be obtained. Indeed, the most favorable conformation identified for the inclusion complex, using all of the methods explored here, corresponded well with the identified crystal structure. In addition, the accepted affinity constant obtained by ITC experiments (Bom, 2022) was closely reproduced by PMF calculations. These results offer validation for the use of an entirely computational method to determine CD inclusion complex conformations as well as affinity constants. This can be extremely powerful for the in silico design of specific CDs, and opens the door for applying AI and ML to CD development.

USC
UNIVERSIDADE DE SANTIAGO DE COMPOSTELA

Chapter 5. Cyclodextrins: Establishing Building Blocks for AI-Driven Drug Design by Determining Affinity Constants *in Silico*[2]

5.1. Preface to Contextualizing the Research: Insights into Authorship, Contributions, and Publication Specifics

The next step of our method validation is aimed at exploring the encapsulation of sterols by modified βCDs - a critical component for designing specific oxysterol encapsulators. Here, we employ PMF calculations obtained from guided metadynamics simulations to characterize the 1:1 inclusion complexes between four different modified βCDs, with different type, number, and location of substitutions, and two sterol molecules (cholesterol and 7KC). Our methods, validated for reproducibility through four independent repeated simulations per system and different post processing techniques, offer new insights into the formation and stability of CD-sterol inclusion complexes. A systematic, distinct orientation preference where the sterol tail projects from the CD's larger face and significant impacts of CD substitutions on binding are observed. Notably, sampling only the CD cavity's wide face during simulations yielded comparable binding energies to full-cavity sampling, but in less time and with reduced statistical uncertainty, suggesting a more efficient approach. Bridging computational methods with complex molecular interactions, our research enables predictive CD designs for diverse applications. Moreover, the high reproducibility, sensitivity, and cost-effectiveness of the studied methods pave the way for extensive studies of massive CD-ligand combinations, enabling AI algorithm training and automated molecular design.

Title: Cyclodextrins: Establishing Building Blocks for AI-Driven Drug Design by Determining Affinity Constants in Silico

Authors: Amelia Anderson, Rebeca García-Fandiño, Ángel Piñeiro, Matthew S. O'Connor

Year: 2024

Publisher: Elsevier Ltd.

ISSN/ISBN: 2001-0370

DOI: https://doi.org/10.1016/j.csbj.2024.02.011

Quality indexes: Computational and Structural Biotechnology Journal is a journal covering the technologies/fields/categories related to Biochemistry (Q1); Biophysics (Q1); Biotechnology (Q1); Computer Science Applications (Q1); Genetics (Q1); Structural Biology (Q2). It is published by Elsevier on behalf of the Research Network of Computational and Structural Biotechnology.

[2] This article/chapter was published in Computational and Structural Biotechnology Journal, Available Online February 16, 2024
Copyright Elsevier 2024

Contributions: As the leading and corresponding author of this work, my involvement was multifaceted and critical to the project's success. My key contributions were: designing and conceptualizing the research study; developing and implementing the computational methodologies employed; analyzing and interpreting the resulting data; writing and preparing the manuscript for publication.

USC
UNIVERSIDADE DE SANTIAGO DE COMPOSTELA

5.1. Introduction

CDs can be chemically modified by substituting the hydroxyls with other functional groups, such as methyl, HP, or SB. These modifications lead to distributions of structures with different numbers and locations of the substitutions which can improve the solubility of the CD and alter their properties in various ways (Chatjigakis et al., 1992; Del Valle, 2004; Frijlink et al., 1990; Irie et al., 1992; Kovac, 2009). The average number of functional groups in the distribution of chemically modified CDs is denoted as the degree of DS. These modifications can also modulate the selectivity for the encapsulation of certain molecules as well as their release rate (Kovac, 2009; Moser et al., 2001; Skanchy et al., 1999), thus opening an opportunity to develop *ad hoc* applications.

The development and optimization of applications based on CDs depend on their ability to encapsulate molecules into their hydrophobic cavity. However, actually measuring the affinity constants between CDs and sterols is difficult and unreliable due to solubility problems, stoichiometric considerations, and the presence of a distribution of CD structures in the case of substituted CDs. Therefore, experimental affinity constants are often reported as "apparent" affinity constants, and there is no accepted experimental value for many of these systems, particularly when the guest is poorly soluble and uncharged, as cholesterol is (Anderson et al., 2024; Schönbeck et al., 2024; Šolínová et al., 2016; Sursyakova et al., 2022). Here, we aim to establish an effective and efficient tool for obtaining reliable affinity constants for individual CD inclusion complexes using in silico methods. If this tool was validated, it could enable the automated production of many association constants for many CD inclusion complexes. This would open the door for AI and ML training on a system for which we have very little practical control over in vitro, but we have very precise control over in silico. Such a tool could revolutionize our understanding of CD inclusion complexation. For certain uses, such as the extraction of harmful or undesirable molecules from organisms or from the environment, a high affinity constant and a very low release rate are required to achieve high specificity. A notable example is the use of the engineered sugammadex to capture the neuromuscular blocker rocuronium (Welliver, 2008) In contrast, employing CDs as excipients necessitates a substantial, though comparatively lower, affinity constant, along with lower specificity and a more flexible release rate. This distinction is critical; using a CD with a very high affinity for an active compound can impede its intended function by preventing its release. Therefore, the accurate quantification of CD-target complexation affinity constants and specificity to distinguish targets/off-targets is key for designing and optimizing CD-based applications.

Historically, this has been achieved through a rational approach, assisted by trial-and-error assays. However, artificial intelligence (AI) algorithms represent a family of promising alternative methods for the same aim; the bottleneck of this approach is the availability of a large volume of high-quality data to effectively train models. Acquiring such data for CD systems is challenging due to several factors, including solubility issues of the compounds involved, the potential presence of impurities, and notably, the diversity in the number and location of substitutions in modified CDs, not to mention the difficulties in correctly analyzing measurements from different sources. Recently, a publicly accessible database that compiles affinity constants for the formation of inclusion complexes between relatively small molecules and CDs, gathered from existing literature, has been published (Tahıl et al., 2023). This information has been obtained from different experimental methods published between the years 1963 and 2021, and includes mainly ITC and various spectroscopic techniques. This publication represents an extraordinary effort to collect affinity data between CDs and ligands, but the sources are highly heterogeneous and difficult to control, reproduce,

USC
UNIVERSIDADE
DE SANTIAGO
DE COMPOSTELA

or scale. Important uncertainties are also present due to the different sources of the samples, experiments, and analysis methods, complicating analysis. Additionally, the employed techniques face challenges both in conducting effective experiments and in analyzing results. This is because complex protocols are often necessary, including competitive experiments with a reference compound, chemical labeling of molecules, or manipulating the solvent.

It is important to keep in mind the fact that none of these methods actually measure affinity constants directly - instead, they rely on the application of thermodynamic models coupled with numerical and statistical calculations. Best practices involve the global fitting of multiple data sets across different concentration ranges, and the employment of advanced mathematical methods, along with estimating reasonable uncertainty values for numerical parameters. The results typically yield apparent values or approaches useful for specific applications within a limited context, rather than direct thermodynamic affinities. Thus, truly direct laboratory measurements of affinity constants remains an unattainable ideal as of yet, but reasonable estimations are possible in many cases by applying robust multidimensional models to multiple experiments (Anderson et al., 2024). In this context, massive production of many thousand *in vitro* systems that include a large variety of CDs with specific types, numbers, and locations of substitutions, along with diverse ligands for the purpose of training AI-based algorithms, presents significant challenges in terms of complexity and cost.

The use of computational modeling represents an exceptional and increasingly realistic complement to *in vitro* assays for characterizing the interaction between molecules - particularly between CDs and small molecules that can potentially be encapsulated in their cavity. These methods can provide important insights to the mechanism of interaction between molecules, saving money, time, and resources by predicting how a molecule might act before synthesizing and/or testing it (Ramírez, 2016). Additionally, they can be fully automated and connected to a database which would be fed with the results. The information contained in such a database would be highly uniform and it would be very easy to scale the production to reach many thousand complexes. The database would enable precise control of the CD structures, including the type, number, and location of substitutions, and cover a variety of targets, considering the ionic state of the molecules, the presence of cosolvents, or any other environmental factor. These data could then be easily utilized to train AI algorithms. Employing such a workflow could significantly enhance the design and optimization of CDs for specific applications. The bottleneck to develop a platform based on this computational workflow is, again, just as with *in vitro*, the availability of accurate and efficient methods to determine the affinity constant of the encapsulation event. Different computational approaches are widely employed for characterizing protein-ligand interactions in both academic research and practical applications, but their use in the characterization of CD systems is quite limited. A reason for this is the lack of specific software available to automatically perform these studies, since the strategies typically employed to build, execute and analyze simulations of protein systems differ significantly from those that are more suitable for CDs (Arsiccio et al., 2021; Cézard et al., 2011; Mazurek & Szeleszczuk, 2022; Ott & Meyer, 1996; Senderowitz et al., 1996). To take advantage of computational simulations, careful parameterization of the involved molecules, efficient sampling algorithms and well-designed analysis methods able to provide as much information as possible, are always required. Specifically, while CDs are often depicted as rigid, truncated cone structures, they are actually quite flexible both in solution and in solid form. Capturing this behavior is crucial for accurately describing interactions in computational studies of CD systems (Dodziuk, 2002; F. Garrido et al., 2020).

USC
UNIVERSIDADE DE SANTIAGO DE COMPOSTELA

In this study, we have adapted and tested different approaches based on metadynamics simulations to simulate and evaluate CD-based inclusion complexes. In order to test these methods, 1:1 βCD-sterol systems were employed. Cholesterol (CHOL) and its oxidized form 7-ketocholesterol (7KC) were used as ligands for βCD structures with different type, number and location of substitutions. The difference between 7KC and native CHOL is miniscule: just one additional atom in 7KC, an oxygen forming a keto group at the position 7 (Fig. 3). This difference, small as it is, is apparently key to the development of many diseases such as atherosclerosis and Alzheimer's (Anderson et al., 2020). Thus, unlike cholesterol, which is essential for various physiological roles including cell membrane composition and hormone precursor functions, 7KC has disastrous effects in living organisms. This is the main reason to look for methods to selectively extract 7KC from cells without significantly affecting the concentration of CHOL. Encapsulation of the oxidized sterol by CDs has been proposed for this end (Anderson et al., 2021).

In this strategy, specificity for the encapsulation of 7KC over CHOL is crucial. Experimental evidence obtained from turbidity studies suggests that, in contrast to the native βCD, HPβCD exhibits specific behavior to capture 7KC over CHOL (Anderson et al., 2021, 2024). The detailed examination of 1:1 βCD-sterol systems featuring CHOL and 7KC serves as a preliminary model for our broader goal, which is to develop accurate and efficient computational methods that can be implemented in an automated workflow to produce affinity constants for thousands of inclusion complexes. These results enable training machine learning algorithms to design optimal modified CDs for specific purposes.

5.2. Specific Methods

The methods employed in this chapter have been detailed in **Chapter 3. Methodological Framework**. However, for clarity, certain specific aspects are outlined here:

5.2.1. Description of the Systems

PMF profiles were obtained to characterize the binding of CHOL and 7KC with native βCD, DS3 HPβCD, and SBβCD with DS3 and DS7 (Fig. 11). Regarding the modified CDs, the two DS3 structures, both with HP substitutions and SB substitutions, have these modifications at the exact same positions on the CD molecule.

USC
UNIVERSIDADE DE SANTIAGO DE COMPOSTELA

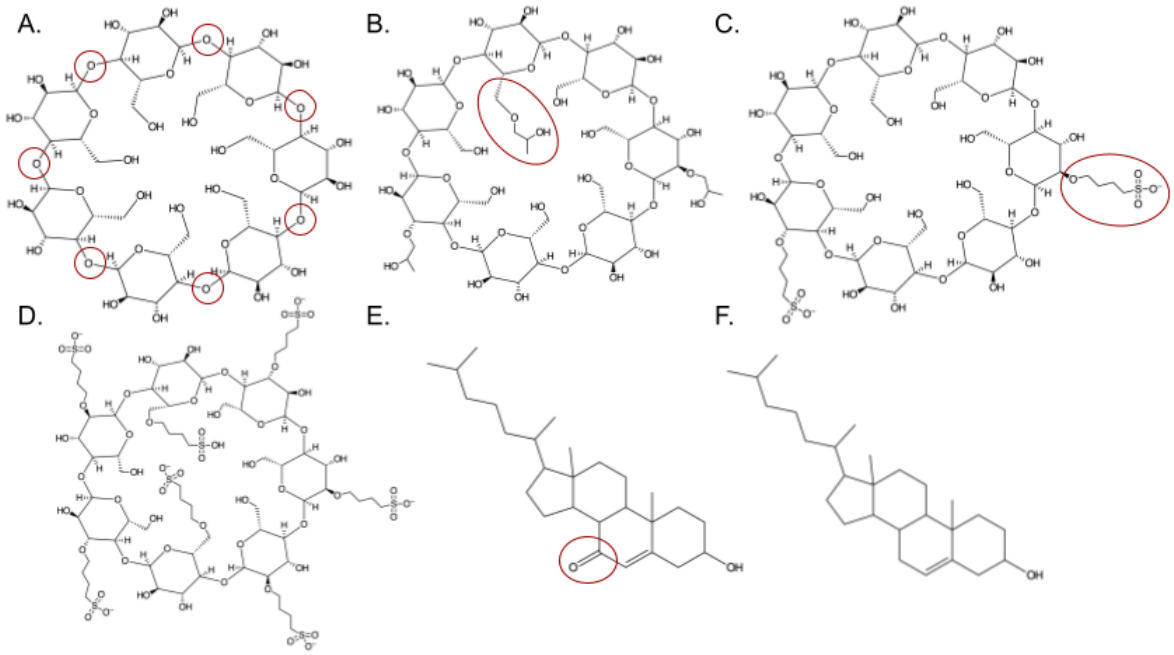


Figure 11. 2D structures of the molecules to be simulated. (A) Native βCD (O4 atoms circled in red) (B) DS3 HPβCD (one HP group circled in red) (C) DS2 SBβCD (one SBE group circled in red) (D) DS7 SBβCD (E) 7KC (oxygen at position 7 circled in red) (F) Cholesterol.

5.2.2. Simulation Parameters

The up orientation corresponds to the complex with the tail of the sterol molecule pointing to the large face of the βCD while the down orientation corresponds to the tail of the sterol molecule pointing to the small face (Fig. 7). Each of the 12 walkers was inserted in a 7x7x7 nm^3 dodecahedral simulation box, which was then filled with approximately 7800 SPC waters. The water molecules overlapping the solute molecules were removed and Na^+ ions were added to neutralize the total charge, when needed.

5.2.3. Metadynamics Simulations

The trajectories were carried out for 300 ns with walls at -2.5 and +2.5 nm between the sterol and the βCD to prevent the sterol from leaving the simulation box and crossing the periodic boundary. Each metadynamics simulation was repeated four times with slightly different distributions of the starting positions to check for reproducibility.

USC
UNIVERSIDADE DE SANTIAGO DE COMPOSTELA

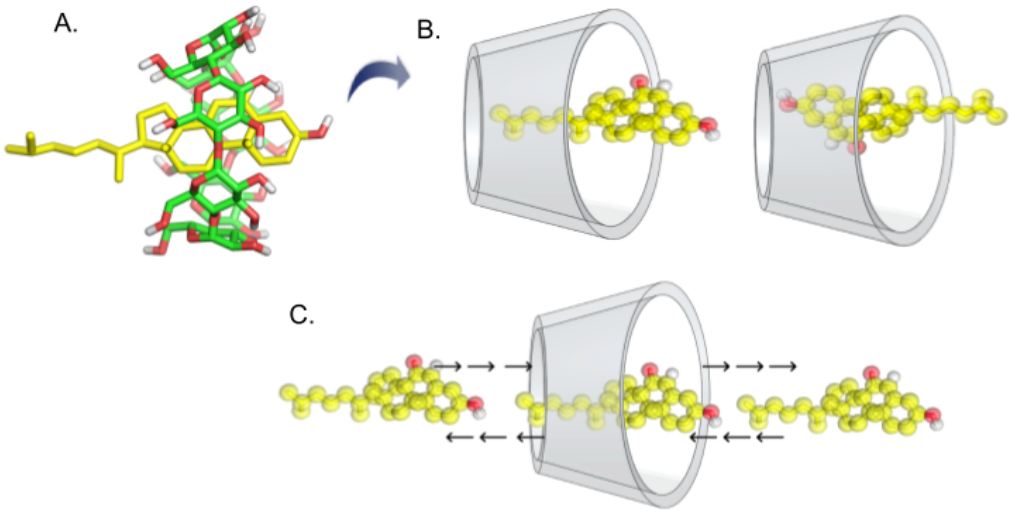


Figure 12. (A) 3D molecular structure of the bCD (green carbons) - 7KC (yellow carbons) inclusion complex. (B) Simplified cone representation of the bCD (where the smaller side is the primary face and the larger side is the secondary face) showing the up (left) and down (right) orientations of the inclusion complex. The target is shown in yellow. (C) Illustration of metadynamics simulations, where the target is guided through the cavity of the CD in each direction and in each orientation.

5.2.4. Potential of Mean Force (PMF)

The PMF calculation was performed two times with different limits of integration: once using the entire distribution of the CV (-2 to 2 nm, the "All Method"), and once considering only the wide face of the βCD (CV from 0 to 2 nm only, the "Wide Face Method"). It is expected that the targets will tend to form complexes via the wide face of the βCD, and sampling only half of the βCD will lead to a faster and still accurate result. In addition to association constants, from PMF profiles we can also get the energy wells and barriers of the encapsulation process as a function of the distance between the center of mass of both molecules and the most stable structures for each complex. By using these systems, we hope to gain insight into the effect of each substitution type on the complex.

5.2.5. Statistical analysis

The ΔG^0 values obtained from the PMF profiles using both integration methods ("All" and "Wide-Face") for the four metadynamics simulations of each CD + sterol combination and for both orientations of each system were plotted to check for reproducibility and systematic differences. A total of 128 ΔG^0 values were collected in this way. Then, several statistical tests were applied to check for the normality of the uncertainty distributions (Shapiro-Wilk (Shapiro & Wilk, 1965) test) and for significant differences between the values (t-test, Mann-Whitney (Mann & Whitney, 1947) test, paired t-test, or Wilcoxon (Wilcoxon, 1945) test, depending on the case) obtained using different integration methods, considering relative orientations of the ligand in the CD cavity, different ligands for the formation of the complexes, and also to compare the uncertainties obtained using the two integration methods. The average values of the repeats under the same conditions were obtained after removing possible outliers (those with a *z*-score > 1.5). The standard deviation was taken as a measurement of the reproducibility for these repeats. Bland-Altman (Altman &

USC UNIVERSIDADE DE SANTIAGO DE COMPOSTELA

Bland, 1983) plots were also generated to highlight possible trends in the differences of ΔG^0 value obtained using different integration methods, relative orientations, and ligands.

5.3. Results

5.3.1. General description of the PMF profiles

PMF profiles were generated for all systems studied by metadynamics simulations, each with 300 ns-long trajectories per walker to ensure simulation convergence. This convergence is demonstrated by the overlapping curves in the PMF profile evolution over time, as shown in Figures 13-14 and in the Supplementary Material. The simulations sampled the displacement of the target along the symmetry axis of the CD ring, with restraints on the relative orientation and on the distance to this axis (see Methods for details). Consequently, two regions with negligible interaction in the PMF are expected at both negative and positive long-distance displacements between the CD and the ligand. In these "unbound" regions, the PMF profile should level off, indicating no change in interaction energy. This behavior was observed in most systems, with some exceptions showing significant differences in the height of the PMF at opposite sides of the CD. These discrepancies contribute to the uncertainties in the calculated ΔG^0 values. Typically, one or more energy barriers are observed for the ligand entry into the CD cavity from the narrower side, presenting a sampling challenge. Conversely, calculating ΔG^0 values might be simpler when integrating the pathway from the bound to the unbound region via the wider cavity side, usually devoid of significant energy barriers. K_A and corresponding ΔG^0 values for all systems were calculated using these two approaches, as shown in the Supplementary Material.

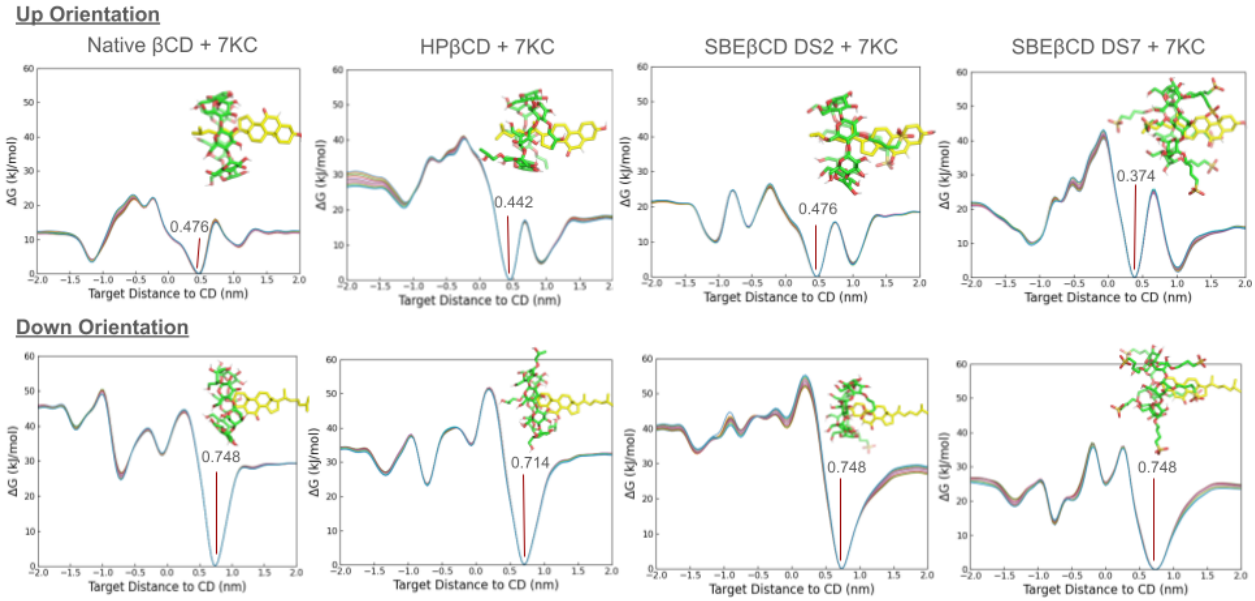


Figure 13. PMF profiles for the four βCDs with 7KC in the up and down orientations, together with the structures of the complexes and the CV value corresponding to the energy minimum. The K_A and ΔG^0 values calculated from both the All and Wide Face method, as well as the additional simulation replicates, are available in the Supplementary Material.

USC
UNIVERSIDADE DE SANTIAGO DE COMPOSTELA

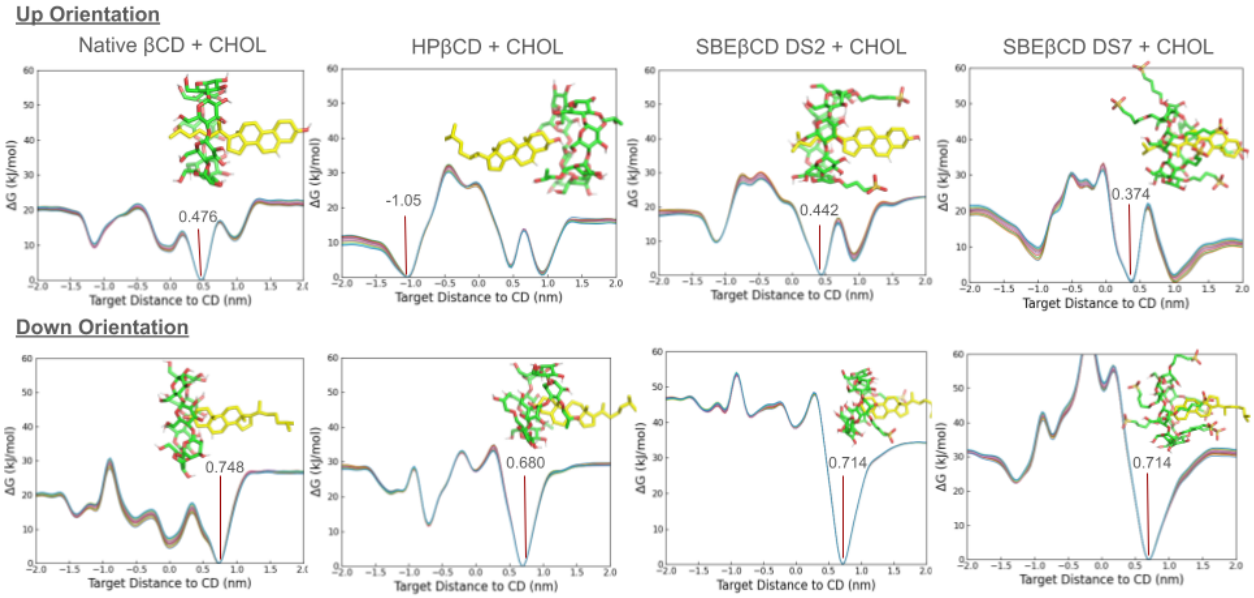


Figure 14. PMF profiles for the four βCDs with cholesterol in the up and down orientations, together with the structures of the complexes and the CV value corresponding to the energy minimum. The K_A and ΔG^0 values calculated from both the All and Wide Face method, as well as the additional simulation replicates, are available in the Supplementary Material.

All employed CDs generally exhibit a marked preference, evidenced by more negative ΔG^0 values, for the down orientation. Specifically, the native βCD monomer shows its lowest energy at exactly 0.748 nm for both sterols in the down orientation, and around 0.4 nm in the up orientation. The positions of these minima are more varied for modified CDs, but they remain fairly consistent for both sterols within each CD and orientation pair, with one notable exception for HPβCD with cholesterol in the up orientation, which shows the absolute minimum at -1.05 nm and secondary minima at approximately 0.5 and 1 nm. While the PMF profiles for both sterols with a given CD are similar, the presence of two local minima of varying depth for both sterols in the up orientation influences these results. Overall, across all systems, the roughness of the energy profile is much more pronounced in the region corresponding to the narrow face of the CD than the wide face, making the former more challenging to sample than the latter. Additionally, it seems that the larger the number of substitutions the more sophisticated the PMF profile is, with more and higher energy barriers for SBβCD (DS7) than for SBβCD (DS3) and a more complex energy profile for both modified CDs with DS3 than for the native βCD.

USC
UNIVERSIDADE DE SANTIAGO DE COMPOSTELA

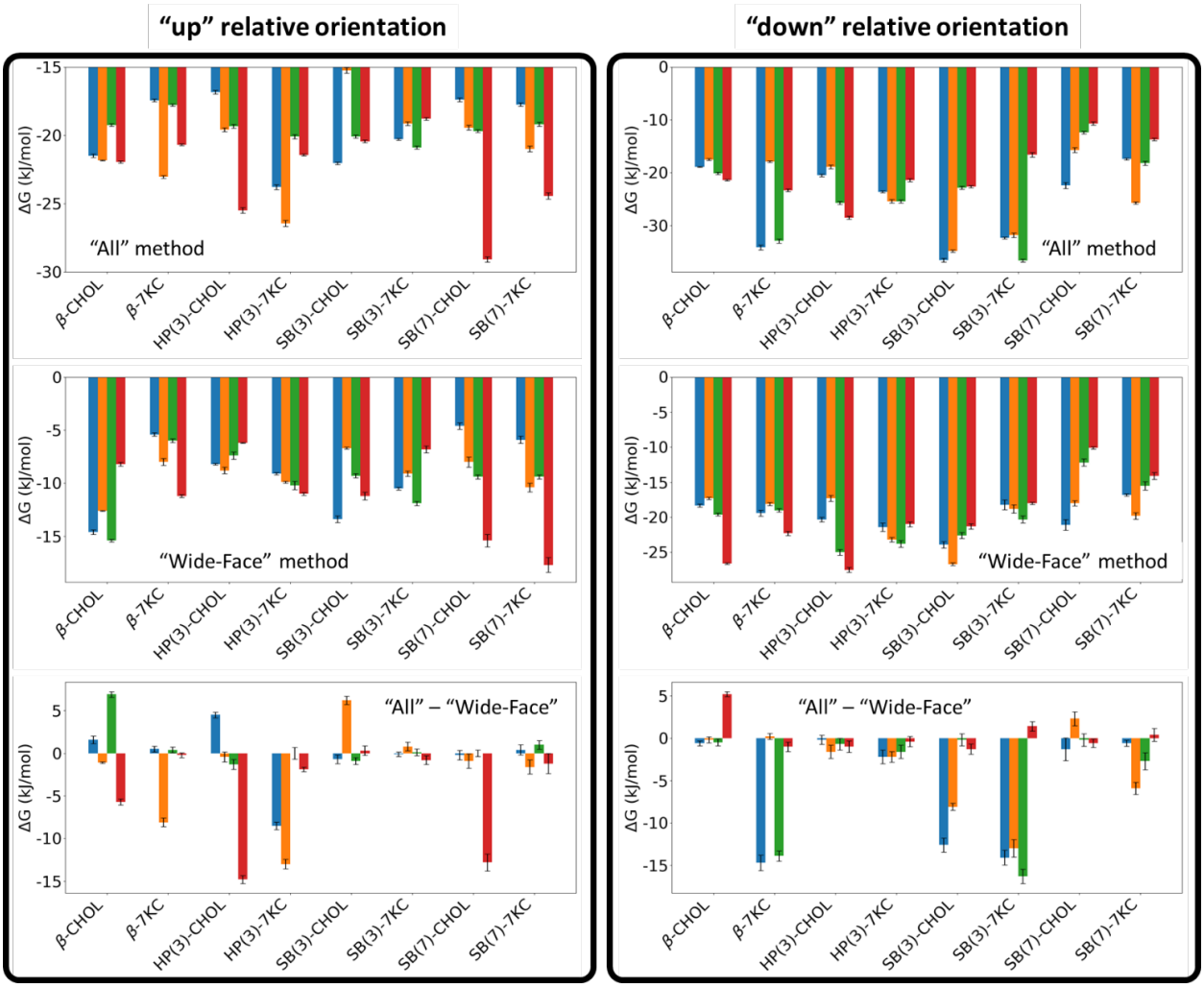


Figure 15. ΔG^0 values obtained from all the PMF profiles calculated in the present work. For each system and integration method, four independent calculations were conducted, represented by the colors blue, orange, green, and red. The top plot displays results utilizing the entire PMF profile. The middle plot shows the results obtained from the integration from the bound region near the global minimum to the unbound region towards the wide face direction. The bottom plots highlight the differences between the two integration methods for identical simulations. The left column contains the results of simulations where the ligand is in the up orientation, while the results for the down orientation are in the right column.

To facilitate comparison of results from various combinations of employed variables (relative orientation, integration method, and ligand name), the average values for each specific combination, along with their standard deviations, were calculated (Fig. 16, Table 2). As mentioned above, the outliers (values with *z*-score > 1.5) were excluded for these calculations (a total of 11 ΔG^0 values). In general, there is a good correlation observed between the two integration methods. Additionally, clear trends are evident in these results, although some are more subtle. A notable example is the difference between the results for the up and down orientations, with the down orientation consistently showing significantly stronger affinity across all CDs. This trend is reproducible with both integration methods. However, the specificity of the CDs for

USC UNIVERSIDADE DE SANTIAGO DE COMPOSTELA

each sterol is less clear. While the native βCD in the up orientation appears to be more specific for CHOL and HPβCD, also in the up orientation, is more specific for 7KC, the overall impact of these differences is limited due to the much lower significance of the up orientation compared to the down orientation. It is important to note that the overall association constant for a given CD is the sum of the association constants from both the up and down orientations. The association constants are proportional to the exponential of ΔG^0 ($K_A = \exp(-\Delta G^0/RT)$), meaning even small differences in ΔG^0 can lead to substantial variations in the association constants. Therefore, in all cases, the contribution of the up orientation to the quantification of binding energies is expected to be low when compared to the down orientation. The results corresponding to the down orientation do not exhibit clear specificity for any of the sterol molecules.

A more robust support for this discussion could be provided by applying appropriate statistical tests.

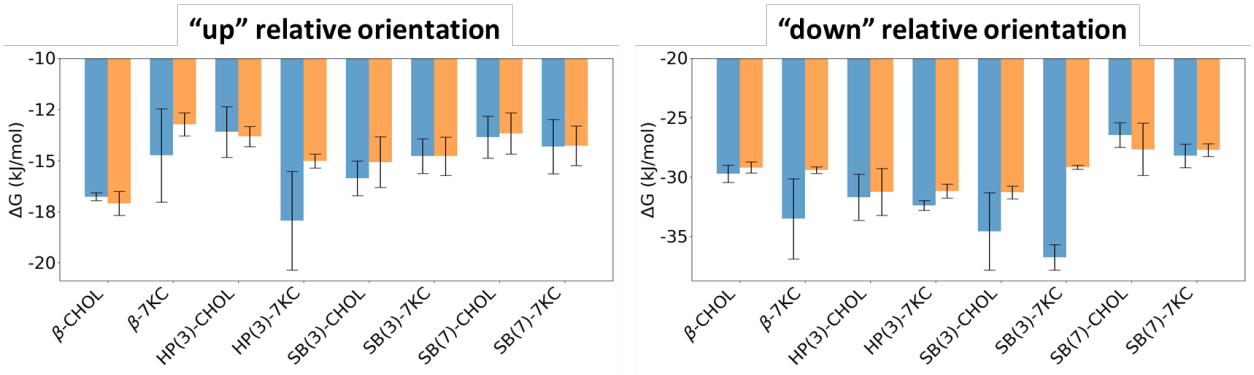


Figure 16. Average ΔG^0 values for each group of experiments together with the corresponding standard deviation (error bars). The results using the 'All' integration method are in blue and those using the 'Wide-Face' method are in orange. Values with z-score > 1 (a total of 11 values) were excluded from the calculations.

Table 2. Average ΔG^0 values for each group of experiments together with the corresponding standard deviation for the All and the Wide-Face integration methods. Values with z-score > 1 (a total of 11 values) were excluded from the calculations.

	up		down	
	all	Wide-Face	all	Wide-Face
β-CHOL	-13.53 ± 0.39	-14.2 ± 1.2	-19.5 ± 1.4	-18.40 ± 0.94
β-7KC	-9.5 ± 4.6	-6.5 ± 1.1	-27.1 ± 6.7	-18.83 ± 0.54
HP(3)-CHOL	-7.2 ± 2.5	-7.7 ± 1.0	-23.4 ± 3.9	-22.5 ± 4.0
HP(3)-7KC	-15.9 ± 4.8	-10.05 ± 0.68	-24.80 ± 0.85	-22.4 ± 1.2
SB(3)-CHOL	-11.7 ± 1.7	-10.2 ± 2.5	-29.2 ± 6.5	-22.6 ± 1.1
SB(3)-7KC	-9.6 ± 1.7	-9.6 ± 1.9	-33.6 ± 2.2	-18.33 ± 0.34
SB(7)-CHOL	-7.7 ± 2.1	-7.3 ± 2.0	-12.9 ± 2.1	-15.4 ± 4.4
SB(7)-7KC	-8.6 ± 2.7	-8.6 ± 1.9	-16.4 ± 2.0	-15.5 ± 1.1

USC UNIVERSIDADE DE SANTIAGO DE COMPOSTELA

5.3.2. Statistical Results

All vs. Wide-Face Methods: To explore the differences in ΔG^0 values, uncertainties, and reproducibility between the two integration methods (All and Wide-Face) across both up and down orientations, the average values shown in Fig. 16 and Table 2 were employed. The standard deviation was taken as a measurement of the reproducibility of the ΔG^0 values in each independent simulation.

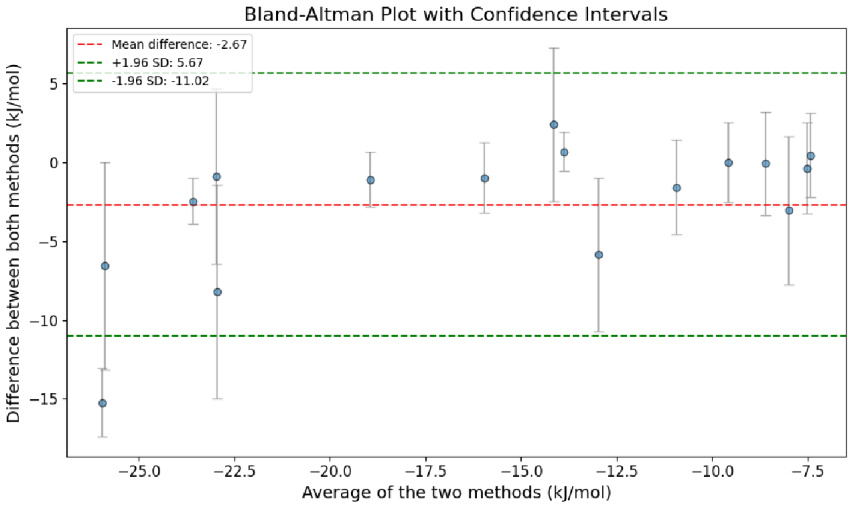


Figure 17. Differences in ΔG^0 values obtained from the integration of the whole PMF profile and using just the wide face ($\Delta G^0_{All} - \Delta G^0_{Wide\text{-}Face}$) as a function of the average of both values ($0.5 \cdot (\Delta G^0_{All} + \Delta G^0_{Wide\text{-}Face})$). The mean of the difference together with the confidence interval (mean difference ± 1.96 times the standard deviation of the differences) are shown as a dashed red line and dashed green lines, respectively.

The Bland-Altman plots suggest a small bias between the two methods (represented by the red line in Fig. 17). In addition to this visual comparison, a quantitative analysis aimed to assess whether or not both methods are equivalent to each other was performed. The analysis was performed in different ways: (*i*) ignoring the uncertainties; and (*ii*) considering the uncertainties to weight the differences in the results obtained from both methods. Note that outliers were excluded from the calculation of the average values. To assess the differences in ΔG^0 values derived from the two integration methods, both the paired t-test and the Wilcoxon test were utilized. Initial comparisons, which did not account for uncertainties, suggested significant differences between the methods. However, when incorporating the standard deviation of the average values into the analysis, there are no significant differences between the two integration methods (p-value > 0.05) (Table 3).

USC
UNIVERSIDADE DE SANTIAGO DE COMPOSTELA

Table 3. Comparison of the average difference in ΔG values ($\Delta G_{all} - \Delta G_{wide}$) obtained from all the PMF plots with different considerations.

Analysis Method	Mean Difference (kJ/mol)	p-value t-test	p-value Wilcoxon
Results using the mean values for each system			
Without Uncertainties	-2.67 ± 1.10	0.028	0.0125
With Uncertainties	-1.96 ± 1.04	0.080	

The t-test for independent samples and the Mann-Whitney test were employed to check for differences in the uncertainties of both methods. Both tests suggest that the uncertainties are significantly different with p-values of 0.030 and 0.018, respectively. The mean difference of the standard deviations is 1.83 ± 0.49 (larger for the All method). This means that the data obtained using the Wide-Face method is significantly more reproducible than those using the All method, even though the two methods provide equivalent mean values.

Up vs. Down Orientation: This analysis was performed using the mean values to determine if significant differences exist between the up and down orientations, independent of the reproducibility of repeated experiments for the same system. It was conducted separately for both the All and Wide-Face integration methods.

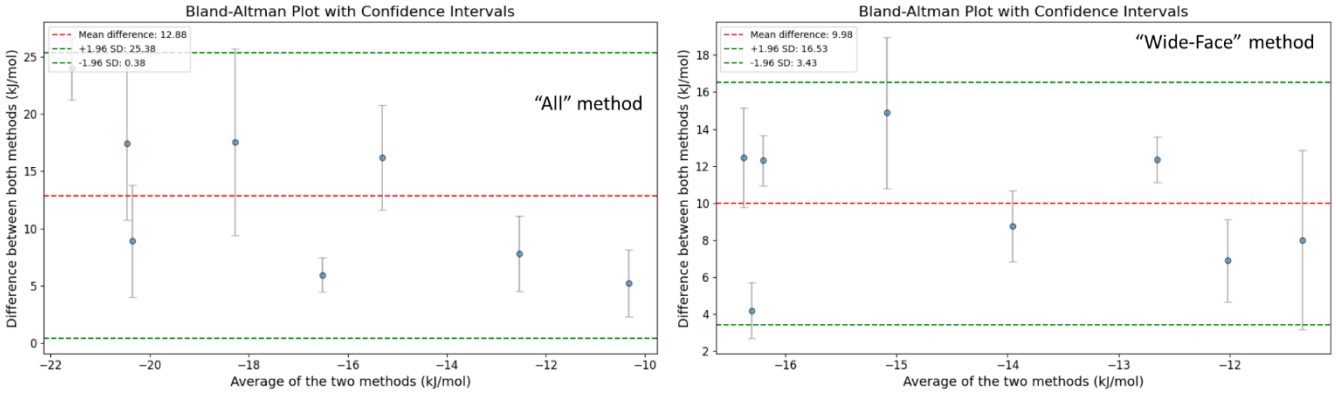


Figure 18. Differences in mean ΔG^0 values obtained for the up and down orientations of each system for the All (left) and Wide-Face (right) integration methods. The mean of the difference together with the confidence interval (mean difference ± 1.96 times the standard deviation of the differences) are shown as a dashed red line and dashed green lines, respectively.

The Bland-Altman plots show a clear systematic bias between the results provided by both orientations, with a negative excess in the ΔG^0 value of more than 10 kJ/mol, as shown in Fig. 18.

USC
UNIVERSIDADE DE SANTIAGO DE COMPOSTELA

Table 4. Comparison of the average difference in ΔG^0 values ($\Delta G^0_{up} - \Delta G^0_{down}$) obtained from the mean values of the four PMF replicas obtained for each system and orientation. Both integration methods were employed, providing similar results, as indicated in the Table. The p-values obtained from both the paired t-test and the Wilcoxon tests are lower than 0.05 in all cases, indicating that the difference between ΔG^0_{up} and ΔG^0_{down} is significant, with lower (more negative) values for ΔG_{down}.

Analysis Method	Mean Difference (kJ/mol)	p-value t-test	p-value Wilcoxon
Results using the All method with mean values of each system			
Without Uncertainties	12.88 ± 2.41	0.0011	0.00781
With Uncertainties	9.79 ± 2.35	0.004	
Results using Wide Face method with mean values of each system			
Without Uncertainties	9.98 ± 1.26	0.0001	0.00781
With Uncertainties	9.92 ± 118	0.0000	

No statistical differences were observed between the uncertainties of the two orientations, the t-test for independent samples, and the Mann-Whitney test providing values of 0.51 and 0.80 for the All method and 0.79 and 0.51 for the Wide-Face method.

Cholesterol vs. 7KC Targets: Again, the same analysis as in the previous section was performed, *i.e.* using the mean values of the four replicas obtained for each system and orientation. Again, the analysis was performed using the two integration methods separately.

USC UNIVERSIDADE DE SANTIAGO DE COMPOSTELA

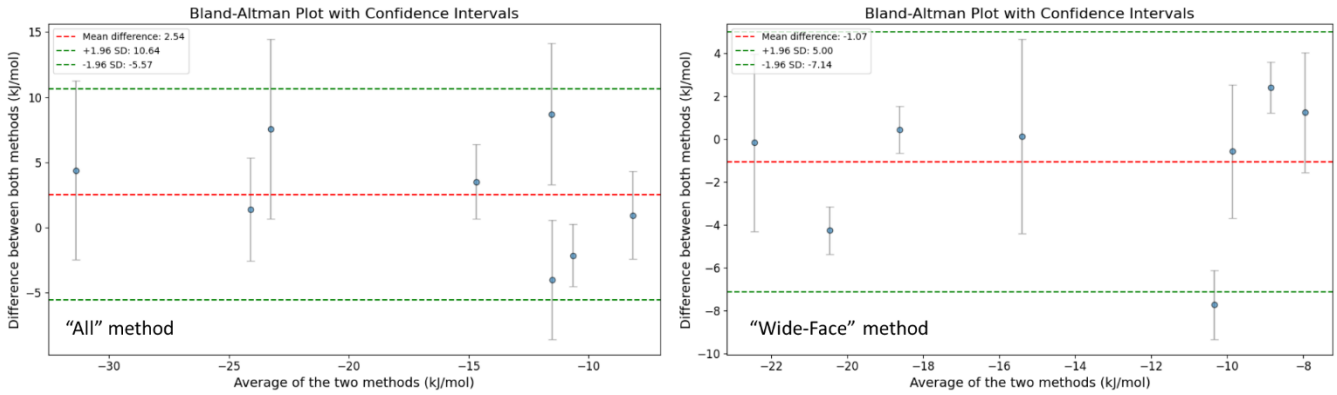


Figure 19. Differences in mean ΔG^0 values obtained for cholesterol and 7KC with the different CDs for the All (left) and Wide-Face (right) integration methods. The mean of the difference together with the confidence interval (mean difference ± 1.96 times the standard deviation of the differences) are shown as a dashed red line and dashed green lines, respectively.

The Bland-Altman plots (Fig. 19) suggest systematic bias of different sign, where the All method is positive and the Wide Face method is negative, depending on the employed method to integrate the PMF profiles. The application of statistical tests also provides contradictory results for both integration methods, but with no significant systematic differences between both sterols (Table 4).

Table 5. Comparison of the average difference in ΔG^0 values ($\Delta G_{cholesterol} - \Delta G_{7KC}$) obtained from the mean values of the four PMF replicas obtained for each system and orientation.

Analysis Method	Mean Difference (kJ/mol)	p-value t-test	p-value Wilcoxon
Results using the All method with mean values of each system			
Without Uncertainties	2.54 ± 1.56	0.148	0.195
With Uncertainties	1.02 ± 1.23	0.433	
Results using Wide Face method with mean values of each system			
Without Uncertainties	-1.07 ± 1.17	0.931	0.742
With Uncertainties	-1.37 ± 1.21	0.295	

Additionally, no statistical differences were observed between the uncertainties of the mean values for both sterols, the t-test for independent samples and the Mann-Whitney test providing values of 0.53 and 0.51 for the All method and 0.073 and 0.16 for the Wide-Face method.

USC
UNIVERSIDADE DE SANTIAGO DE COMPOSTELA

5.4. Discussion

The present study provides a comprehensive investigation into the inclusion complexes formed between different βCDs (βCD, HPβCD with DS3, and SBβCD with DS3 and DS7) and sterol molecules, specifically CHOL and 7KC, through guided metadynamics simulations followed by PMF calculations. The research aims to establish robust and efficient methods to characterize the interaction between CDs and small ligands. For this, a relatively large set of trajectories is used to assess the reproducibility in the determination and accuracy of ΔG^0 values by different approaches. Additionally, the ability of the different CDs to distinguish the two sterols and their relative orientation into the cavity are assessed. Complementarily, the obtained results shed light on the interactions between the molecules employed in our calculations.

All employed CDs display a strong preference for the down orientation, indicated by more negative ΔG^0 values by ~10 kJ/mol, compared to the opposite orientation of the sterol in the CD cavity. The positions of all minima (displacement between the CD and the sterol) vary for different CDs, but they are consistent for both sterols within each CD and orientation. SBβCD with DS=7 is the only exception to this behavior due to the presence of two local minima in the up orientation at similar locations but with different depths for both sterols. This preference could be due to the fact that the hydrophobic headgroup of the sterol is in better contact with the hydrophobic CD cavity, while the hydrophilic tail of the sterol is in better contact with water in this orientation. Subtle differences in sterol specificity among CDs was observed. This could be due to the significant differences in ΔG^0 values in the up orientation, and the impact of this contribution to the overall association constant is limited due to the much higher significance of the down orientation. Note that the total association constant for the interaction between a given CD-ligand pair results from the sum of the association constants in the two orientations and the transformation from the ΔG^0 to the K_A space is performed by the exponential function. Thus, relatively small differences in ΔG^0 are magnified when they are transformed to K_A, as it happens for all the studied systems when combining ΔG^0 values obtained from both orientations of the sterol in the CD cavity.

The roughness of the energy profile is evident around the narrow face of the CD, in contrast to the wide face, making it harder to sample. The results obtained from the two integration methods (All and Wide-Face) were consistent, with no significant differences between them. However, the Wide-Face method was significantly more reproducible and it is cheaper, from the computational point of view, than the All method, since the former requires the sampling of a much smaller range of the CV used in the metadynamics simulations. This method is expected to be sufficient for randomly substituted or unsubstituted CDs interacting with steroidal target molecules.

The study successfully reveals energy profiles, optimized complex structures, and quantitative estimations of binding affinities for the inclusion complexes between βCDs and sterols. The computed PMF profiles offer a detailed understanding of the energy landscapes governing the association between the host βCDs and the guest sterols. The rationalization of these energy landscapes provides insights into the mechanisms of inclusion, shedding light on the interactions and driving forces governing the formation of inclusion complexes. The employed approach to exploring selective sequestration of specific molecules using modified βCDs opens up possibilities for designing novel molecular systems for targeted drug delivery or other applications. Our study is focused only on 1:1 complexes, but it is worth mentioning that other stoichiometries such as 2:1 (two CD molecules threaded by the same ligand), 1:2 (one CD molecule simultaneously binding 2 sterol molecules), or even aggregates of higher order could significantly

USC
UNIVERSIDADE DE SANTIAGO DE COMPOSTELA

contribute to the solubilization of a given ligand by CDs (Castagne et al., 2010; Christoforides et al., 2018; Kučáková & Dolenský, 2020; Loftsson et al., 2019; Messner et al., 2010; Nishijo et al., 2004; Ravichandran & Divakar, 1998). However, inclusion complexes are of special interest because the interaction mechanism leading to these structures is expected to take advantage of the particular design of the CD molecules to specifically distinguish between different ligands. The CDs employed in this study did not successfully differentiate CHOL from 7KC, but it has been demonstrated, with approaches similar to those employed in the present work, that CD dimers, with the monomers joined by a chemical linker, are indeed able to distinguish these two sterol molecules.

Overall, in addition to the new insight that our calculations provide on the specific interactions between different CDs and the two studied sterol molecules, we propose a protocol that could be employed in massive PMF calculations of CD-ligand systems. This protocol is based on metadynamics simulations that only require the sampling in one dimension (the displacement of the ligand along the symmetry axis of the CD) in the direction of the wide face of the cavity with some restraints (the relative orientation of the ligand with respect to the CD and the distance from the ligand to the symmetry axis of the CD). The ΔG^0 and association constant values obtained from these calculations were highly reproducible and allowed us to save significant computational resources compared to other methods. We intend to implement this method into an automated workflow for designing modified CDs tailored for specific applications.

5.6. Conclusion

This study focuses on the computational study of inclusion complexes between multiple βCDs and sterols, using metadynamics simulations and PMF calculations to understand their interactions. The methods reveal that CDs-sterol inclusion complexes are generally preferred in the "down" orientation, with notable differences in binding affinities and energy profiles among different CDs. These differences highlight the impact of number and type of substitution on the characteristics of CD inclusion complexes. The research demonstrates the consistency and efficiency of the Wide-Face integration method in these calculations, offering insights for designing faster, specialized methods to analyze CD-sterol inclusion complexes in silico. These results are significant for various applications, including targeted drug delivery and novel drug design. Finally, the automated techniques presented here showcase the potential of accelerating CD development by creating and using large amounts of data for training AI and ML algorithms. These advancements are poised to not only improve our understanding of CD inclusion complexes, but also open new horizons for a world where tailored, CD-based solutions can be developed more efficiently and effectively than ever before.

USC
UNIVERSIDADE DE SANTIAGO DE COMPOSTELA

Chapter 6. Addressing the Complexities in Measuring Cyclodextrin-Sterol Binding Constants: a Multidimensional Study[3]

6.1. Preface to Contextualizing the Research: Insights into Authorship, Contributions, and Publication Specifics

The final experimental chapter of this thesis is aimed at exploring the encapsulation of sterols by novel CD dimers. This class of CD dimers has emerged as a potential new treatment for atherosclerosis; they work by forming strong, soluble inclusion complexes with oxysterols, allowing the body to reduce and heal arterial plaques. However, characterizing the interactions between CD dimers and oxysterols presents formidable challenges due to low sterol solubility, the synthesis of modified CDs resulting in varying number and position of molecular substitutions, and the diversity of interaction mechanisms. To address these challenges and illuminate the nuances of CD-sterol interactions, we have used multiple orthogonal approaches for a comprehensive characterization. Results obtained from three independent techniques - metadynamics simulations, competitive isothermal titration calorimetry, and circular dichroism - to quantify CD-sterol binding are presented. The objective of this study is to obtain the binding constants and gain insights into the intricate nature of the system, while accounting for the advantages and limitations of each method. Notably, our findings demonstrate ~1000× stronger affinity of the CD dimer for 7KC in comparison to cholesterol for the 1:1 complex in direct binding assays. These methodologies and findings not only enhance our understanding of CD dimer-sterol interactions, but could also be generally applicable to prediction and quantification of other challenging host-guest complex systems. A rigorous computational method for determining accurate binding constants for CD dimers greatly benefits our CD development process and offers new insights that could impact how the CD dimer might work *in vivo*.

Title: Addressing the Complexities in Measuring Cyclodextrin-Sterol Binding Constants: a Multidimensional Study

Authors: Amelia M. Anderson, Ilse Manet, Milo Malanga, Daniel M. Clemens, Keivan Sadrerafi, Rebeca García-Fandiño, Ángel Piñeiro, Matthew S. O'Connor

Year: 2024

Publisher: Elsevier Ltd.

ISSN/ISBN: 0144-8617

DOI: https://doi.org/10.1016/j.carbpol.2023.121360

[3] This article/chapter was published in Carbohydrate Polymers, Volume 323, 121360, ISSN 0144-8617, https://doi.org/10.1016/j.carbpol.2023.121360
Copyright Elsevier 2024

Quality indexes: Carbohydrate Polymers is a journal covering the technologies/fields/categories related to Materials Chemistry (Q1); Organic Chemistry (Q1); Polymers and Plastics (Q1). The overall impact score is 11.93.

Contributions: As the leading and corresponding author of this work, my involvement was multifaceted and critical to the project's success. My key contributions were: designing and conceptualizing the research study; developing and implementing the computational methodologies employed; analyzing and interpreting the resulting data; writing and preparing the manuscript for publication.

USC
UNIVERSIDADE DE SANTIAGO DE COMPOSTELA

6.1. Introduction

CDs are in wide use for industrial and drug delivery applications and have an excellent safety profile (Schmid, Gerhard, 2001); when used in medicine, CDs are usually employed as excipients and are not considered pharmaceutically active themselves. There are two notable exceptions to this: Bridion™, a CD API (active pharmaceutical ingredient) drug widely approved and used for reversal of neuromuscular block during surgical procedures (Merck and Co, Inc., 2015), and clinical trials are being conducted using Hydroxypropyl-β-cyclodextrin (HPβCD)to treat Niemann Pick Type C disease, a debilitating disease of cholesterol metabolism (*Safety and Efficacy of Intravenous Trappsol Cyclo (HPBCD) in Niemann-Pick Type C Patients from ClinicalTrials.Gov*, 2019), however with serious side effects due to the incredibly high doses of monomer necessary (Puglisi & Yagci, 2019). Both of these APIs take advantage of CDs forming inclusion complexes with target molecules, and it has been shown that CD dimers can further enhance the solubility of CHOL in water (Alcalde et al., 2009; Anderson et al., 2021; Breslow & Zhang, 1996).

The crystal structure of the inclusion complex of cholesterol in unsubstituted βCD monomers reveals CHOL encapsulated inside of a naturally formed (not covalently linked) head-to-head βCD dimer, which has been recapitulated in computational studies (Christoforides et al., 2018; Hayashino et al., 2018; Kučáková & Dolenský, 2020). Other CD dimers have been synthesized for various purposes (Aime et al., 2009; Alcalde et al., 2009; Anderson et al., 2021; Aykaç et al., 2012; Blaszkiewicz et al., 2013; Breslow & Zhang, 1996; Casas-Solvas et al., 2011; Chmurski et al., 2016; de Jong et al., 2000; Lebedinskiy et al., 2022; Shuang et al., 2020). Regarding head-to-head dimers complexing CHOL, corresponding to the crystal structure and NMR structure (Christoforides et al., 2018; Kučáková & Dolenský, 2020), little research has been conducted and sterol solubility remains an issue. The binding affinity of CHOL for linked tail-to-tail CD dimers has been shown to be enhanced due to a chelate effect by phase-solubility (Alcalde et al., 2009; Breslow & Zhang, 1996), but a more reliable method for determining binding constants remains elusive due to the very low aqueous solubility of CHOL.

Recently, Cyclarity Therapeutics has engineered CD dimers as innovative APIs for the treatment of atherosclerosis, a leading cause of cardiovascular diseases (Anderson et al., 2020, 2021). Current treatments for atherosclerosis primarily focus on managing risk factors and alleviating symptoms (Banach et al., 2016; Katzmann et al., 2020; Strandberg et al., 2020), but it is proposed that CD dimers can effectively reverse arterial plaque formation by specifically encapsulating atherosclerotic and cytotoxic oxysterols (Anderson et al., 2021; Breslow & Zhang, 1996; Coisne et al., 2016; Kim et al., 2020; Kritharides et al., 1996; Martinet et al., 2008). In this case, the challenge lies in selectively encapsulating toxic 7-ketocholesterol (7KC) over essential cholesterol (CHOL), as these sterol molecules only differ by a single heavy atom - an oxygen doubly-bound to carbon 7 - making them difficult to distinguish. Selectivity for 7KC over CHOL is important because CHOL plays a crucial role in maintaining cell membrane integrity, fluidity, and functionality, whereas 7KC is a cytotoxic oxysterol that can contribute to the development of various pathologies, including atherosclerosis (Anderson et al., 2020). This research focuses on CD dimers as they exhibit several advantages over monomers, including their enhanced affinity for encapsulating sterol molecules, and a higher density of functional groups that can be substituted within a single molecule, facilitating the potential for specificity of the modified structure (Anderson et al., 2021; Breslow et al., 1995; Kritharides et al., 1996; Voskuhl et al., 2011). Furthermore, the chemical linker connecting the two CD monomers can be tailored to optimize the recognition and encapsulation of particular ligands (Breslow

USC UNIVERSIDADE DE SANTIAGO DE COMPOSTELA

et al., 1989; Breslow & Zhang, 1996; Chmurski et al., 2016; Liu & Chen, 2006; Shuang et al., 2020; Soto Tellini et al., 2006).

The capacity of a macrocycle to accurately identify and bind to a particular ligand can be quantified in terms of the standard Gibbs energy (ΔG^0) associated with the formation of the resultant supramolecular complex. In general, the change in any macroscopic physical observable as a function of the concentration ratio of the CD and ligand can be used to determine ΔG^0 or, equivalently, the corresponding association/binding constant(s) ($K_A = \exp(-\Delta G^0/RT)$) (Connors, 1987; Piñeiro et al., 2019). The determination of this parameter is essential to understanding the molecular interactions and to design drugs with improved efficacy and specificity. However, a universal, rapid, precise, and cost-effective approach to measure ΔG^0 values has not yet been developed. Many wet lab-based methods have been proposed for this aim in the field of the CDs, including isothermal titration calorimetry (ITC) (Peluso et al., 2023; Piñeiro et al., 2022), surface plasmon resonance (SPR)(Hayashi et al., 2010), nuclear magnetic resonance (NMR) (Doan et al., 2022), microscale thermophoresis (MST) (Niether et al., 2017), circular dichroism spectrophotometry (CiDi, so as not to be confused with CD for cyclodextrin) (Wankar et al., 2017), fluorescence spectroscopy (Al-Soufi et al., 2008; Anand et al., 2012; Salzano et al., 2017), surface tension (Piñeiro et al., 2007), mass spectroscopy (Jankowski et al., 2016), and capillary electrophoresis (Aksamija et al., 2022; Peluso et al., 2023).

Although numerous methods for measuring K_A and ΔG^0 are available, they exhibit certain limitations for CD dimer-sterol systems, such as the requisite concentration and solubility of the compounds involved, the signal-to-noise ratio, or artifacts associated with sample labeling (Flood et al., 2001; Mura, 2014). The binding constants must also be measured in biologically relevant solvent if they are to be used for drug development, and sterols are highly insoluble in aqueous media. A range of computational methods have been proposed as alternatives to determine ΔG^0 values but, again, none of them provides a universal solution to the problem (Hayashino et al., 2018; López et al., 2011, 2013). The most common issues with these approaches are the production of unrealistic results due to oversimplifications of the studied systems and the excessive consumption of computational resources for obtaining reliable energy values.

Here, we present an orthogonal characterization of the complexes between HPβCD dimers and CHOL or 7KC using one computational and two wet lab methods: computational metadynamics simulations followed by PMF calculations, ITC, and CiDi. Each of these methods has required significant optimization for these kinds of host-guest systems. They provide cooperative insight on the interaction between the CD dimer and the sterol molecules, including energy profiles, optimized structures for the supramolecular complexes and independent quantitative estimations of the corresponding binding affinities. This approach is expected to contribute to the development of novel therapies and other technologies targeting the selective sequestration of small hydrophobic molecules, offering new possibilities for the treatment of ailments involving the accumulation of hydrophobic toxins. Our ultimate goal is to develop CDs as APIs for the treatment and reversal of all cholesterol-related dyslipidemia, but the methodologies presented here could also be applied to a range of complex molecular systems.

Our hypothesis posits that the complexity of CD dimer-sterol inclusion complexes necessitates the integration of multiple methods rather than relying on a single approach. Factors like flexibility, solubility variations, diverse substitutions, and multiple stoichiometries contribute to this complexity, and our multi-method approach illuminates CD dimer-sterol behavior comprehensively. These orthogonal techniques

USC UNIVERSIDADE DE SANTIAGO DE COMPOSTELA

independently estimate K_A and ΔG^0 values, showcasing selective 7KC encapsulation by the CD dimer. This approach underscores how a multidimensional analysis deepens understanding of CD-sterol inclusion complex formation, both qualitatively and quantitatively.

6.2. Materials

2.1 Carbohydrate Characterization

The same HPβCD dimer was used for both ITC and CiDi experiments, custom synthesized by Cyclarity Therapeutics. 98.60% purity (Fig. 20).

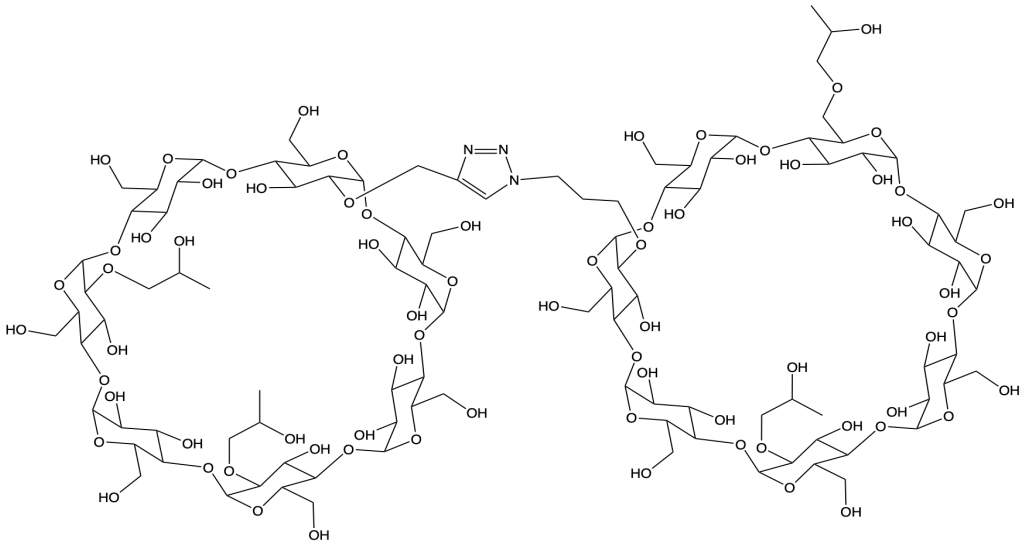


Figure 20. Structure of the head-to-head HPβCD dimer used for CiDi and ITC. Note that the actual product is an isomeric mixture of HPβCD dimers, this structure represents just one isomer of the HPβCD dimer. The narrow side, or "primary face", is facing outside (where the O6 oxygens reside), while the wide side, or "secondary face", of each CD monomer is facing inside (where the O2 and O3 oxygens reside).

NMR experiments (Figs. S6-1 to S6-9) were performed using two different spectrometers: a 600 MHz Varian DDR NMR spectrometer equipped with a 5 mm inverse-detection gradient (IDPFG) probehead, and a Bruker Advance III HD 600 MHz spectrometer equipped with a QCI 1H/13C/15N/31P proton-optimized quadrupole inverse cryoprobe with 1H and 13C cryochannels. The standard pulse sequences and processing routines available in VnmrJ 3.2 C/Chempack 5.1 or Bruker TopSpin 3.6.2 software were used for structure identifications. The experiments were conducted at a temperature of 298 K using standard 5 mm NMR tubes. Chemical shifts (δ) are reported in parts per million (ppm) and referenced to the residual signals of the NMR solvents: dimethyl sulfoxide-d6 (δ1H = 1.25 ppm, δ13C = 39.52 ppm) or D2O (δ1H = 4.79 ppm). J values are reported in hertz (Hz). Samples were prepared by dissolving 10 mg of solid in 0.7 mL of deuterated solvent. The identification of the HPβCD dimer using NMR spectroscopy involved cross-linking the data obtained from 1H, 13C, COSY, DEPT-edited HSQC, and HMBC spectra in DMSO-d6.

The HPβCD dimer is an isomeric mixture of differently substituted βCD dimer core derivatives with varying degrees of substitution (DS). The determination of the average DS was based on 1H NMR measurements in D2O (Fig. S6-1 and S6-2). The signals in the anomeric region (4.9-5.3 ppm) were

USC UNIVERSIDADE DE SANTIAGO DE COMPOSTELA

integrated together and set to be 14.00. The methyl signal at 1.08 ppm was then divided by three to calculate the average number of 2-hydroxypropyl units on the HPβCD dimer.

The DS distribution of the HPβCD dimer was also examined using a MALDI spectrum (Fig. S6-8). The spectrum exhibited a typical Gaussian-shaped distribution, indicating a composite isomeric mixture. The peak values corresponded to the sodium adduct of the selected DS. For instance, the value 2412.374/DS0 represented the molecular weight of the βCD dimer core plus one sodium unit, while the value 2470.590/DS1 represented the molecular weight of the βCD dimer core bearing one 2-hydroxypropyl moiety (DS1) plus one sodium unit, and so on.

The purity of the HPβCD dimer was determined using High-Performance Liquid Chromatography with Charged Aerosol Detection (HPLC-CAD), and it was measured to be greater than 96% based on the area percentage (Fig. S6-9). Lastly, the pH of a 30% (w/v) aqueous solution of the HPβCD dimer at 25 °C was measured to be 8.3.

Additional characterization data and NMR spectra can be found in the supplemental information.

7KC was sourced from Cayman Chemicals (Ann Arbor, MI, USA), catalog number 16339, with a molecular weight of 400.6. Cholesterol was sourced from Sigma-Aldrich (St. Louis, MO, USA), catalog number C8667-5G, with a molecular weight of 386.65. Randomly Methylated βCD Monomers (RAMEB) were sourced from CycloLab (Budapest, HU). The molecular formula for RAMEB is $C_{42}H_{70-n}O_{35} \cdot (CH3)n$, the catalog number is CY-2004.1, and the CAS is CAS 128446-36-6. RAMEB has a molecular weight of 1135.0 + n·(14.0) and >95% purity. The HPβCD monomer used in CiDi techniques was also sourced from CycloLab (Budapest, HU), catalog number CYL-4584, 96% purity. Ethanol (EtOH) absolute was sourced from HiPerSolv Chromanorm, purity > 99.7%.

6.3. Specific Methods

This chapter utilizes methods that are comprehensively described in **Chapter 3. Methodological Framework**. Additional specific details are provided in this section to enhance clarity.

6.3.1 Computational methods

6.3.1.1. Description of the structures employed for the computational simulations

One of the challenges in studying modified CDs, both computationally and experimentally, is that they are often not synthesized as a single isomer, but as a distribution of multiple molecular entities with different numbers and locations of substitutions and thus represented by an average DS. In contrast to *in vitro* experiments, it is feasible to consider a limited number of individual chemical species from a computational perspective. Therefore, in this work, we will examine four distinct structures of HPβCD dimers (Fig. 21) which are expected to be present in the synthesized isomeric mixture, based on the selected synthetic conditions and on steric considerations, and as strongly suggested by the 1D and 2D in-depth NMR analysis (Fig. S6-1 to S6-9), to represent the distribution. To simulate the entire distribution of thousands of isomers in an isomeric mixture is, up to now, an elusive goal due to the calculation power required, so the discussion of the computational results will be limited to these reduced number of structures that will be taken as representative of the whole distribution.

USC UNIVERSIDADE DE SANTIAGO DE COMPOSTELA

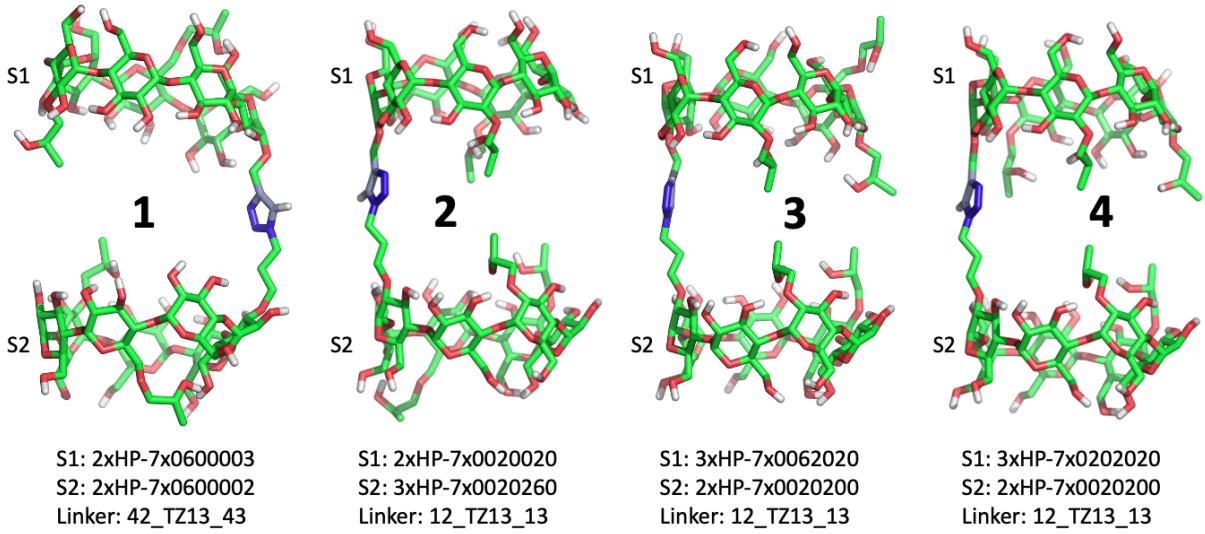


Figure 21. Representation of the four CD dimers considered in our computational simulations. The sequence of each monomer subunit (S1 on top and S2 beneath) is indicated in the labels with the number of HP substitutions per monomer followed by the sequence of native or substituted glucopyranoside (GPU) units in the anticlockwise direction: 0 indicates no substitution (excluding the linker) in the corresponding GPU residue, while 2, 3 and 6 indicate the positions of the hydroxyl groups of the corresponding GPU residues. The location of the connection of the chemical linker to each CD monomer is also indicated with two digits per subunit as a prefix and a suffix to the acronym of the linker: 42_TZ13_43 indicates that the TZ13 linker is connected to the glucopyranoside number 4 of S1 at position 2 and to the glucopyranoside number 4 of S2 at position 3. The standard coloring of atoms is used, where carbon is green, oxygen is red, hydrogens are white, and nitrogen is blue. The number between both subunits in bold will be used to identify the structures along the text.

The four structures have an asymmetric linker with 1 or 3 carbon atoms between the triazole ring and the first and second monomer, respectively. Although the 4 structures share the same linker, the number and location of the HP substituents are different. The first structure has only 2 substitutions at the interface between the two monomers and no substitutions within two GPU units of the linker. The second structure has four substitutions at the interface between the two monomers, and the last structure has all five substitutions located at the wide face of the monomers that face each other. Notably, S2 in structures 3 and 4 are identical.

CHOL and 7KC were employed as ligands to be encapsulated by the CD dimers. Unlike CDs, the chemical structures of these sterol molecules are well-defined (see Fig. 3). Our primary objective is to develop methods to selectively encapsulate 7KC without affecting CHOL concentration, as disrupting CHOL balance could have detrimental effects.

6.3.1.2. Simulation Parameters

After inserting the solute molecules (CHOL/7KC and CD) in a 10x10x10 nm^3 dodecahedral simulation box, it was filled with approximately 23000 SPC (simple point charge) waters (Berendsen et al., 1981), removing those overlapping the solute molecules. The “up” orientation corresponds to the complex with the tail of the sterol molecule pointing to the CD monomer joined to the shorter arm of the linker while the “down” orientation corresponds to the opposite orientation of the ligand in the CD dimer.

USC
DE SANTIAGO
DE COMPOSTELA

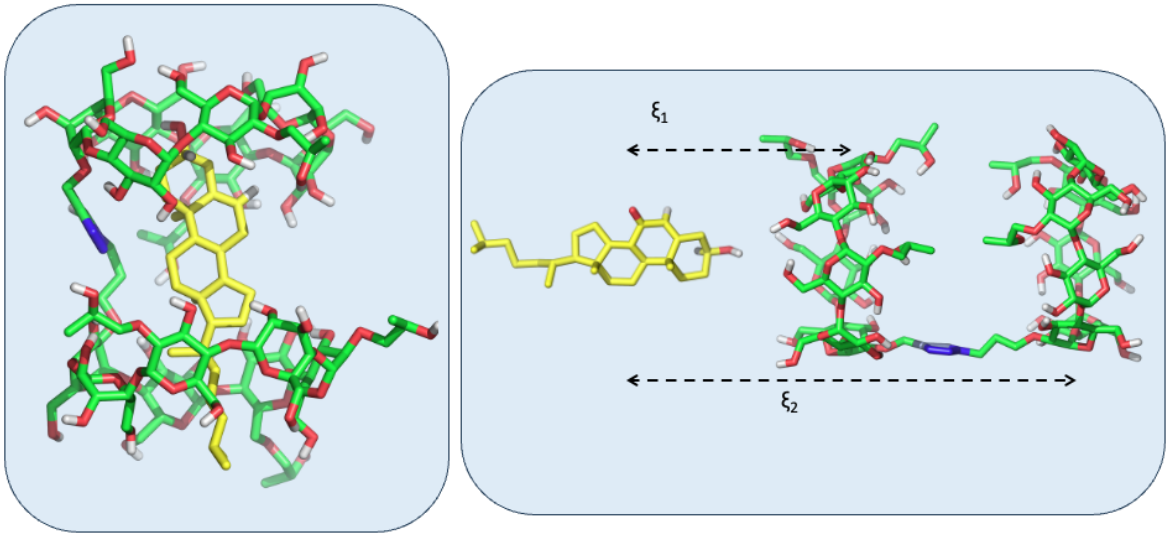


Figure 22. Structure of a DIC comprising a HPβCD dimer with CHOL (left) together with the image of the separated sterol and CD dimer molecules illustrating the CVs (1 and 2) used for metadynamics simulations: the distances between the COM of the ligand and the COM of the O4 atoms of each CD monomer in the dimer.

6.4. Results

6.4.1. Metadynamics Simulations

Two-dimensional PMF profiles, the structures of the optimized supramolecular complexes with 1:1 stoichiometry, and an estimation of the corresponding binding constants were obtained from metadynamics simulations (Fig. 23 and Table 4). The structures of the four dimers are shown in Fig. 21.

The analysis obtained from metadynamics simulations provides a significant amount of energetic and structural information showing clear trends. It is worth keeping in mind that the two relative orientations of the sterol molecule in the cavity of the CD dimer are not equivalent, as the linker is asymmetrical, which explains the different results for both orientations of the ligand. For CD dimer 1, which has the fewest number of HP substituents at the interface, the minimum energy structures for the "down" orientation are tightly packed for both sterol molecules, with the COM of the ligand at only 0.106 nm of S1 for CHOL and 0.105 nm of the same subunit for 7KC, while the distances to S2 are 0.706 and 0.671, respectively. Although the structures appear similar, the energy well for 7KC is much deeper, resulting in a considerably larger binding constant. This is a clear indication of specificity, as the same CD dimer can effectively distinguish between the two sterol molecules. Note that the "down" orientation corresponds to the complex with the tail of the sterol molecule pointing towards the CD monomer connected to the longer arm of the linker. In contrast, the structures corresponding to the "up" orientation are less compact, with the monomers more separated from each other, and the corresponding binding constants significantly lower than those for the "down" orientation.

In general, the PMF profiles for the same CD dimer and orientation are similar for both sterol molecules with surprisingly high reproducibility of the distances between the sterol and each of the CD subunits (Table S6-1). However, there are substantial quantitative differences in the energy values. The most similar energy profiles between the sterol molecules correspond to CD dimers 2 and 3. Notably, several PMF profiles,

USC
UNIVERSIDADE DE SANTIAGO DE COMPOSTELA

mainly those corresponding to the “up” orientation, contain two energy wells, suggesting that the same CD dimer could simultaneously bind two sterol molecules at different locations.

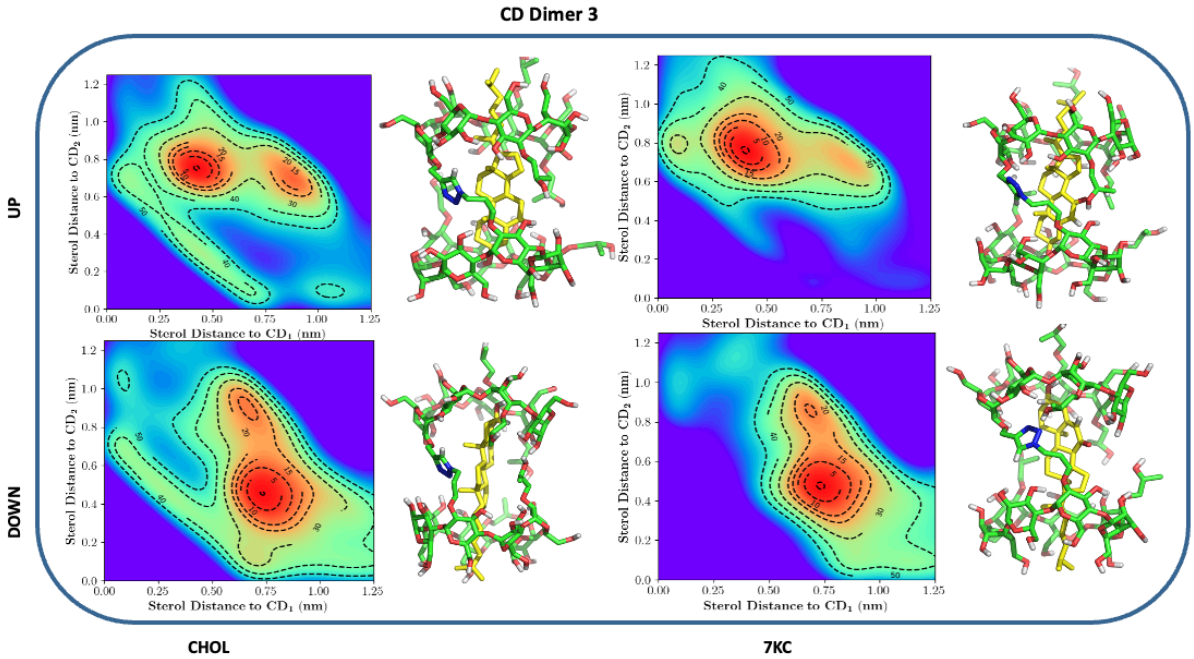


Figure 23. PMF profiles obtained from metadynamics simulations together with the minimum energy structure for each case. Results for each CD dimer structure are separated and labeled. The upper row of each panel presents the "up" relative orientation of the ligand within the CD cavity, while the bottom row shows the "down" orientation. CHOL results are displayed on the left side, and 7KC results are on the right side of each panel. The full PMF results are supplemented in Fig. S6-10.

It can easily be demonstrated that the overall binding constant corresponding to a given complex, considering both possible orientations, can be obtained by adding the separate values obtained for each orientation. To facilitate a clearer comparison between the results obtained for the four structures and the two sterol molecules, the results were summarized in Table 6, considering just one binding constant per system.

Table 6. Binding constants in M^{-1} for the different CD dimers and sterol molecules used in the metadynamics simulations, obtained from the sum of K_{av} shown in Table S6-1. The uncertainties are given in percentages.

CD dimer:	1	2	3	4
CHOL	$2.66 \cdot 10^5 \pm 17\%$	$2.00 \cdot 10^7 \pm 5.6\%$	$2.12 \cdot 10^6 \pm 9.8\%$	$5.97 \cdot 10^7 \pm 8.9\%$
7KC	$4.25 \cdot 10^8 \pm 7.0\%$	$3.16 \cdot 10^7 \pm 6.7\%$	$2.56 \cdot 10^8 \pm 12\%$	$2.49 \cdot 10^6 \pm 6.0\%$

These results clearly indicate that the structure **1**, with (1) the lowest number of substituents in the interface between both CD monomers, (2) the fewest number of substitutions close to the linker, and (3) the lowest

USC UNIVERSIDADE DE SANTIAGO DE COMPOSTELA

number of substitutions overall, exhibits the highest specificity towards 7KC. Moreover, it is evident that, on average, these isomers of the HPβCD dimer prefer to encapsulate 7KC over CHOL. This is in agreement with previously published relative affinities estimated in vitro by turbidity assay and NMR (Anderson et al., 2021). Structure **2**, with the most substitutions on the CD bound to the short side of the linker, shows poor specificity for 7KC, indicating that the number and position of substitutions on each monomer in an asymmetrically linked dimer may contribute to specificity. Only the structure **4**, with both the highest number of substitutions at the interface and the highest number of substitutions closest to the linker, shows a preference for CHOL over 7KC, indicating that the substitutions at the CD-CD interface may contribute more to specificity than other factors. These results indicate that the number and location of the substitutions in each subunit relative to each other and the linker are important factors in inclusion complex formation, and may be the key to improving specificity for particular guest molecules.

6.4.2 Competitive Isothermal Titration Calorimetry

Before studying the sterol-dimer interaction in competition experiments using ITC, dilution experiments were performed with the sterol-RAMEB mixtures. Interestingly, the energy profiles of the dilution experiments for the mixtures of RAMEB CD monomers with 7KC and CHOL are strikingly different (Fig. 25, top). This indicates that ITC clearly distinguishes the interaction between each sterol and the CD monomer, which is apparent by eye without the application of any theoretical model, despite the subtle difference between the structures of these two sterols (Fig. 3). For CHOL + RAMEB CD monomers, a global analysis of the different experiments, using multiple seeds for the numerical calculations as implemented in AFFINImeter, was performed (Piñeiro et al., 2019). A model that incorporates both 1:1 and 2:1 (CD_2:$CHOL_1$) complexes was required to fairly describe the experimental isotherms (equations [8] and [9]). The binding constants resulting from this global fitting of the monomer data reveals that the formation of 1:1 complexes is unfavorable compared to 2:1 complexes. Despite its very low concentration in the explored conditions, the presence of the 1:1 complex is essential for an accurate depiction of the curvature changes for CHOL. For 7KC, the dilution experiments clearly show a different profile compared to that of CHOL (Fig. 25, top). Global analysis of the 7KC ITC data also required a model with two complexes of 1:1 and 2:1 stoichiometry, but with a much more favorable binding constant for 1:1 complexes.

USC
UNIVERSIDADE DE SANTIAGO DE COMPOSTELA

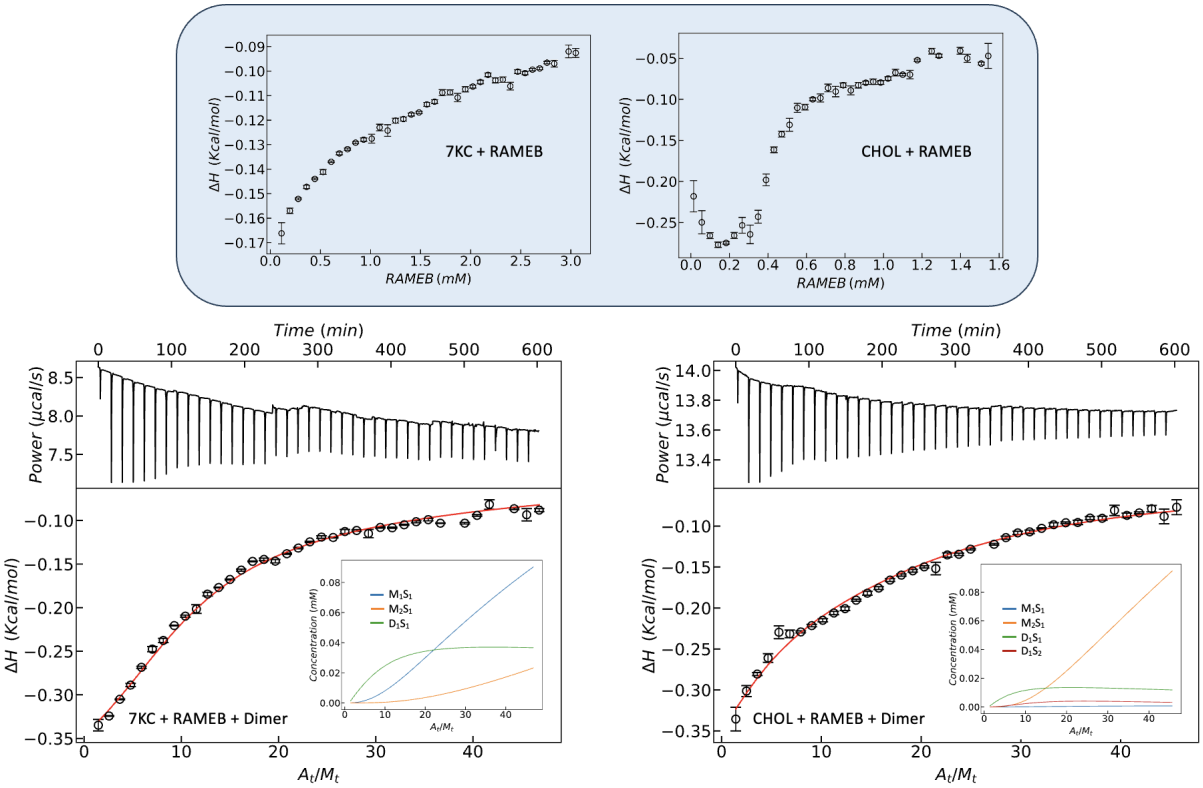


Figure 25. ITC results corresponding to the ITC dilution experiments (top) of RAMEB + sterol and the global fitting of sterol + RAMEB + CD dimer (bottom) for 7KC (left) and CHOL (right). The dilution experiments (top) show that ITC clearly distinguishes the interaction between the sterol and the CD monomer, and that 7KC has a simpler and stronger interaction than CHOL. The competitive experiments (bottom) show much stronger binding between sterols and CD dimers than monomers. The insets show the concentration of M_1S_1 (blue line), M_2S_1 (orange line), D_1S_1 (green line) and D_1S_2 (red line). The concentrations employed for each experiment are indicated in the plots. The full ITC results are supplemented in Fig. S6-11.

The thermodynamic parameters corresponding to the interaction between CHOL and RAMEB were considered to analyze the competitive experiments including the CD dimer. Three independent repeats of these experiments at slightly different concentrations were performed and, again, they were globally analyzed. Fittings assuming that CHOL and the dimer form only a 1:1 complex were unable to successfully describe the experimental data, so it was necessary to consider the presence of an additional chemical species. After several tests, it was observed that the data can be reasonably well described considering also the presence of 1:2 complexes, where two CHOL molecules interact with a single dimer (Fig. S6-12), albeit with high uncertainties in the thermodynamic parameters. The possible encapsulation of two sterol molecules by a single CD dimer is consistent with the presence of two energy wells observed in some of the PMF profiles (e.g. that corresponding to the CD dimer 3 interacting with CHOL in the "up" relative orientation shown in Fig. 23), and this phenomenon has been observed in unrestrained simulations by our group (data not shown). The high uncertainties of the parameters could be attributed to the fact that both CDs are a distribution of multiple molecules with different locations and numbers of substituents, introducing additional uncertainty and complexity. Therefore, we propose the thermodynamic parameters

USC
UNIVERSIDADE DE SANTIAGO DE COMPOSTELA

obtained from this analysis (Tables 5 and 6) are representative values for the entire CD distribution in the sample.

It is worth mentioning that both the 1:1 and the 1:2 complexes between the CD dimer and CHOL are present in the sample at significant concentrations, in contrast to what was observed for the interaction between RAMEB and this sterol molecule, which displays a clear cooperative behavior in favor of the 2:1 ($CD_2Sterol_1$) complexes. The binding constants corresponding to the formation of the 1:1 and 1:2 complexes, as described in equations [10] and [11], cannot be compared as they correspond to reactions of different degrees, thus resulting in different units. However, it is possible to compare the K-value of equation [10] with the *ratio* between the K-values of equations [11] and [10], which represents the formation of the 1:2 complexes from the addition of a second sterol molecule to the already formed 1:1 complex. This latter value, approximating the overall affinity between the steroid and the CD, is (1.79 x 10^9) / (6.5 x 10^4) = 2.75 x 10^4 M^{-1}. This is slightly lower than the K-value corresponding to the formation of the 1:1 complexes from the free molecules.

$$K_{stepwise} = \frac{[D_1S_2]}{[D_1S_1][S]} \qquad [13]$$

Table 5. binding constants and enthalpies for the equilibria indicated in the first column, where M stands for RAMEB, D for the CD dimer, and S for the sterol, obtained from the analysis of dilution and competitive ITC experiments.

S = CHOL	K (M^{-n})	ΔH (kcal/mol)
$M + S \leftrightarrow M_1S_1$	58.2 ± 3.0 M^{-1}	-121 ± 54
$2M + S \leftrightarrow M_2S_1$	(5.631 ± 0.050) x 10^6 M^{-2}	2.2345 ± 0.008
$D + S \leftrightarrow D_1S_1$	(6.5 ± 20) x 10^4 M^{-1}	-1.59 ± 0.11
$D + 2S \leftrightarrow D_1S_2$	(1.79 ± 0.36) x 10^9 M^{-2}	7.3 ± 4.3

For 7KC, the competitive experiments involving the CD dimer were satisfactorily described considering just a 1:1 complex between 7KC and the dimer, with an binding constant of ~$2.0 \cdot 10^7$ M^{-1} (Table 6). This binding constant is similar to the values determined from metadynamics simulations, although a direct comparison should not be made because the ITC experiments consider all the chemical species collectively while the computational calculations distinguish structures with specific numbers and locations of the HP substituents. In contrast to what was observed for the interaction with CHOL, the enthalpies corresponding to 7KC were found to be positive in all cases. This explains the qualitatively different behavior between both sterols observed in Fig. 24.

Overall, it can be concluded that ITC is able to effectively differentiate between the two sterol molecules, despite differing by only 1 atom, not only from the quantitative point of view but also by identifying different interaction schemes. Importantly, it was also found that the affinity of the dimer for 7KC is significantly higher than that for CHOL.

USC
UNIVERSIDADE DE SANTIAGO DE COMPOSTELA

Table 6. binding constants and enthalpies for the equilibria indicated in the first column, for 7KC, obtained from the global analysis of dilution and competitive ITC experiments.

S = 7KC	K (M^{-n})	ΔH (kcal/mol)
$M + S \leftrightarrow M_1S_1$	$(5.01 \pm 0.35) \times 10^4 M^{-1}$	5.18 ± 0.42
$2M + S \leftrightarrow M_2S_1$	$(4.49 \pm 0.34) \times 10^6 M^{-2}$	8.09 ± 0.42
$D + S \leftrightarrow D_1S_1$	$(2.02 \pm 0.15) \times 10^7 M^{-1}$	0.99 ± 0.43
$D + 2S \leftrightarrow D_1S_2$	N/A	N/A

6.4.3 Circular Dichroism

Fig. 7A and 7E show the CiDi spectra obtained by titrating CHOL or 7KC with increasing dimer concentrations. Tables 7 and 8 report the binding constants for the equilibria in Eq. 10 and 12 obtained with the CiDi technique.

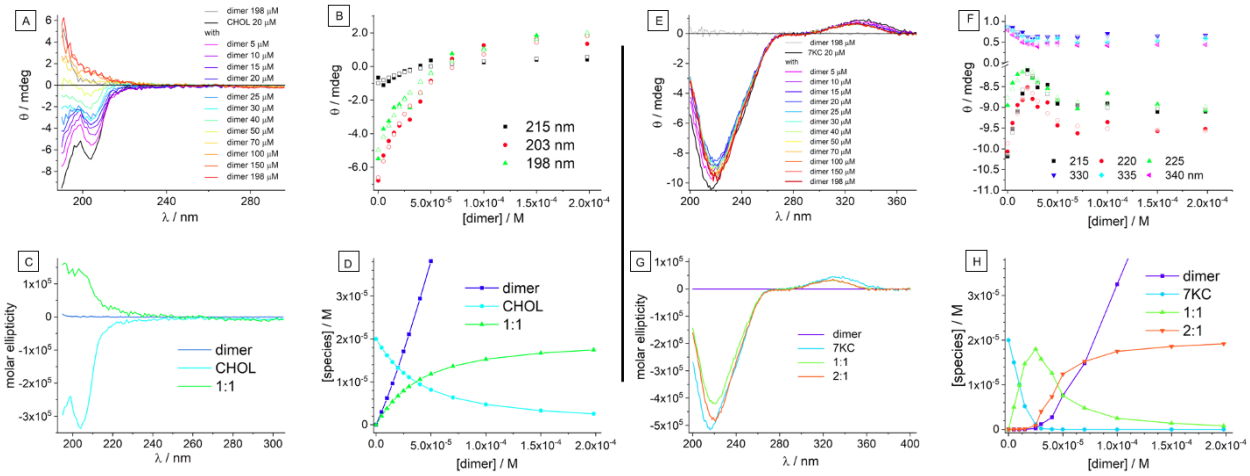


Figure 25. Original CiDi spectra of 20 μM solutions of CHOL (left, A) and 7KC (E) with increasing dimer concentrations (5-200 μM) in a 1 cm cuvette; (B, F) plots of absolute (full symbols) and calculated ellipticity values (empty symbols) at selected wavelengths (nm) for CHOL (B) and 7KC (F); (C, G) calculated spectra of the free components and complexes of the best models for CHOL (C) and 7KC (G); (D, H) species distribution vs total dimer concentration for CHOL (D) and 7KC (H).

In the case of CHOL, it was possible to monitor the intrinsic sterol CiDi signal at 205 nm becoming less intense with increasing CD dimer concentration (Fig. 25). The absorption spectra are dominated by the dimer triazole absorbance (Fig. S6-14). Differently from 7KC, analysis does not converge when applying a model with the simultaneous presence of two complexes with different stoichiometries. The CiDi and absorption data (Table S6-3, Fig. S6-14) both converged when fitted to a model with only one complex with 1:1 stoichiometry, and the binding constants were similar between the two methods. Table 7 reports the binding constant obtained with CiDi. The result of the fitting with the 1:1 model is in good agreement with the ITC results.

USC UNIVERSIDADE DE SANTIAGO DE COMPOSTELA

Table 7. Binding constants for the equilibria indicated in the first column for CHOL, obtained from the global analysis of CiDi experiments, converging with the model in the presence of a single complex for CHOL.

S = CHOL	K (M^{-n})
$D + S \leftrightarrow D_1S_1$	$(3.8 \pm 0.2) \times 10^4\ M^{-1}$

Regarding 7KC, analysis of CiDi data required a model with two complexes with different stoichiometries when analyzing the entire range from 200 to 400 nm. The analysis does not converge when fitting with a model of only one complex with 1:1 or 2:1 (dimer:7KC) stoichiometry. This is not surprising, considering the ellipticity plots at selected wavelengths shown in Fig. 25F. In particular, for the negative band in the 216 nm region of 7KC, there is an ellipticity trend that inverts halfway through titration, different from the positive band in the 300-350 nm region, due to the C=O functionality where there is a small decrease and shift in maximum (Marconi et al., 2011). Analysis of the 7KC absorption spectra confirmed the model with 2 complexes of different stoichiometry, but yielded binding constant values that were lower (Fig. S6-13, S6-14), perhaps because CiDi can more easily sense when changes occur in complex stoichiometry and geometry compared to the absorption technique. Indeed, the CiDi spectrum of the dimer is almost flat in the 200-400 nm range, and the CiDi signal is therefore due to 7KC (with a very intense intrinsic signal). Complexation and interaction with the dimer triazole unit may give rise to an induced signal in the complex, but the shape of the collected CiDi spectra along titration suggests the origin of the observed signal is mainly due to the 7KC unit in the complex. Moreover, the UV changes are very small for 7KC and no relevant trend inversion was observed at any wavelength.

As for the spectral characteristics for the 7KC complexes, the positive band at 350 nm is typical of the C=O bond and the more intense negative band at 220 nm is typical of the conjugated system C=C-C=O, due to n-π* and π-π* transitions, respectively. It is likely that they are both strongly influenced in the 1:1 complex, where we can envision a rigid geometry. A more flexible geometry in the 2:1 complex may allow the π-π* transition to recover in intensity. The lone electron pair of the carbonyl oxygen may be involved in hydrogen bonding in both complexes, thus explaining why its signal does not change when going from 1:1 to 2:1 stoichiometry.

Table 8. Binding constants for the equilibria indicated in the first column, for 7KC, obtained from the global analysis of CiDi experiments, converging with the model in presence of two complexes for 7KC.

S = 7KC	K (M^{-n})
$D + S \leftrightarrow D_1S_1$	$(7.05 \pm 2.20) \times 10^7\ M^{-1}$
$2D + S \leftrightarrow D_2S_1$	$(1.51 \pm 0.48) \times 10^{13}\ M^{-2}$

An additional study has been conducted using CiDi to characterize the interaction of 7KC and CHOL with the HPβCD monomer. In this case, a single trend of decreasing ellipticity was observed around 220 nm and

USC UNIVERSIDADE DE SANTIAGO DE COMPOSTELA

in the 300-350 nm range for 7KC and 205 nm for CHOL (Fig. S6-15, S6-16). Analysis converged with the exclusive presence of a 2:1 complex of 2 CD monomers for one steroid molecule (Table S6-4). The overall binding constant of the 2:1 complexes of 7KC and CHOL with the monomer were much lower compared to the dimer. A similar preference of HPβCD monomers for 7KC over cholesterol was also observed.

The results ultimately show that the CD dimer has very high affinity for 7KC. Furthermore, the CD dimer has higher affinity for 7KC than it does for CHOL. Monomeric HPβCD has a much lower affinity for both CHOL and 7KC. The dimer binding constants are in line with values reported in literature for other CD dimers complexing CHOL (Alcalde et al., 2009; Breslow & Zhang, 1996; Kritharides et al., 1996; Nishijo et al., 2003).

6.5. Discussion

This study forms part of a broader project aimed at designing modified CDs capable of encapsulating toxic biomolecules with high affinity and specificity. This project aims to quantify this interaction by obtaining binding constants for the CD dimer - sterol inclusion complex, but is applicable to any CD dimer inclusion complex. Numerous methods may be employed to perform this characterization, but none of them represent a universal solution for every system. In the case of the interaction between CD dimers and sterol molecules, several difficulties are evident: first, modified CDs are often constituted by a mixture of numerous species with varying number and location of modified groups; second, the sterols targeted in this study are highly insoluble in aqueous media; finally, there are multiple stoichiometries at play, and accounting for all of them is challenging. Here we have utilized one *in silico* and two *in vitro* techniques to synergistically address these problems; namely: PMF calculations from metadynamics simulations, as well as global analysis of multiple competitive ITC and CiDi measurements.

In Silico **-** The convergence of the metadynamics simulations using the distance between the COM of the ligand and of each monomer as collective variables was satisfactory at time scales of 300 ns using 12 walkers and a combination of restraints designed to bias the reversible formation of 1:1 DICs. Under these conditions, the obtained binding constants indicate that the presence of 2-hydroxypropyl substituents at the interface between both monomers in the CD dimer hinder the ability of the CD dimer to distinguish between the sterol molecules. Thus, the CD with a lower number of HP groups in that region shows the highest affinity for 7KC as well as the highest specificity to capture this sterol molecule. This is consistent with previously published work using less quantitative methods for comparing the complexes (Anderson et al., 2021). Previous unbiased molecular dynamics simulations suggested that CD dimers form more stable complexes with sterols than do monomers , and that there was some preference for complexing with 7KC over CHOL, however such calculations did not allow the quantitative characterization of the interactions. Previous crude turbidity tests showed that CD dimers could solubilize 50% of 7KC at a ~10x lower concentration of CD than CHOL, but the difference in concentration does not reflect even the relative difference in actual affinity demonstrated in the present work, which was closer to 1000x using rigorous biophysical methods. It is worth noting that turbidity measurements can be affected by different molecular interaction mechanisms other than the simple formation of 1:1 inclusion complexes. NMR has also shown the same dimer encapsulating both 7KC and CHOL predominantly in 1:1 double-inclusion complexes, but the model proposed for the 7KC complex appeared to be more clear and consistent than that with CHOL (Anderson et al., 2021). The computational method employed in the present work is exceptional for studying specific modified CD molecules with a predetermined number and location of the substituted

USC
UNIVERSIDADE DE SANTIAGO DE COMPOSTELA

groups, but it cannot be directly employed to derive the apparent binding constant for a whole distribution formed by an astronomical number of different structures present in a non-isomeric mixture typical of randomly substituted CDs.

In Vitro - Both ITC and CiDi enable quantification while considering the overall contribution of the entire distribution of different molecular structures that are present in the sample, and distinguish between the different stoichiometries in the mixture, while the simulations currently focus on a single isomer at a time in the 1:1-DIC complex. CiDi has an advantage over ITC in that the technique does not require competition between two encapsulators for these systems, in this case the dimer and RAMEB. ITC, on the other hand, by virtue of the fact that it directly measures the heat (energy) difference between states, might be considered a more direct and empirical quantification of binding. Both *in vitro* methods indicate that the 1:1 complexes have the most favorable binding constant especially for 7KC, and to a lesser extent for CHOL. Further, both *in vitro* techniques reveal complexes with additional stoichiometries to be considered, and that those stoichiometric contributions are different between 7KC and CHOL (which is surprising, considering the molecules differ by only one atom, but also encouraging as we are seeking selectivity for 7KC over cholesterol (Anderson et al., 2021). Importantly, the concentration ratio of CD to sterol is different between CiDi and ITC, which could impact the interpretation of the stoichiometry and/or binding constants. For example, the CiDi concentration range accounts for the 2:1 (CD:sterol) complex, while ITC accounts for the 1:2 (CD:sterol) complex, making the methods complementary in this respect, but the obtained binding constants broadly agree between the two *in vitro* methods. By most measures, 1:1 complexes dominate the interaction, while ITC suggests that there may be a significant presence of 1:2 complexes between the CD dimer and CHOL. Interestingly, ITC clearly shows that both sterol molecules can be distinguished by RAMEB CD monomers, even at the qualitative level and out of model considerations, which was a surprising result. Noticeably, in the case of 7KC, the interaction is always entropy driven. A possible reason may be the more rigid skeleton of 7KC compared to CHOL (due to sp2 hybridization of the 7 carbon in 7KC compared to sp3 of the same carbon in CHOL), preventing 7KC from optimizing the non-covalent interactions with the CD. The interaction may thus be exclusively entropy driven in the case of 7KC, and solvation effects are likely important. Another hypothesis, which supports entropy-driven processes, is the co-existence of more conformations for a single complex, as suggested by the calculations that find two energy wells in several cases. Finally, in the case of CHOL, the 1:1 complex with the dimer has favorable enthalpy, likely due to multiple optimized non-covalent interactions. In the complex with two sterols, solvation effects are expected to be more important, and also multiple conformations may exist.

The structure of CD inclusion complexes is pivotal in their ability to effectively distinguish between 7KC and CHOL, and therefore potentially mitigate 7KC toxicity in a biological setting. For the studied CD dimers, the 1:1 complex is the strongest, and computational studies indicate that this complex is likely a DIC (Fig. 23). This complex is more favorable for 7KC than for CHOL, despite the only subtle difference between the molecular structures of 7KC and CHOL. Noncovalent interactions stabilize the inclusion complex, so a slight difference in rigidity and/or hydrophobicity can convey a significant difference in binding constant for CD inclusion complexes. Additionally, our previous publication details the impact of the substitutions and linker on the strength and specificity of the interaction compared to other dimers. In this previous study, a small number of HP groups in combination with the triazole group on the linker exhibited the best 7KC specificity at a qualitative level (possibly caused by a destabilizing effect on the

USC
UNIVERSIDADE DE SANTIAGO DE COMPOSTELA

cholesterol inclusion complex) (Anderson et al., 2021). The present study supports that hypothesis, and elucidates quantitative binding constants for this one dimer.

6.6. Conclusion

The combined results of these experiments demonstrate that the CD dimer has ~1000 fold stronger affinity for 7KC than for CHOL. The binding constants obtained from the *in vitro* methods compare well to those obtained from metadynamics simulations, and they are comparable or even higher than other values reported in literature for similar systems of steroid complexes with CD dimers (Christoforides et al., 2018; Kritharides et al., 1996; Piñeiro et al., 2007). While some of the inclusion complex properties remain difficult to characterize, the combined methods demonstrate the ability of CD dimers to quantitatively differentiate between very similar guest molecules.

This work underscores the challenges in obtaining realistic binding constants for complex systems, as well as the advantages and disadvantages of three different methods. Here, specific protocols have been developed to optimize the characterization of these systems by conducting an orthogonal study based on three different methods to obtain complementary information. In particular, the power of iterating between multiple simulations of single isomers and empirical *in vitro* data from non-isomeric mixtures of host molecules should not be under-appreciated. While computational data always needs to be validated with physical data, simulations allow for predictions, enriched interpretation of empirical experiments, and the isolation of questions that cannot be asked in real-world experiments. The combination of the two help explain the true nature of the complex better than either on its own. This study is expected to serve as a benchmark in the characterization of other, similarly complex systems. The remarkable capability of these CD dimers to discriminate between targets as similar as CHOL and 7KC, both qualitatively and quantitatively, highlights the potential for leveraging CDs in the specific encapsulation of particular small molecules for diverse applications.

USC
UNIVERSIDADE DE SANTIAGO DE COMPOSTELA

Chapter 7. General Conclusions

USC
UNIVERSIDADE
DE SANTIAGO
DE COMPOSTELA

This thesis serves as a benchmark in characterizing complex cyclodextrin inclusion systems, and highlights the value of integrating computational and wet laboratory techniques to unravel the intricacies of molecular interactions. We have used multiple computational techniques, automated to be a simple workflow, to assess multiple CD inclusion complexes, both CD monomers and CD dimers. Our results suggest that our computational methods are robust enough to show realistic inclusion dynamics and conformations, and even estimate affinity constants using only *in silico* tools. Given how difficult it can be to measure these constants *in vitro*, the ability to calculate these values greatly enhances our ability to design and craft CDs for specific purposes without spending prohibitive amounts of time or money in the lab. Moreover, computational simulations can provide information which is inaccessible or difficult to access in the lab, both in regards to the dynamics of the complex and the structure of the CD. The research not only advances our understanding of CD binding but also provides a framework for investigating similar complex systems in the future.

We have shown in this work that our methods can successfully reproduce known characteristics of known systems, such as the sugammadex-rocuronium system. This system was chosen to validate our methods because it is well characterized and currently used as an NMB reversal agent in humans. Additionally, sugammadex exists as a single isomer, unlike many other substituted CDs, making its computational study simpler. In this study, we used docking, unbiased MD, and metadynamics coupled with PMF to analyze the sugammadex-rocuronium system. We were able to recapitulate the crystal structure of the sugammadex-rocuronium inclusion complex using MD, docking, and metadynamics/PMF, as well as calculate the binding constant for the interaction using the PMF. These encouraging results suggest that we are effectively capturing the important characteristics of the inclusion complex using our methods, and that we could use them to extrapolate onto other CD systems. Our simulations also indicated that a secondary inclusion complex, one with the opposite orientation of that in the crystal structure, may exist in solution. We have also shown that the Lennard-Jones interactions of the complex are exceptionally strong, which could explain the viability of this secondary orientation despite its less favorable electrostatic interactions.

We also set out to validate our PMF method against a series of CD monomer systems, not only sugammadex-rocuronium but also βCD monomers complexing with steroids, which are more similar systems to the novel CD dimer system. Except for native βCD, these systems exist in solution as a series of isomers, making their *in silico* study more nuanced than that of sugammadex. We executed a total of 384 metadynamics simulations (4 CDs, 2 orientations, 12 walkers, 4 runs), which was enough to do a statistical analysis on the data distribution. We determined that the preferred orientation for sterols and βCDs was one in which the hydrophobic headgroup was deeply embedded in the cavity of the CD, while the more hydrophilic tail group extended out of the wide face (the down orientation). We also found a more efficient method for sampling randomly substituted CDs interacting with sterols, in which only the wide face of the CD is sampled. This method was explored due to the roughness of the energy profile on the small face, which impacts the ease of sampling on that side, but this is not expected to be valid for CDs that are not randomly substituted, such as sugammadex. This protocol, based on metadynamics simulations focusing on a single dimension (displacement along the CD's symmetry axis), offers high reproducibility, and sampling of only half of the CD can conserve computational resources while maintaining accuracy.

The final study was aimed at computationally quantifying the specificity for binding 7KC over cholesterol by the novel CD dimers developed by Cyclarity Therapeutics. The purpose of this novel CD dimer is to have high affinity and specificity for 7KC over cholesterol so that it can be used as a treatment for

USC
UNIVERSIDADE
DE SANTIAGO
DE COMPOSTELA

atherosclerosis. In the future, we aim to design more CD dimers to specifically encapsulate other molecules for a variety of purposes, such as those outlined in the introduction of this thesis. Obtaining a reliable binding constant for this system is exceedingly difficult due to multiple factors - an entirely computational method would offer an expedited route to obtaining these important values. This study set out to compare multiple *in vitro* methods (CiDi, ITC) with an entirely *in silico* method, aiming to provide a more complete picture of the interaction from multiple viewpoints. For the computational part, a series of CD dimers were chosen to account for some variability in isomeric structures. Each method had significant advantages and drawbacks, but together they provide a comprehensive analysis of the CD dimer inclusion complex. The binding constants obtained through both computational and laboratory methods reveal that CD dimers exhibit approximately 1,000-fold higher affinity for 7KC compared to cholesterol. Computationally, we were able to determine the structures of the inclusion complexes, as well as the subtle differences between the complexes with 7KC and cholesterol. The combined results underscore the capability of CD dimers to differentiate between closely related molecules such as cholesterol and 7KC, both qualitatively and quantitatively. This suggests the potential of CDs in specific small molecule encapsulation for various applications, establishing a benchmark for characterizing similar complex systems.

This research emphasizes the remarkable binding affinity of this CD dimer for 7KC, showcasing its potential for specific encapsulation of this toxic biomolecule. Moreover, we underscore the challenges inherent in obtaining and validating realistic binding constants for complex systems, particularly when dealing with mixtures of CD species and subtle structural differences between guest molecules. By leveraging multi-method approaches, both computationally and with empirical laboratory data, we can gain a more comprehensive understanding of the interactions. Computational methods make it possible to understand the CD inclusion complex at a level of detail and certainty impossible to achieve *in vitro*, and we hope the methods presented here will set the stage for future *in silico* research of CD applications.

Final Thoughts

The research presented here underscores the importance of a multifaceted approach in scientific inquiry. By combining computational modeling methods with experimental validation, a deeper insight can be found into complex molecular interactions, offering possible reasons for observed phenomena. Computational methods can be validated by known systems, and even shed light on the mechanism of important drugs that are used every day in hospitals. Once validated, *in silico* methods are an effective tool for understanding both known and unknown systems in great detail.

The *in silico* modeling of CDs has led to the synthesis of novel CD dimers as a treatment for atherosclerosis by encapsulating and sequestering 7KC. These CD dimers have high potential as versatile tools for selectively encapsulating specific biomolecules - in particular, the ability to distinguish between structurally similar molecules like cholesterol and 7KC. This has significant implications in disease treatment and overall understanding of the mechanistic underpinnings driving complex diseases related to 7KC, such as atherosclerosis. Moreover, researchers can use this knowledge about CD encapsulation to design targeted delivery systems, improve drug and product formulations, and enhance the effectiveness of CD-based agents in many different contexts. CDs are already valuable tools for multiple industries, and improving them by modifying their structures based on computational simulations could greatly expand their utility.

At Cyclarity Therapeutics, the primary goal of these studies was to build, assess, and validate a platform technology for evaluating CD inclusion complexes *in silico*. We have reached a point where our simulations

USC UNIVERSIDADE DE SANTIAGO DE COMPOSTELA

and analyses are satisfactorily automated and uploaded to a private database, which we maintain with thousands of CD simulations. The goal of this database is to implement AI and ML algorithms to help us understand the CD inclusion complex and its many facets, as well as to propose new CD structures for particular purposes. Validation is ongoing to ensure that our inclusion complexes are accurately captured and analyzed, and the sugammadex study presented in this thesis was critical to our confidence in the models. One of the primary challenges in CD research, especially in designing CDs for specific uses, is the chemical modification of CDs, which can lead to a large number of isomers due to their cyclic structures. AI and machine learning technologies could play an important role here, aiding in the modeling of inclusion complexes with specific CD isomers and assisting in the identification of reliable descriptors within large datasets. This approach not only streamlines the development process but also increases the precision in targeting specific molecules. By assessing system 'pseudoaffinity' and other metaparameters, these AI-driven models can predict optimal CD structures for specific targets. This advancement is not just limited to theoretical modeling but extends to practical applications in medicine, where CDs can be used to create safe and effective drug delivery systems, and beyond. By enhancing the precision and efficiency of CD development, AI-powered approaches have the potential to drive significant innovation across a variety of fields.

In concluding this exploration into the captivating world of CDs, we not only understand their interactions with multiple guest molecules using multiple *in vitro* and *in silico* methods, but also open new horizons for predictive design and diverse applications. As scientific research continues to advance, interdisciplinary collaborations and the integration of computational and experimental techniques will play a pivotal role in unlocking new discoveries and addressing complex challenges. From therapeutic interventions for atherosclerosis and beyond, the implications of our research are expansive. This thesis bridges the gap between computational methods and complex molecular interactions, advancing the boundaries of knowledge in the study of CDs, and laying a robust foundation for future investigations and innovations.

USC
UNIVERSIDADE DE SANTIAGO DE COMPOSTELA

References

Abraham, M. J., Murtola, T., Schulz, R., Páll, S., Smith, J. C., Hess, B., & Lindahl, E. (2015). GROMACS: High performance molecular simulations through multi-level parallelism from laptops to supercomputers. *SoftwareX*, *1–2*, 19–25. https://doi.org/10.1016/j.softx.2015.06.001

Aime, S., Gianolio, E., Arena, F., Barge, A., Martina, K., Heropoulos, G., & Cravotto, G. (2009). New cyclodextrin dimers and trimers capable of forming supramolecular adducts with shape-specific ligands. *Org. Biomol. Chem.*, *7*(2), 370–379. https://doi.org/10.1039/B812172A

Aksamija, A., Tomao, V., Dangles, O., & Plasson, R. (2022). Encapsulation of phenolic acids into cyclodextrins: A global statistical analysis of the effects of pH, temperature and concentrations on binding constants measured by ACE methods. *ELECTROPHORESIS*, *43*(23–24), 2290–2301. https://doi.org/10.1002/elps.202200075

Alcalde, M. A., Antelo, A., Jover, A., Meijide, F., & Tato, J. V. (2009). Solubilization of cholesterol in aqueous solution by two β-cyclodextrin dimers and a negatively charged β-cyclodextrin derivative. *Journal of Inclusion Phenomena and Macrocyclic Chemistry*, *63*(3–4), 309–317. https://doi.org/10.1007/s10847-008-9524-3

Allenmark, S. (2003). Induced circular dichroism by chiral molecular interaction. *Chirality*, *15*(5), 409–422. https://doi.org/10.1002/chir.10220

Almeida, B., Domingues, C., Mascarenhas-Melo, F., Silva, I., Jarak, I., Veiga, F., & Figueiras, A. (2023). The Role of Cyclodextrins in COVID-19 Therapy—A Literature Review. *International Journal of Molecular Sciences*, *24*(3), Article 3. https://doi.org/10.3390/ijms24032974

Al-Soufi, W., Reija, B., Felekyan, S., Seidel, C. A. M., & Novo, M. (2008). Dynamics of Supramolecular Association Monitored by Fluorescence Correlation Spectroscopy. *ChemPhysChem*, *9*(13), 1819–1827. https://doi.org/10.1002/cphc.200800330

Altman, D. G., & Bland, J. M. (1983). Measurement in Medicine: The Analysis of Method Comparison Studies. *The Statistician*, *32*(3), 307. https://doi.org/10.2307/2987937

Anand, R., Ottani, S., Manoli, F., Manet, I., & Monti, S. (2012). A close-up on doxorubicin binding to γ-cyclodextrin: An elucidating spectroscopic, photophysical and conformational study. *RSC Advances*, *2*(6), 2346–2357. https://doi.org/10.1039/C2RA01221A

Andersen, H. C. (1980). Molecular dynamics simulations at constant pressure and/or temperature. *The Journal of Chemical Physics*, *72*(4), 2384–2393. https://doi.org/10.1063/1.439486

Anderson, A. M., Campo, A., Fulton, E., Corwin, A., Jerome, W. G., & O'Connor, M. S. (2020). 7-Ketocholesterol in disease and aging. *Redox Biology*, *29*, 101380. https://doi.org/10.1016/j.redox.2019.101380

Anderson, A. M., Kirtadze, T., Malanga, M., Dinh, D., Barnes, C., Campo, A., Clemens, D. M., Garcia-Fandiño, R., Piñeiro, Á., & O'Connor, M. S. (2021). Cyclodextrin dimers: A versatile approach to optimizing encapsulation and their application to therapeutic extraction of toxic oxysterols. *International Journal of Pharmaceutics*, *606*, 120522. https://doi.org/10.1016/j.ijpharm.2021.120522

Anderson, A. M., Manet, I., Malanga, M., Clemens, D. M., Sadrerafi, K., Piñeiro, Á., García-Fandiño, R., & O'Connor, M. S. (2024). Addressing the complexities in measuring cyclodextrin-sterol binding constants: A multidimensional study. *Carbohydrate Polymers*, *323*, 121360. https://doi.org/10.1016/j.carbpol.2023.121360

Angelova, A., Ringard-Lefebvre, C., & Baszkin, A. (1999). Drug-Cyclodextrin Association Constants Determined by Surface Tension and Surface Pressure Measurements. *Journal of Colloid and Interface Science 212, 275–279 (1999)*, *212*, 275–279.

Aprà, E., Bylaska, E. J., De Jong, W. A., Govind, N., Kowalski, K., Straatsma, T. P., Valiev, M., Van Dam, H. J. J., Alexeev, Y., Anchell, J., Anisimov, V., Aquino, F. W., Atta-Fynn, R., Autschbach, J., Bauman, N. P., Becca, J. C., Bernholdt, D. E., Bhaskaran-Nair, K., Bogatko, S., … Harrison, R. J. (2020). NWChem: Past, present, and future. *The Journal of Chemical Physics*, *152*(18), 184102. https://doi.org/10.1063/5.0004997

USC UNIVERSIDADE DE SANTIAGO DE COMPOSTELA

Archambault, J.-C., Djedaini-Pilard, F., Ouvrard-Baraton, F., & Weisse, S. (2004). *Utilisation cosmetique ou dermatologique de la vitamine a ou de ses esters, en association avec une bêta-cyclodextrine partiellement methylee* (World Intellectual Property Organization Patent WO2003063805A3). https://patents.google.com/patent/WO2003063805A3/en?oq=WO2003063805

Arima, H., Motoyama, K., & Higashi, T. (2017). Potential Use of Cyclodextrins as Drug Carriers and Active Pharmaceutical Ingredients. *Chemical and Pharmaceutical Bulletin*, *65*(4), 341–348. https://doi.org/10.1248/cpb.c16-00779

Arsiccio, A., Rospiccio, M., Shea, J.-E., & Pisano, R. (2021). Force Field Parameterization for the Description of the Interactions between Hydroxypropyl-β-Cyclodextrin and Proteins. *The Journal of Physical Chemistry B*, *125*(27), 7397–7405. https://doi.org/10.1021/acs.jpcb.1c04033

Astray, G., Mejuto, J. C., & Simal-Gandara, J. (2020). Latest developments in the application of cyclodextrin host-guest complexes in beverage technology processes. *Food Hydrocolloids*, *106*, 105882. https://doi.org/10.1016/j.foodhyd.2020.105882

Aykaç, A., Martos-Maldonado, M. C., Casas-Solvas, J. M., García-Fuentes, L., & Vargas-Berenguel, A. (2012). Binding ability properties of β-cyclodextrin dimers linked through their secondary faces towards cancer chemotherapeutic agent methotrexate. *J. Drug Del. Sci. Tech.*, *22*(3), 270–272.

Badruddoza, A. Z. M., Shawon, Z. B. Z., Tay, W. J. D., Hidajat, K., & Uddin, M. S. (2013). Fe3O4/cyclodextrin polymer nanocomposites for selective heavy metals removal from industrial wastewater. *Carbohydrate Polymers*, *91*(1), 322–332. https://doi.org/10.1016/j.carbpol.2012.08.030

Balaka, C., Poulida, S., Miliatou, M., Roussakis, A., Lavranou, V., Moshaki, M., Komi, L., & Romana, C. (2011). O-52 Comparison of sugammadex to neostigmine reversal of neuromuscular blockade in patients with myasthenia gravis. *Journal of Cardiothoracic and Vascular Anesthesia*, *25*(3), S22–S23. https://doi.org/10.1053/j.jvca.2011.03.065

Banach, M., Stulc, T., Dent, R., & Toth, P. P. (2016). Statin non-adherence and residual cardiovascular risk: There is need for substantial improvement. *International Journal of Cardiology*, *225*, 184–196. https://doi.org/10.1016/j.ijcard.2016.09.075

Barbosa, P. F. P., Cumba, L. R., Andrade, R. D. A., & do Carmo, D. R. (2019). Chemical Modifications of Cyclodextrin and Chitosan for Biological and Environmental Applications: Metals and Organic Pollutants Adsorption and Removal. *Journal of Polymers and the Environment*, *27*(6), 1352–1366. https://doi.org/10.1007/s10924-019-01434-x

Barducci, A., Bonomi, M., & Parrinello, M. (2011). Metadynamics. *WIREs Computational Molecular Science*, *1*(5), 826–843. https://doi.org/10.1002/wcms.31

Barducci, A., Bussi, G., & Parrinello, M. (2008). Well-Tempered Metadynamics: A Smoothly Converging and Tunable Free-Energy Method. *Physical Review Letters*, *100*(2), 020603. https://doi.org/10.1103/PhysRevLett.100.020603

Bartlett, R. J., & Musiał, M. (2007). Coupled-cluster theory in quantum chemistry. *Reviews of Modern Physics*, *79*(1), 291–352. https://doi.org/10.1103/RevModPhys.79.291

Bartlett, R. J., & Purvis, G. D. (1978). Many-body perturbation theory, coupled-pair many-electron theory, and the importance of quadruple excitations for the correlation problem. *International Journal of Quantum Chemistry*, *14*(5), 561–581. https://doi.org/10.1002/qua.560140504

Berendsen, H. J. C., Postma, J. P. M., Van Gunsteren, W. F., & Hermans, J. (1981). Interaction Models for Water in Relation to Protein Hydration. In B. Pullman (Ed.), *Intermolecular Forces* (Vol. 14, pp. 331–342). Springer Netherlands. https://doi.org/10.1007/978-94-015-7658-1_21

Berendsen, H. J. C., van der Spoel, D., & van Drunen, R. (1995). GROMACS: A message-passing parallel molecular dynamics implementation. *Computer Physics Communications*, *91*(1–3), 43–56. https://doi.org/10.1016/0010-4655(95)00042-E

Bertaut, E., & Landy, D. (2014). Improving ITC studies of cyclodextrin inclusion compounds by global analysis of conventional and non-conventional experiments. *Beilstein Journal of Organic Chemistry*, *10*, 2630–2641. https://doi.org/10.3762/bjoc.10.275

Blanco-González, A., Marrink, S. J., Piñeiro, Á., & García-Fandiño, R. (2023). Molecular insights into the

USC DE SANTIAGO DE COMPOSTELA

effects of focused ultrasound mechanotherapy on lipid bilayers: Unlocking the keys to design effective treatments. *Journal of Colloid and Interface Science*, *650*, 1201–1210. https://doi.org/10.1016/j.jcis.2023.07.077

Blaszkiewicz, C., Bricout, H., Léonard, E., Len, C., Landy, D., Cézard, C., Djedaïni-Pilard, F., Monflier, E., & Tilloy, S. (2013). A cyclodextrin dimer as a supramolecular reaction platform for aqueous organometallic catalysis. *Chemical Communications*, *49*(62), 6989. https://doi.org/10.1039/c3cc43647k

Bom, A., Bradley, M., Cameron, K., Clark, J. K., van Egmond, J., Feilden, H., MacLean, E. J., Muir, A. W., Palin, R., Rees, D. C., & Zhang, M.-Q. (2002). A Novel Concept of Reversing Neuromuscular Block: Chemical Encapsulation of Rocuronium Bromide by a Cyclodextrin-Based Synthetic Host *Angewandte Chemie International Edition*, *41*(2), 265. https://doi.org/10.1002/1521-3773(20020118)41:2<265::AID-ANIE265>3.0.CO;2-Q

Bonnet, P., Jaime, C., & Morin-Allory, L. (2001). α-, β-, and γ-Cyclodextrin Dimers. Molecular Modeling Studies by Molecular Mechanics and Molecular Dynamics Simulations. *The Journal of Organic Chemistry*, *66*(3), 689–692. https://doi.org/10.1021/jo0008284

Bonnet, P., Jaime, C., & Morin-Allory, L. (2002). Structure and Thermodynamics of α-, β-, and γ-Cyclodextrin Dimers. Molecular Dynamics Studies of the Solvent Effect and Free Binding Energies. *The Journal of Organic Chemistry*, *67*(24), 8602–8609. https://doi.org/10.1021/jo026166v

Bonomi, M., Branduardi, D., Bussi, G., Camilloni, C., Provasi, D., Raiteri, P., Donadio, D., Marinelli, F., Pietrucci, F., Broglia, R. A., & Parrinello, M. (2009). PLUMED: A portable plugin for free-energy calculations with molecular dynamics. *Computer Physics Communications*, *180*(10), 1961–1972. https://doi.org/10.1016/j.cpc.2009.05.011

Bonomi, M., Bussi, G., Camilloni, C., Tribello, G. A., Banáš, P., Barducci, A., Bernetti, M., Bolhuis, P. G., Bottaro, S., Branduardi, D., Capelli, R., Carloni, P., Ceriotti, M., Cesari, A., Chen, H., Chen, W., Colizzi, F., De, S., De La Pierre, M., … The PLUMED consortium. (2019). Promoting transparency and reproducibility in enhanced molecular simulations. *Nature Methods*, *16*(8), Article 8. https://doi.org/10.1038/s41592-019-0506-8

Bonomi, M., & Parrinello, M. (2010). Enhanced Sampling in the Well-Tempered Ensemble. *Physical Review Letters*, *104*(19), 190601. https://doi.org/10.1103/PhysRevLett.104.190601

Bouchemal, K., & Mazzaferro, S. (2012). How to conduct and interpret ITC experiments accurately for cyclodextrin–guest interactions. *Drug Discovery Today*, *17*(11–12), 623–629. https://doi.org/10.1016/j.drudis.2012.01.023

Breslow, R., Greenspoon, N., Guo, T., & Zarzycki, R. (1989). Very strong binding of appropriate substrates by cyclodextrin dimers. *Journal of the American Chemical Society*, *111*(21), 8296–8297. https://doi.org/10.1021/ja00203a050

Breslow, R., Halfon, S., & Zhang, B. (1995). Molecular recognition by cyclodextrin dimers. *Tetrahedron*, *51*(2), 377–388. https://doi.org/10.1016/0040-4020(94)00903-8

Breslow, R., & Zhang, B. (1996). Cholesterol Recognition and Binding by Cyclodextrin Dimers. *Journal of the American Chemical Society*, *118*(35), 8495–8496. https://doi.org/10.1021/ja961567b

Brewster, M. E., & Loftsson, T. (2007). Cyclodextrins as pharmaceutical solubilizers. *Advanced Drug Delivery Reviews*, *59*(7), 645–666. https://doi.org/10.1016/j.addr.2007.05.012

Bursulaya, B. D., Totrov, M., Abagyan, R., & Brooks, C. L. (2003). Comparative study of several algorithms for flexible ligand docking. *Journal of Computer-Aided Molecular Design*, *17*(11), 755–763. https://doi.org/10.1023/b:jcam.0000017496.76572.6f

Buschmann, H.-J., & Schollmeyer, E. (2002). Applications of cyclodextrins in cosmetic products: A review. *Journal of Cosmetic Science*, *53*(3), 185–191.

Bussi, G., & Laio, A. (2020). Using metadynamics to explore complex free-energy landscapes. *Nature Reviews Physics*, *2*(4), Article 4. https://doi.org/10.1038/s42254-020-0153-0

Casas-Solvas, J. M., Quesada-Soriano, I., Carreño-Gázquez, D., Giménez-Martínez, J. J., García-Fuentes, L., & Vargas-Berenguel, A. (2011). β-Cyclodextrin Dimers Linked through Their Secondary Faces

USC UNIVERSIDADE DE SANTIAGO DE COMPOSTELA

with Rigid Spacer Arms as Hosts for Bile Salts. *Langmuir*, *27*(16), 9729–9737. https://doi.org/10.1021/la201180u

Castagne, D., Dive, G., Evrard, B., Frédérich, M., & Piel, G. (2010). Spectroscopic studies and molecular modeling for understanding the interactions between cholesterol and cyclodextrins. *Journal of Pharmacy & Pharmaceutical Sciences*, *13*(3), Article 3. https://doi.org/10.18433/J3BS34

Cézard, C., Trivelli, X., Aubry, F., Djedaïni-Pilard, F., & Dupradeau, F.-Y. (2011). Molecular dynamics studies of native and substituted cyclodextrins in different media: 1. Charge derivation and force field performances. *Physical Chemistry Chemical Physics*, *13*(33), 15103. https://doi.org/10.1039/c1cp20854c

Chatjigakis, A. K., Donze, C., Coleman, A. W., & Cardot, P. (1992). Solubility behavior of .beta.-cyclodextrin in water/cosolvent mixtures. *Analytical Chemistry*, *64*(14), 1632–1634. https://doi.org/10.1021/ac00038a022

Chmurski, K., Stepniak, P., & Jurczak, J. (2016). Long-chain-linked β-cyclodextrin dimers: Synthesis and relationship between reactivity and inclusion complex formation. *Carbohydrate Polymers*, *138*, 8–15. https://doi.org/10.1016/j.carbpol.2015.11.054

Cho, A. E., Guallar, V., Berne, B. J., & Friesner, R. (2005). Importance of accurate charges in molecular docking: Quantum mechanical/molecular mechanical (QM/MM) approach. *Journal of Computational Chemistry*, *26*(9), 915–931. https://doi.org/10.1002/jcc.20222

Choi, Y.-H., Yang, C.-H., Kim, H.-W., & Jung, S. (2000). *Molecular Modeling Studies of the β-Cyclodextrin in Monomer and Dimer Form as Hosts for the Complexation of Cholesterol*. 6.

Christoforides, E., Papaioannou, A., & Bethanis, K. (2018). Crystal structure of the inclusion complex of cholesterol in β-cyclodextrin and molecular dynamics studies. *Beilstein Journal of Organic Chemistry*, *14*, 838–848. https://doi.org/10.3762/bjoc.14.69

Coisne, C., Tilloy, S., Monflier, E., Wils, D., Fenart, L., & Gosselet, F. (2016). Cyclodextrins as Emerging Therapeutic Tools in the Treatment of Cholesterol-Associated Vascular and Neurodegenerative Diseases. *Molecules*, *21*(12), 1748. https://doi.org/10.3390/molecules21121748

Connors, K. A. (1987). *Binding constants: The measurement of molecular complex stability*. Wiley.

Cornell, W. D., Cieplak, P., Bayly, C. I., Gould, I. R., Merz, K. M., Ferguson, D. M., Spellmeyer, D. C., Fox, T., Caldwell, J. W., & Kollman, P. A. (1995). A Second Generation Force Field for the Simulation of Proteins, Nucleic Acids, and Organic Molecules. *Journal of the American Chemical Society*, *117*(19), 5179–5197. https://doi.org/10.1021/ja00124a002

Crini, G., Fourmentin, S., Fenyvesi, É., Torri, G., Fourmentin, M., & Morin-Crini, N. (2018). Cyclodextrins, from molecules to applications. *Environmental Chemistry Letters*, *16*(4), 1361–1375. https://doi.org/10.1007/s10311-018-0763-2

Darden, T., York, D., & Pedersen, L. (1993). Particle mesh Ewald: An $N \cdot \log(N)$ method for Ewald sums in large systems. *The Journal of Chemical Physics*, *98*(12), 10089–10092. https://doi.org/10.1063/1.464397

de Jong, M. R., Engbersen, J. F., Huskens, J., & Reinhoudt, D. N. (2000). Cyclodextrin dimers as receptor molecules for steroid sensors. *Chemistry (Weinheim an Der Bergstrasse, Germany)*, *6*(21), 4034–4040. https://doi.org/10.1002/1521-3765(20001103)6:21<4034::aid-chem4034>3.0.co;2-3

Del Valle, E. M. M. (2004). Cyclodextrins and their uses: A review. *Process Biochemistry*, *39*(9), 1033–1046. https://doi.org/10.1016/S0032-9592(03)00258-9

Ding, B., Yu, Y., Geng, S., Liu, B., Hao, Y., & Liang, G. (2022). Computational Methods for the Interaction between Cyclodextrins and Natural Compounds: Technology, Benefits, Limitations, and Trends. *Journal of Agricultural and Food Chemistry*, *70*(8), 2466–2482. https://doi.org/10.1021/acs.jafc.1c07018

Doan, A. T. N., Doan, V. T. H., Katsuki, J., Fujii, S., Kono, H., & Sakurai, K. (2022). Dramatically Increased Binding Constant of Water-Soluble Cyclodextrin Hyperbranched Polymers: Explored with Diffusion Ordered NMR Spectroscopy (DOSY). *ACS Omega*, *7*(13), 10890–10900. https://doi.org/10.1021/acsomega.1c06194

Dodziuk, H. (2002). Rigidity versus flexibility. A review of experimental and theoretical studies pertaining

USC DE SANTIAGO DE COMPOSTELA

to the cyclodextrin nonrigidity. *Journal of Molecular Structure*, *614*(1), 33–45. https://doi.org/10.1016/S0022-2860(02)00236-3

European Medicines Agency. (2017). *Cyclodextrins used as excipients*.

Ezri, T., Boaz, M., Sherman, A., Armaly, M., & Berlovitz, Y. (2016). Sugammadex: An Update. *The Journal of Critical Care Medicine*, *2*(1), 16–21. https://doi.org/10.1515/jccm-2016-0005

F. Garrido, P., Calvelo, M., Garcia-Fandiño, R., & Piñeiro, Á. (2020). Rings, Hexagons, Petals, and Dipolar Moment Sink-Sources: The Fanciful Behavior of Water around Cyclodextrin Complexes. *Biomolecules*, *10*(3), 431. https://doi.org/10.3390/biom10030431

Feng, J., Ding, S.-Y., Tucker, M. P., Himmel, M. E., Kim, Y.-H., Zhang, S. B., Keyes, B. M., & Rumbles, G. (2005). Cyclodextrin driven hydrophobic/hydrophilic transformation of semiconductor nanoparticles. *Applied Physics Letters*, *86*(3), 033108. https://doi.org/10.1063/1.1854739

Fenyvesi, É. (2011). *CYCLODEXTRINS IN BIOREMEDIATION OF CONTAMINATED SOIL*. *25*(5).

Fenyvesi, E., & Szente, L. (2016). 18—Nanoencapsulation of flavors and aromas by cyclodextrins. In A. M. Grumezescu (Ed.), *Encapsulations* (pp. 769–792). Academic Press. https://doi.org/10.1016/B978-0-12-804307-3.00018-1

Fenyvesi, É., Vikmon, M., & Szente, L. (2016). Cyclodextrins in Food Technology and Human Nutrition: Benefits and Limitations. *Critical Reviews in Food Science and Nutrition*, *56*(12), 1981–2004. https://doi.org/10.1080/10408398.2013.809513

Ferrenberg, A. M., & Swendsen, R. H. (1989). Optimized Monte Carlo data analysis. *Physical Review Letters*, *63*(12), 1195–1198. https://doi.org/10.1103/PhysRevLett.63.1195

Final Progress Reports: CycloPure, Inc.: Remediation of Perfluorinated Chemicals in Water Using Novel High-Affinity Polymer Adsorbents (Superfund Research Program). (2018). National Institute of Environmental Health Sciences. https://tools.niehs.nih.gov/srp/programs/progress_report.cfm?Project_ID=R43ES029401

Flood, K. G., Reynolds, E. R., & Snow, N. H. (2001). Determination of apparent association constants of steroid–cyclodextrin inclusion complexes using a modification of the Hummel–Dreyer method. *Journal of Chromatography A*, *913*(1–2), 261–268. https://doi.org/10.1016/S0021-9673(01)00567-2

French, D. (1957). The Schardinger Dextrins. In M. L. Wolfrom & R. S. Tipson (Eds.), *Advances in Carbohydrate Chemistry* (Vol. 12, pp. 189–260). Academic Press. https://doi.org/10.1016/S0096-5332(08)60209-X

Frenkel, D., Smit, B., & Ratner, M. A. (1997). *Understanding Molecular Simulation: From Algorithms to Applications*. *Physics Today*, *50*(7), 66–66. https://doi.org/10.1063/1.881812

Frijlink, H. W., Visser, J., Hefting, N. R., Oosting, R., Meijer, D. K. F., & Lerk, C. F. (1990). The Pharmacokinetics of β-Cyclodextrin and Hydroxypropyl-β-cyclodextrin in the Rat. *Pharmaceutical Research*, *7*(12), 1248–1252. https://doi.org/10.1023/A:1015929720063

Frisch, M. J., Trucks, G. W., Schlegel, H. B., & G. E. Scuseria, M. A. Robb, J. R. Cheeseman, G. Scalmani, V. Barone, G. A. Petersson, H. Nakatsuji, X. Li, M. Caricato, A. V. Marenich, J. Bloino, B. G. Janesko, R. Gomperts, B. Mennucci, H. P. Hratchian, J. V. Ortiz, A. F. Izmaylov, J. L. Sonnenberg, D. Williams-Young, F. Ding, F. Lipparini, F. Egidi, J. Goings, B. Peng, A. Petrone, T. Henderson, D. Ranasinghe, V. G. Zakrzewski, J. Gao, N. Rega, G. Zheng, W. Liang, M. Hada, M. Ehara, K. Toyota, R. Fukuda, J. Hasegawa, M. Ishida, T. Nakajima, Y. Honda, O. Kitao, H. Nakai, T. Vreven, K. Throssell, J. A. Montgomery, Jr., J. E. Peralta, F. Ogliaro, M. J. Bearpark, J. J. Heyd, E. N. Brothers, K. N. Kudin, V. N. Staroverov, T. A. Keith, R. Kobayashi, J. Normand, K. Raghavachari, A. P. Rendell, J. C. Burant, S. S. Iyengar, J. Tomasi, M. Cossi, J. M. Millam, M. Klene, C. Adamo, R. Cammi, J. W. Ochterski, R. L. Martin, K. Morokuma, O. Farkas, J. B. Foresman, and D. J. Fox, G. E. (2016). *Gaussian* (Version 16) [Computer software]. Gaussian, Inc., Wallingford CT, 2016.

Gao, J., & Truhlar, D. G. (2002). Quantum Mechanical Methods for Enzyme Kinetics. *Annual Review of Physical Chemistry*, *53*(1), 467–505. https://doi.org/10.1146/annurev.physchem.53.091301.150114

Garrido, P. F., Calvelo, M., Blanco-González, A., Veleiro, U., Suárez, F., Conde, D., Cabezón, A., Piñeiro,

USC DE SANTIAGO DE COMPOSTELA

Á., & Garcia-Fandino, R. (2020). The Lord of the NanoRings: Cyclodextrins and the battle against SARS-CoV-2. *International Journal of Pharmaceutics*, *588*, 119689. https://doi.org/10.1016/j.ijpharm.2020.119689

Gebhardt, J., Kleist, C., Jakobtorweihen, S., & Hansen, N. (2018). Validation and Comparison of Force Fields for Native Cyclodextrins in Aqueous Solution. *The Journal of Physical Chemistry B*, *122*(5), 1608–1626. https://doi.org/10.1021/acs.jpcb.7b11808

Giannozzi, P., Baroni, S., Bonini, N., Calandra, M., Car, R., Cavazzoni, C., Ceresoli, D., Chiarotti, G. L., Cococcioni, M., Dabo, I., Dal Corso, A., De Gironcoli, S., Fabris, S., Fratesi, G., Gebauer, R., Gerstmann, U., Gougoussis, C., Kokalj, A., Lazzeri, M., … Wentzcovitch, R. M. (2009). QUANTUM ESPRESSO: A modular and open-source software project for quantum simulations of materials. *Journal of Physics: Condensed Matter*, *21*(39), 395502. https://doi.org/10.1088/0953-8984/21/39/395502

Grønlund, A., Larsen, K. G., Mathiasen, A., Nielsen, J. S., Schneider, S., & Song, M. (2018). *Fast Exact k-Means, k-Medians and Bregman Divergence Clustering in 1D* (arXiv:1701.07204). arXiv. http://arxiv.org/abs/1701.07204

Guo, J., Li, D., Tao, H., Li, G., Liu, R., Dou, Y., Jin, T., Li, L., Huang, J., Hu, H., & Zhang, J. (2019). Cyclodextrin-Derived Intrinsically Bioactive Nanoparticles for Treatment of Acute and Chronic Inflammatory Diseases. *Advanced Materials*, *31*(46), 1904607. https://doi.org/10.1002/adma.201904607

Haerter, F., & Eikermann, M. (2016). Reversing neuromuscular blockade: Inhibitors of the acetylcholinesterase versus the encapsulating agents sugammadex and calabadion. *Expert Opinion on Pharmacotherapy*, *17*(6), 819–833. https://doi.org/10.1517/14656566.2016.1145667

HALFORD, B. (2019). CycloPure. *C&EN Global Enterprise*, *97*(44), 30–31. https://doi.org/10.1021/cen-09744-cover2

Hann, M. M., Leach, A. R., & Harper, G. (2001). Molecular Complexity and Its Impact on the Probability of Finding Leads for Drug Discovery. *Journal of Chemical Information and Computer Sciences*, *41*(3), 856–864. https://doi.org/10.1021/ci000403i

Hansson, T., Oostenbrink, C., & van Gunsteren, W. F. (2002). *Molecular dynamics simulations*. 7.

Harata, K., & Uedaira, H. (1975). The Circular Dichroism Spectra of the β-Cyclodextrin Complex with Naphthalene Derivatives. *Bulletin of the Chemical Society of Japan*, *48*(2), 375–378. https://doi.org/10.1246/bcsj.48.375

Harris, C. R., Millman, K. J., van der Walt, S. J., Gommers, R., Virtanen, P., Cournapeau, D., Wieser, E., Taylor, J., Berg, S., Smith, N. J., Kern, R., Picus, M., Hoyer, S., van Kerkwijk, M. H., Brett, M., Haldane, A., del Río, J. F., Wiebe, M., Peterson, P., … Oliphant, T. E. (2020). Array programming with NumPy. *Nature*, *585*(7825), Article 7825. https://doi.org/10.1038/s41586-020-2649-2

Hartree, D. R. (1928). The Wave Mechanics of an Atom with a Non-Coulomb Central Field. Part II. Some Results and Discussion. *Mathematical Proceedings of the Cambridge Philosophical Society*, *24*(1), 111–132. https://doi.org/10.1017/S0305004100011920

Hata, S., Mihara, T., Shiraishi, M., Yamaguchi, Y., Du, Y., Shiraishi, Y., & Toshima, N. (2020). Development of carbon nanotube organic thermoelectric materials using cyclodextrin polymer: Control of semiconductor characteristics by the solvent effect. *Japanese Journal of Applied Physics*, *59*(SD), SDDD05. https://doi.org/10.7567/1347-4065/ab6341

Hayashi, N., Chen, R., Hiraoka, M., Ujihara, T., & Ikezaki, H. (2010). Beta-cyclodextrin/surface plasmon resonance detection system for sensing bitter-astringent taste intensity of green tea catechins. *Journal of Agricultural and Food Chemistry*, *58*(14), 8351–8356. https://doi.org/10.1021/jf1012693

Hayashino, Y., Sugita, M., Arima, H., Irie, T., Kikuchi, T., & Hirata, F. (2018). Predicting the Binding Mode of 2-Hydroxypropyl-β-cyclodextrin to Cholesterol by Means of the MD Simulation and the 3D-RISM-KH Theory. *The Journal of Physical Chemistry B*, *122*(21), 5716–5725. https://doi.org/10.1021/acs.jpcb.8b02098

Hedges, A. R., Shieh, W. J., & Sikorski, C. T. (1995). Use of Cyclodextrins for Encapsulation in the Use

USC DE SANTIAGO DE COMPOSTELA

and Treatment of Food Products. In S. J. Risch & G. A. Reineccius (Eds.), *Encapsulation and Controlled Release of Food Ingredients* (Vol. 590, pp. 60–71). American Chemical Society. https://doi.org/10.1021/bk-1995-0590.ch006

Hernandez-Pascacio, J., Piñeiro, Á., Ruso, J. M., Hassan, N., Campbell, R. A., Campos-Terán, J., & Costas, M. (2016). Complex Behavior of Aqueous α-Cyclodextrin Solutions. Interfacial Morphologies Resulting from Bulk Aggregation. *Langmuir*, *32*(26), 6682–6690. https://doi.org/10.1021/acs.langmuir.6b01646

Hess, B., Bekker, H., Berendsen, H. J. C., & Fraaije, J. G. E. M. (1997). LINCS: A linear constraint solver for molecular simulations. *Journal of Computational Chemistry*, *18*(12), 1463–1472. https://doi.org/10.1002/(SICI)1096-987X(199709)18:12<1463::AID-JCC4>3.0.CO;2-H

Holland, L., Rizzi, G., & Malton, P. (2000). *Cosmetic compositions comprising cyclic oligosaccharide and fragrance* (World Intellectual Property Organization Patent WO2000067716A1). https://patents.google.com/patent/WO2000067716A1/en?oq=WO2000067716

Hünenberger, P. H. (2005). Thermostat Algorithms for Molecular Dynamics Simulations. In C. Dr. Holm & K. Prof. Dr. Kremer (Eds.), *Advanced Computer Simulation* (Vol. 173, pp. 105–149). Springer Berlin Heidelberg. https://doi.org/10.1007/b99427

Hunter, J. D. (2007). Matplotlib: A 2D Graphics Environment. *Computing in Science & Engineering*, *9*(3), 90–95. https://doi.org/10.1109/MCSE.2007.55

Irani, A. H., Voss, L., Whittle, N., & Sleigh, J. W. (2023). Encapsulation Dynamics of Neuromuscular Blocking Drugs by Sugammadex. *Anesthesiology*, *138*(2), 152–163. https://doi.org/10.1097/ALN.0000000000004442

Irie, T., Fukunaga, K., & Pitha, J. (1992). Hydroxypropylcyclodextrins in Parenteral use. I: Lipid Dissolution and Effects on Lipid Transfers in Vitro. *Journal of Pharmaceutical Sciences*, *81*(6), 521–523. https://doi.org/10.1002/jps.2600810609

Irie, T., & Uekama, K. (1997). Pharmaceutical Applications of Cyclodextrins. III. Toxicological Issues and Safety Evaluation. *Journal of Pharmaceutical Sciences*, *86*(2), 147–162. https://doi.org/10.1021/js960213f

Isik, Y., Palabiyik, O., Cegin, B. M., Goktas, U., & Kati, I. (2016). Effects of Sugammadex and Neostigmine on Renal Biomarkers. *Medical Science Monitor*, *22*, 803–809. https://doi.org/10.12659/MSM.897608

Jankowski, C. K., Lamouroux, C., Jiménez-Estrada, M., Arseneau, S., & Wagner, B. D. (2016). Factors Affecting the Formation of 2:1 Host:Guest Inclusion Complexes of 2-[(R-Phenyl)amine]-1,4-naphthalenediones (PAN) in β- and γ-Cyclodextrins. *Molecules*, *21*(11), Article 11. https://doi.org/10.3390/molecules21111568

Jansook, P., Kurkov, S. V., & Loftsson, T. (2010). Cyclodextrins as solubilizers: Formation of complex aggregates. *Journal of Pharmaceutical Sciences*, *99*(2), 719–729. https://doi.org/10.1002/jps.21861

Jorgensen, W. L., & Tirado-Rives, J. (1988). The OPLS [optimized potentials for liquid simulations] potential functions for proteins, energy minimizations for crystals of cyclic peptides and crambin. *Journal of the American Chemical Society*, *110*(6), 1657–1666. https://doi.org/10.1021/ja00214a001

Jung, J., Kobayashi, C., Kasahara, K., Tan, C., Kuroda, A., Minami, K., Ishiduki, S., Nishiki, T., Inoue, H., Ishikawa, Y., Feig, M., & Sugita, Y. (2021). New parallel computing algorithm of molecular dynamics for extremely huge scale biological systems. *Journal of Computational Chemistry*, *42*(4), 231–241. https://doi.org/10.1002/jcc.26450

Karplus, M., & Petsko, G. A. (1990). *Molecular dynamics simulations in biology*. *347*, 9.

Katzmann, J. L., Gouni-Berthold, I., & Laufs, U. (2020). PCSK9 Inhibition: Insights From Clinical Trials and Future Prospects. *Frontiers in Physiology*, *11*, 595819. https://doi.org/10.3389/fphys.2020.595819

Keating, G. M. (2016). Sugammadex: A Review of Neuromuscular Blockade Reversal. *Drugs*, *76*(10), 1041–1052. https://doi.org/10.1007/s40265-016-0604-1

USC UNIVERSIDADE DE SANTIAGO DE COMPOSTELA

Kerdpol, K., Kicuntod, J., Wolschann, P., Mori, S., Rungnim, C., Kunaseth, M., Okumura, H., Kungwan, N., & Rungrotmongkol, T. (2019). Cavity Closure of 2-Hydroxypropyl-β-Cyclodextrin: Replica Exchange Molecular Dynamics Simulations. *Polymers*, *11*(1), 145. https://doi.org/10.3390/polym11010145

Kim, H., Kumar, S., Kang, D.-W., Jo, H., & Park, J.-H. (2020). Affinity-Driven Design of Cargo-Switching Nanoparticles to Leverage a Cholesterol-Rich Microenvironment for Atherosclerosis Therapy. *ACS Nano*, *14*(6), 6519–6531. https://doi.org/10.1021/acsnano.9b08216

Kiss, E., Szabó, V. A., & Horváth, P. (2019). Simple circular dichroism method for selection of the optimal cyclodextrin for drug complexation. *Journal of Inclusion Phenomena and Macrocyclic Chemistry*, *95*(3), 223–233. https://doi.org/10.1007/s10847-019-00938-2

Kohn, W., Becke, A. D., & Parr, R. G. (1996). Density Functional Theory of Electronic Structure. *The Journal of Physical Chemistry*, *100*(31), 12974–12980. https://doi.org/10.1021/jp960669l

Kovac, A. L. (2009). Sugammadex: The first selective binding reversal agent for neuromuscular block. *Journal of Clinical Anesthesia*, *21*(6), 444–453. https://doi.org/10.1016/j.jclinane.2009.05.002

Kritharides, L., Kus, M., Brown, A. J., Jessup, W., & Dean, R. T. (1996). Hydroxypropyl-β-cyclodextrin-mediated Efflux of 7-Ketocholesterol from Macrophage Foam Cells. *Journal of Biological Chemistry*, *271*(44), 27450–27455. https://doi.org/10.1074/jbc.271.44.27450

Kučáková, K., & Dolenský, B. (2020). Molecular structure study of a heptakis(2,3,6-tri-O-methyl)-β-cyclodextrin complex of cholesterol. *Steroids*, *155*, 108555. https://doi.org/10.1016/j.steroids.2019.108555

Kumar, S., Rosenberg, J. M., Bouzida, D., Swendsen, R. H., & Kollman, P. A. (1992). THE weighted histogram analysis method for free-energy calculations on biomolecules. I. The method. *Journal of Computational Chemistry*, *13*(8), 1011–1021. https://doi.org/10.1002/jcc.540130812

Kuntz, I. D., Blaney, J. M., Oatley, S. J., Langridge, R., & Ferrin, T. E. (1982). A geometric approach to macromolecule-ligand interactions. *Journal of Molecular Biology*, *161*(2), 269–288. https://doi.org/10.1016/0022-2836(82)90153-X

Kurkov, S. V., & Loftsson, T. (2013). Cyclodextrins. *International Journal of Pharmaceutics*, *453*(1), 167–180. https://doi.org/10.1016/j.ijpharm.2012.06.055

Laio, A., & Parrinello, M. (2002). Escaping free-energy minima. *Proceedings of the National Academy of Sciences*, *99*(20), 12562–12566. https://doi.org/10.1073/pnas.202427399

Landy, D., Mallard, I., Ponchel, A., Monflier, E., & Fourmentin, S. (2012). Remediation technologies using cyclodextrins: An overview. *Environmental Chemistry Letters*, *10*(3), 225–237. https://doi.org/10.1007/s10311-011-0351-1

Lebedinskiy, K., Lobaz, V., & Jindřich, J. (2022). Preparation of β-cyclodextrin-based dimers with selectively methylated rims and their use for solubilization of tetracene. *Beilstein Journal of Organic Chemistry*, *18*, 1596–1606. https://doi.org/10.3762/bjoc.18.170

Li, L., Zhou, Y., Wang, Z., Wu, C., Li, Z., Sun, C., & Sun, T. (2018). Theoretical studies on the mechanism of sugammadex for the reversal of aminosteroid-induced neuromuscular blockade. *Journal of Molecular Liquids*, *265*, 450–456. https://doi.org/10.1016/j.molliq.2018.06.033

Li, S., & Purdy, W. C. (2002, May 1). *Cyclodextrins and their applications in analytical chemistry* (world) [Research-article]. ACS Publications; American Chemical Society. https://doi.org/10.1021/cr00014a009

Li, T., Guo, R., Zong, Q., & Ling, G. (2022). Application of molecular docking in elaborating molecular mechanisms and interactions of supramolecular cyclodextrin. *Carbohydrate Polymers*, *276*, 118644. https://doi.org/10.1016/j.carbpol.2021.118644

Liu, Y., & Chen, Y. (2006). Cooperative Binding and Multiple Recognition by Bridged Bis(*β* -cyclodextrin)s with Functional Linkers. *Accounts of Chemical Research*, *39*(10), 681–691. https://doi.org/10.1021/ar0502275

Loftsson, T., & Duchene, D. (2007). Cyclodextrins and their pharmaceutical applications. *International Journal of Pharmaceutics*, *329*(1–2), 1–11. https://doi.org/10.1016/j.ijpharm.2006.10.044

Loftsson, T., Saokham, P., & Sá Couto, A. R. (2019). Self-association of cyclodextrins and cyclodextrin

USC DE SANTIAGO DE COMPOSTELA

complexes in aqueous solutions. *International Journal of Pharmaceutics*, *560*, 228–234. https://doi.org/10.1016/j.ijpharm.2019.02.004

López, C. A., de Vries, A. H., & Marrink, S. J. (2011). Molecular Mechanism of Cyclodextrin Mediated Cholesterol Extraction. *PLoS Computational Biology*, *7*(3), e1002020. https://doi.org/10.1371/journal.pcbi.1002020

López, C. A., de Vries, A. H., & Marrink, S. J. (2013). Computational microscopy of cyclodextrin mediated cholesterol extraction from lipid model membranes. *Scientific Reports*, *3*(1), 2071. https://doi.org/10.1038/srep02071

Lyu, J., Wang, S., Balius, T. E., Singh, I., Levit, A., Moroz, Y. S., O'Meara, M. J., Che, T., Algaa, E., Tolmachova, K., Tolmachev, A. A., Shoichet, B. K., Roth, B. L., & Irwin, J. J. (2019). Ultra-large library docking for discovering new chemotypes. *Nature*, *566*(7743), 224–229. https://doi.org/10.1038/s41586-019-0917-9

Mackerell Jr., A. D. (2004). Empirical force fields for biological macromolecules: Overview and issues. *Journal of Computational Chemistry*, *25*(13), 1584–1604. https://doi.org/10.1002/jcc.20082

Makieła, D., Janus-Zygmunt, I., Górny, K., & Gburski, Z. (2018). Investigation of the influence of β-cyclodextrin on cholesterol lodgement—A molecular dynamics simulation study. *Journal of Molecular Liquids*, *262*, 451–459. https://doi.org/10.1016/j.molliq.2018.04.098

Malde, A. K., Zuo, L., Breeze, M., Stroet, M., Poger, D., Nair, P. C., Oostenbrink, C., & Mark, A. E. (2011). An Automated Force Field Topology Builder (ATB) and Repository: Version 1.0. *Journal of Chemical Theory and Computation*, *7*(12), 4026–4037. https://doi.org/10.1021/ct200196m

Mann, H. B., & Whitney, D. R. (1947). On a Test of Whether one of Two Random Variables is Stochastically Larger than the Other. *The Annals of Mathematical Statistics*, *18*(1), 50–60. https://doi.org/10.1214/aoms/1177730491

Marconi, G., Mezzina, E., Manet, I., Manoli, F., Zambelli, B., & Monti, S. (2011). Stereoselective interaction of ketoprofen enantiomers with β-cyclodextrin: Ground state binding and photochemistry. *Photochemical & Photobiological Sciences*, *10*(1), 48–59. https://doi.org/10.1039/c0pp00262c

Marques, H. M. C. (2010). A review on cyclodextrin encapsulation of essential oils and volatiles. *Flavour and Fragrance Journal*, *25*(5), 313–326. https://doi.org/10.1002/ffj.2019

Martinet, W., Schrijvers, D. M., Timmermans, J.-P., & Bult, H. (2008). Interactions between cell death induced by statins and 7-ketocholesterol in rabbit aorta smooth muscle cells. *British Journal of Pharmacology*, *154*(6), 1236–1246. https://doi.org/10.1038/bjp.2008.181

Mazurek, A. H., & Szeleszczuk, Ł. (2022). Current Status of Quantum Chemical Studies of Cyclodextrin Host–Guest Complexes. *Molecules*, *27*(12), Article 12. https://doi.org/10.3390/molecules27123874

Mazurek, A. H., Szeleszczuk, Ł., & Gubica, T. (2021). Application of Molecular Dynamics Simulations in the Analysis of Cyclodextrin Complexes. *International Journal of Molecular Sciences*, *22*(17), 9422. https://doi.org/10.3390/ijms22179422

McCammon, J. A., Gelin, B. R., & Karplus, M. (1977). Dynamics of folded proteins. *Nature*, *267*(5612), Article 5612. https://doi.org/10.1038/267585a0

McKinney, W. (2010). Data Structures for Statistical Computing in Python. *PROC. OF THE 9th PYTHON IN SCIENCE CONF. (SCIPY 2010)*, 56–61.

Meng, E. C., Shoichet, B. K., & Kuntz, I. D. (1992). Automated docking with grid-based energy evaluation. *Journal of Computational Chemistry*, *13*(4), 505–524. https://doi.org/10.1002/jcc.540130412

Merck and Co, Inc. (2015). *BRIDION® (sugammadex) Injection Drug Label*.

Messner, M., Kurkov, S. V., Jansook, P., & Loftsson, T. (2010). Self-assembled cyclodextrin aggregates and nanoparticles. *International Journal of Pharmaceutics*, *387*(1–2), 199–208. https://doi.org/10.1016/j.ijpharm.2009.11.035

Mixcoha, E., Campos-Terán, J., & Piñeiro, Á. (2014). Surface Adsorption and Bulk Aggregation of Cyclodextrins by Computational Molecular Dynamics Simulations as a Function of Temperature: α-CD vs β-CD. *The Journal of Physical Chemistry B*, *118*(25), 6999–7011.

USC UNIVERSIDADE DE SANTIAGO DE COMPOSTELA

https://doi.org/10.1021/jp412533b
Miyamoto, S., & Kollman, P. A. (1992). Settle: An analytical version of the SHAKE and RATTLE algorithm for rigid water models. *Journal of Computational Chemistry*, *13*(8), 952–962. https://doi.org/10.1002/jcc.540130805
Morris, G. M., Goodsell, D. S., Halliday, R. S., Huey, R., Hart, W. E., Belew, R. K., & Olson, A. J. (1998). Automated docking using a Lamarckian genetic algorithm and an empirical binding free energy function. *Journal of Computational Chemistry*, *19*(14), 1639–1662. https://doi.org/10.1002/(SICI)1096-987X(19981115)19:14<1639::AID-JCC10>3.0.CO;2-B
Morris, G. M., Huey, R., Lindstrom, W., Sanner, M. F., Belew, R. K., Goodsell, D. S., & Olson, A. J. (2009). AutoDock4 and AutoDockTools4: Automated docking with selective receptor flexibility. *Journal of Computational Chemistry*, *30*(16), 2785–2791. https://doi.org/10.1002/jcc.21256
Moser, J. G., Rose, I., Wagner, B., Wieneke, T., & Vervoorts, A. (2001). Taxol Inclusion Complexes with a Cyclodextrin Dimer: Possibilities to Detoxify Chemotherapeutics and to Target Drugs Specifically to Tumors? *Journal of Inclusion Phenomena and Macrocyclic Chemistry*, *39*(1), 13–18. https://doi.org/10.1023/A:1008114826524
Mura, P. (2014). Analytical techniques for characterization of cyclodextrin complexes in aqueous solution: A review. *Journal of Pharmaceutical and Biomedical Analysis*, *101*, 238–250. https://doi.org/10.1016/j.jpba.2014.02.022
Nag, K., Singh, D., Shetti, A., Kumar, H., Sivashanmugam, T., & Parthasarathy, S. (2013). Sugammadex: A revolutionary drug in neuromuscular pharmacology. *Anesthesia: Essays and Researches*, *7*(3), 302. https://doi.org/10.4103/0259-1162.123211
Niether, D., Kawaguchi, T., Hovancová, J., Eguchi, K., Dhont, J. K. G., Kita, R., & Wiegand, S. (2017). Role of Hydrogen Bonding of Cyclodextrin–Drug Complexes Probed by Thermodiffusion. *Langmuir*, *33*(34), 8483–8492. https://doi.org/10.1021/acs.langmuir.7b02313
Nishijo, J., Moriyama, S., & Shiota, S. (2003). Interactions of cholesterol with cyclodextrins in aqueous solution. *Chemical & Pharmaceutical Bulletin*, *51*(11), 1253–1257. https://doi.org/10.1248/cpb.51.1253
Nishijo, J., Moriyama, S., Shiota, S., Kamigauchi, M., & Sugiura, M. (2004). *Interaction of Heptakis (2,3,6-Tri-O-methyl)-b-cyclodextrin with Cholesterol in Aqueous Solution*. *52*(12).
Ogoshi, T., & Harada, A. (2008). Chemical Sensors Based on Cyclodextrin Derivatives. *Sensors*, *8*(8), Article 8. https://doi.org/10.3390/s8084961
Oostenbrink, C., Villa, A., Mark, A. E., & Van Gunsteren, W. F. (2004). A biomolecular force field based on the free enthalpy of hydration and solvation: The GROMOS force-field parameter sets 53A5 and 53A6. *Journal of Computational Chemistry*, *25*(13), 1656–1676. https://doi.org/10.1002/jcc.20090
Ott, K.-H., & Meyer, B. (1996). Parametrization of GROMOS force field for oligosaccharides and assessment of efficiency of molecular dynamics simulations. *Journal of Computational Chemistry*, *17*(8), 1068–1084. https://doi.org/10.1002/(SICI)1096-987X(199606)17:8<1068::AID-JCC14>3.0.CO;2-A
Pahuja, P., Kashyap, H., & Pawar, P. (2014). Design and evaluation of HP-β-CD based voriconazole formulations for ocular drug delivery. *Current Drug Delivery*, *11*(2), 223–232. https://doi.org/10.2174/15672018106661312241052 05
Park, S., & Schulten, K. (2004). Calculating potentials of mean force from steered molecular dynamics simulations. *The Journal of Chemical Physics*, *120*(13), 5946–5961. https://doi.org/10.1063/1.1651473
Parrinello, M., & Rahman, A. (1981). Polymorphic transitions in single crystals: A new molecular dynamics method. *Journal of Applied Physics*, *52*(12), 7182–7190. https://doi.org/10.1063/1.328693
Peluso, P., Landy, D., Nakhle, L., Dallocchio, R., Dessì, A., Krait, S., Salgado, A., Chankvetadze, B., & Scriba, G. K. E. (2023). Isothermal titration calorimetry and molecular modeling study of the complex formation of daclatasvir by γ-cyclodextrin and trimethyl-β-cyclodextrin. *Carbohydrate Polymers*, *313*, 120870. https://doi.org/10.1016/j.carbpol.2023.120870

USC UNIVERSIDADE DE SANTIAGO DE COMPOSTELA

Piñeiro, Á., Banquy, X., Pérez-Casas, S., Tovar, E., García, A., Villa, A., Amigo, A., Mark, A. E., & Costas, M. (2007). On the Characterization of Host−Guest Complexes: Surface Tension, Calorimetry, and Molecular Dynamics of Cyclodextrins with a Non-ionic Surfactant. *The Journal of Physical Chemistry B*, *111*(17), 4383–4392. https://doi.org/10.1021/jp0688815

Piñeiro, Á., Muñoz, E., Sabín, J., Costas, M., Bastos, M., Velázquez-Campoy, A., Garrido, P. F., Dumas, P., Ennifar, E., García-Río, L., Rial, J., Pérez, D., Fraga, P., Rodríguez, A., & Cotelo, C. (2019). AFFINImeter: A software to analyze molecular recognition processes from experimental data. *Analytical Biochemistry*, *577*, 117–134. https://doi.org/10.1016/j.ab.2019.02.031

Piñeiro, Á., Pipkin, J., Antle, V., & Garcia-Fandino, R. (2021). Aggregation versus inclusion complexes to solubilize drugs with cyclodextrins. A case study using sulphobutylether-β-cyclodextrins and remdesivir. *Journal of Molecular Liquids*, *343*, 117588. https://doi.org/10.1016/j.molliq.2021.117588

Piñeiro, Á., Pipkin, J., Antle, V., & Garcia-Fandino, R. (2022). Remdesivir interactions with sulphobutylether-β-cyclodextrins: A case study using selected substitution patterns. *Journal of Molecular Liquids*, *346*, 117157. https://doi.org/10.1016/j.molliq.2021.117157

Poltev, V. (2015). Molecular Mechanics: Principles, History, and Current Status. In J. Leszczynski (Ed.), *Handbook of Computational Chemistry* (pp. 1–48). Springer Netherlands. https://doi.org/10.1007/978-94-007-6169-8_9-2

Ponder, J. W., & Case, D. A. (2003). Force Fields for Protein Simulations. In *Advances in Protein Chemistry* (Vol. 66, pp. 27–85). Academic Press. https://doi.org/10.1016/S0065-3233(03)66002-X

Prabaharan, M., & Mano, J. F. (2006). Chitosan derivatives bearing cyclodextrin cavitiesas novel adsorbent matrices. *Carbohydrate Polymers*, *63*(2), 153–166. https://doi.org/10.1016/j.carbpol.2005.08.051

Prochowicz, D., Kornowicz, A., & Lewiński, J. (2017). Interactions of Native Cyclodextrins with Metal Ions and Inorganic Nanoparticles: Fertile Landscape for Chemistry and Materials Science. *Chemical Reviews*, *117*(22), 13461–13501. https://doi.org/10.1021/acs.chemrev.7b00231

PubChem. (n.d.). *Sugammadex*. Retrieved May 17, 2023, from https://pubchem.ncbi.nlm.nih.gov/compound/6918585

Puglisi, A., & Yagci, Y. (2019). Cyclodextrin-Based Macromolecular Systems as Cholesterol-Mopping Therapeutic Agents in Niemann-Pick Disease Type C. *Macromolecular Rapid Communications*, *40*(1), 1800557. https://doi.org/10.1002/marc.201800557

Ramírez, D. (2016). Computational Methods Applied to Rational Drug Design. *The Open Medicinal Chemistry Journal*, *10*, 7–20. https://doi.org/10.2174/1874104501610010007

Ramsey, J. D., Stewart, I. E., Madden, E. A., Lim, C., Hwang, D., Heise, M. T., Hickey, A. J., & Kabanov, A. V. (2022). Nanoformulated Remdesivir with Extremely Low Content of Poly(2-oxazoline)-Based Stabilizer for Aerosol Treatment of COVID-19. *Macromolecular Bioscience*, *22*(8), 2200056. https://doi.org/10.1002/mabi.202200056

Ravichandran, R., & Divakar, S. (1998). Inclusion of Ring A of Cholesterol Inside the -Cyclodextrin Cavity: Evidence from Oxidation Reactions and Structural Studies. *Journal of Inclusion Phenomena and Molecular Recognition in Chemistry*, *30*, 253–270.

Rousseeuw, P. J. (1987). Silhouettes: A graphical aid to the interpretation and validation of cluster analysis. *Journal of Computational and Applied Mathematics*, *20*, 53–65. https://doi.org/10.1016/0377-0427(87)90125-7

Safety and Efficacy of Intravenous Trappsol Cyclo (HPBCD) in Niemann-Pick Type C Patients from ClinicalTrials.gov. (2019, November 7). ClinicalTrials.Gov. https://clinicaltrials.gov/ct2/show/NCT02912793

Salzano, G., Wankar, J., Ottani, S., Villemagne, B., Baulard, A. R., Willand, N., Brodin, P., Manet, I., & Gref, R. (2017). Cyclodextrin-based nanocarriers containing a synergic drug combination: A potential formulation for pulmonary administration of antitubercular drugs. *International Journal of Pharmaceutics*, *531*(2), 577–587. https://doi.org/10.1016/j.ijpharm.2017.05.030

Sandilya, A. A., Natarajan, U., & Priya, M. H. (2020). Molecular View into the Cyclodextrin Cavity: Structure and Hydration. *ACS Omega*, *5*(40), 25655–25667.

USC UNIVERSIDADE DE SANTIAGO DE COMPOSTELA

https://doi.org/10.1021/acsomega.0c02760
Schmid, Gerhard, S. (2001). *Original Submission—Notice of GRAS Exemption for Beta-Cyclodextrin*. Wacker Biochem Corp.
Schönbeck, C., Kari, J., & Westh, P. (2024). ITC analysis of polydisperse systems: Unravelling the impact of sample heterogeneity. *Analytical Biochemistry*, *687*, 115446. https://doi.org/10.1016/j.ab.2023.115446
Schönbeck, C., Westh, P., & Holm, R. (2014). Complexation Thermodynamics of Modified Cyclodextrins: Extended Cavities and Distorted Structures. *The Journal of Physical Chemistry B*, *118*(34), 10120–10129. https://doi.org/10.1021/jp506001j
Senderowitz, H., Parish, C., & Still, W. C. (1996). Carbohydrates: United Atom AMBER* Parameterization of Pyranoses and Simulations Yielding Anomeric Free Energies. *Journal of the American Chemical Society*, *118*(8), 2078–2086. https://doi.org/10.1021/ja9529652
Senn, H. M., & Thiel, W. (2009). QM/MM Methods for Biomolecular Systems. *Angewandte Chemie International Edition*, *48*(7), 1198–1229. https://doi.org/10.1002/anie.200802019
Shapiro, S. S., & Wilk, M. B. (1965). An analysis of variance test for normality (complete samples). *Biometrika*, *52*(3–4), 591–611. https://doi.org/10.1093/biomet/52.3-4.591
Shavitt, I., & Bartlett, R. J. (2009). *Many-Body Methods in Chemistry and Physics: MBPT and Coupled-Cluster Theory*. Cambridge University Press.
Shen, Q., Shen, Y., Jin, F., Du, Y.-Z., & Ying, X.-Y. (2020). Paclitaxel/hydroxypropyl-β-cyclodextrin complex-loaded liposomes for overcoming multidrug resistance in cancer chemotherapy. *Journal of Liposome Research*, *30*(1), 12–20. https://doi.org/10.1080/08982104.2019.1579838
Shuang, Y., Liao, Y., Wang, H., Wang, Y., & Li, L. (2020). Preparation and evaluation of a triazole-bridged bis(β-cyclodextrin)–bonded chiral stationary phase for HPLC. *Chirality*, *32*(2), 168–184. https://doi.org/10.1002/chir.23147
Skanchy, D. J., Xie, G.-H., Tait, R. J., Luna, E., Demarest, C., & Stobaugh, J. F. (1999). Application of sulfobutylether-β-cyclodextrin with specific degrees of substitution for the enantioseparation of pharmaceutical mixtures by capillary electrophoresis. *Electrophoresis*, *20*(13), 2638–2649. https://doi.org/10.1002/(SICI)1522-2683(19990901)20:13<2638::AID-ELPS2638>3.0.CO;2-Z
Slater, J. C. (1951). A Simplification of the Hartree-Fock Method. *Physical Review*, *81*(3), 385–390. https://doi.org/10.1103/PhysRev.81.385
Šolínová, V., Mikysková, H., Kaiser, M. M., Janeba, Z., Holý, A., & Kašička, V. (2016). Estimation of apparent binding constant of complexes of selected acyclic nucleoside phosphonates with β-cyclodextrin by affinity capillary electrophoresis. *ELECTROPHORESIS*, *37*(2), 239–247. https://doi.org/10.1002/elps.201500337
Soto Tellini, V. H., Jover, A., García, J. C., Galantini, L., Meijide, F., & Tato, J. V. (2006). Thermodynamics of Formation of Host−Guest Supramolecular Polymers. *Journal of the American Chemical Society*, *128*(17), 5728–5734. https://doi.org/10.1021/ja0572809
Sousa, S. F., Fernandes, P. A., & Ramos, M. J. (2006). Protein-ligand docking: Current status and future challenges. *Proteins*, *65*(1), 15–26. https://doi.org/10.1002/prot.21082
Strandberg, T. E., Libby, P., & Kovanen, P. T. (2020). A tale of two therapies lipid-lowering vs. anti-inflammatory therapy: A false dichotomy? *European Heart Journal — Cardiovascular Pharmacotherapy*, *7*(3), 238–241. https://doi.org/10.1093/ehjcvp/pvaa131
Sursyakova, V. V., Levdansky, V. A., & Rubaylo, A. I. (2022). Evaluation of the effect of background electrolyte composition and independence of parameters in determining binding constants of betulin derivatives to β- and dimethyl-β-cyclodextrins by affinity capillary electrophoresis. *Journal of Separation Science*, *45*(19), 3745–3753. https://doi.org/10.1002/jssc.202200453
Szabo, A., & Ostlund, N. S. (1996). *Modern quantum chemistry: Introduction to advanced electronic structure theory*. Dover Publications.
Szejtli, J. (1998). Introduction and General Overview of Cyclodextrin Chemistry. *Chemical Reviews*, *98*(5), 1743–1754. https://doi.org/10.1021/cr970022c
Szente, L., Sohajda, T., & Fenyvesi, É. (2021). Encapsulation for Masking Off-Flavor and Off-Tasting in

USC DE SANTIAGO DE COMPOSTELA

Food Production. In T. M. Ho, H. Yoshii, K. Terao, & B. R. Bhandari (Eds.), *Functionality of Cyclodextrins in Encapsulation for Food Applications* (pp. 223–253). Springer International Publishing. https://doi.org/10.1007/978-3-030-80056-7_12

Szente, L., & Szejtli, J. (2004). Cyclodextrins as food ingredients. *Trends in Food Science & Technology*, *15*(3), 137–142. https://doi.org/10.1016/j.tifs.2003.09.019

Szente, L., & Szemán, J. (2013). Cyclodextrins in Analytical Chemistry: Host–Guest Type Molecular Recognition. *Analytical Chemistry*, *85*(17), 8024–8030. https://doi.org/10.1021/ac400639y

Tahıl, G., Delorme, F., Le Berre, D., Monflier, É., Sayede, A., & Tilloy, S. (2023). Curated dataset of association constants between a cyclodextrin and a guest for machine learning. *Chemical Data Collections*, *45*, 101022. https://doi.org/10.1016/j.cdc.2023.101022

team, T. pandas development. (2023). *pandas-dev/pandas: Pandas* [Computer software]. Zenodo. https://doi.org/10.5281/zenodo.7794821

Topuz, F., Holtzl, T., & Szekely, G. (2021). Scavenging organic micropollutants from water with nanofibrous hypercrosslinked cyclodextrin membranes derived from green resources. *Chemical Engineering Journal*, *419*, 129443. https://doi.org/10.1016/j.cej.2021.129443

Torrie, G. M., & Valleau, J. P. (1977). Nonphysical sampling distributions in Monte Carlo free-energy estimation: Umbrella sampling. *Journal of Computational Physics*, *23*(2), 187–199. https://doi.org/10.1016/0021-9991(77)90121-8

Tribello, G. A., Bonomi, M., Branduardi, D., Camilloni, C., & Bussi, G. (2014). PLUMED 2: New feathers for an old bird. *Computer Physics Communications*, *185*(2), 604–613. https://doi.org/10.1016/j.cpc.2013.09.018

Trott, O., & Olson, A. J. (2009). AutoDock Vina: Improving the speed and accuracy of docking with a new scoring function, efficient optimization, and multithreading. *Journal of Computational Chemistry*, NA-NA. https://doi.org/10.1002/jcc.21334

Van Gunsteren, W. F., & Berendsen, H. J. C. (1988). A Leap-frog Algorithm for Stochastic Dynamics. *Molecular Simulation*, *1*(3), 173–185. https://doi.org/10.1080/08927028808080941

Vanommeslaeghe, K., Hatcher, E., Acharya, C., Kundu, S., Zhong, S., Shim, J., Darian, E., Guvench, O., Lopes, P., Vorobyov, I., & MacKerell, A. D. (2010). CHARMM General Force Field (CGenFF): A force field for drug-like molecules compatible with the CHARMM all-atom additive biological force fields. *Journal of Computational Chemistry*, *31*(4), 671–690. https://doi.org/10.1002/jcc.21367

Villiers. (1891). *Comptes Rendus de l'Académie Des Sciences*.

Voskuhl, J., Schaepe, K., & Ravoo, B. J. (2011). Enhanced Chiral Recognition by Cyclodextrin Dimers. *International Journal of Molecular Sciences*, *12*(7), 4637–4646. https://doi.org/10.3390/ijms12074637

Wang, J., Wolf, R. M., Caldwell, J. W., Kollman, P. A., & Case, D. A. (2004). Development and testing of a general amber force field. *Journal of Computational Chemistry*, *25*(9), 1157–1174. https://doi.org/10.1002/jcc.20035

Wang, W., Shao, H., Zhou, S., Zhu, D., Jiang, X., Yu, G., & Deng, S. (2021). Rapid Removal of Perfluoroalkanesulfonates from Water by β-Cyclodextrin Covalent Organic Frameworks. *ACS Applied Materials & Interfaces*, *13*(41), 48700–48708. https://doi.org/10.1021/acsami.1c14043

Wang, Z., Landy, D., Sizun, C., Cézard, C., Solgadi, A., Przybylski, C., De Chaisemartin, L., Herfindal, L., Barratt, G., & Legrand, F.-X. (2020). Cyclodextrin complexation studies as the first step for repurposing of chlorpromazine. *International Journal of Pharmaceutics*, *584*, 119391. https://doi.org/10.1016/j.ijpharm.2020.119391

Wankar, J., Salzano, G., Pancani, E., Benkovics, G., Malanga, M., Manoli, F., Gref, R., Fenyvesi, E., & Manet, I. (2017). Efficient loading of ethionamide in cyclodextrin-based carriers offers enhanced solubility and inhibition of drug crystallization. *International Journal of Pharmaceutics*, *531*(2), 568–576. https://doi.org/10.1016/j.ijpharm.2017.05.041

Welliver, M. (2008). Discovery, development, and clinical application of sugammadex sodium, a selective relaxant binding agent. *Drug Design, Development and Therapy*, 49.

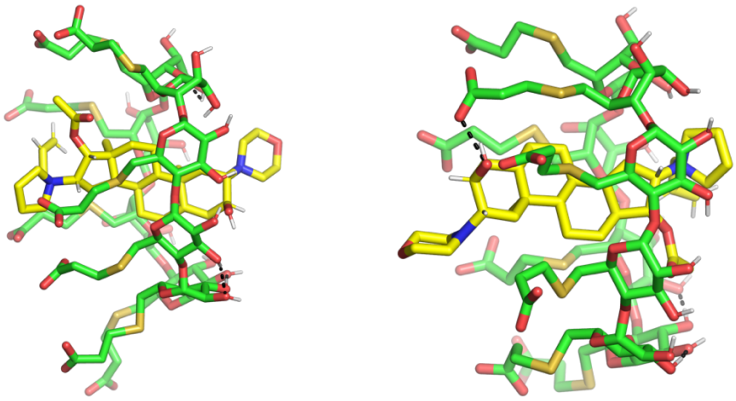
USC UNIVERSIDADE DE SANTIAGO DE COMPOSTELA

https://doi.org/10.2147/DDDT.S2757
Wilcoxon, F. (1945). Individual comparisons by ranking methods. *Biom. Bull.*, *1*(6).
Williams, K. R., Colina, C. J., Eylem, C., & Montgomery, L. (2016). *(54) FRESHENING COMPOSITIONS*.
Wolf, S., Lickert, B., Bray, S., & Stock, G. (2020). Multisecond ligand dissociation dynamics from atomistic simulations. *Nature Communications*, *11*(1), 2918. https://doi.org/10.1038/s41467-020-16655-1
Wu, X. (1991). Optimal quantization by matrix searching. *Journal of Algorithms*, *12*(4), 663–673. https://doi.org/10.1016/0196-6774(91)90039-2
Xu, M., & Lill, M. A. (2013). Induced fit docking, and the use of QM/MM methods in docking. *Drug Discovery Today: Technologies*, *10*(3), e411–e418. https://doi.org/10.1016/j.ddtec.2013.02.003
Xu, Z., Wauchope, O. R., & Frank, A. T. (2021). Navigating Chemical Space by Interfacing Generative Artificial Intelligence and Molecular Docking. *Journal of Chemical Information and Modeling*, *61*(11), 5589–5600. https://doi.org/10.1021/acs.jcim.1c00746
Yadav, M., Thakore, S., & Jadeja, R. (2022). A review on remediation technologies using functionalized Cyclodextrin. *Environmental Science and Pollution Research*, *29*(1), 236–250. https://doi.org/10.1007/s11356-021-15887-y
Yang, S., Yan, Y., Huang, J., Petukhov, A. V., Kroon-Batenburg, L. M. J., Drechsler, M., Zhou, C., Tu, M., Granick, S., & Jiang, L. (2017). Giant capsids from lattice self-assembly of cyclodextrin complexes. *Nature Communications*, *8*(1), Article 1. https://doi.org/10.1038/ncomms15856
You, W., Tang, Z., & Chang, C. A. (2019). Potential Mean Force from Umbrella Sampling Simulations: What Can We Learn and What Is Missed? *Journal of Chemical Theory and Computation*, *15*(4), 2433–2443. https://doi.org/10.1021/acs.jctc.8b01142

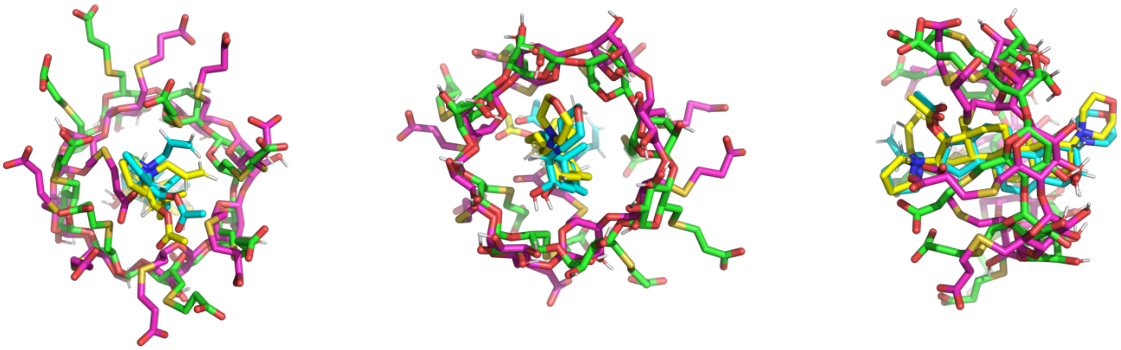
USC
UNIVERSIDADE DE SANTIAGO DE COMPOSTELA

Supplemental Information

USC
UNIVERSIDADE DE SANTIAGO DE COMPOSTELA



Supplemental Figure S4-1. Hydrogen bonds in the up (left) and down (right) orientations. Hydrogen bonds are shown as black dashed lines.

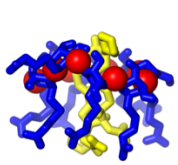


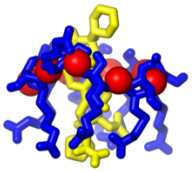
Supplemental Figure S4-2. Alignment of the docking output (magenta CD, blue rocuronium) with the PMF minimum in the up orientation (green CD, yellow rocuronium) from three different angles. The RMSD for the whole complex was 1.875 Å. The alignment is good but it is clear that the complex is quite flexible, especially regarding the substitutions on the CD.

USC
UNIVERSIDADE DE SANTIAGO DE COMPOSTELA

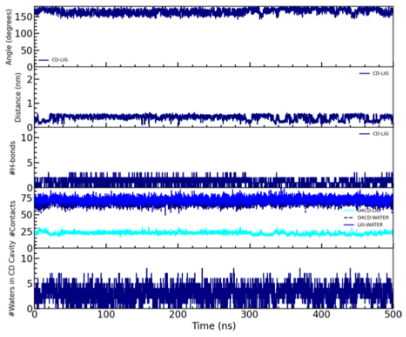
Additional Supplemental Information for Chapter 4: MD and Docking Results for All Eight Centroids

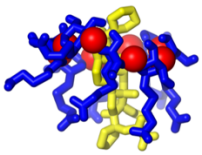
Centroid 1





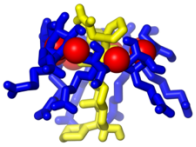
Docking Energy = −5.6111 kJ/mol

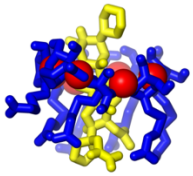




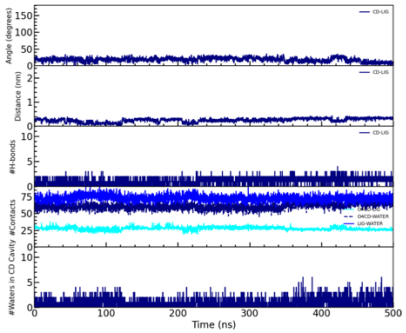
MD Energy: −269 ± 37 kJ/mol
Coulomb: −94 ± 24 kJ/mol
L-J: −175 ± 13 kJ/mol

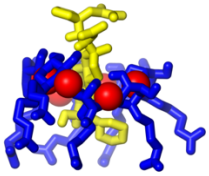
Centroid 2





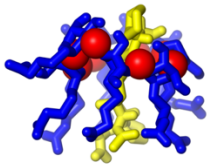
Docking Energy = −5.4041 kJ/mol

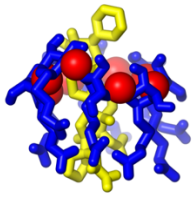




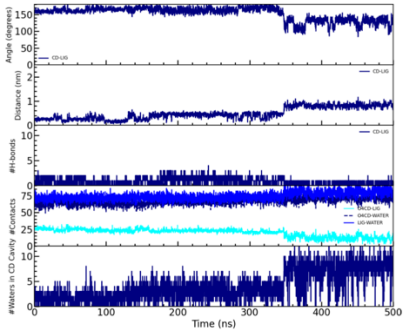
MD Energy: −244 ± 44 kJ/mol
Coulomb: −75 ± 31 kJ/mol
L-J: −169 ± 13 kJ/mol

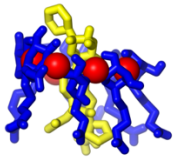
Centroid 3





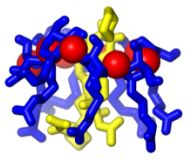
Docking Energy = −5.6039 kJ/mol

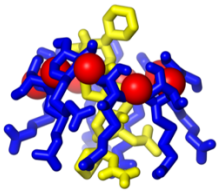




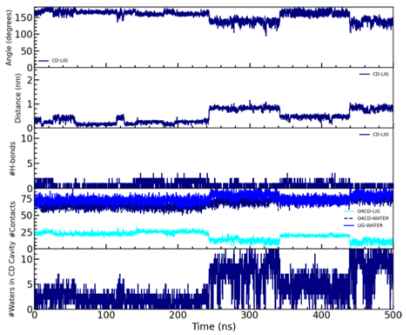
MD Energy: −238 ± 53 kJ/mol
Coulomb: −72 ± 30 kJ/mol
L-J: −166 ± 23 kJ/mol

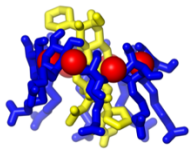
Centroid 4





Docking Energy = −5.7555 kJ/mol

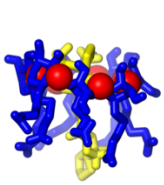


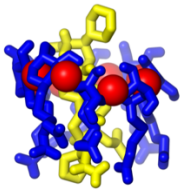


MD Energy: −236 ± 49 kJ/mol
Coulomb: −68 ± 28 kJ/mol
L-J: −168 ± 21 kJ/mol

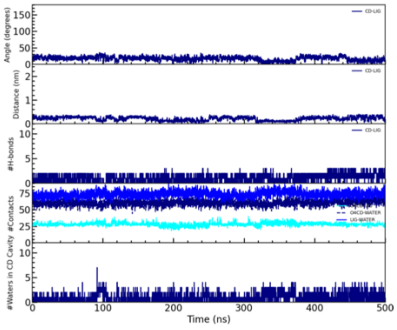
USC
UNIVERSIDADE DE SANTIAGO DE COMPOSTELA

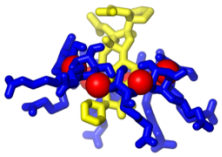
Centroid 5





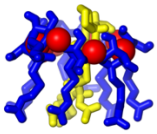
Docking Energy = −5.7244 kJ/mol

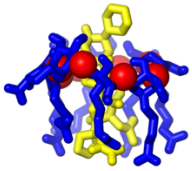




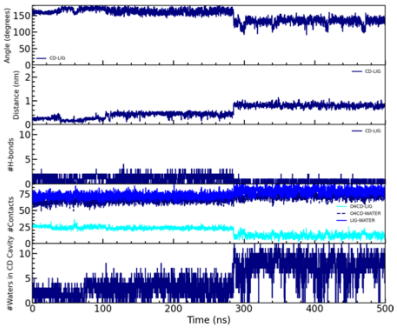
MD Energy: -236 ± 44 kJ/mol
Coulomb: -70 ± 31 kJ/mol
L-J: -166 ± 13 kJ/mol

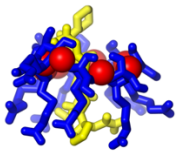
Centroid 6





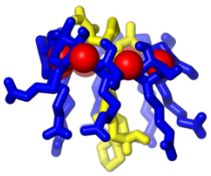
Docking Energy = −5.7203 kJ/mol

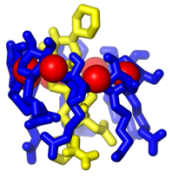




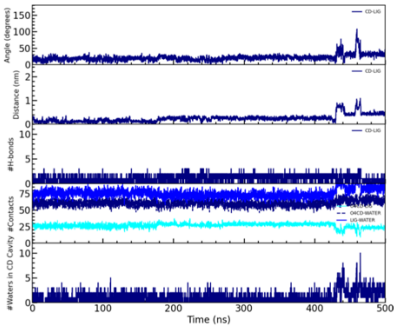
MD Energy: -234 ± 54 kJ/mol
Coulomb: -71 ± 32 kJ/mol
L-J: -163 ± 22 kJ/mol

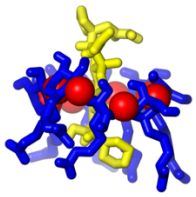
Centroid 7





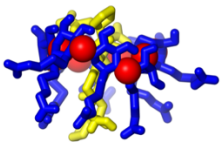
Docking Energy = −5.4696 kJ/mol

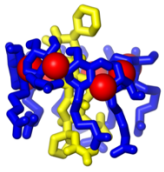




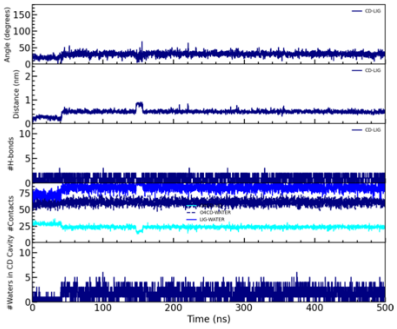
MD Energy: -218 ± 55 kJ/mol
Coulomb: -60 ± 31 kJ/mol
L-J: -158 ± 24 kJ/mol

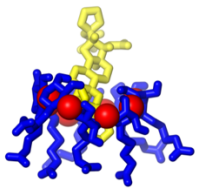
Centroid 8





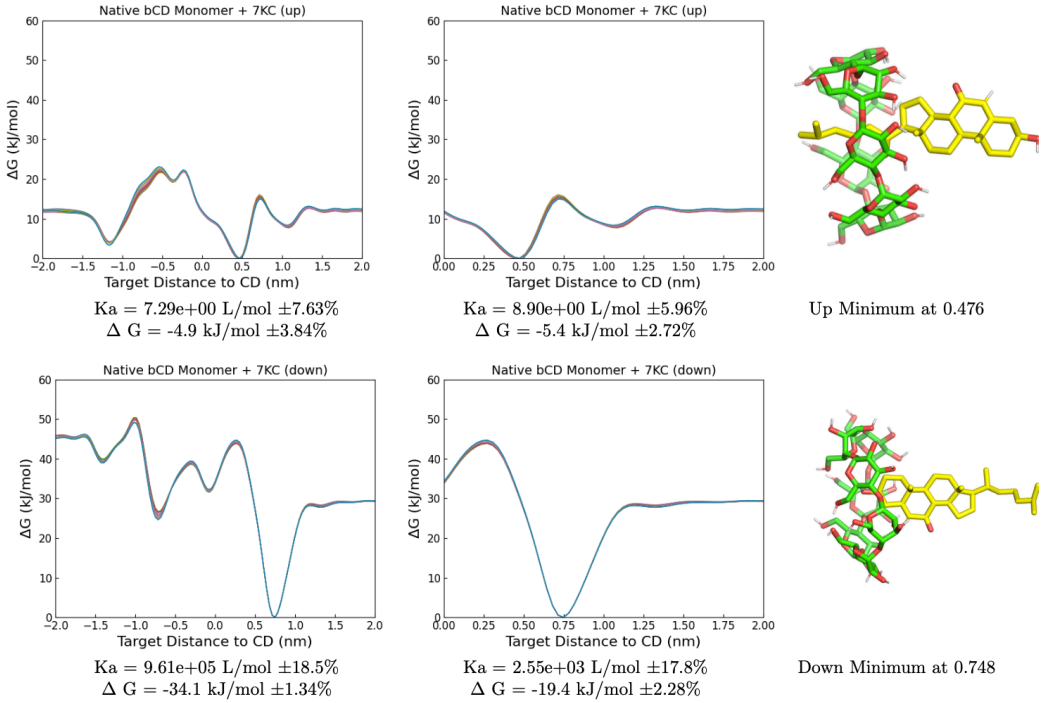
Docking Energy = −5.3831 kJ/mol





MD Energy: -158 ± 40 kJ/mol
Coulomb: -34 ± 21 kJ/mol
L-J: -124 ± 19 kJ/mol

USC
UNIVERSIDADE DE SANTIAGO DE COMPOSTELA



Ka = 7.29e+00 L/mol ±7.63%
Δ G = -4.9 kJ/mol ±3.84%

Ka = 8.90e+00 L/mol ±5.96%
Δ G = -5.4 kJ/mol ±2.72%

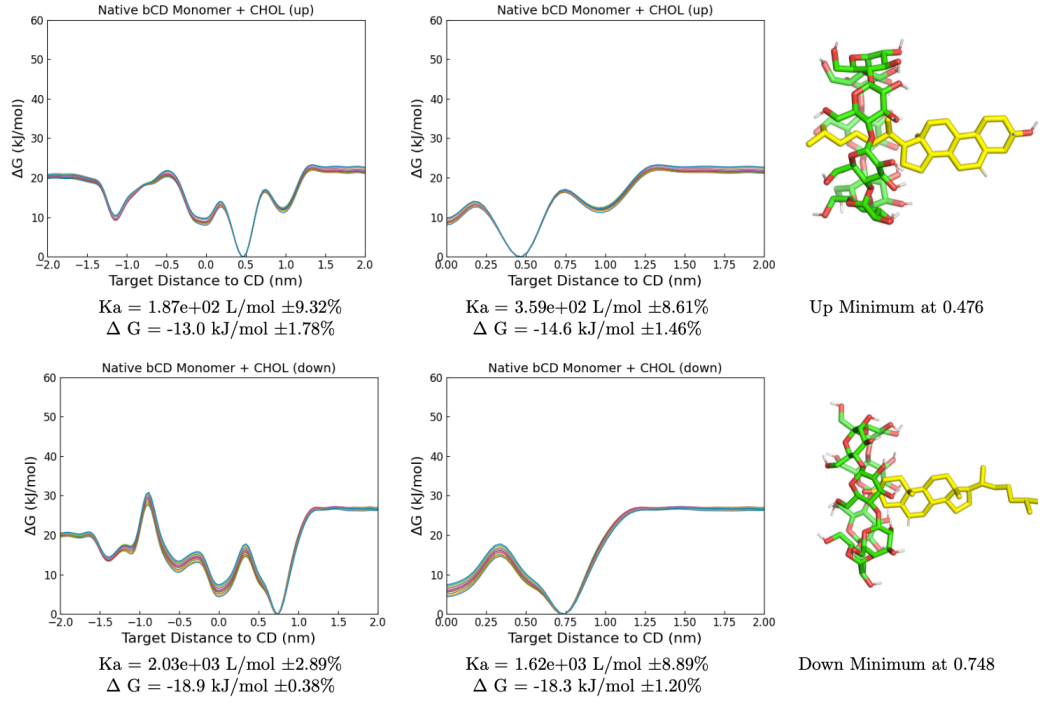
Up Minimum at 0.476

Ka = 9.61e+05 L/mol ±18.5%
Δ G = -34.1 kJ/mol ±1.34%

Ka = 2.55e+03 L/mol ±17.8%
Δ G = -19.4 kJ/mol ±2.28%

Down Minimum at 0.748

Figure S5-1. Native βCD with 7KC in up (top) and down (bottom) orientation, sampling either the entire βCD cavity (left) or only the secondary (wide) face of the βCD (middle), along with the associated K and ΔG values, and the configuration at the energy minimum (right).



Ka = 1.87e+02 L/mol ±9.32%
Δ G = -13.0 kJ/mol ±1.78%

Ka = 3.59e+02 L/mol ±8.61%
Δ G = -14.6 kJ/mol ±1.46%

Up Minimum at 0.476

Ka = 2.03e+03 L/mol ±2.89%
Δ G = -18.9 kJ/mol ±0.38%

Ka = 1.62e+03 L/mol ±8.89%
Δ G = -18.3 kJ/mol ±1.20%

Down Minimum at 0.748

Figure S5-2. Native βCD with cholesterol in up (top) and down (bottom) orientation, sampling either the entire βCD cavity (left) or only the secondary (wide) face of the βCD

USC UNIVERSIDADE DE SANTIAGO DE COMPOSTELA

(middle), along with the associated K and ΔG values, and the configuration at the energy minimum (right).

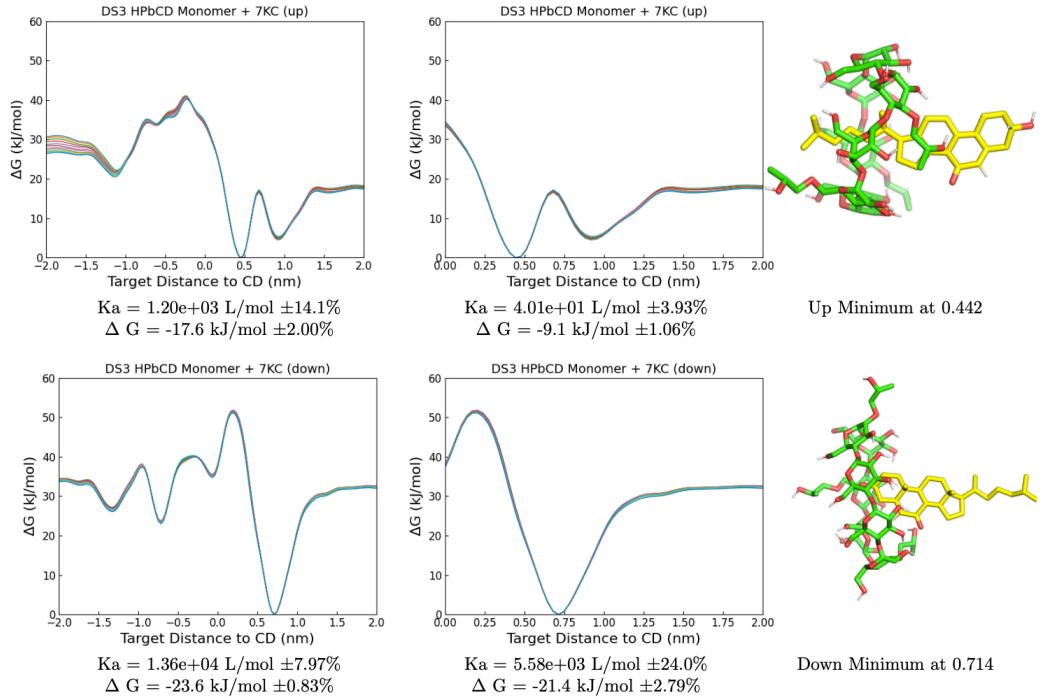


Figure S5-3. DS3 HPβCD with 7KC in up (top) and down (bottom) orientation, sampling either the entire βCD cavity (left) or only the secondary (wide) face of the βCD (middle), along with the associated K and ΔG values, and the configuration at the energy minimum (right).

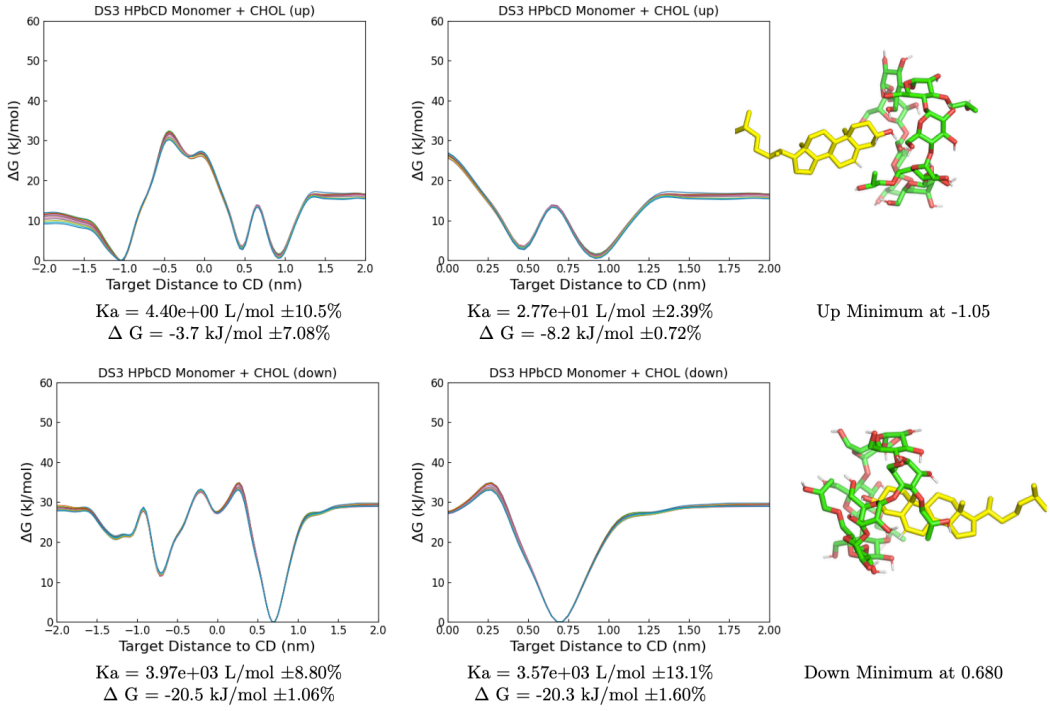


Figure S5-4. DS3 HPβCD with cholesterol in up (top) and down (bottom) orientation, sampling either the entire βCD cavity (left) or only the secondary (wide) face of the βCD

USC UNIVERSIDADE DE SANTIAGO DE COMPOSTELA

(middle), along with the associated K and ΔG values, and the configuration at the energy minimum (right).

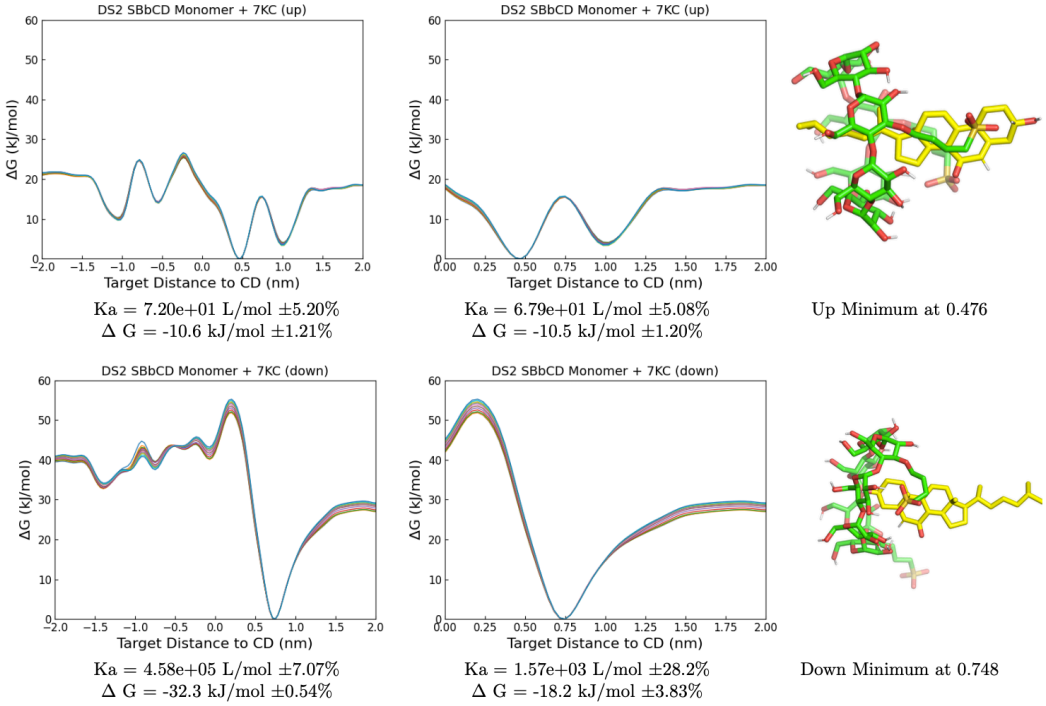


Figure S5-5. DS2 SBβCD monomer with 7KC in up (top) and down (bottom) orientation, sampling either the entire βCD cavity (left) or only the secondary (wide) face of the βCD (middle), along with the associated K and ΔG values, and the configuration at the energy minimum (right).

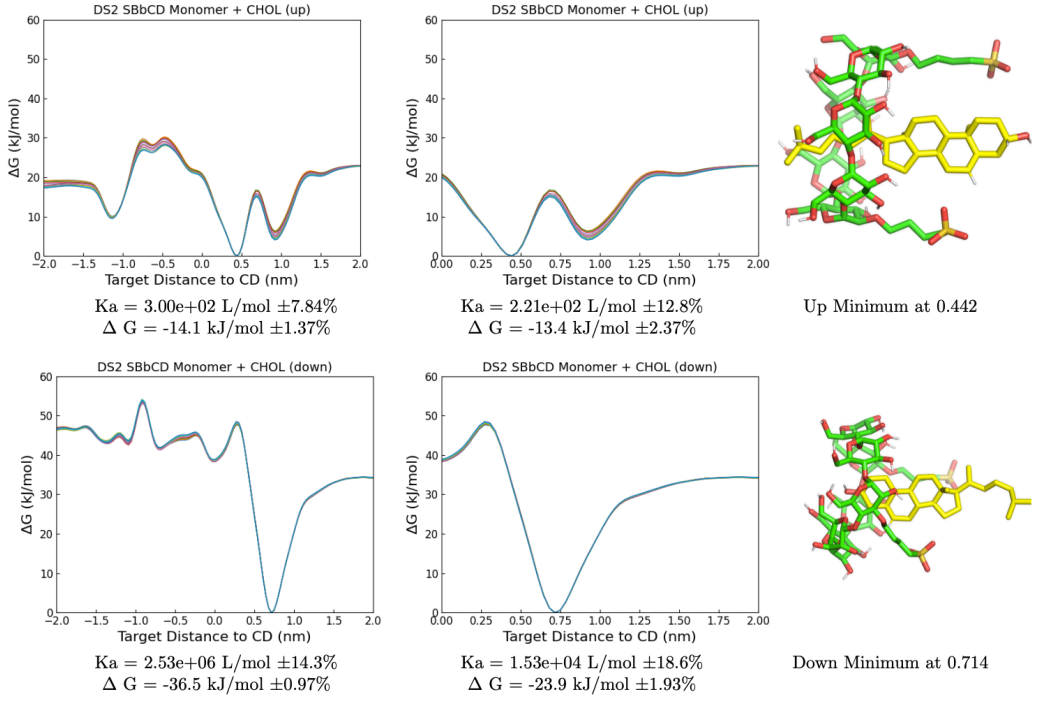


Figure S5-6. DS2 SBβCD monomer with cholesterol in up (top) and down (bottom) orientation, sampling either the entire βCD cavity (left) or only the secondary (wide) face

USC UNIVERSIDADE DE SANTIAGO DE COMPOSTELA

of the βCD (middle), along with the associated K and ΔG values, and the configuration at the energy minimum (right).

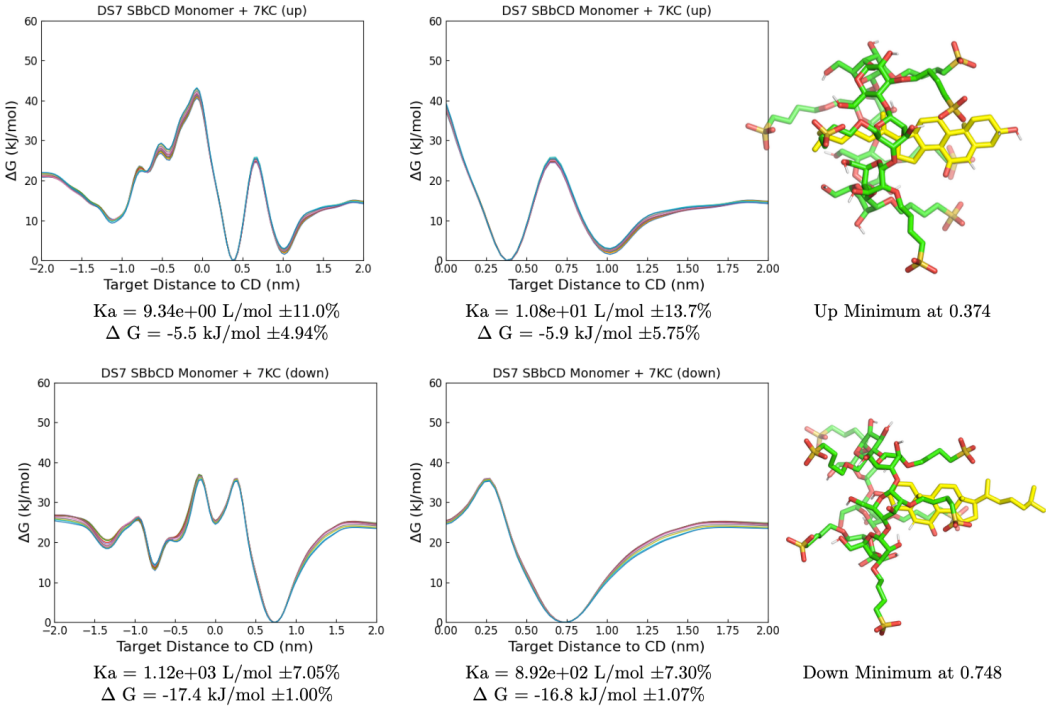


Figure S5-7. DS7 SBβCD monomer with 7KC in up (top) and down (bottom) orientation, sampling either the entire βCD cavity (left) or only the secondary (wide) face of the βCD (middle), along with the associated K and ΔG values, and the configuration at the energy minimum (right).

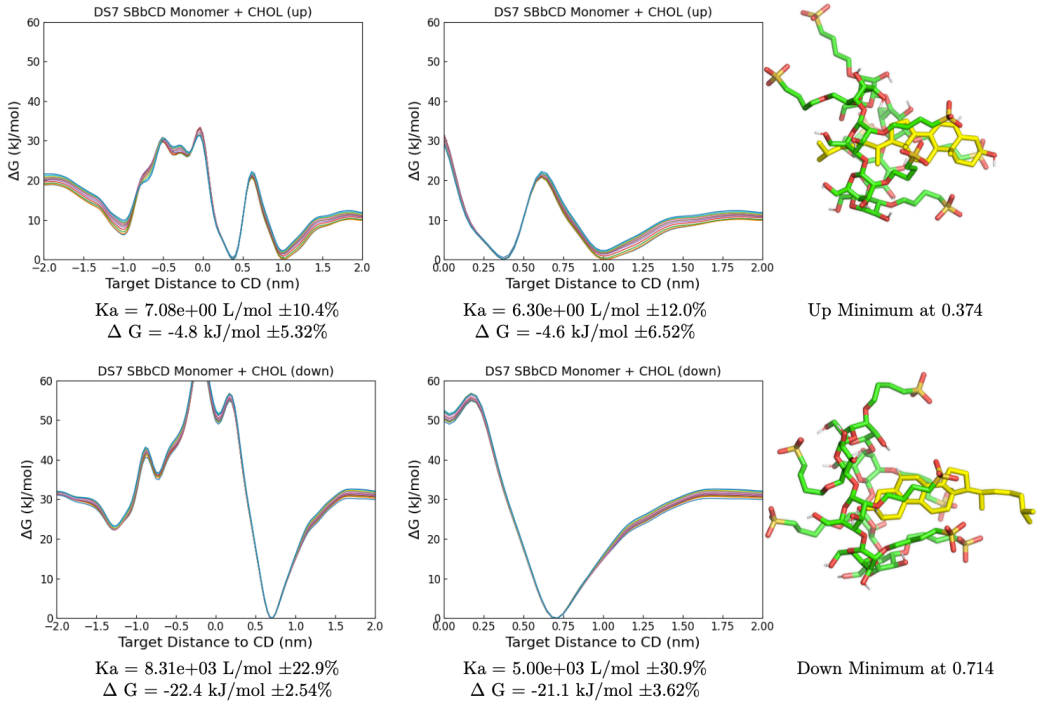


Figure S5-8. DS7 SBβCD monomer with cholesterol in up (top) and down (bottom) orientation, sampling either the entire βCD cavity (left) or only the secondary (wide) face

USC UNIVERSIDADE DE SANTIAGO DE COMPOSTELA

of the βCD (middle), along with the associated K and ΔG values, and the configuration at the energy minimum (right).

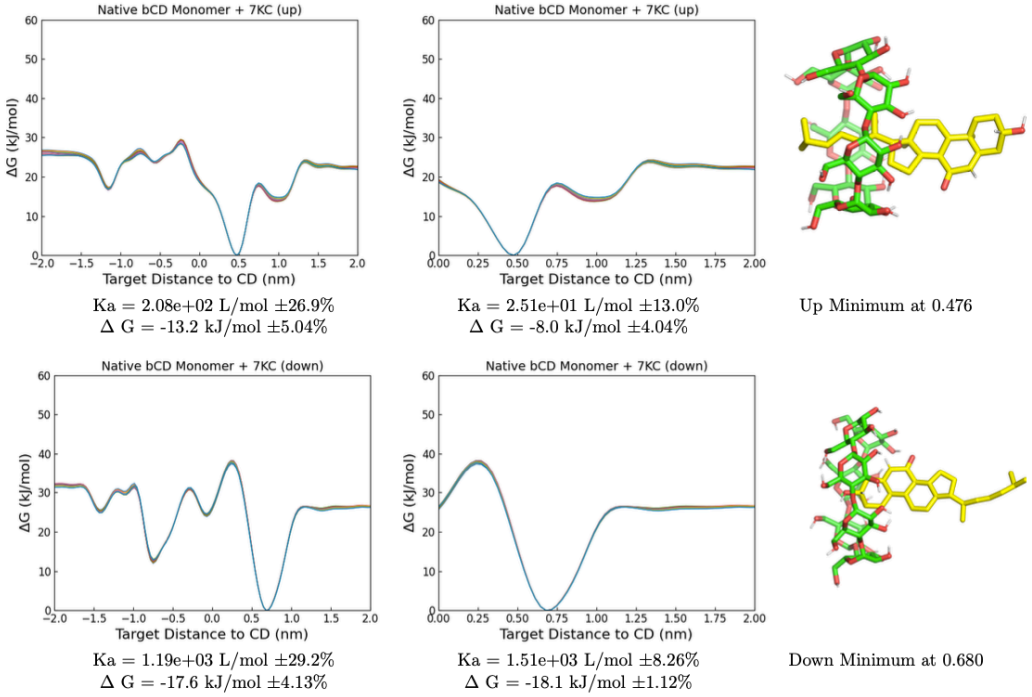


Figure S5-9. Second run of walkers placed every 5Å along the CD cavity. Native βCD with 7KC in up (top) and down (bottom) orientation, sampling either the entire βCD cavity (left) or only the secondary (wide) face of the βCD (middle), along with the associated K and ΔG values, and the configuration at the energy minimum (right).

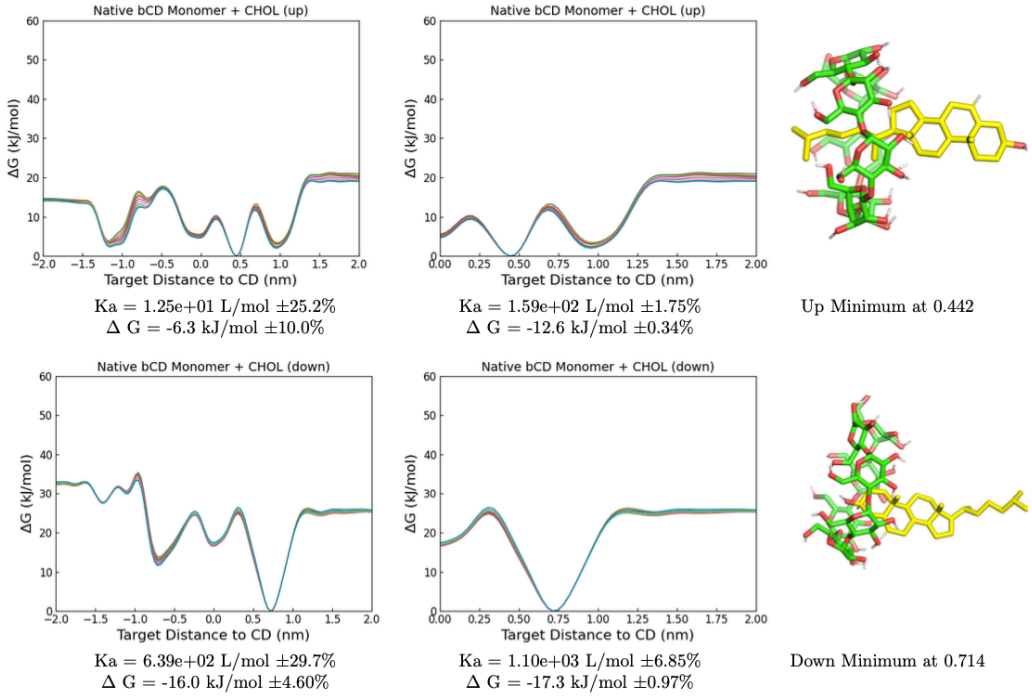


Figure S5-10. Second run of walkers placed every 5Å along the CD cavity. Native βCD with cholesterol in up (top) and down (bottom) orientation, sampling either the entire βCD

USC UNIVERSIDADE DE SANTIAGO DE COMPOSTELA

cavity (left) or only the secondary (wide) face of the βCD (middle), along with the associated K and ΔG values, and the configuration at the energy minimum (right).

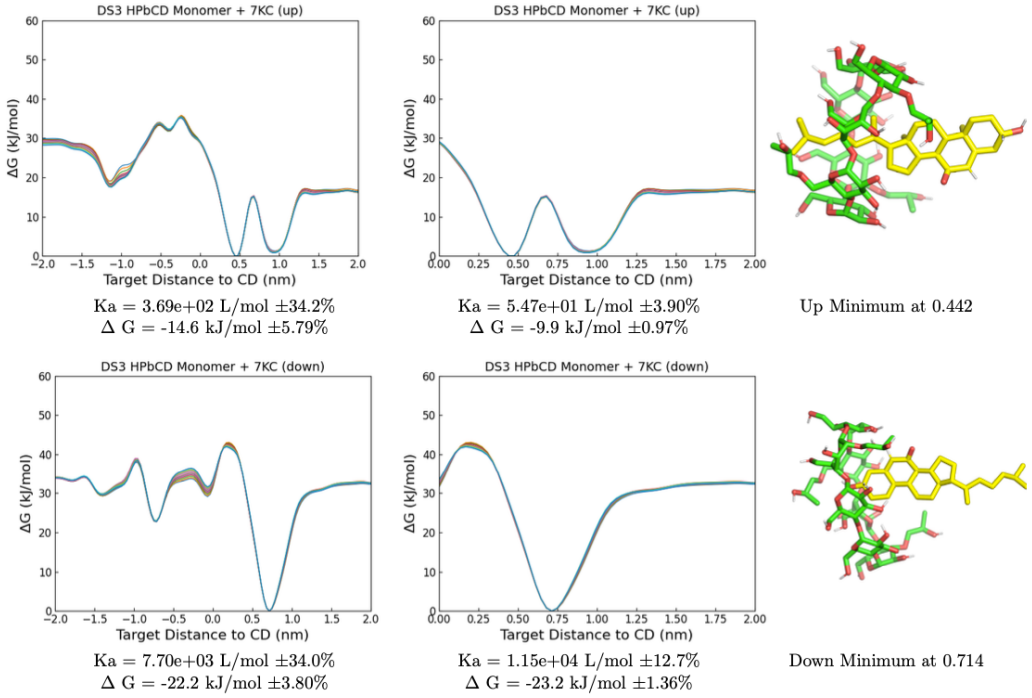


Figure S5-11. Second run of walkers placed every 5Å along the CD cavity. DS3 HPβCD with 7KC in up (top) and down (bottom) orientation, sampling either the entire βCD cavity (left) or only the secondary (wide) face of the βCD (middle), along with the associated K and ΔG values, and the configuration at the energy minimum (right).

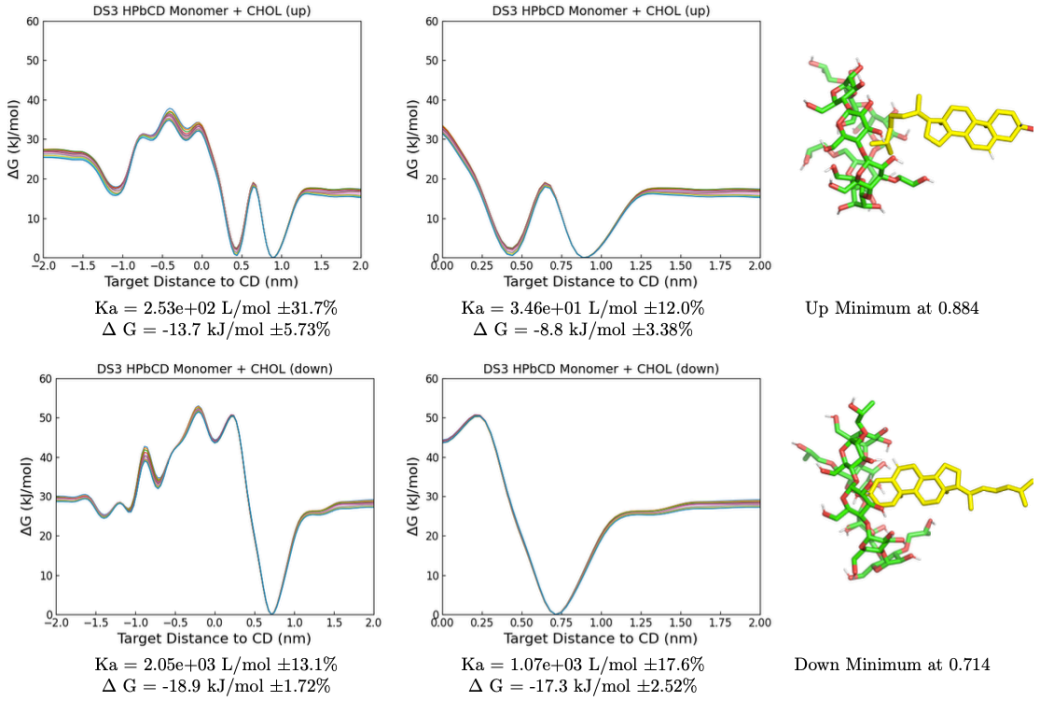


Figure S5-12. Second run of walkers placed every 5Å along the CD cavity. DS3 HPβCD with cholesterol in up (top) and down (bottom) orientation, sampling either the entire βCD

USC UNIVERSIDADE DE SANTIAGO DE COMPOSTELA

cavity (left) or only the secondary (wide) face of the βCD (middle), along with the associated K and ΔG values, and the configuration at the energy minimum (right).

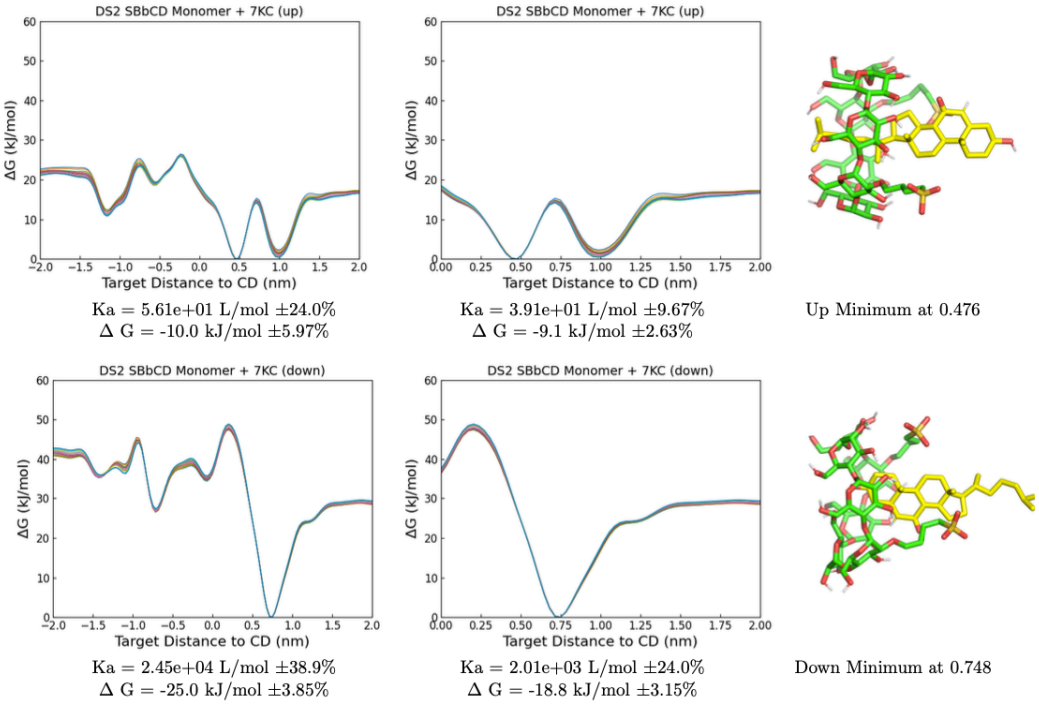


Figure S5-13. Second run of walkers placed every 5Å along the CD cavity. DS2 SBβCD monomer with 7KC in up (top) and down (bottom) orientation, sampling either the entire βCD cavity (left) or only the secondary (wide) face of the βCD (middle), along with the associated K and ΔG values, and the configuration at the energy minimum (right).

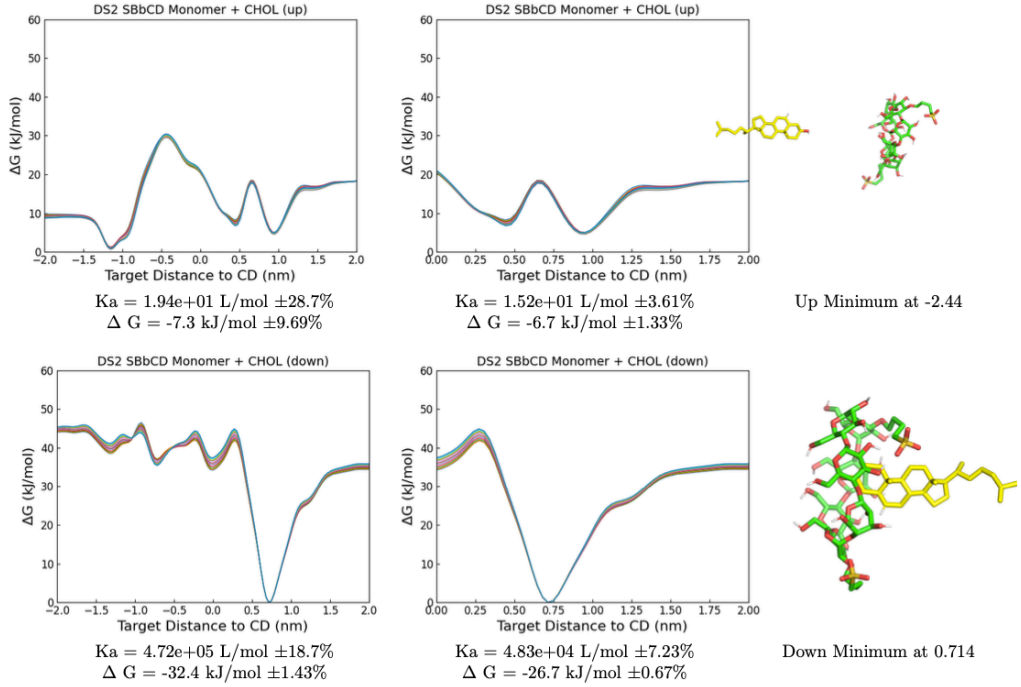


Figure S5-14. Second run of walkers placed every 5Å along the CD cavity. DS2 SBβCD monomer with cholesterol in up (top) and down (bottom) orientation, sampling either the

USC UNIVERSIDADE DE SANTIAGO DE COMPOSTELA

entire βCD cavity (left) or only the secondary (wide) face of the βCD (middle), along with the associated K and ΔG values, and the configuration at the energy minimum (right).

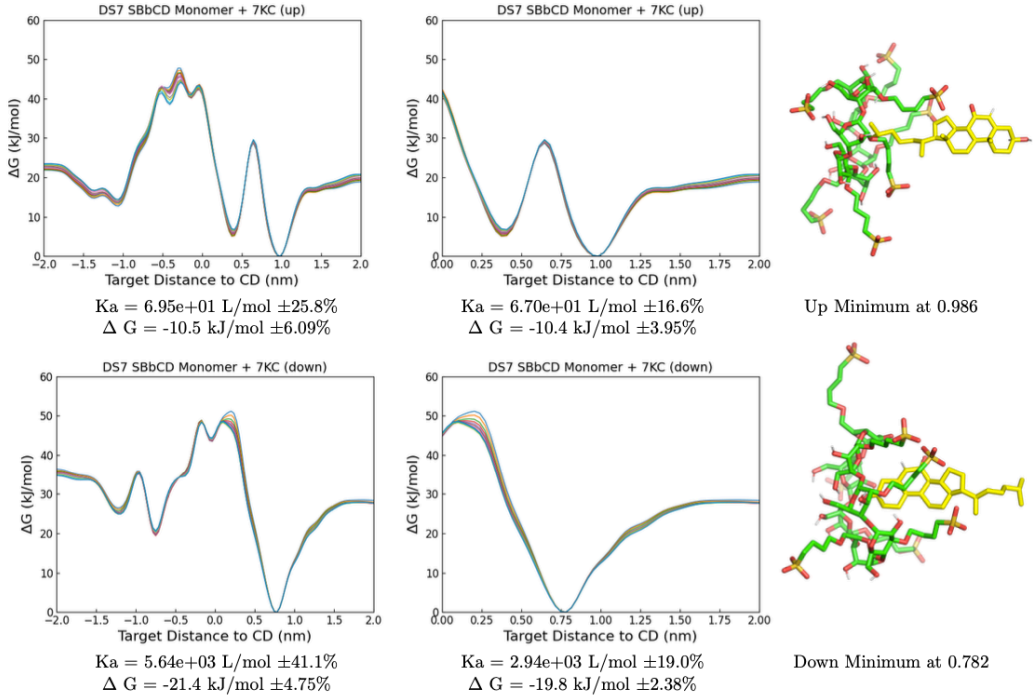


Figure S5-15. Second run of walkers placed every 5Å along the CD cavity. DS7 SBβCD monomer with 7KC in up (top) and down (bottom) orientation, sampling either the entire βCD cavity (left) or only the secondary (wide) face of the βCD (middle), along with the associated K and ΔG values, and the configuration at the energy minimum (right).

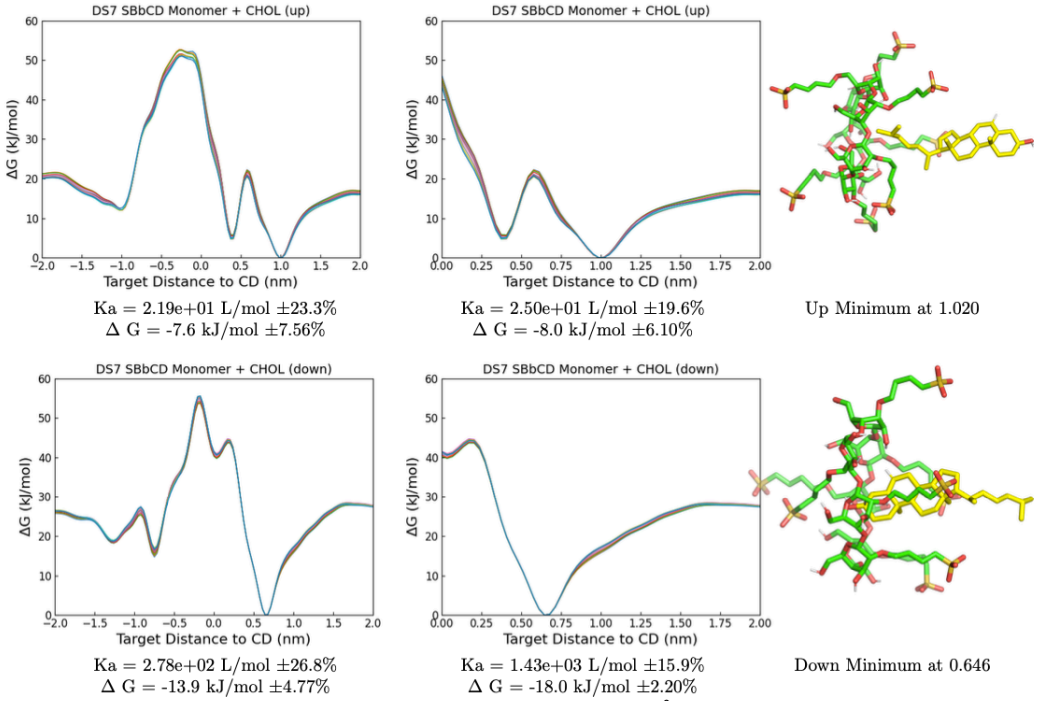


Figure S5-16. Second run of walkers placed every 5Å along the CD cavity. DS7 SBβCD monomer with cholesterol in up (top) and down (bottom) orientation, sampling either the

USC UNIVERSIDADE DE SANTIAGO DE COMPOSTELA

entire βCD cavity (left) or only the secondary (wide) face of the βCD (middle), along with the associated K and ΔG values, and the configuration at the energy minimum (right).

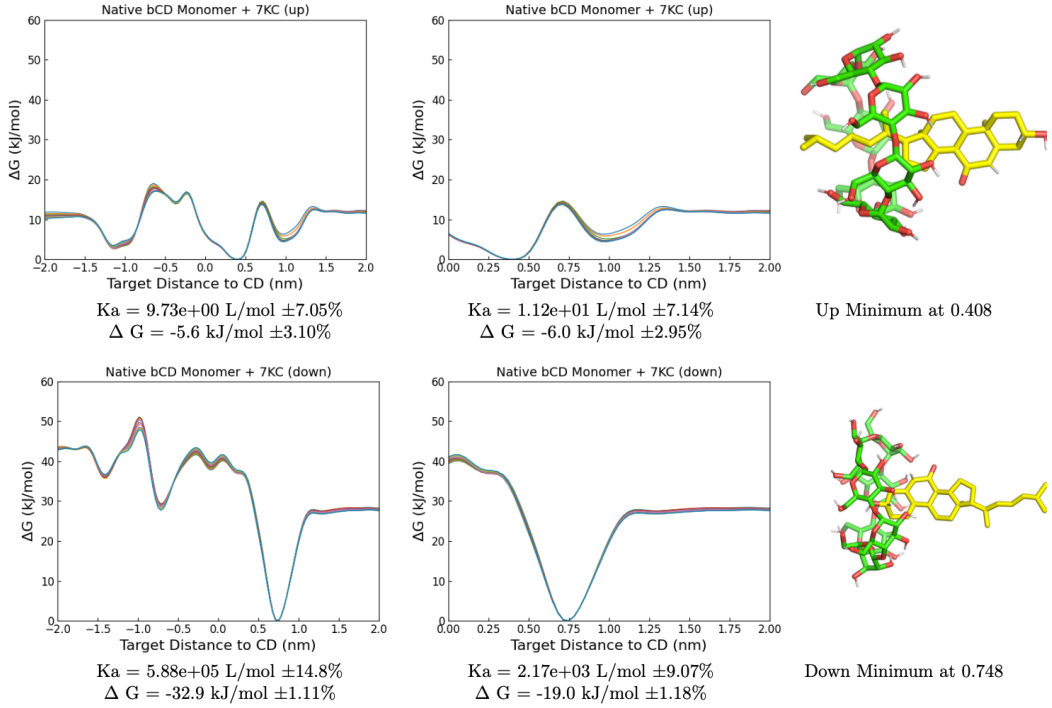


Figure S5-17. Walkers placed every 4Å along the CD cavity. Native βCD with 7KC in up (top) and down (bottom) orientation, sampling either the entire βCD cavity (left) or only the secondary (wide) face of the βCD (middle), along with the associated K and ΔG values, and the configuration at the energy minimum (right).

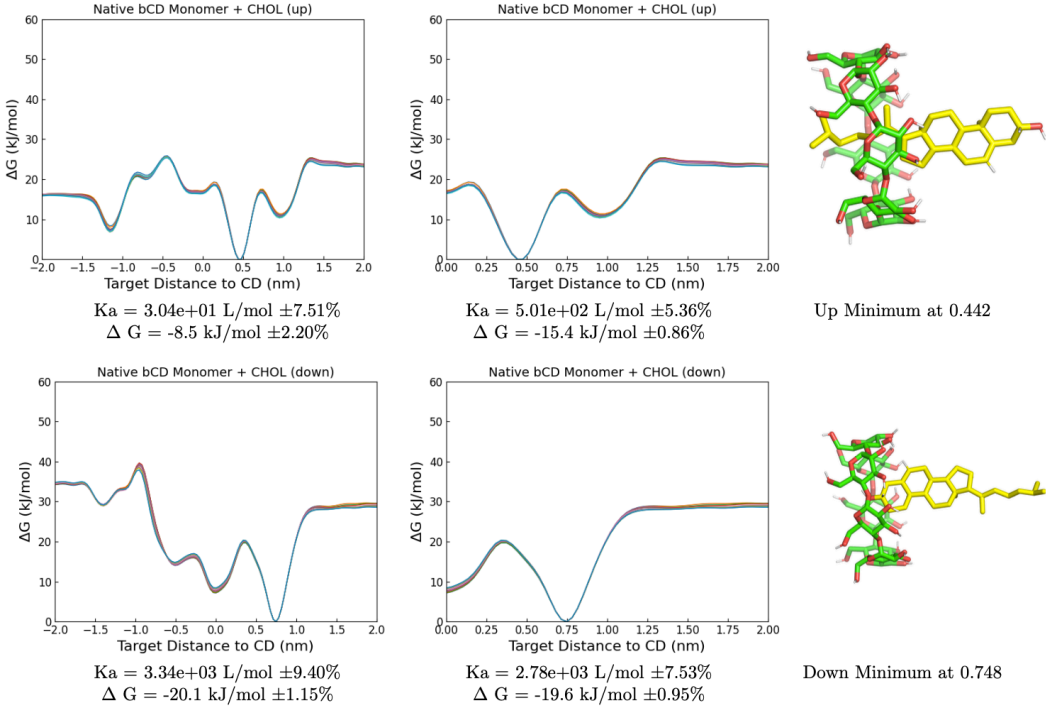


Figure S5-18. Walkers placed every 4Å along the CD cavity. Native βCD with cholesterol in up (top) and down (bottom) orientation, sampling either the entire βCD cavity (left) or

USC UNIVERSIDADE DE SANTIAGO DE COMPOSTELA

only the secondary (wide) face of the βCD (middle), along with the associated K and ΔG values, and the configuration at the energy minimum (right).

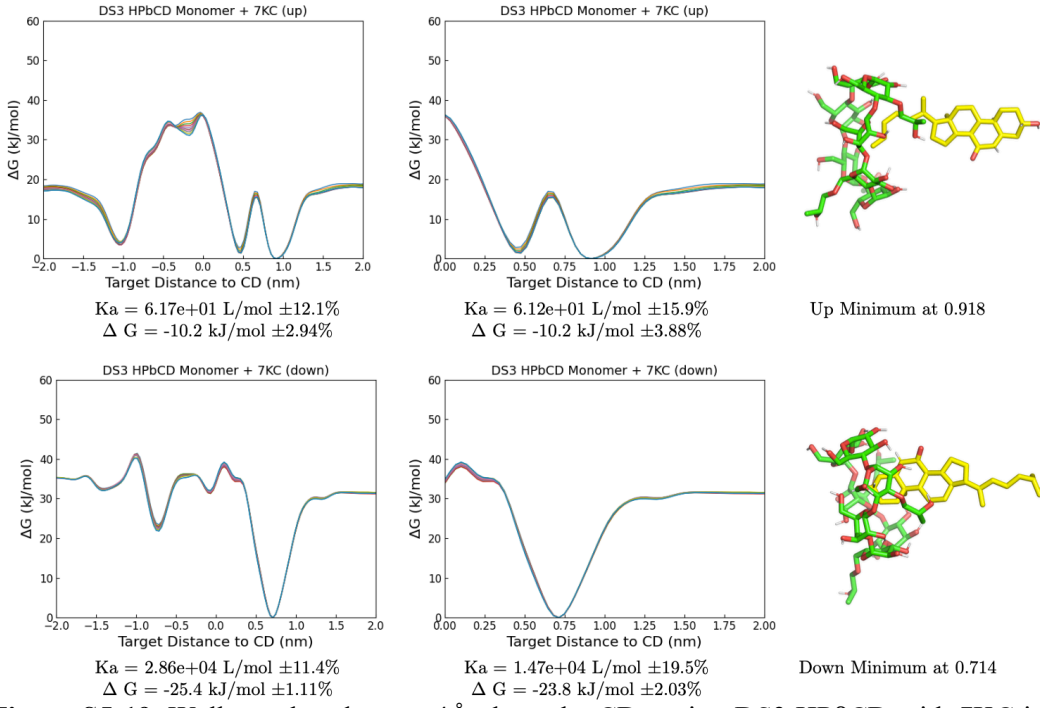


Figure S5-19. Walkers placed every 4Å along the CD cavity. DS3 HPβCD with 7KC in up (top) and down (bottom) orientation, sampling either the entire βCD cavity (left) or only the secondary (wide) face of the βCD (middle), along with the associated K and ΔG values, and the configuration at the energy minimum (right).

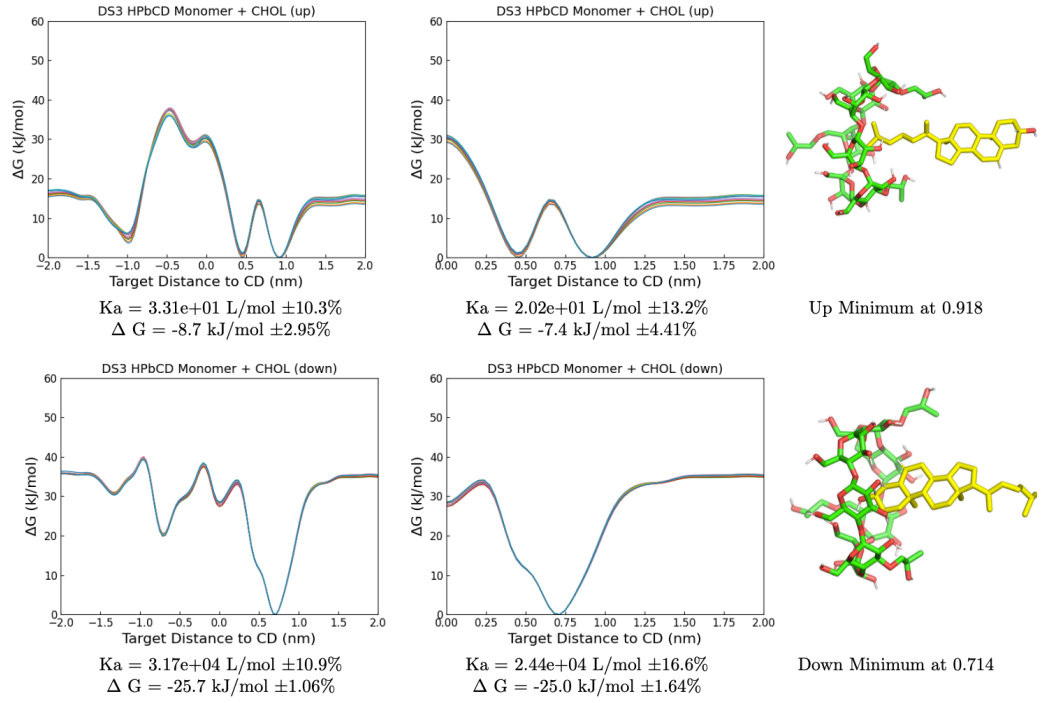


Figure S5-20. Walkers placed every 4Å along the CD cavity. DS3 HPβCD with cholesterol in up (top) and down (bottom) orientation, sampling either the entire βCD cavity (left) or

USC UNIVERSIDADE DE SANTIAGO DE COMPOSTELA

only the secondary (wide) face of the βCD (middle), along with the associated K and ΔG values, and the configuration at the energy minimum (right).

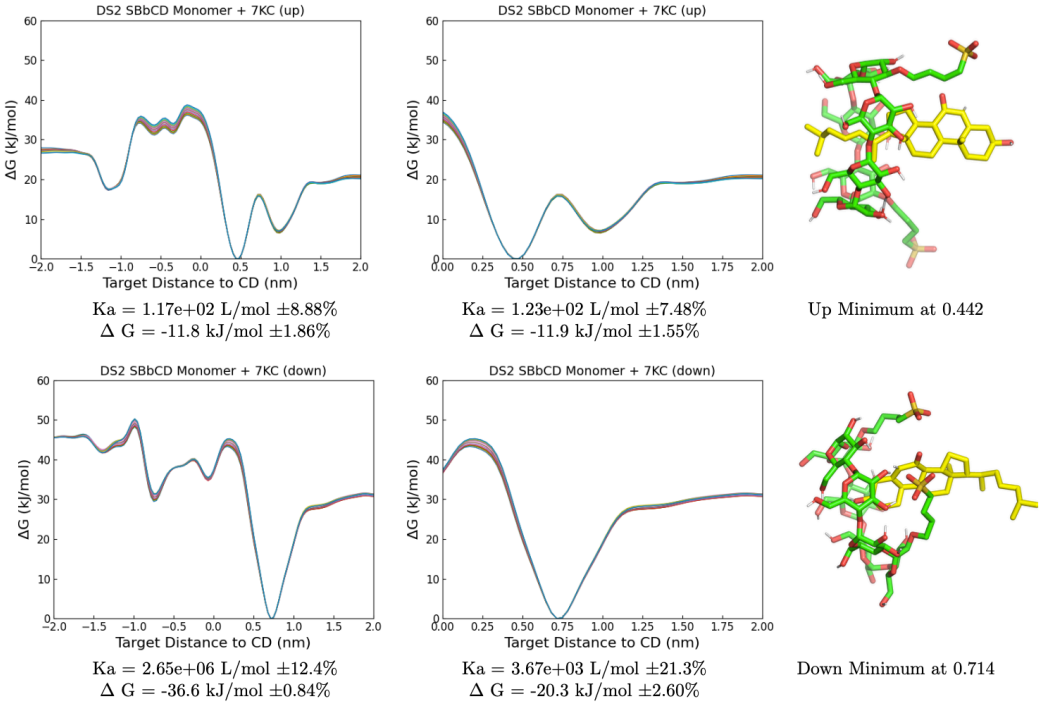


Figure S5-21. Walkers placed every 4Å along the CD cavity. DS2 SBβCD monomer with 7KC in up (top) and down (bottom) orientation, sampling either the entire βCD cavity (left) or only the secondary (wide) face of the βCD (middle), along with the associated K and ΔG values, and the configuration at the energy minimum (right).

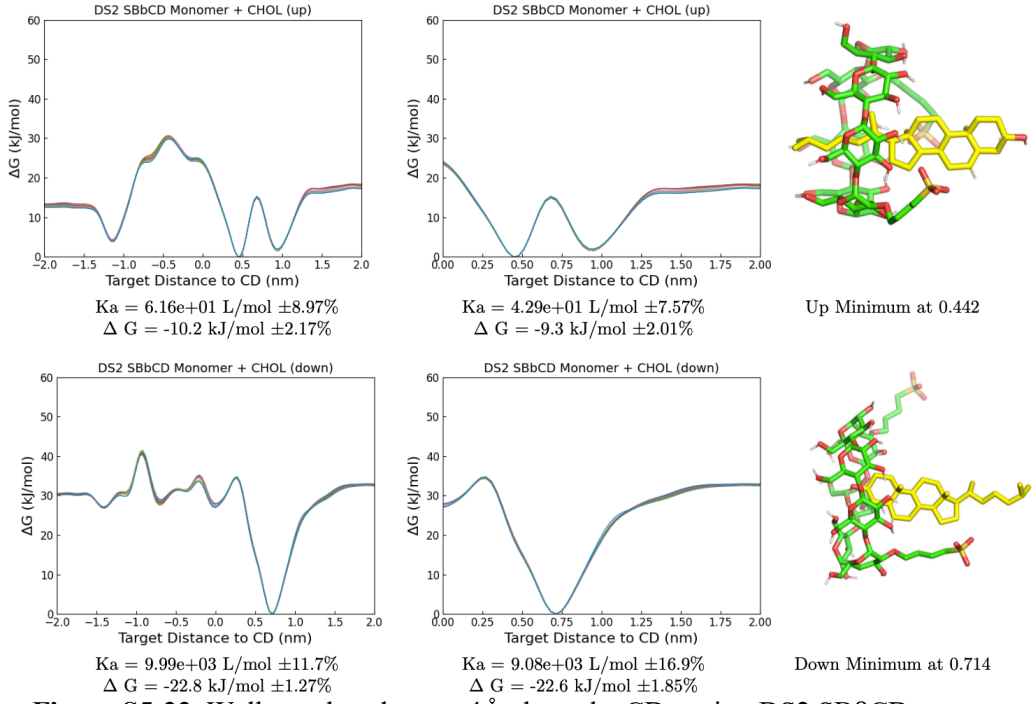


Figure S5-22. Walkers placed every 4Å along the CD cavity. DS2 SBβCD monomer with cholesterol in up (top) and down (bottom) orientation, sampling either the entire βCD

USC UNIVERSIDADE DE SANTIAGO DE COMPOSTELA

cavity (left) or only the secondary (wide) face of the βCD (middle), along with the associated K and ΔG values, and the configuration at the energy minimum (right).

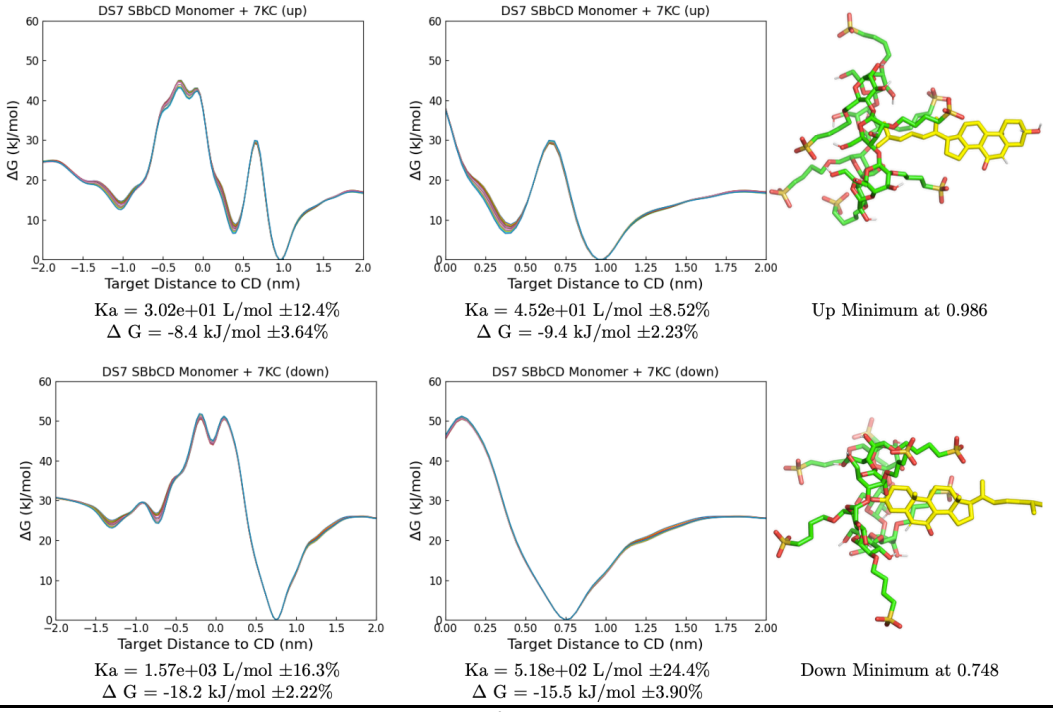


Figure S5-23. Walkers placed every 4Å along the CD cavity. DS7 SBβCD monomer with 7KC in up (top) and down (bottom) orientation, sampling either the entire βCD cavity (left) or only the secondary (wide) face of the βCD (middle), along with the associated K and ΔG values, and the configuration at the energy minimum (right).

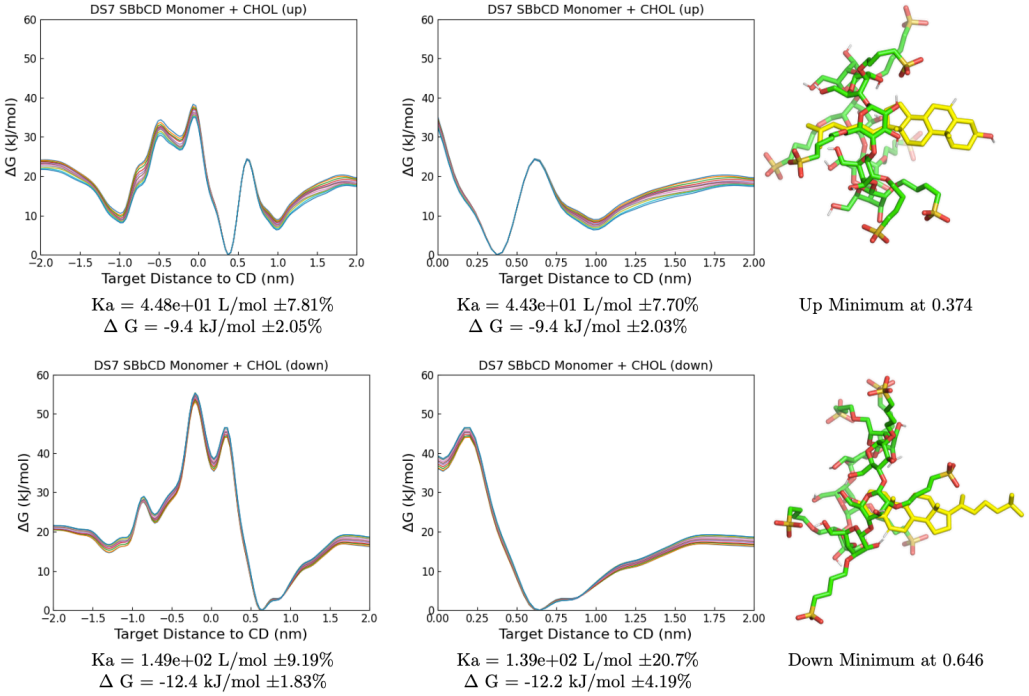


Figure S5-24. Walkers placed every 4Å along the CD cavity. DS7 SBβCD monomer with cholesterol in up (top) and down (bottom) orientation, sampling either the entire βCD

USC UNIVERSIDADE DE SANTIAGO DE COMPOSTELA

cavity (left) or only the secondary (wide) face of the βCD (middle), along with the associated K and ΔG values, and the configuration at the energy minimum (right).

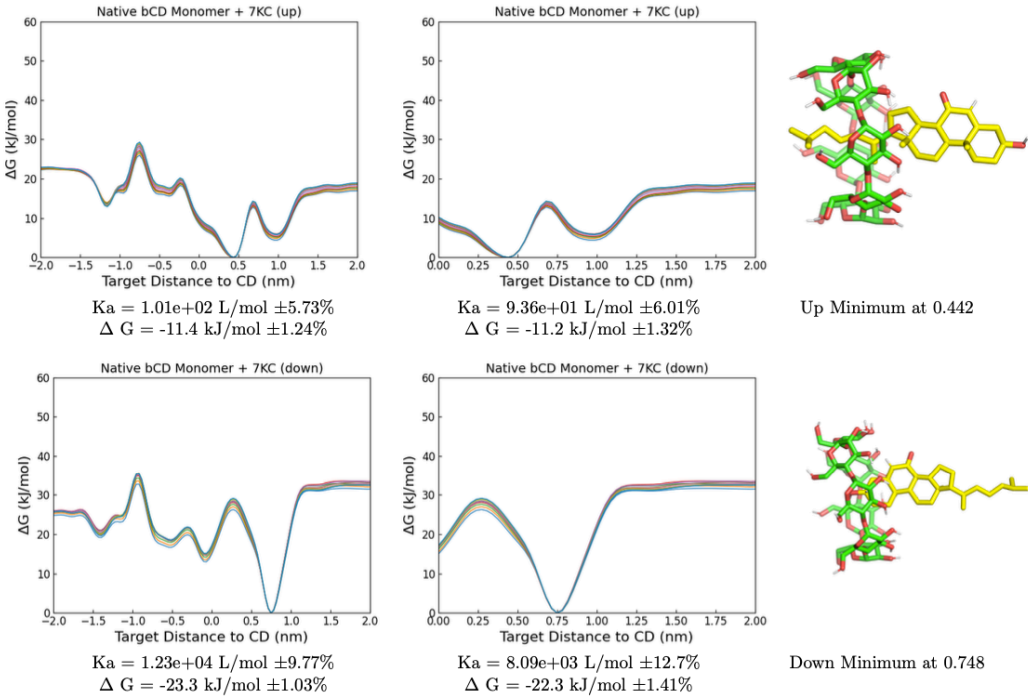


Figure S5-25. Walkers placed every 6Å along the CD cavity. Native βCD with 7KC in up (top) and down (bottom) orientation, sampling either the entire βCD cavity (left) or only the secondary (wide) face of the βCD (middle), along with the associated K and ΔG values, and the configuration at the energy minimum (right).

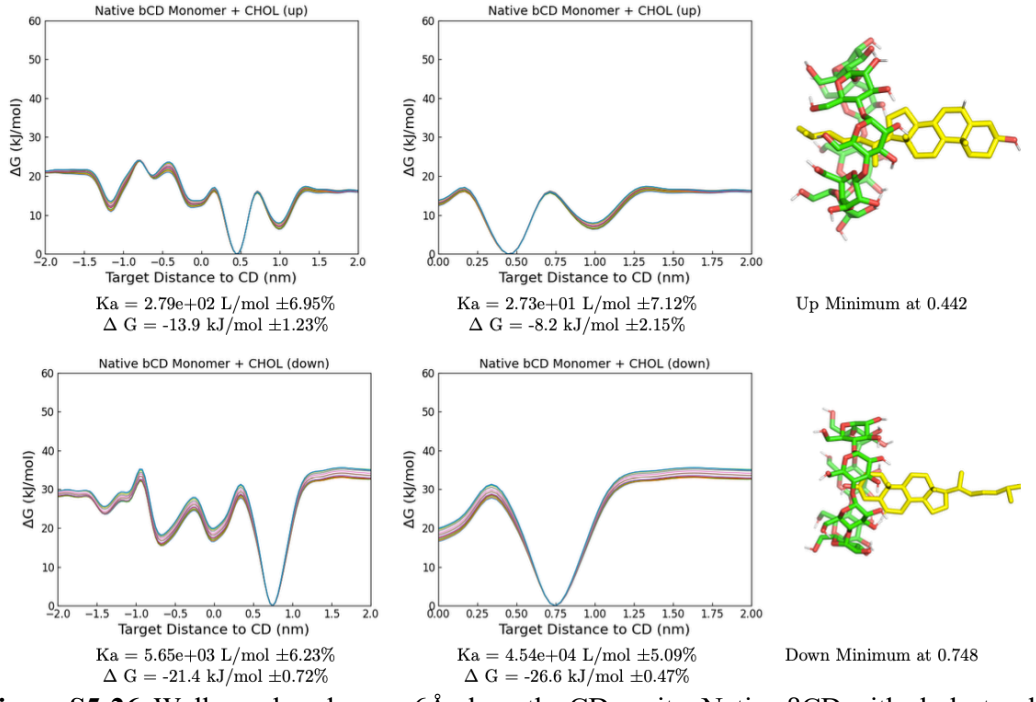


Figure S5-26. Walkers placed every 6Å along the CD cavity. Native βCD with cholesterol in up (top) and down (bottom) orientation, sampling either the entire βCD cavity (left) or

USC UNIVERSIDADE DE SANTIAGO DE COMPOSTELA

only the secondary (wide) face of the βCD (middle), along with the associated K and ΔG values, and the configuration at the energy minimum (right).

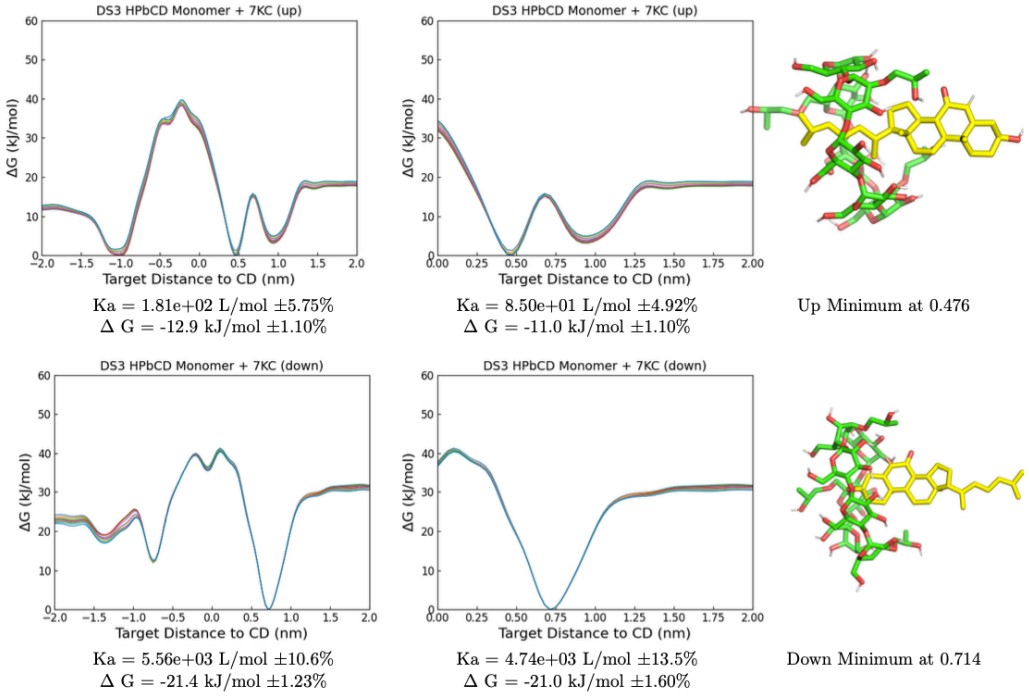


Figure S5-27. Walkers placed every 6Å along the CD cavity. DS3 HPβCD with 7KC in up (top) and down (bottom) orientation, sampling either the entire βCD cavity (left) or only the secondary (wide) face of the βCD (middle), along with the associated K and ΔG values, and the configuration at the energy minimum (right).

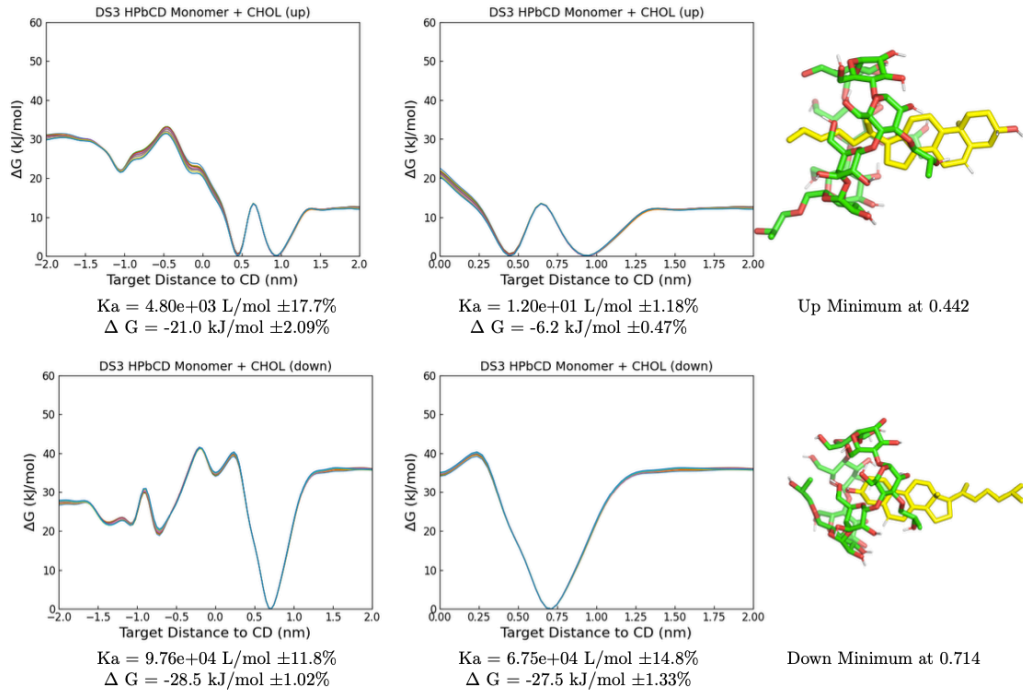


Figure S5-28. Walkers placed every 6Å along the CD cavity. DS3 HPβCD with cholesterol in up (top) and down (bottom) orientation, sampling either the entire βCD cavity (left) or

USC UNIVERSIDADE DE SANTIAGO DE COMPOSTELA

only the secondary (wide) face of the βCD (middle), along with the associated K and ΔG values, and the configuration at the energy minimum (right).

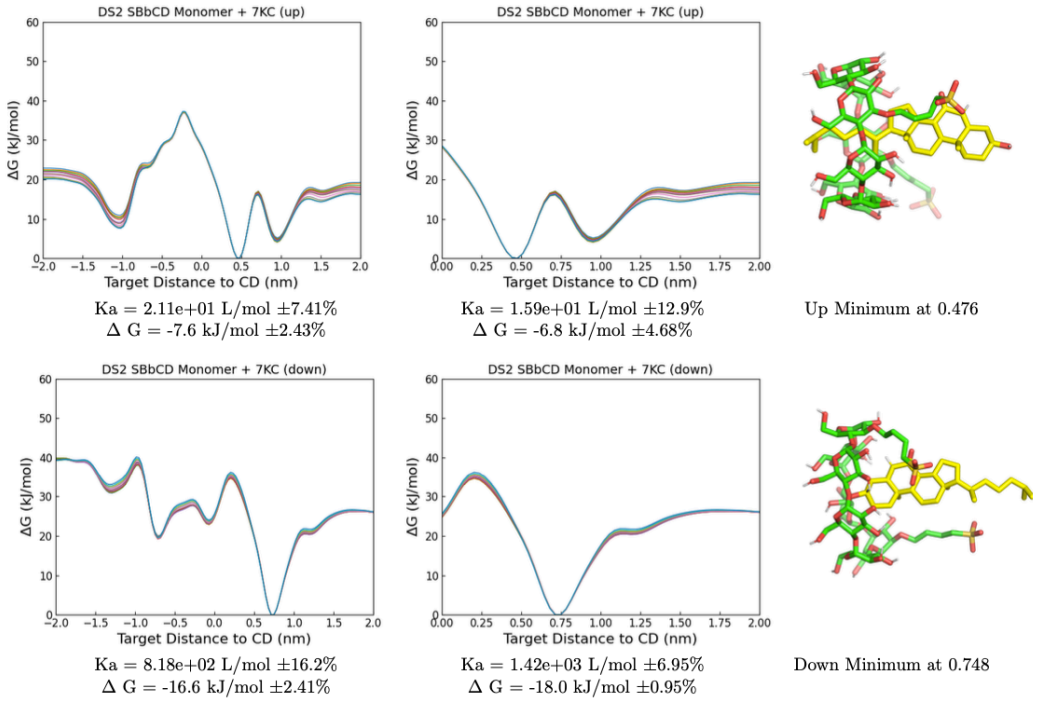


Figure S5-29. Walkers placed every 6Å along the CD cavity. DS2 SBβCD monomer with 7KC in up (top) and down (bottom) orientation, sampling either the entire βCD cavity (left) or only the secondary (wide) face of the βCD (middle), along with the associated K and ΔG values, and the configuration at the energy minimum (right).

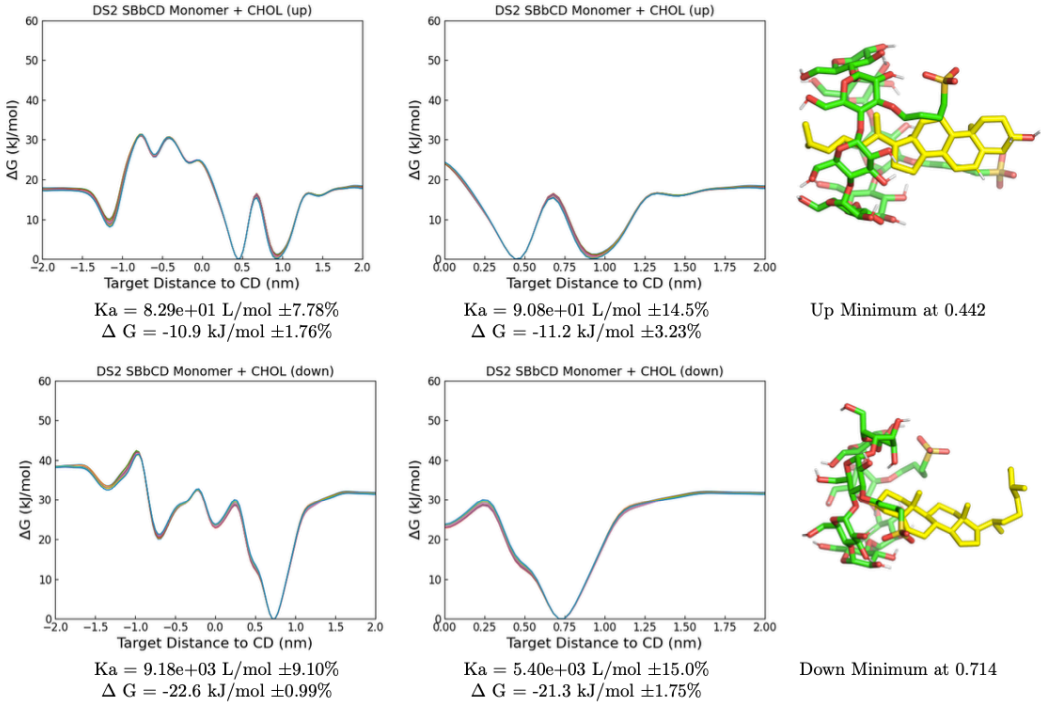


Figure S5-30. Walkers placed every 6Å along the CD cavity. DS2 SBβCD monomer with cholesterol in up (top) and down (bottom) orientation, sampling either the entire βCD

USC UNIVERSIDADE DE SANTIAGO DE COMPOSTELA

cavity (left) or only the secondary (wide) face of the βCD (middle), along with the associated K and ΔG values, and the configuration at the energy minimum (right).

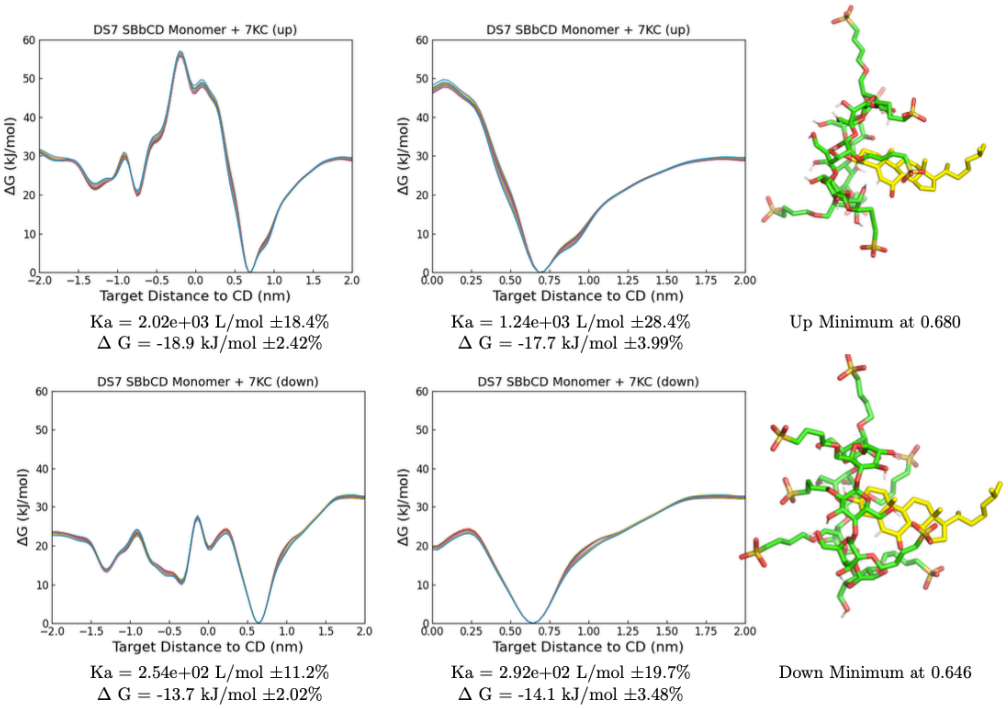


Figure S5-31. Walkers placed every 6Å along the CD cavity. DS7 SBβCD monomer with 7KC in up (top) and down (bottom) orientation, sampling either the entire βCD cavity (left) or only the secondary (wide) face of the βCD (middle), along with the associated K and ΔG values, and the configuration at the energy minimum (right).

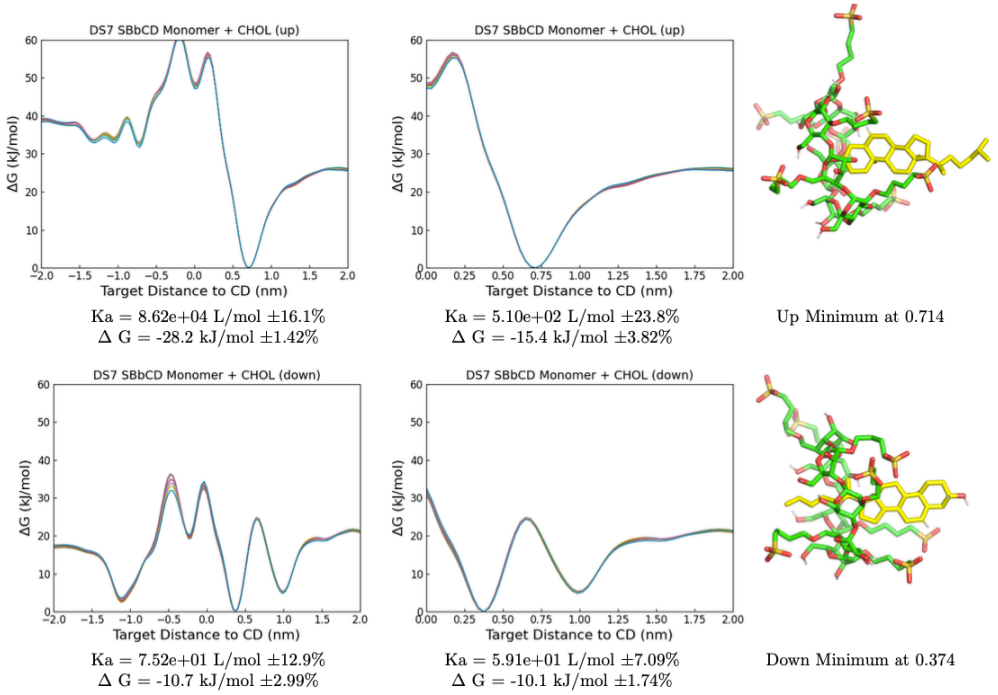


Figure S5-32. Walkers placed every 6Å along the CD cavity. DS7 SBβCD monomer with cholesterol in up (top) and down (bottom) orientation, sampling either the entire βCD

USC UNIVERSIDADE DE SANTIAGO DE COMPOSTELA

cavity (left) or only the secondary (wide) face of the βCD (middle), along with the associated K and ΔG values, and the configuration at the energy minimum (right).

Chapter 6 Supplemental Information

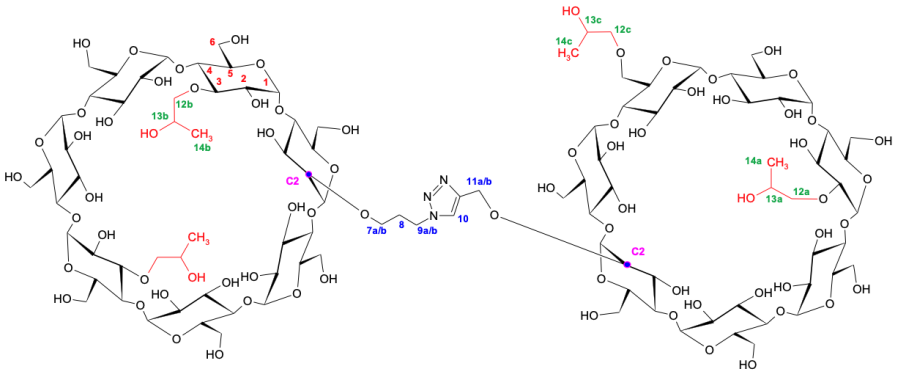


Figure S6-1. Structure of HPβCD dimer with assignment.

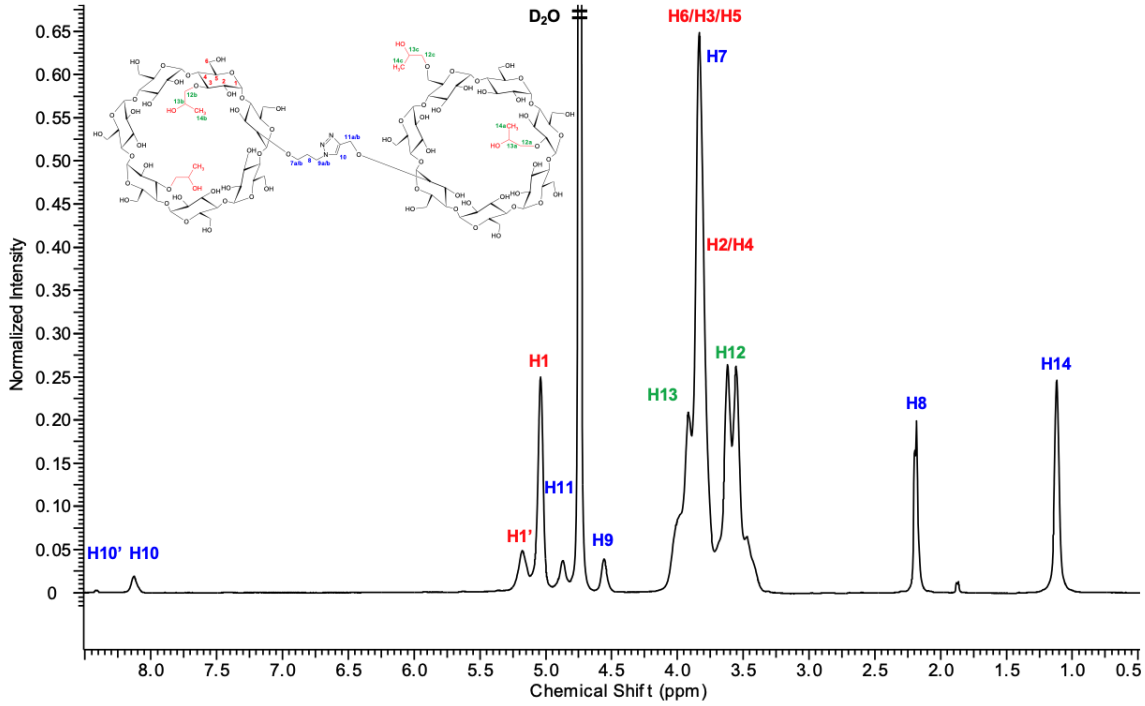


Figure S6-2. ^{1}H spectrum of HPβCD dimer with assignment (D_2O, 600 MHz, 298.15 K).

USC UNIVERSIDADE DE SANTIAGO DE COMPOSTELA

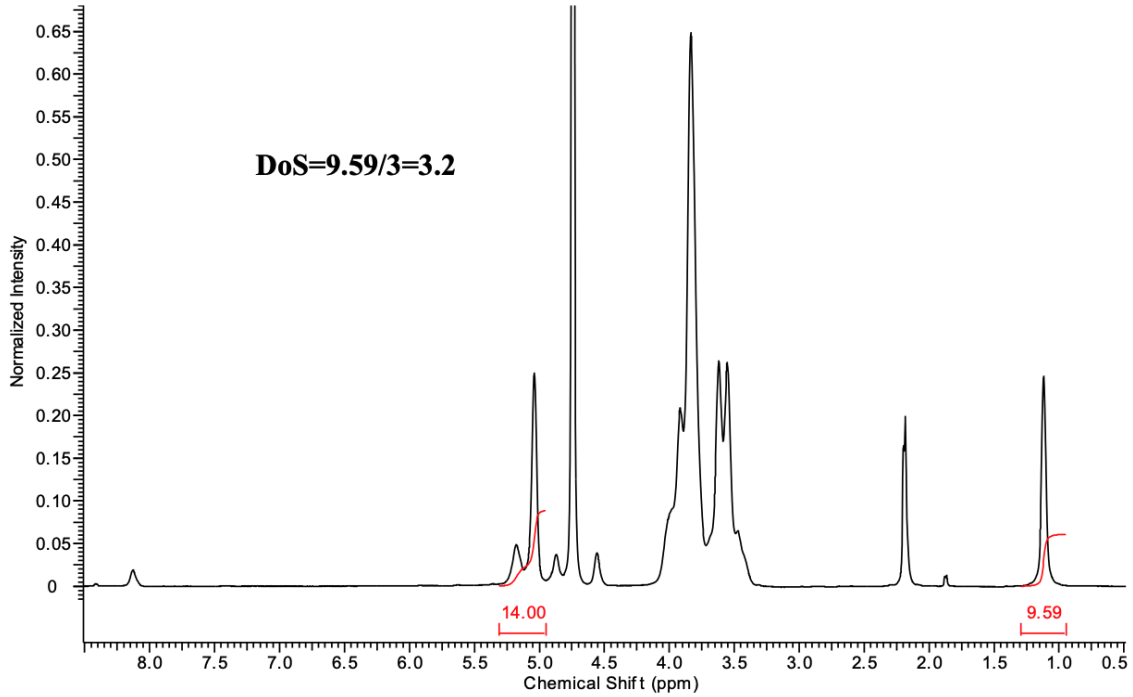


Figure S6-3. ^{1}H spectrum of HPβCD dimer with DoS calculation (D_2O, 600 MHz, 298.15 K).

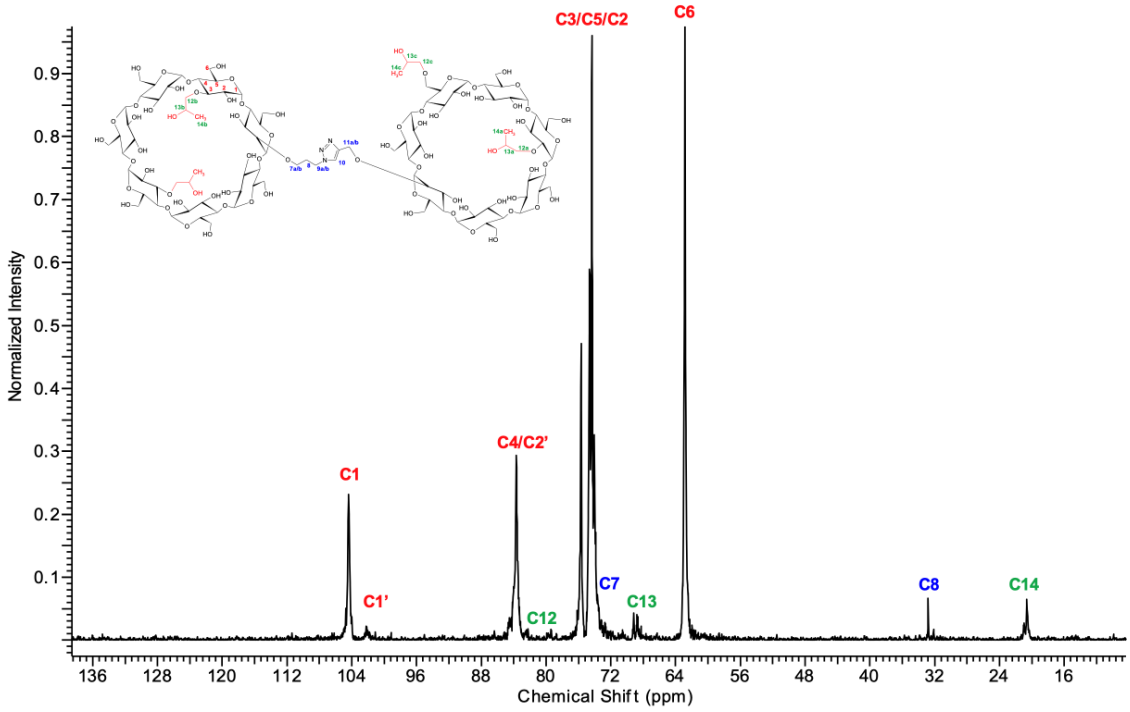


Figure S6-4. ^{13}C spectrum of HPβCD dimer (D_2O, 150 MHz, 298.15 K).

USC
UNIVERSIDADE DE SANTIAGO DE COMPOSTELA

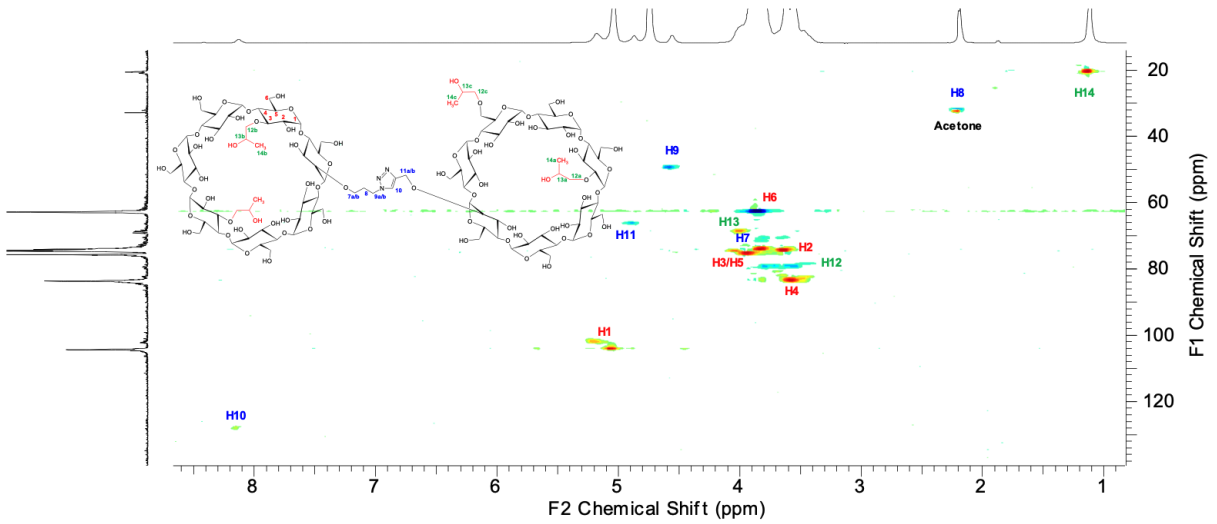


Figure S6-5. DEPT-edited HSQC spectrum of HPβCD dimer with assignment (DMSO-d_6, 600 MHz, 298.15 K).

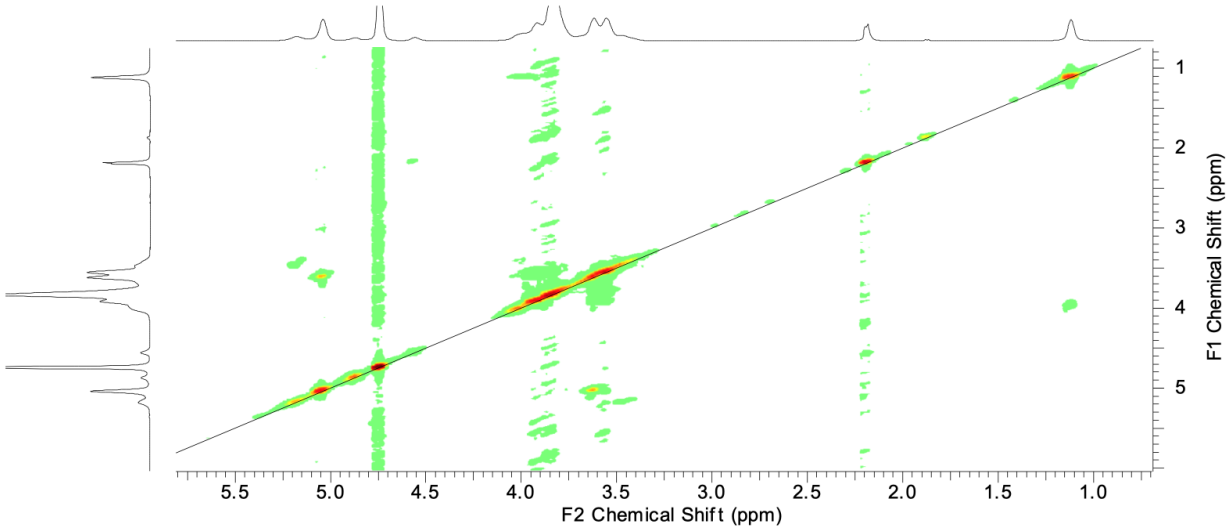


Figure S6-6. COSYspectrum of HPβCD dimer (D_2O, 600 MHz, 298.15 K).

USC
UNIVERSIDADE DE SANTIAGO DE COMPOSTELA

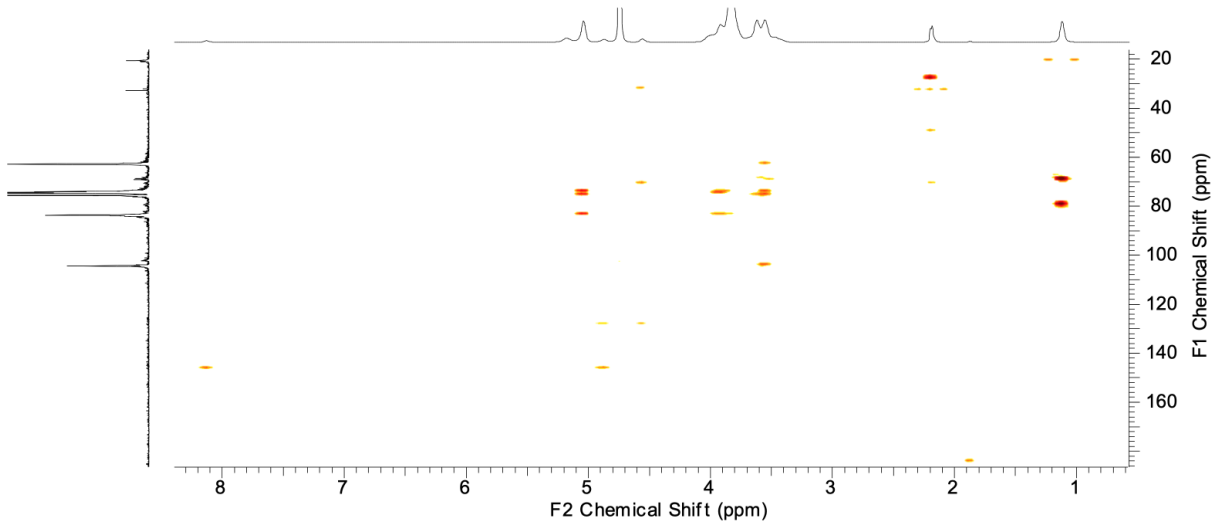


Figure S6-7. HMBC spectrum of HPβCD dimer (DMSO-d_6, 600 MHz, 298.15 K).

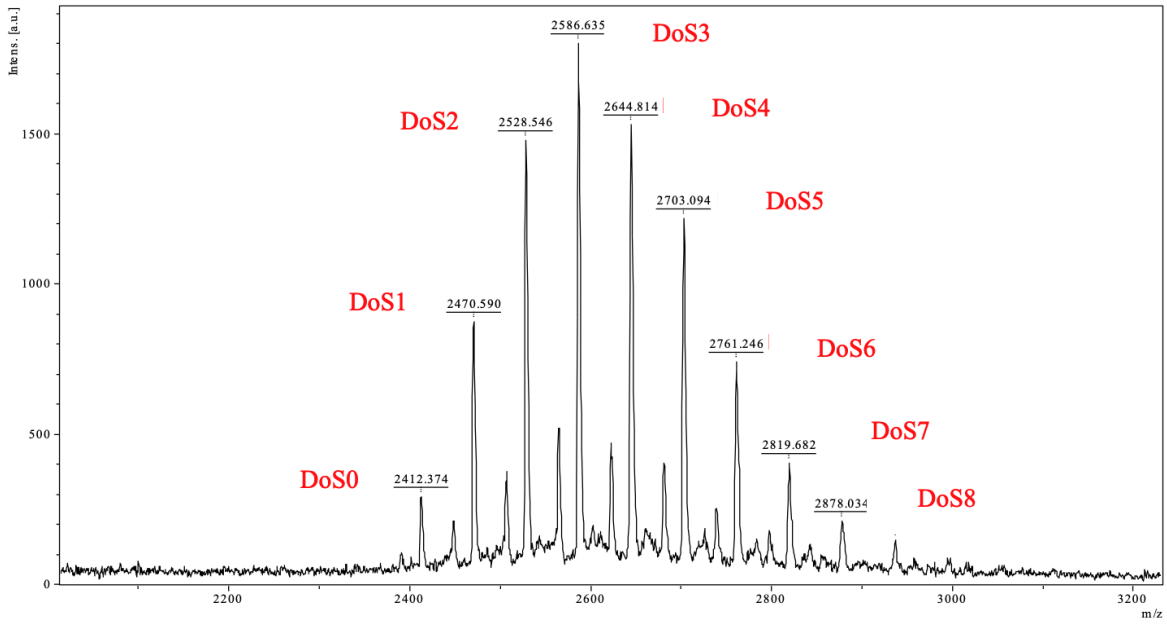


Figure S6-8. MALDI-TOF spectrum of HPβCD dimer with DS (DoS) assignment.

USC
UNIVERSIDADE DE SANTIAGO DE COMPOSTELA

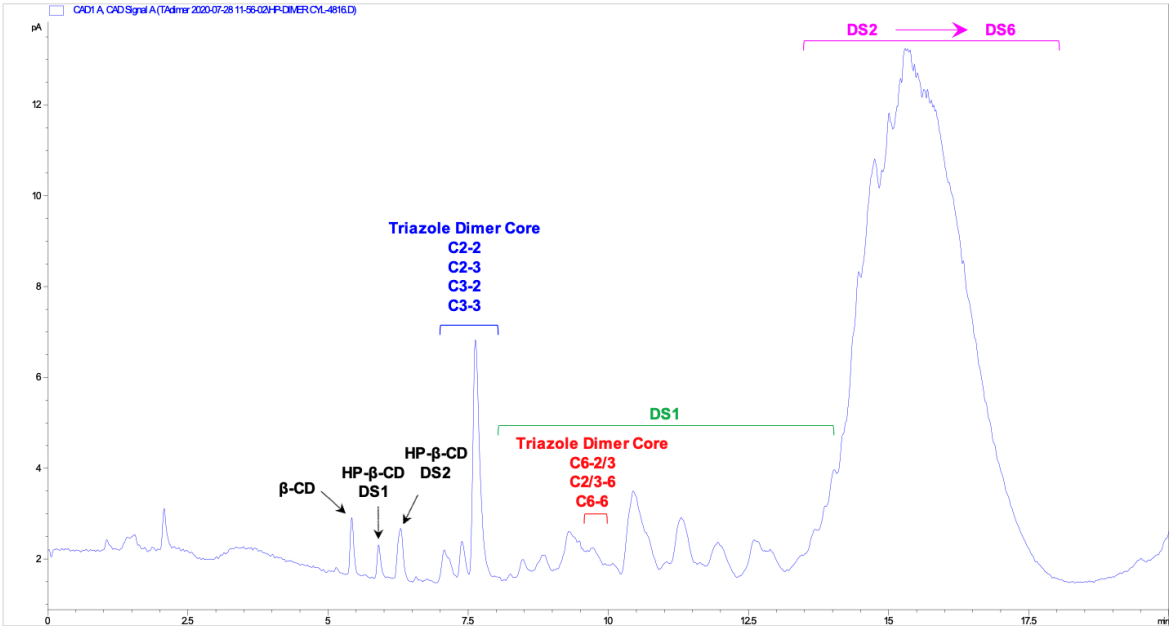


Figure S6-9. Typical HPLC-CAD chromatogram for HPβCD dimer with signals/regions identification.

USC
UNIVERSIDADE DE SANTIAGO DE COMPOSTELA

CHOL		d_1 (nm)	d_2 (nm)	K_1 (M^{-1})	K_2 (M^{-1})	K_{av} (M^{-1})	ΔG_1 (kJ/mol)	ΔG_2 (kJ/mol)	ΔG_{av} (kJ/mol)	Time (ns)	%Δ
1	up	0.494	0.741	3.39E+04 ± 4.8	9.07E+03 ± <1	1.74E+04 ± 4.8	-25.8 ± 0.5	-22.6 ± <0.1	-24.2 ± 0.5	314	13
	down	0.706	0.106	3.49E+05 ± <1	1.82E+05 ± 12	2.49E+05 ± 12	-31.6 ± 0.0	-30.0 ± 1.0	-30.8 ± 1.0	316	5.2
2	up	0.459	0.776	2.83E+07 ± <1	1.27E+07 ± <1	1.86E+07 ± <1	-42.5 ± 0.0	-40.5 ± <0.1	-41.5 ± <0.1	303	4.8
	down	0.741	0.424	6.52E+05 ± <1	2.70E+06 ± 5.6	1.33E+06 ± 5.6	-33.2 ± 0.0	-36.7 ± 0.4	-35.0 ± 0.4	314	10
3	up	0.424	0.741	1.90E+07 ± <1	1.99E+05 ± <1	1.91E+06 ± 0.3	-41.5 ± 0.0	-30.2 ± <0.1	-35.9 ± <0.1	309	32
	down	0.741	0.459	1.98E+06 ± <1	2.26E+04 ± 9.5	2.08E+05 ± 9.5	-35.9 ± 0.0	-24.8 ± 0.9	-30.4 ± 0.9	316	37
4	up	0.388	0.742	1.87E+08 ± <1	1.85E+07 ± 6.8	5.89E+07 ± 6.8	-47.2 ± 0.0	-41.5 ± 0.4	-44.4 ± 0.4	313	13
	down	0.741	0.423	3.00E+06 ± <1	2.13E+05 ± 2.1	8.02E+05 ± 2.1	-37.0 ± 0.0	-30.4 ± 0.2	-33.7 ± 0.2	304	20
1	up	0.529	0.777	1.71E+03 ± <1	6.78E+02 ± <1	1.07E+03 ± <1	-18.4 ± 0.0	-16.2 ± <0.1	-17.3 ± <0.1	309	13
	down	0.671	0.105	8.91E+08 ± <1	2.01E+08 ± 7	4.25E+08 ± 7	-51.1 ± 0.0	-47.4 ± 0.4	-49.3 ± 0.4	308	7.5
2	up	0.423	0.742	5.79E+06 ± <1	6.02E+06 ± <1	5.90E+06 ± <1	-38.6 ± 0.0	-38.7 ± <0.1	-38.7 ± <0.1	300	0.3
	down	0.741	0.424	8.36E+07 ± <1	8.14E+06 ± 6.7	2.57E+07 ± 6.7	-45.2 ± 0.0	-39.4 ± 0.4	-42.3 ± 0.4	302	14
3	up	0.388	0.777	4.47E+07 ± 7.6	1.28E+09 ± <1	2.37E+08 ± 7.6	-43.6 ± 0.4	-52.0 ± <0.1	-47.8 ± 0.4	324	18
	down	0.742	0.459	1.52E+07 ± <1	2.38E+07 ± 4.0	1.90E+07 ± 4.0	-41.0 ± 0.0	-42.1 ± 0.2	-41.6 ± 0.2	301	3
4	up	0.388	0.777	1.48E+04 ± <1	2.11E+05 ± <1	5.59E+04 ± <1	-23.8 ± 0.0	-30.4 ± <0.1	-27.1 ± <0.1	326	24
	down	0.706	0.459	6.15E+06 ± <1	9.75E+05 ± 6.0	2.43E+06 ± 6.0	-38.7 ± 0.0	-34.2 ± 0.4	-36.5 ± 0.4	304	12

Table S6-1. PMF results corresponding to the interaction between CHOL (top) and 7KC (bottom) and the 4 studied CD dimers. The distance between the center of mass of the ligand and the center of mass of the O4 atoms of each monomer are represented by the parameters d1 and d2, the association constant and corresponding DG calculated from the projection of the PMF on each CV are labeled with subscript 1 or 2. The average association constants and DG considering both CVs are included with the subscript "av". The simulation time of each simulation, always using 12 walkers is indicated, and the percentual difference between the standard free energies obtained independently using both CVs is added in the last column as an extra indication of the reliability of each quantitative result.

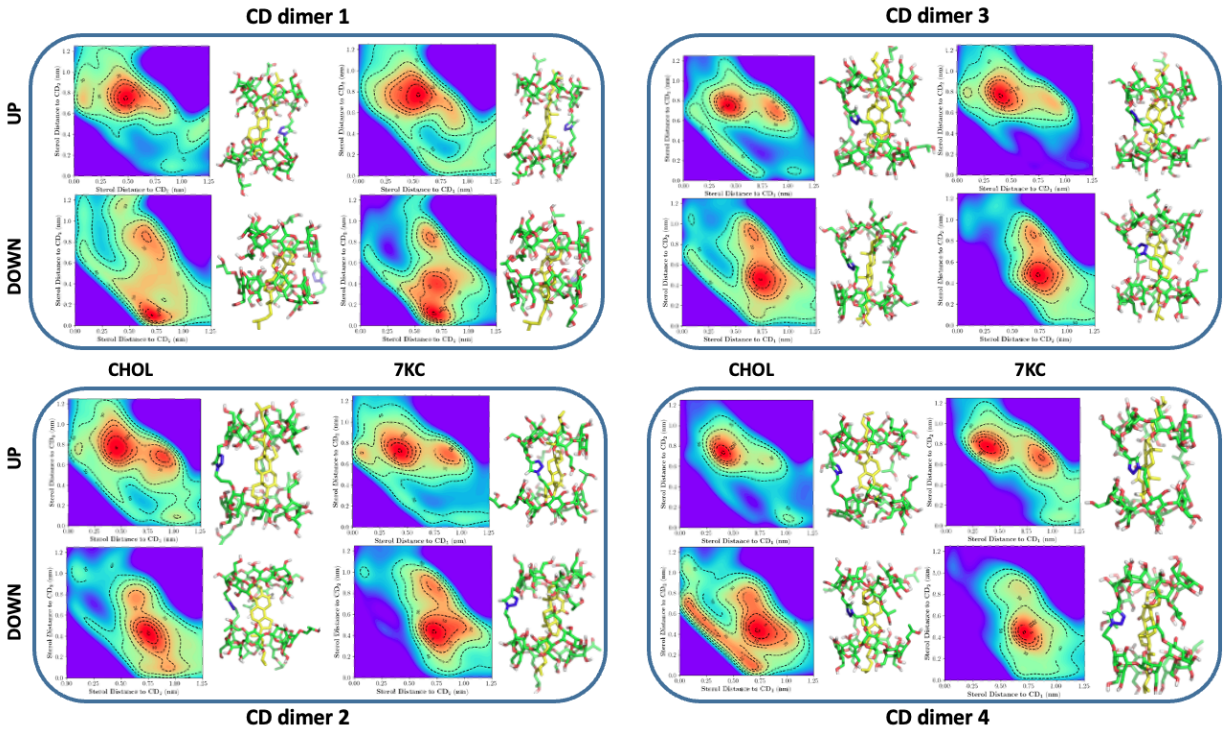


Figure S6-10. PMF profiles obtained from metadynamics simulations together with the minimum energy structure for each case. Results for each CD dimer structure are separated and labeled. The upper row of each panel presents the "up" relative orientation of the ligand within the CD cavity, while the bottom row

USC UNIVERSIDADE DE SANTIAGO DE COMPOSTELA

shows the "down" orientation. CHOL results are displayed on the left side, and 7KC results are on the right side of each panel.

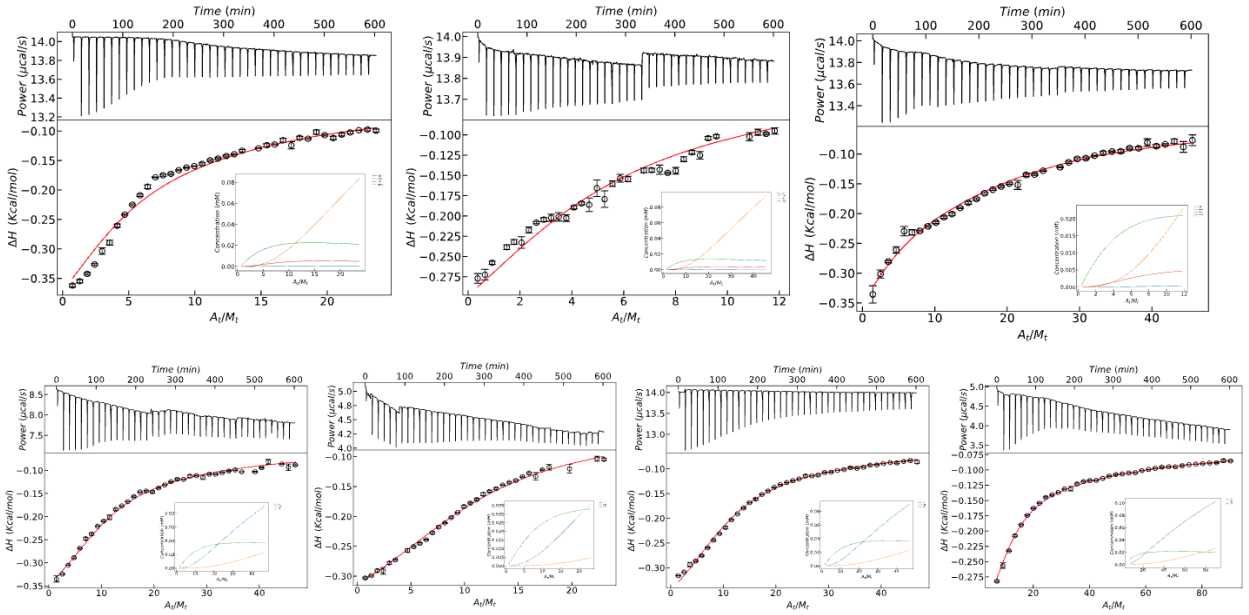


Figure S6-11. ITC results corresponding to the global fitting of the competitive experiments with CHOL (top) and 7KC (bottom) solutions. The insets show the concentration of M1S1 (blue line), M2S1 (orange line), D1S1 (green line) and D1S2 (red line). The concentrations employed for each experiment are indicated in the plots.

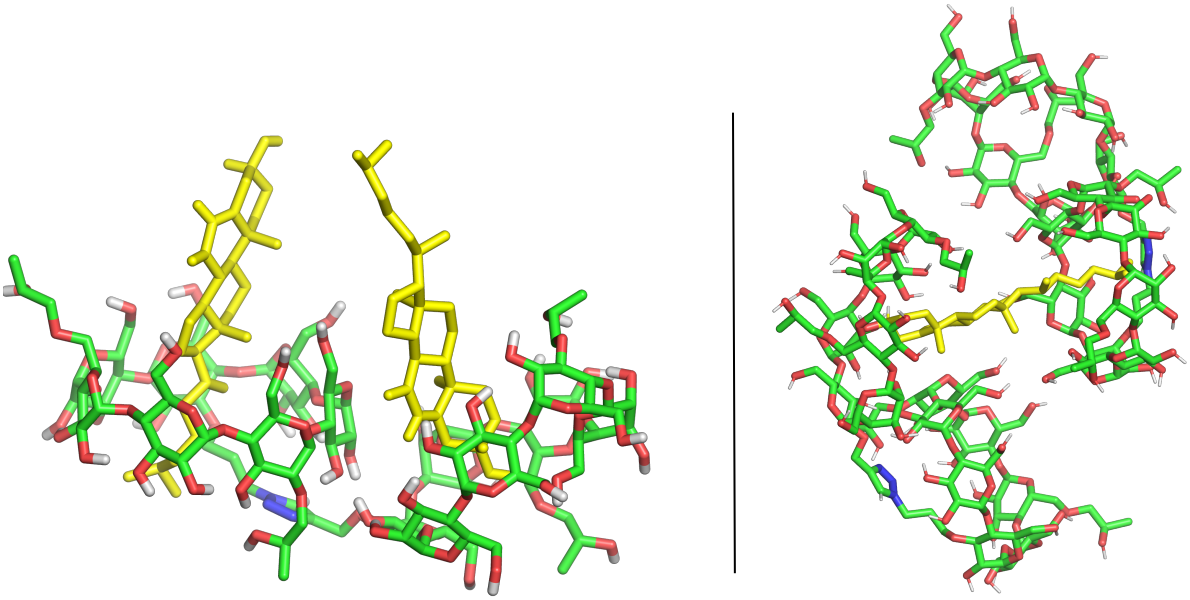


Figure S6-12. Representation of the 1:2 (left, CD_1CHOL_2) and the 2:1 (CD_2CHOL_1) complexes for CD *dimers*. ITC accounts for the 1:2 complex, while CiDi accounts for the 2:1 complex. CDs are represented in green, while CHOL is represented in yellow.

USC
UNIVERSIDADE DE SANTIAGO DE COMPOSTELA

Absorption spectra have been registered on a Perkin Elmer l950 spectrophotometer. The intrinsic absorption of the triazole linker in the dimer was used with a molar absorption coefficient of 4000 $M^{-1}cm^{-1}$ at 215 nm to estimate the CD concentration.

Table S6-2. Association constants corresponding to the reactions indicated in the first column for CHOL, considering both orientations, obtained from the analysis of UV-Vis experiments.

S = CHOL	K (M^{-n})
$D + S \leftrightarrow D_1S_1$	$(3.47 \pm 0.09) \times 10^4\ M^{-1}$
$2D + S \leftrightarrow D_2S_1$	$(2.34 \pm 0.1) \times 10^9\ M^{-2}$

Table S6-3. Association constants corresponding to the reactions indicated in the first column, for 7KC, obtained from the global analysis of UV-Vis experiments.

S = 7KC	K (M^{-n})
$D + S \leftrightarrow D_1S_1$	$(2.09 \pm 0.25) \times 10^6\ M^{-1}$
$2D + S \leftrightarrow D_2S_1$	$(1.26 \pm 0.15) \times 10^{12}\ M^{-2}$

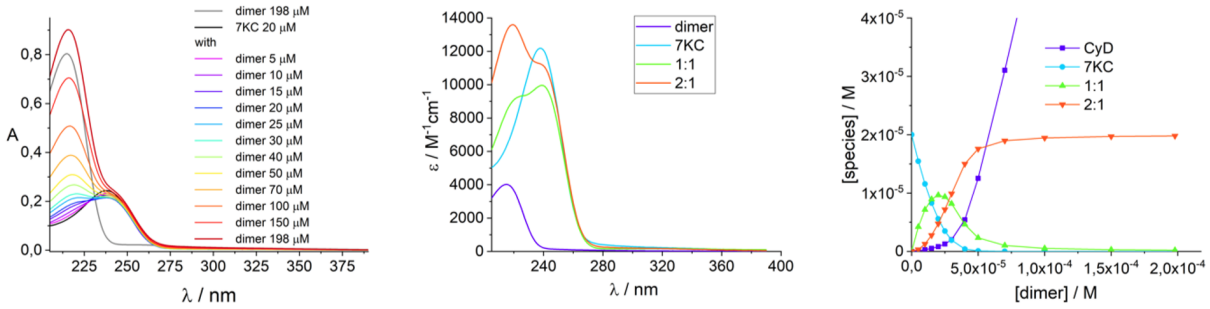


Figure S6-13. UV-Vis Absorption data for 7KC + HPβCD Dimer.

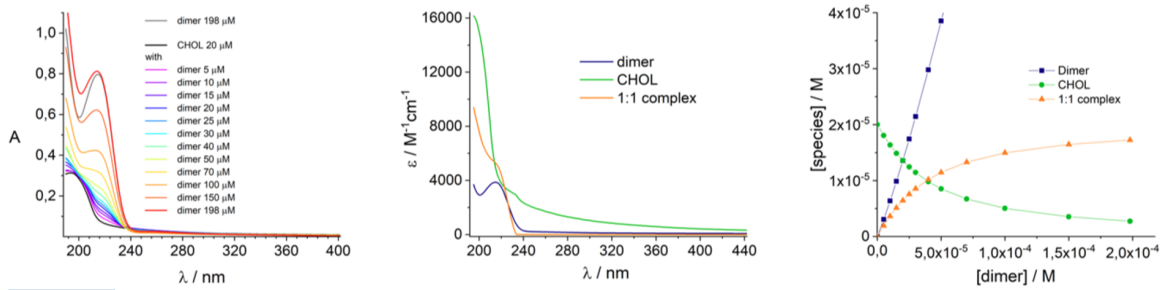


Figure S6-14. UV-Vis absorption data for CHOL + HPβCD dimer.

USC UNIVERSIDADE DE SANTIAGO DE COMPOSTELA

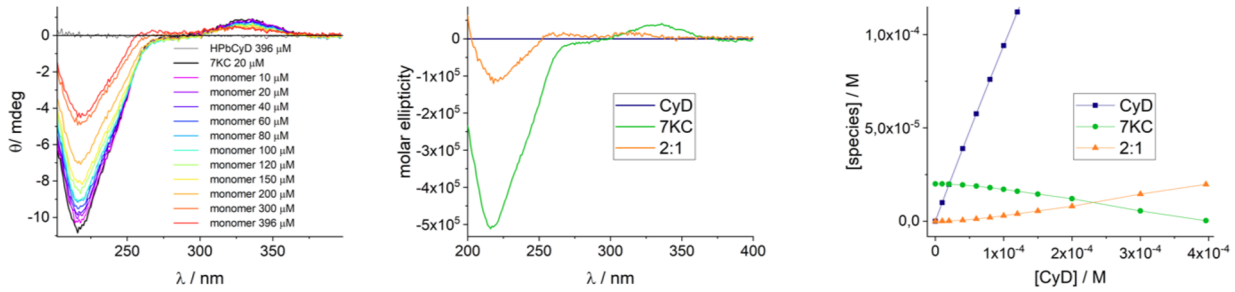


Figure S6-15. CiDi data for 7KC + HPβCD monomer.

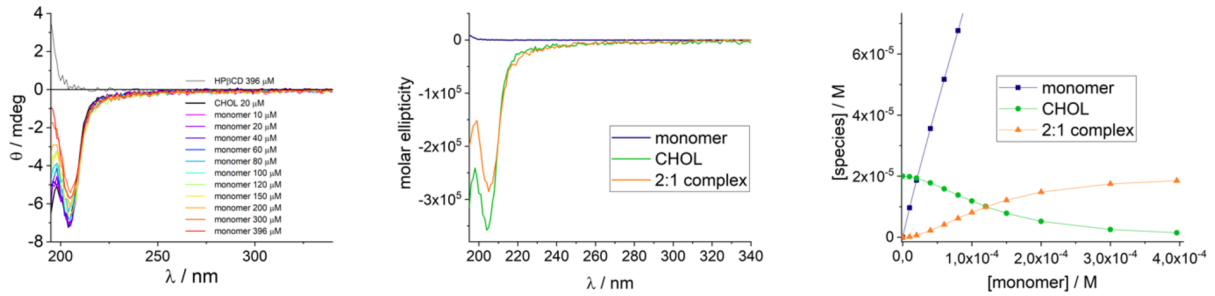


Figure S6-16. CiDi data for CHOL + HPβCD monomer.

Table S6-4. Association constants corresponding to the equilibria indicated in the first column, for the steroid and HPβCD monomer, obtained from the global analysis of CiDi spectra in Figure S14-15 converging with the model consisting in a single 2:1 (monomer:sterol) complex, where M indicates the HPβCD monomer and S indicates the sterol.

	K_{CHOL} (M^{-2})	K_{7KC} (M^{-2})
$2M + S \leftrightarrow M_2S_1$	$(1.99 \pm 0.03) \times 10^7$	$(5.01 \pm 0.21) \times 10^7$

USC
UNIVERSIDADE DE SANTIAGO DE COMPOSTELA

Annex 1: Publications Included in the Thesis and Authorizations for the Published Content

USC
UNIVERSIDADE DE SANTIAGO DE COMPOSTELA

List of Included Publications

Title: Unraveling the Molecular Dynamics of Sugammadex-Rocuronium Complexation: A Blueprint for Cyclodextrin Drug Design

Authors: Amelia Anderson, Rebeca García-Fandiño, Ángel Piñeiro, Matthew S. O'Connor
Year: 2024
Publisher: Elsevier Ltd.
ISSN/ISBN: 01448617
DOI: https://doi.org/10.1016/j.carbpol.2024.122018
Quality indexes: Carbohydrate Polymers is a journal covering the technologies/fields/categories related to Materials Chemistry (Q1); Organic Chemistry (Q1); Polymers and Plastics (Q1). It is published by Elsevier Ltd.. The overall impact score is 11.93.

Title: Cyclodextrins: Establishing Building Blocks for AI-Driven Drug Design by Determining Affinity Constants *in Silico*

Authors: Amelia Anderson, Rebeca García-Fandiño, Ángel Piñeiro, Matthew S. O'Connor
Year: 2024
Publisher: Elsevier Ltd.
ISSN/ISBN: 2001-0370
DOI: https://doi.org/10.1016/j.csbj.2024.02.011
Quality indexes: Computational and Structural Biotechnology Journal is a journal covering the technologies/fields/categories related to Biochemistry (Q1); Biophysics (Q1); Biotechnology (Q1); Computer Science Applications (Q1); Genetics (Q1); Structural Biology (Q2). It is published by Elsevier on behalf of the Research Network of Computational and Structural Biotechnology. The overall impact score is 6.0.

Title: Addressing the Complexities in Measuring Cyclodextrin-Sterol Binding Constants: a Multidimensional Study

Authors: Amelia M. Anderson, Ilse Manet, Milo Malanga, Daniel M. Clemens, Keivan Sadrerafi, Rebeca García-Fandiño, Ángel Piñeiro, Matthew S. O'Connor
Year: 2024
Publisher: Elsevier Ltd.
ISSN/ISBN: 0144-8617
DOI: https://doi.org/10.1016/j.carbpol.2023.121360
Quality indexes: Carbohydrate Polymers is a journal covering the technologies/fields/categories related to Materials Chemistry (Q1); Organic Chemistry (Q1); Polymers and Plastics (Q1). The overall impact score is 11.93.

Copyright Elsevier 2024. Permission was obtained via email on December 12, 2023 from Elsevier to publish manuscripts in this thesis subject to proper acknowledgement.

USC UNIVERSIDADE DE SANTIAGO DE COMPOSTELA

As ciclodextrinas (CDs) son oligosacáridos cíclicos que forman complexos con diversas moléculas, o que as fai extremadamente valiosas en numerosas aplicacións industriais e farmacéuticas. Esta tese explora o uso das CDs para tratar a aterosclerose, enfocándose na eliminación selectiva do colesterol oxidado nocivo, 7-ketocholesterol (7KC), sobre o colesterol. A integración de métodos computacionais e experimentais, incluíndo dinámica molecular e metadinámica, así como medicións isotérmicas de titulación calorimétrica e dicroísmo circular, permitiu unha mellor comprensión destas interaccións a nivel cuantitativo e cualitativo. Os díMeros de CD modificados mostraron unha afinidade mellorada para 7KC sobre o colesterol, resaltando a adaptabilidade das CDs e o seu potencial en aplicacións personalizadas.